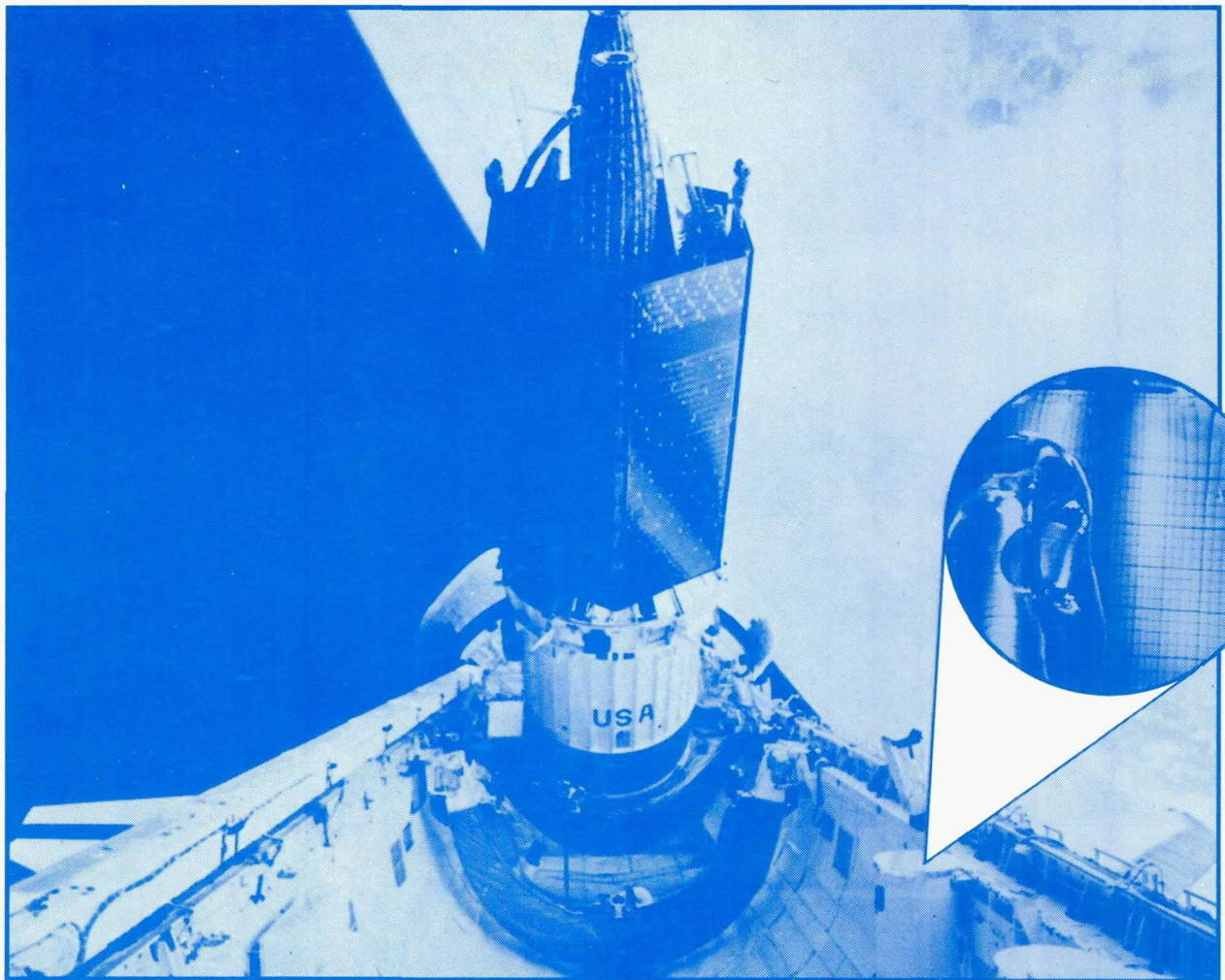


E6677

# **RT** 1991 **Research & Technology**



**NASA**

Lewis Research Center  
Cleveland, Ohio

TECHNICAL MEMORANDUM 105320

**About the cover:**

The Tank Pressure Control Experiment (TPCE) was one of three Lewis experiments aboard the Space Shuttle *Atlantis* on mission STS-43 in August 1991. The TPCE flew in a Get Away Special (GAS) canister visible in the lower right. The inset photograph shows the effect of a liquid jet on the vapor bubble during low-gravity fluid mixing. The results proved the effectiveness of this technique for controlling tank pressures in space. This technology will be applied in cryogenic propellant tanks for many future space missions.



# **Research & Technology 1991**



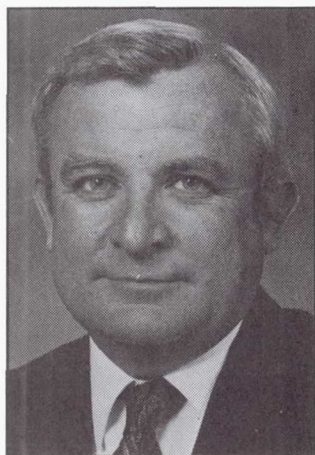
National Aeronautics and  
Space Administration

**Lewis Research Center**  
Cleveland, Ohio 44135

TM-105320

**Page intentionally left blank**





## Introduction

As we enter the next 50 years at the Lewis Research Center, we embark on a journey that will take us to a permanently manned presence in space, exploration of Mars, and beyond. Here at home, we will help the Nation unlock the mysteries of advanced technology and science to make life better for those on Earth. The 1991 Research & Technology Report highlights Lewis' many contributions as we continue down the path that began in 1941.

The report is organized so that a broad cross section of the community can readily use it. A short introductory paragraph begins each article and will prove to be an invaluable reference tool for the layperson. The more than 150 articles summarize the progress made during the year in various technical areas and portray the technical and administrative support associated with Lewis technology programs. If additional information is desired, the reader is encouraged to contact the authors identified in the articles.

The principal purpose of this report is to give a brief but comprehensive review of the technical accomplishments of the Center during the past year. It is a testimony to the dedication and competence of all the employees, civil servants and contractors, who make up the staff.

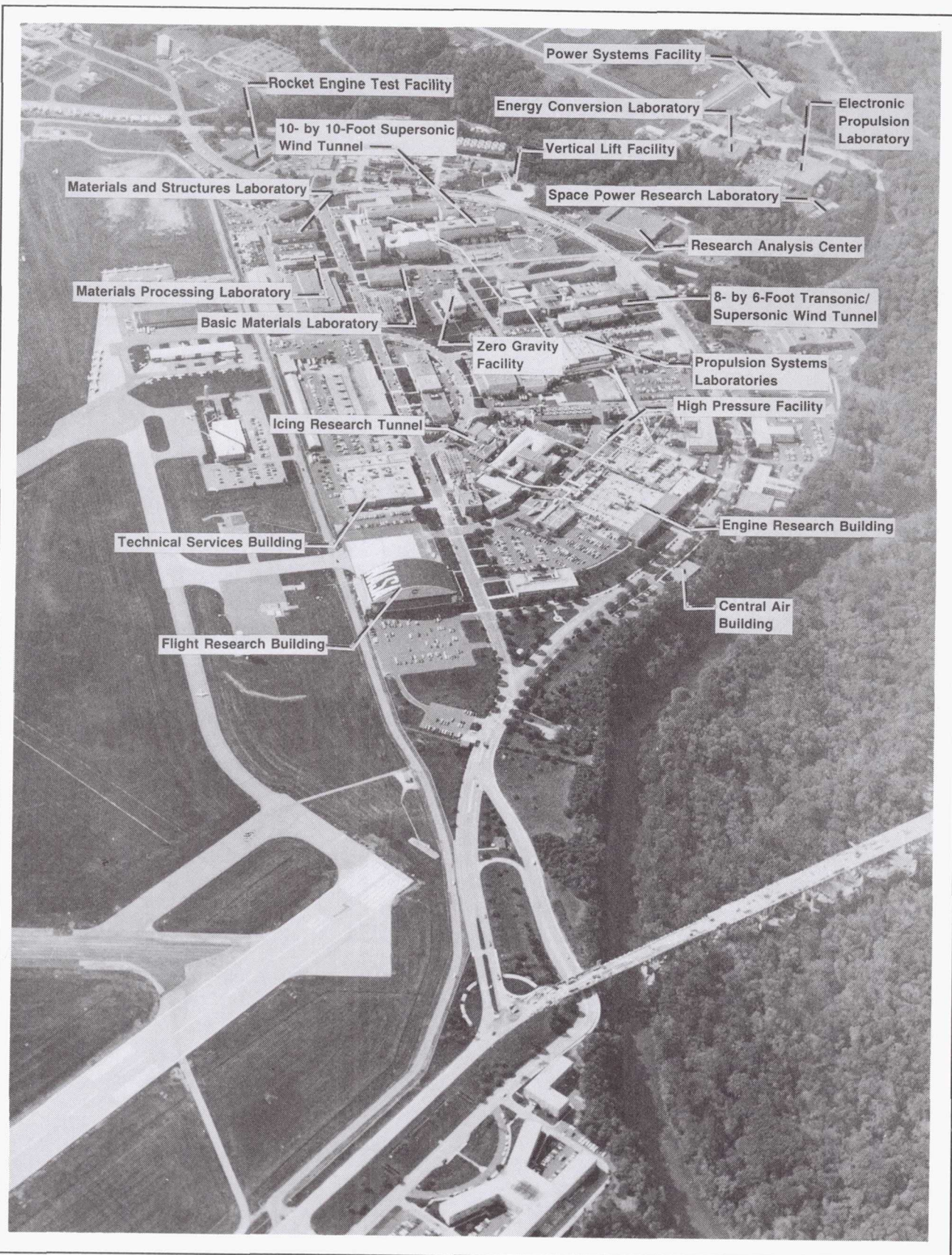
The Lewis Research Center is a unique facility, located in an important geographic sector, with a long and distinguished history of performing research and technology development in support of NASA's mission and the Nation's needs.

A handwritten signature in cursive script that reads "L J Ross".

Lawrence J. Ross  
Director

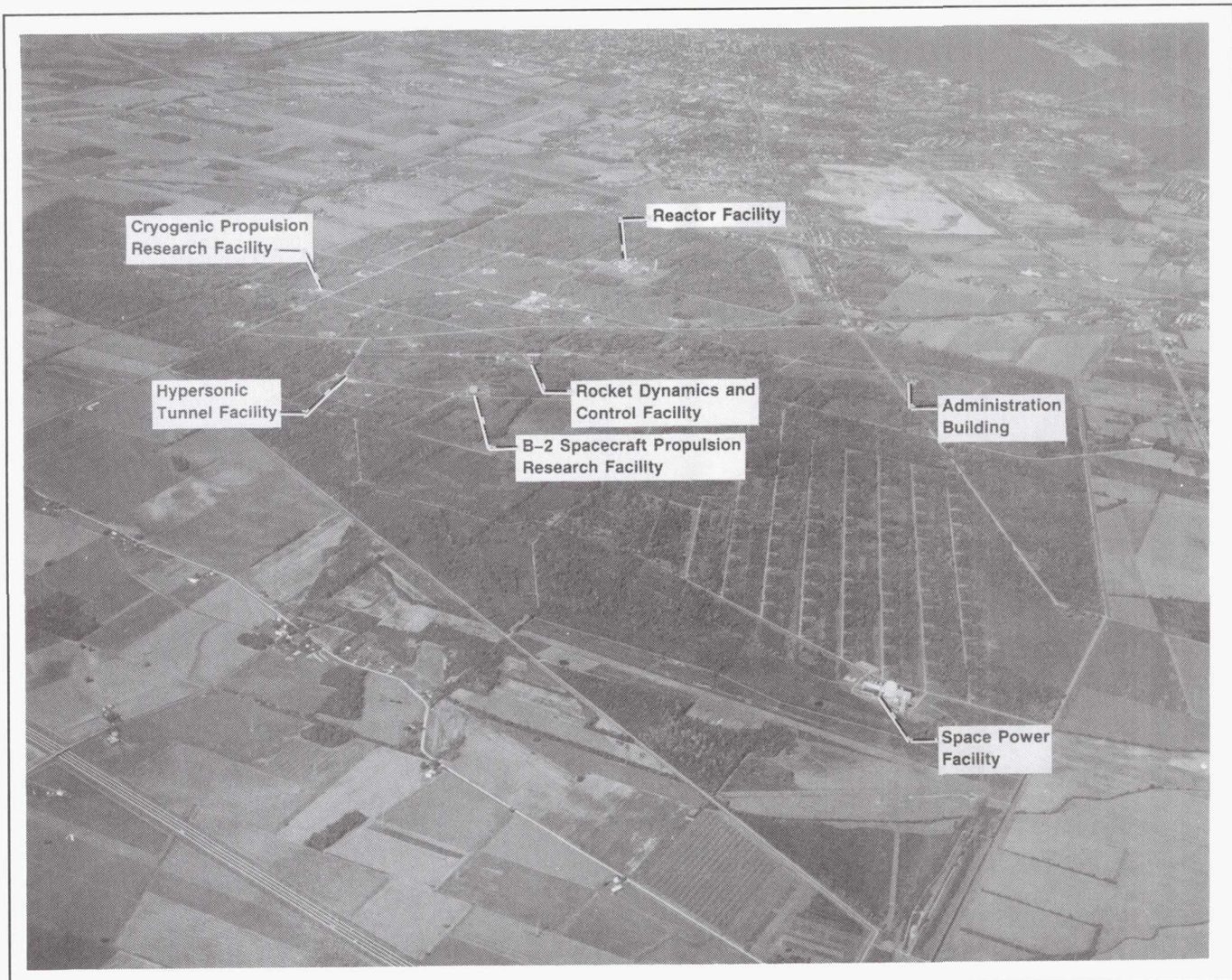
Inquiries regarding this report can be addressed to the Office of Interagency and Industry Programs, Mail Stop 3-17. The telephone number is (216) 433-5382 or FTS 297-5382.





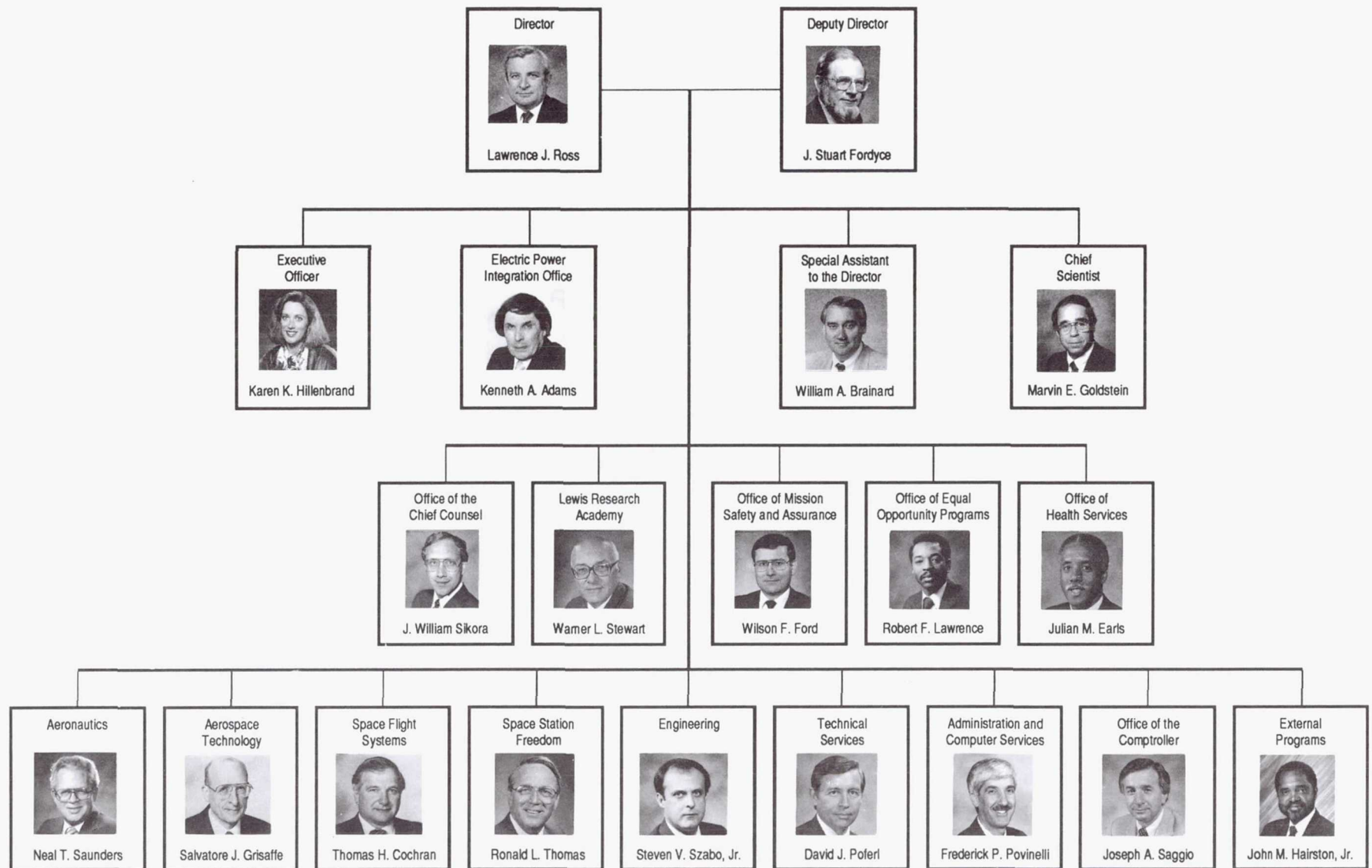
Lewis Research Center, Cleveland, Ohio





Plum Brook Station, Sandusky, Ohio

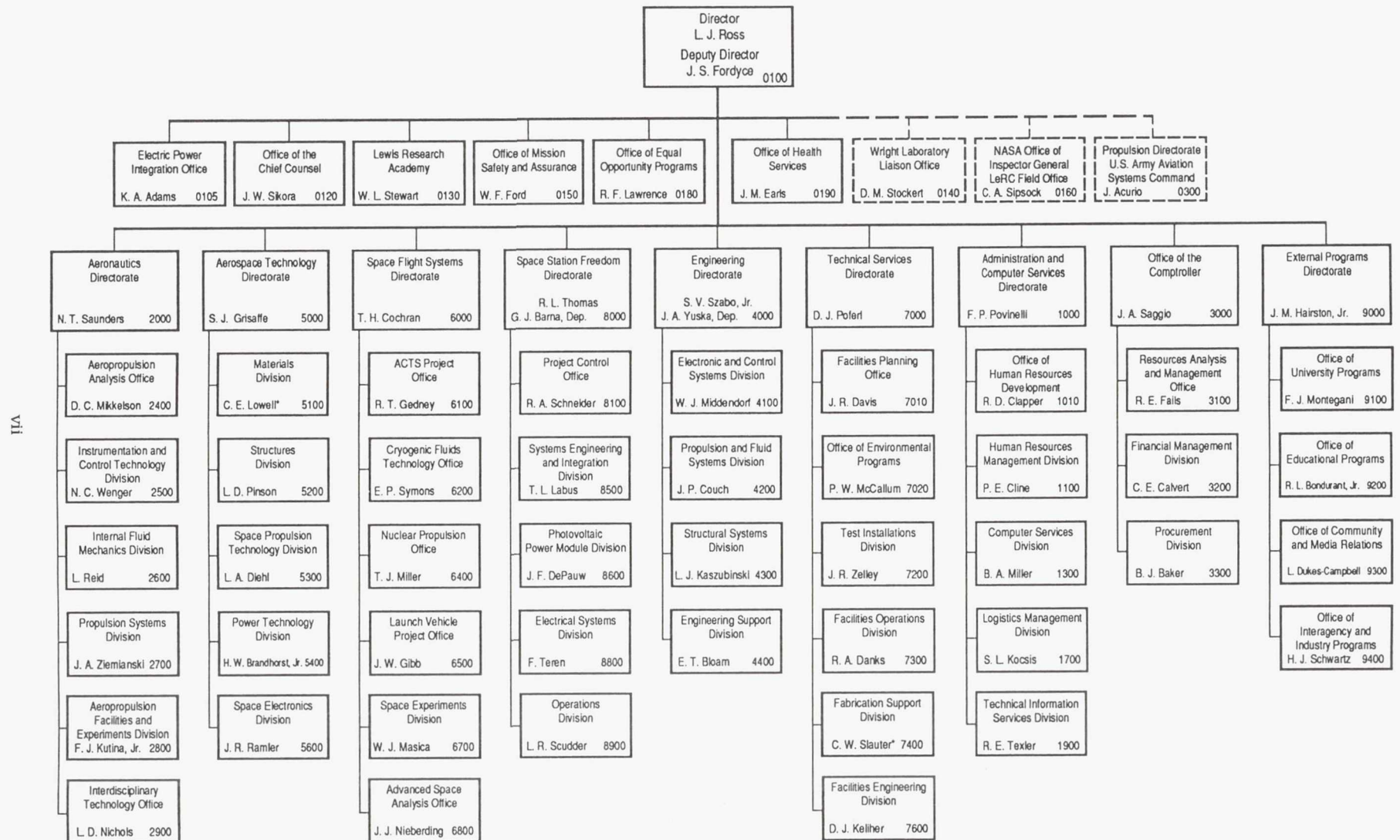
# NASA Lewis Research Center Senior Management



December 17, 1991  
CD-91-48534



# NASA Lewis Research Center



\*Acting

CD-44972  
January 28, 1992

**Page intentionally left blank**



# Contents

<b>Aeronautics</b> .....	1
<b>Aeropropulsion Analysis</b> .....	1
Graphical User Interface Speeds Engine Cycle Analysis .....	1
Beta II Shows Promise for Reduced Cost and Assured Manned Access to Space .....	2
<b>Instrumentation and Control Technology</b> .....	3
*High-Temperature Resistance Static Strain Gage Developed .....	3
Thin-Film Thermocouples Measure Ceramic Surface Temperatures to 1500 °C .....	4
X-Ray-Based Extensometry Eases Displacement Measurements in Hostile Environments .....	5
Nonintrusive Laser-Based Measurements Support Hypersonic Propulsion System Experiments .....	6
Alignment of Optical Measurement Systems Automated .....	7
Neural-Network-Based Control Designed .....	8
Sensor Validated by Autoassociative Neural Networks .....	9
Design Methodology Developed for Integrated Flight/Propulsion Control Systems .....	10
<b>Internal Fluid Mechanics</b> .....	11
Parallel Computation Uses Lagrangian Formulation .....	11
Progress Made Toward Developing Parallel Turbomachinery Code .....	12
Centrifugal Compressor Flow Physics Studied .....	13
Progress Made Toward Evaluating Multiphase-Flow Computer Codes .....	14
Hot-Gas Ingestion Calculated for STOVL Aircraft Model .....	15
All-Speed Reacting Flow Code Developed for Engine Simulations .....	16
Enhanced Mixing Tested and Modeled .....	17
Jet Mixing Increased by Using Tabs .....	17
Microgravity Fluid Mechanics Studied With CFD .....	18
Computational Fluid Dynamics Simulations Performed for Space Propulsion Rockets .....	19
<b>Propulsion Systems</b> .....	20
Ceramic Components for Gas Turbine Engines Tested to 2500 °F .....	20
Low-NO <sub>x</sub> Combustor Concepts Reach Goal .....	21
Code Numerically Simulates Icing, Deicing, and Shedding .....	22
Automated Spiral Bevel Gear Grinding and Inspection Enhanced .....	23
Gearbox Acoustic Code Validated .....	24
Transonic Performance of NASP Nozzle Evaluated in Wind Tunnel Tests .....	25
Data Base Compiled for Thrust-Augmenting Ejector .....	26
Analytical Tool Developed for Ventral/Cruise Exhaust Nozzles .....	27
Radial Rotor Cooling Studied .....	28
Viscous Three-Dimensional Codes Predict Transonic Fan Performance .....	29
Euler/Navier-Stokes Code Predicts Unsteady Ducted-Propfan Aerodynamics .....	30
Novel Method Allows Direct Measurement of Acoustic Modes in Fan Engine .....	31
Takeoff Noise Tests Completed on a Model Advanced Ducted Propeller .....	32
Stationary Blockage Devices Simulate Inlet Separation Angle of Attack in an ADP Simulator .....	33
F-18 Inlet Flow Calculated at High Angles of Attack .....	34
Acoustic Dome Constructed .....	35

<b>Aerospace Technology</b> .....	36
<b>Materials</b> .....	36
Advanced High-Temperature Engine Materials Technology Continues Progress .....	36
Materials Program Supports HSCT .....	36
Laser Light Scattering Opens New Frontiers .....	37
New High-Temperature Composite Strengthened .....	38
<sup>†</sup> $\gamma'$ Coarsening in High Volume Fraction Nickel-Base Alloys .....	40
Processing Improved for Single-Crystal Turbine Blades .....	41
Engineered Interface Eliminates Thermal Ratcheting in Graphite-Fiber-Reinforced Copper-Matrix Composites .....	41
Stability of Ceramics in Hydrogen Evaluated .....	43
Creep Modeled for Polycrystalline Ceramic Fibers .....	43
Processing Optimization Improves Flexural Creep Resistance of Sintered Silicon Nitride .....	44
Oxidation-Resistant Coatings Tested on High-Temperature Polymer Composites .....	44
Beryllium Oxide Identified as an Effective Reaction Barrier for NiAl/Nb <sub>2</sub> Be <sub>17</sub> Composite to 1373 K .....	45
Persian Gulf Sand Deposits on Helicopter Turbine Vanes Analyzed .....	46
Approach Defined for Modeling Continuous-Fiber Chemical Vapor Deposition Processes .....	47
Application-Critical Engineering Properties Determined for PM212, Self-Lubricating High-Temperature Composite .....	48
Techniques Developed To Lubricate Ceramics With Solid-Lubricant Films .....	49
*High-Temperature Nitrogen Postcure Developed for Polymer Matrix Composites .....	50
<b>Structures</b> .....	52
New Equations Show Oil Filtration Effect on Bearing Life .....	52
Hot Composites Assessed for Adverse Thermal and Structural Loads .....	52
Acoustic Fatigue of Hot Composite Structures Simulated .....	53
Effects of Interply Damping Layers Simulated on Dynamic Response of Composite Structures .....	54
Nonlinear Finite Element Analysis Proves Viable for Investigating Composite Materials Behavior .....	55
Artificial Neural Networks Simulate Composite Hygrothermal Properties .....	56
Structural NDE Approach Used in Health-Monitoring System .....	57
Computational Simulation of Metal-Matrix Composites Verified .....	58
Method Developed for Observing Matrix Plasticity in Metal-Matrix Composites .....	58
Interphase Layer of Metal-Matrix Composites Tailored With Fabrication Considerations .....	59
Aeroelastic Vibration of Rogue Blades in Turbomachinery Demonstrated .....	60
Unified Motion Planning Approach Developed for Redundant Manipulators .....	61
High-Temperature Ceramic-Wafer Seal Leakage Assessed .....	61
Efficient Flutter Analysis Developed for Cambered Compressor and Turbine Blades .....	63
Integrated Design Program Predicts Life of Monolithic Ceramic Components .....	63
Reliability Evaluated for Laminated CMC Components .....	65
Ultrasonic Test Determines Superconductivity Variations Caused by Porosity Gradient .....	66
Processing Changes in YBa <sub>2</sub> Cu <sub>3</sub> O <sub>7-x</sub> Ultrasonically Evaluated .....	67
<b>Space Propulsion Technology</b> .....	68
Combustion-Wave Ignition Demonstrated for Multiple Engines .....	68
Atomic Implants Investigated for Spectroscopic Wear Detection .....	68
Rocket Engine Advanced Cooling Techniques Evaluated .....	69
Tubular Copper Thrust Chamber Fabricated and Tested .....	70

<sup>†</sup>The 1991 Lewis Research Center Distinguished Publication Award.

\*R&D 100 Award.



Slush Hydrogen Experiments Conducted at K-Site Facility . . . . .	71
Performance Characteristics of Liquid Hydrogen Foil Bearing Demonstrated . . . . .	72
Advanced Method Tracks Evolution of Fatigue Damage in Reusable Space Propulsion Systems . . . . .	73
Brush Seals for Cryogenic Turbopumps Studied . . . . .	73
Advanced Concepts Program Studies High-Energy-Density Propellants . . . . .	74
Metallized Propellant Program Develops New Technologies . . . . .	75
Lunar Indigenous Monopropellants Formulated and Characterized . . . . .	76
Neural Networks Predict Critical Parameters During SSME Startup Transient . . . . .	77
Expert System Analyzes Chemical and Nuclear Rocket Nozzle Performance . . . . .	77
<b>Power Technology . . . . .</b>	<b>79</b>
Flight Hardware Developed for Mini-Dome Fresnel Lens Photovoltaic Concentrator Array . . . . .	79
Mars Insolation Model Expanded . . . . .	80
Advanced Induction Motor Developed . . . . .	81
*Fiber-Optic Sensor Measures Electrical Current . . . . .	83
Photovoltaic Power System Planned for Use in Antarctica . . . . .	83
Small Free-Piston Stirling DIPS Being Designed for Robotic Space Missions . . . . .	85
Free-Piston Stirling Space Power Research Engine Demonstrates Highly Efficient Linear Alternator . . . . .	86
Hydrostatic Gas Bearings Successfully Tested in Free-Piston Stirling Engine . . . . .	87
Model Predicts Focusing of Plasma Ions Into Insulation Holes . . . . .	88
LEO Atomic Oxygen Undercutting Documented at Protective Coating Defect Sites on LDEF . . . . .	89
Experiments Will Evaluate Oxygen-Material Interactions . . . . .	90
Fabrication Techniques Developed for All-Metal Advanced Solar Concentrators . . . . .	91
Thermal Control Concepts Selected for Advanced Space Power Electronics . . . . .	92
<b>Space Electronics . . . . .</b>	<b>93</b>
Breadboard Testing of Ka-Band MMIC Microstrip Subarray Completed . . . . .	93
Optical Control Designed for Phased-Array Antennas . . . . .	94
Packaging Developed for Monolithic Microwave Integrated Circuits . . . . .	95
High-Efficiency Traveling Wave Tube Amplifiers Demonstrated for Deep-Space Communications . . . . .	96
60-GHz Traveling Wave Tube Designed for Intersatellite Communications . . . . .	96
Submillimeter-Wavelength Backward-Wave Oscillator Designed . . . . .	97
Cryogenic High-Electron-Mobility Transistor Studied . . . . .	98
High-Temperature Superconducting Space Experiment Begins Development . . . . .	99
Four-Element Array Tested for Ka-Band Superconducting Microstrip Antenna . . . . .	99
Flexible High-Speed Codec Designed . . . . .	100
Design of Programmable Digital Modem Nears Completion . . . . .	101
Flexible Trellis Modem and Codec Being Developed . . . . .	102
Neurocomputing Pursued for Space Communications . . . . .	103
Advanced GaAs Monolithic Switch Matrix Built and Tested . . . . .	104
SITE Space Communications System Simulator and Testbed Expanded . . . . .	104
ACTS High-Burst-Rate Link Evaluation Terminal Being Developed . . . . .	106
Flexible-Rate High-Definition Television Study Completed . . . . .	106
Subband Coding Improved . . . . .	108
<b>Space Flight Systems . . . . .</b>	<b>109</b>
<b>Cryogenic Fluids Technology . . . . .</b>	<b>109</b>
Tank Pressure Control Experiment Flies on Shuttle . . . . .	109
Cryogenic Component Characterized With Liquid Hydrogen . . . . .	109

\*R&D 100 Award.



Lunar Thermal Environment Simulated for Cryogenic Storage Tests . . . . .	110
Vented-Tank Resupply Experiment Being Designed . . . . .	111
No-Vent Fill Method Modeled for Orbital Propellant Transfer . . . . .	112
Tank Chilldown Demonstrated at K-Site Facility . . . . .	113
Cryogenic Fluid Management Technology Benefits Quantified for Lunar Transfer Vehicles . . . . .	113
<b>Nuclear Propulsion . . . . .</b>	<b>114</b>
Common Lunar/Mars Space Transportation System Is Based on Nuclear Thermal Rocket Technology . . . . .	114
Nuclear Electric Propulsion Vehicle Studied for Piloted Mars Mission . . . . .	116
<b>Space Experiments . . . . .</b>	<b>117</b>
GaAs Crystal Growth Experiment Flown on Shuttle . . . . .	117
Apparatus Being Fabricated for Isothermal Dendritic Growth Experiment . . . . .	118
Design Completed for Critical Fluid Light-Scattering Experiment . . . . .	119
Surface-Tension-Driven Convection Experiment Nears Flight-Readiness . . . . .	120
Space Acceleration Measurement System Flown on Two Shuttle Missions . . . . .	122
Glovebox Experiments Being Developed for USML-1 . . . . .	123
Pool Boiling Experiment Prepared . . . . .	125
Solid Surface Combustion Experiment Analyzed . . . . .	126
Solar Array Module Plasma Interactions Experiment Being Developed . . . . .	127
<b>Space Station Freedom . . . . .</b>	<b>129</b>
<b>Systems Engineering and Integration . . . . .</b>	<b>129</b>
Reliability Computer Program Developed . . . . .	129
Computer Code Analyzes Electric Power System Performance . . . . .	130
Hypervelocity Impact Testing Performed on Solar Dynamic Radiator . . . . .	131
<b>Photovoltaic Power Module . . . . .</b>	<b>132</b>
Plasma Testing Performed on Solar Array and Structure . . . . .	132
Nickel/Hydrogen Cells Tested . . . . .	132
<b>Electrical Systems . . . . .</b>	<b>133</b>
Power System Monitor Design and Implementation Completed . . . . .	133
Development of High-Voltage, Direct-Current Spacecraft Fuse Completed . . . . .	135
Electric Power System Diagnostic Program Tested . . . . .	135
<b>Engineering and Computational Support . . . . .</b>	<b>136</b>
<b>Electronic and Control Systems . . . . .</b>	<b>136</b>
Video Signal Analyzer Provides Trigger Pulse Based on Sensing Motion in Image . . . . .	136
<b>Structural Systems . . . . .</b>	<b>137</b>
Test Verification of Spacecraft Dynamic Models Applied to ACTS . . . . .	137
Space Station <i>Freedom</i> Photovoltaic Array Feathering Reduces Loads . . . . .	138
VAPEPS Predicts Acoustic Environment for ELV Payloads . . . . .	139
Advanced Propfan Technology Works for Cruise Missiles . . . . .	140
Penetrable Linear-Gap Pressure Seal Designed . . . . .	141
<b>Computational Support . . . . .</b>	<b>142</b>
Distributed Resource Computing Speeds Information Delivery . . . . .	142
Multigrid Biharmonic Solver on a Parallel Computer . . . . .	143
High-Speed Fiber Networks Arrive at NASA Lewis . . . . .	143
ISDN at NASA Lewis Explored . . . . .	144
Aerospace Analysis Center Opens . . . . .	146

<b>Lewis Research Academy</b> .....	148
<b><i>Internal Fluid Mechanics</i></b> .....	148
Boundary Layer Transition Explained Further .....	148
Insight Gained on Three-Dimensional Boundary Layer Separation .....	149
Turbomachinery Flow Modeling Continues .....	149
Characterization of Turbulence Shows That Nonlinearity Can Be Negligible .....	150
Nonlinear Dynamics Studied for Mixing and Transition Control .....	150
Modeling of Unsteady Turbulent Flows Aided by Rapid-Distortion Theory .....	151
<b><i>Materials</i></b> .....	152
New Method Calculates Material Properties .....	152
Radiation Heat Transfer Characteristics Obtained in Semitransparent Materials .....	153
<b>Author Index</b> .....	155

# Aeronautics

## Aeropropulsion Analysis

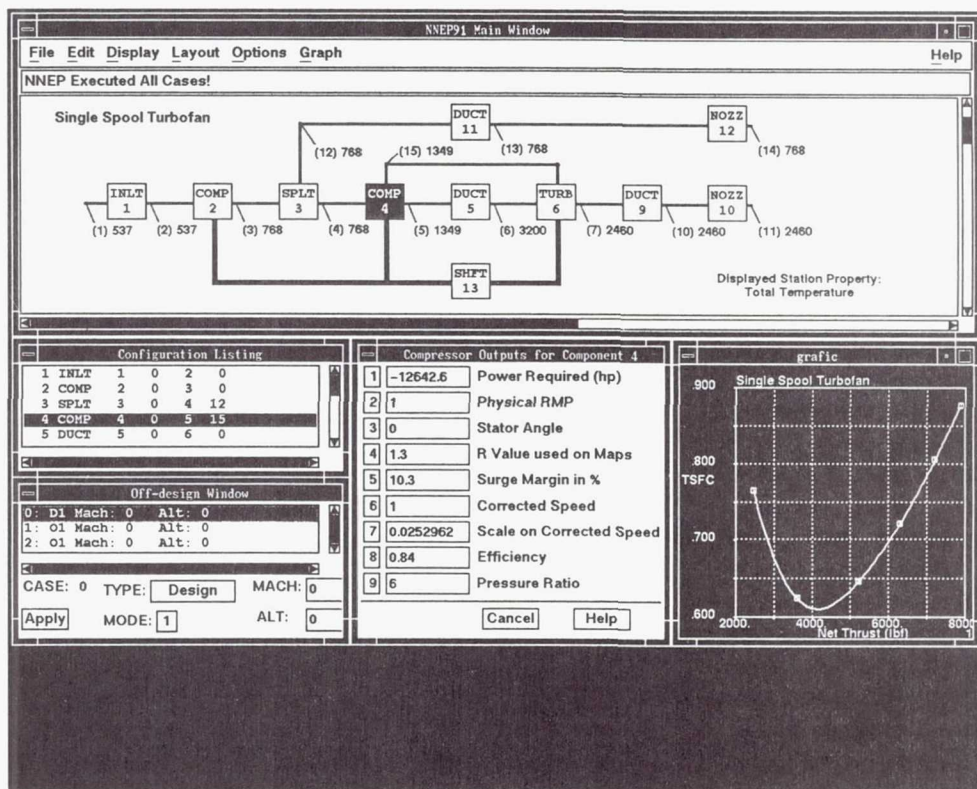
### Graphical User Interface Speeds Engine Cycle Analysis

With recent gains in computer technology it is now possible to move complex engineering analysis away from mainframe computers to a distributed computing environment. This environment consists mostly of high-performance Unix workstations. These high-speed computers allow engineering design and analysis programs, once written for batch processing, to be used in a highly interactive fashion. Research at NASA Lewis has been directed toward improving the human/computer interface to help engineers become more productive in this new computing environment.

NASA's thermodynamic engine cycle simulation program (NNEP) has been reprogrammed to use a graphical user interface. This interface allows the engineer to configure an engine cycle and deter-

mine its performance in a fraction of the previously required time. The engineer can now lay out an engine configuration schematically on the computer screen by using a mouse. Numerical inputs are entered by using forms. A form consists of a set of numeric input fields, each with its own descriptive label and a help button. The help button calls up a detailed explanation of the input and, if applicable, a list of possible choices. Each numeric input field is tied to a scientific calculator program with a variable naming capability. This allows complex functions to be used in place of simple numerical values. Output data can be displayed in numerous ways, including graphically, in forms similar to the input forms, tabular, and/or directly on the schematic—whichever is the most convenient for the engineer. The execution of the program is controlled through a pulldown menu system. Additionally, the user interface has a built-in help system and complete on-line documentation for the engine cycle simulation program.

Perhaps the most beneficial aspect of the NNEP graphical user interface is its high degree of interactivity. A change in any input parameter is immediately reflected as a change in output. This



NNEP graphical user interface.



fast turnaround allows the engineer to more quickly narrow down the design space of the engine configuration. This is very important in the conceptual design process because of the large latitude the engineer has in varying the design parameter. Numerical optimization can be used to refine a small set of design parameters after the engineer has finalized an engine configuration.

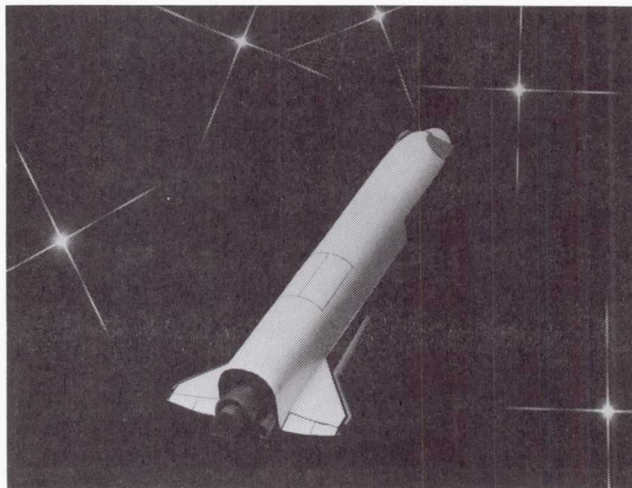
**Lewis contact:** Brian P. Curlett, (216) 977-7041  
**Headquarters program office:** OAST

### **Beta II Shows Promise for Reduced Cost and Assured Manned Access to Space**

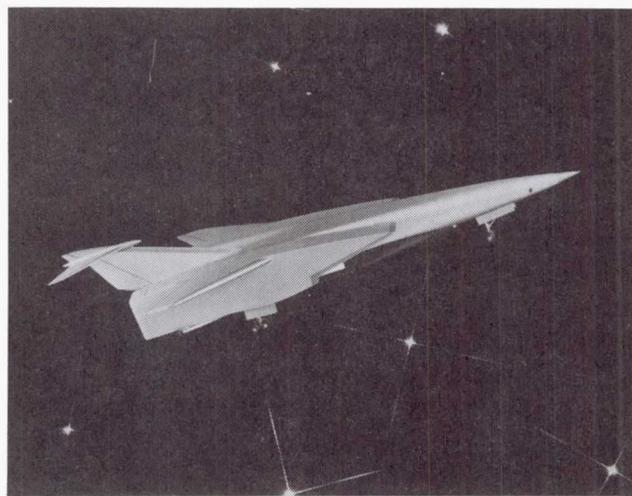
Initial Space Station *Freedom* operations will magnify the need for low-cost, rapid manned access to space. It is generally agreed that vehicles capable of horizontal takeoff and landing (HTOL) and airplane-like operations would be very attractive for this mission. Current studies have been concentrating on single-stage-to-orbit (SSTO) designs. However, SSTO launch vehicles require very advanced materials, structures, and propulsion technologies to achieve the mission, making it difficult to develop an SSTO vehicle in the timeframe required by the Space Station. A study was performed to determine if a nearer term vehicle that could meet the same mission requirements is feasible.

In order to meet the near-term requirement the study ground rules required a two-stage system with the second stage being rocket powered. It was also desired that the first stage be powered by airbreathing engines. The vehicle was to be manned and fully recoverable and was to take off and land horizontally. Staging Mach number was to be as high as possible to reduce gross takeoff weight but limited to avoid active airframe cooling and very advanced airbreathing propulsion systems.

A Government-industry team including NASA Lewis, the Air Force's Wright Laboratory, and Boeing Defense and Space Group was formed to perform the study. The Air Force had previously defined a conceptual HTOL two-stage-to-orbit vehicle known as Beta that has many of the attributes we are looking for. It is fully recoverable and consists of a combination rocket/



*Beta orbiter.*



*Beta booster.*

airbreathing-powered first stage and a rocket-powered second stage. It uses near-term materials, Space Shuttle main engine rockets, and Advanced Tactical Fighter-derived turbojets. It also includes two novel and very practical features. The orbiter is bottom mounted, embedded in a cavity in the booster in a fashion that allows the orbiter to simply be rolled under the booster for stage mating. This, in combination with horizontal takeoff and landing, greatly reduces ground handling and launch facility requirements. Second, although the booster is basically hydrogen fueled, the turbojets are fueled with standard jet propulsion fuel (similar to kerosene) to allow the booster to ferry the orbiter between bases without requiring hydrogen to be available along the route.

Beta has a much larger payload than the current study requires. It can launch 50,000 lb to low polar orbit, whereas the payload for the current study is 10,000 lb to low polar orbit. Although Beta uses a turboramjet airbreathing propulsion system for the first stage, it relies heavily on rocket propulsion to reach ramjet operating speed. The turbojets provide only a small portion of the required thrust. The orbiter is an advanced lifting-body design.

The current study consisted of redesigning the vehicle to accommodate a downsized payload of 10,000 lb, removing the first-stage rocket, increasing turbojet thrust by replacing the ATF turbojets with larger High Speed Civil Transport-derived engines, reducing the staging Mach number from 8 to a more conservative 6.5, and designing a more conservative wing-body Shuttle-like orbiter.

The resulting vehicle, known as Beta II, is a manned, fully recoverable HTOL launch vehicle with a fully airbreathing first stage and a Shuttle-like rocket second stage. It has gross takeoff weight of about 1 million lb, similar to advanced versions of the 747. It is a robust design that meets the near-term technology requirements of the study. It has the potential for low-cost, all-weather, airplane-like operations with simple stage-mating procedures. Beta II is a versatile multimission vehicle that is capable of launching 10,000 lb to low polar orbit, 10 men plus 10,000 lb to the Space Station, or 30,000 lb to the Space Station with an expendable second stage and is capable of performing as a hypersonic research vehicle.

#### Bibliography

Plencner, R.M.: Overview of the Beta II Two-Stage-to-Orbit Vehicle Design. AIAA Paper 91-3175, Sept. 1991.

**Lewis contact:** Leo A. Burkardt, (216) 977-7021  
**Headquarters program office:** OAST

## Instrumentation and Control Technology

### *R&D 100 Award*

#### **High-Temperature Resistance Static Strain Gage Developed**

A resistance strain gage that can provide accurate static strain measurements at high temperatures is urgently needed in the development of hypersonic aerospace vehicles and advanced gas turbine engines. The requirement for good accuracy in the whole operating temperature range up to very high temperatures exceeds the present capability of resistance static strain gages, which has generally been limited to 400 °C.

A temperature-compensated wire resistance strain gage that can provide static strain measurements from ambient temperature to at least 800 °C has been developed at NASA Lewis. This compensated wire gage has dual elements: the gage element is made with 25- $\mu$ m-diameter palladium chromium (PdCr) wire, and the compensator element is made with 25- $\mu$ m-diameter platinum (Pt) wire. The Pt compensator is located around the periphery of the PdCr gage grid to minimize the temperature gradient effect. The temperature compensation is achieved by connecting the Pt resistor to the adjacent arm of a Wheatstone bridge circuit to cancel the thermally induced resistance change that occurs in PdCr. This technique provides the unique ability to compensate for temperature effects on materials with a wide range of thermal expansion coefficients by varying the parameters of a simple external circuit.

The gage can be mounted to the test articles with either high-temperature ceramic cements or flame-sprayed powders. A mixture of alumina and 4- to 6-wt % zirconia is applied to the gage as the protective overcoat. The cemented gage can be used to approximately 600 °C. At the higher temperatures the porous cement is insufficient to prevent the gage system from oxidizing and shorting to ground. The flame-sprayed gage works reasonably well to 800 °C, because flame spraying usually produces a denser film.

This compensated wire gage has been tested on Hastelloy-X, Inconel 718, and IN100 substrates. The strain sensitivity of this compensated wire

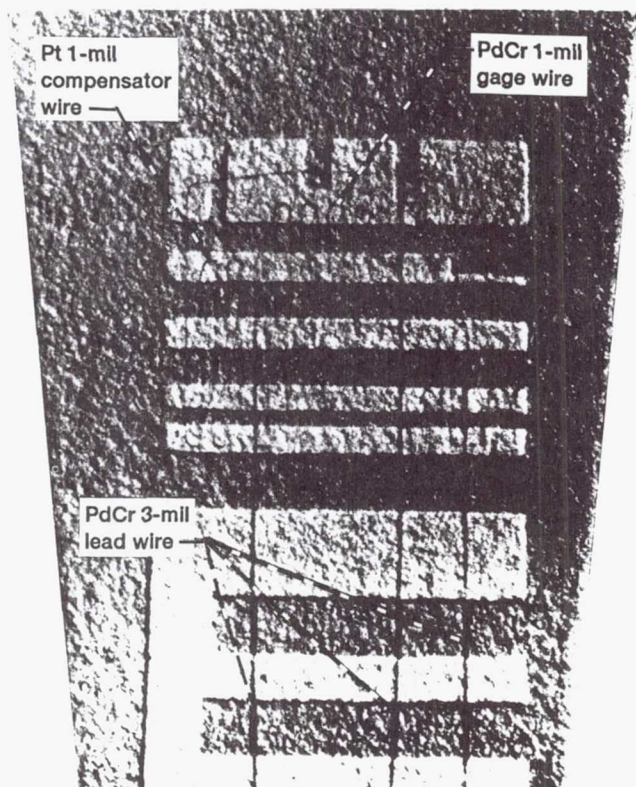


gage is approximately 1.3 at room temperature. The gage responds linearly to the imposed strain to at least  $\pm 2000$  microstrain. Furthermore, its strain sensitivity does not vary much with temperature. The changes in apparent strain of a prestabilized gage on three different substrate materials were all within 750 microstrain with a reproducibility within 100 microstrain between thermal cycles to 800 °C. The apparent strain of the gage can therefore be corrected to 800 °C because of its repeatability and small value. This is a significant advance over the 400 °C barrier of previous techniques for resistance static strain gages.

#### Bibliography

Lei, J.-F.: Case Study: Palladium-Chromium Strain Gages for High Temperatures, *Materials & Design*, vol. 12, no. 4, Aug. 1991.

**Lewis contact: Dr. Jih-Fen Lei, (216) 433-3922**  
**Headquarters program office: OAST**



*PdCr temperature-compensated strain gage.*

#### Thin-Film Thermocouples Measure Ceramic Surface Temperatures to 1500 °C

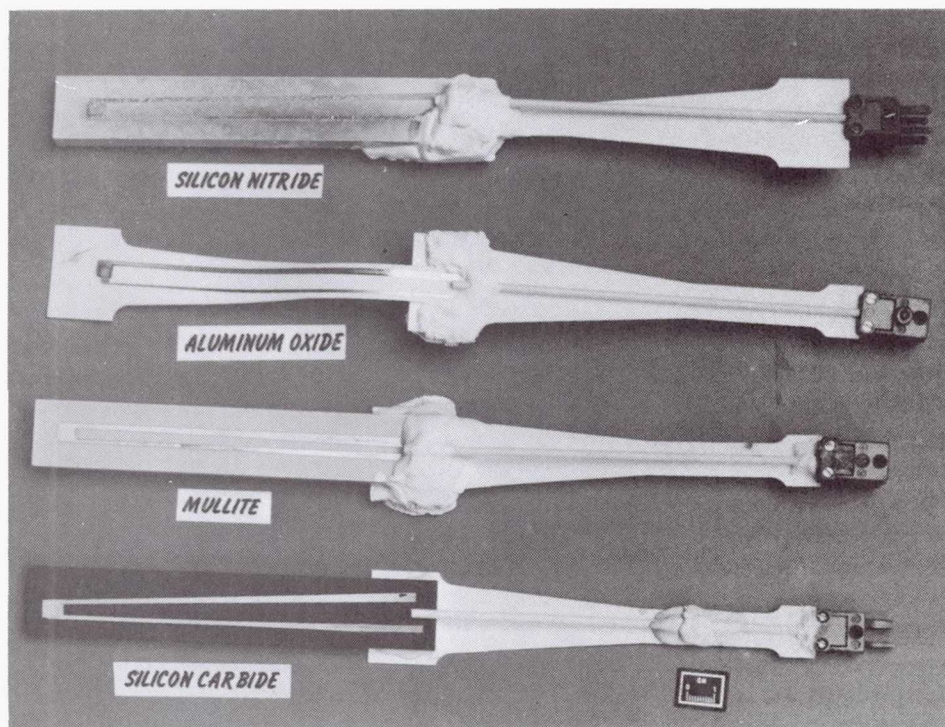
Minimally intrusive measurements are needed for measuring surface temperatures on ceramic materials for advanced propulsion systems. Thin-film thermocouples have been developed for use on metal parts in jet engines to 1000 °C. Advanced propulsion systems are being developed that will use ceramic materials and have the capability of attaining higher temperatures in their operation. Therefore, NASA Lewis is developing thin-film thermocouples for use on ceramic materials to 1500 °C. Thin-film thermocouples of platinum-13 percent rhodium/platinum were fabricated by the sputtering process with lead wires attached by the parallel-gap welding process. The ceramic materials of interest were silicon nitride, silicon carbide, aluminum oxide, and mullite.

Steady-state and thermal cycling tests were performed in a laboratory tube furnace up to 1500 °C. Thermocouples, about 5  $\mu\text{m}$  thick, were deposited on the ceramic materials, which were 15 cm long and were attached to mounting plates for insertion into the furnace hot zone.

Drift rates were determined for the thin-film thermocouples in steady-state tests. Drift rates were low on all ceramic materials in the temperature range 1000 to 1200 °C and increased gradually to 2 deg C/hr at 1500 °C. The drift rate is primarily caused by interdiffusion of sensor and substrate material as a function of temperature and time. Sensor life is primarily associated with the stability of the ceramic materials. Up to 1250 °C all ceramic materials were very stable. Above this temperature the silicon carbide substrate was transformed to a glassy appearance and silicon nitride oxidized, leading to sensor failure. Sensors on aluminum oxide and mullite were tested to 1500 °C and met life goals of more than 50 hr with small bubbling of the sensor, probably caused by the volatility of the substrate material at these temperatures. Complete details of test results are given in reference 1.

Sensors were also tested at high heating rates in an arc-lamp heat flux calibration facility. Thin-film thermocouples on silicon nitride and mullite were subjected to heat flux levels in the range 0.1 to 2.5 MW/m<sup>2</sup> and heating rates in the range 10





Thin-film thermocouples.

to 700 deg C/sec. The thin-film sensors on the silicon nitride substrate survived these test conditions with little or no degradation to 1450 °C.

#### Reference

1. Holanda, R., et al.: Development of Thin-film Temperature Sensors for Surface Temperature Measurement on High-Temperature Engine Materials. *HITEMP Review 1990*, NASA CP-10051, 1990, pp. 71-1 to 71-9.

**Lewis contact: Raymond Holanda, (216) 433-3738**  
**Headquarters program office: OAST**

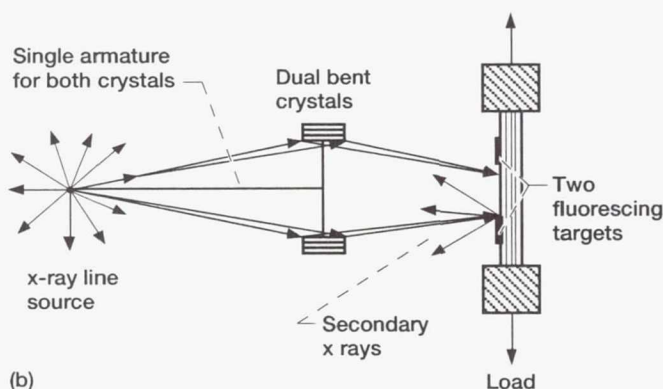
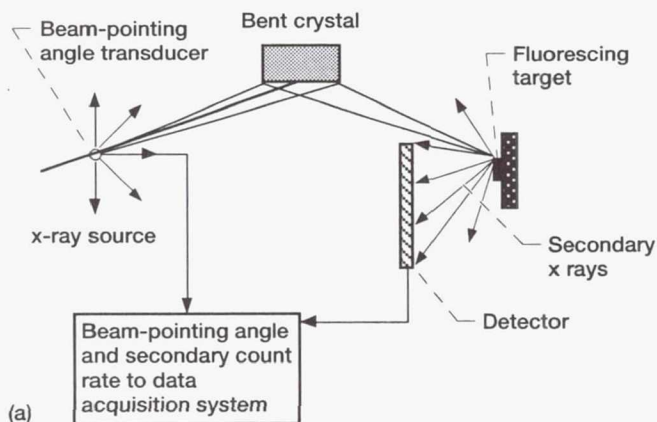
#### X-Ray-Based Extensometry Eases Displacement Measurements in Hostile Environments

Better engineering components for hostile environments are needed for continued increases in the efficiency of fuel-burning engines. They are a prerequisite for successful development of the more ambitious hypersonic flight vehicles, such as the National Aerospace Plane (NASP). A fundamental requirement of these and other advanced programs is the ability to measure the mechani-

cal response of newly available materials under realistic operating conditions. These conditions may include high-temperature, high-velocity gas flows, significant pressure gradients, or the presence of flames and smoke.

The measurement of strain and displacement under such conditions is challenging. Only a limited number of methods are available. These include high-temperature strain gages, ceramic rod extensometers, and laser optical systems. They all have limitations. Strain gages seem to be limited to temperatures below 1000 °C and strains of only a few thousand microstrain. Contacting extensometers present access problems in some cases and cannot be used in the presence of high-velocity gas flows. Laser-based optical methods appear to be the least restrictive, but hot gases above ambient pressure are a severe problem because they refract the source laser beam. In addition, smoke and dust greatly degrade the accuracy of such systems.

A completely new method of noncontacting, high-temperature extensometry based on the focus and scanning of x rays is currently under development. It shows great promise of overcoming



X-ray-based displacement measurement systems: (a) with one fluorescing target; (b) with two fluorescing targets.

many of the limitations associated with available techniques. The system is based on the ability to focus and scan low-energy, hard x rays such as those emanating from copper or molybdenum sources. The x rays are focused into a narrow and intense line image that can be scanned onto targets which fluoresce secondary x-ray radiation. This radiation is monitored, and target edge position can be determined by measuring the beam pointing angle when the marker begins to fluoresce. The main advantage of the technique lies in the penetrating nature of x rays, which are not affected by the presence of refracting gas layers, smoke, flame, or intense thermal radiation, all of which render conventional extensometry methods inoperative or greatly compromise their performance.

Current work has been limited to displacement measurement of a single target with a resolution of  $1.1 \mu\text{m}$  at target temperatures of  $1200^\circ\text{C}$ , directly through an open flame. The final goal of the system is to be able to conduct macroscopic strain measurements in hostile environments by utilizing two or more fluorescing targets.

## Bibliography

Jordan, E.H., et al: High Temperature Displacement Measurement Using a Scanning Focused X-Ray Line Source. *Advances in X-Ray Analysis*, Pergamon Press, New York, 1991.

Lewis contact: Gustave C. Fralick, (216) 433-3645  
Headquarters program office: OAST

## Nonintrusive Laser-Based Measurements Support Hypersonic Propulsion System Experiments

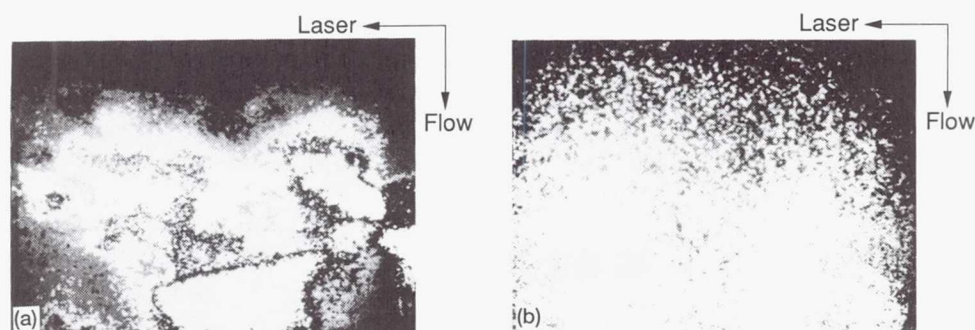
Gas path measurements in hypersonic (greater than Mach 6) propulsion system research present some demanding measurement system design problems. Requirements for nonintrusive measurement, high-temperature operation, and high temporal and spatial resolution are typical.

Hypersonic flow diagnostic instrumentation must be nonintrusive so that it does not affect the flow in unpredictable ways either upstream or downstream. Intrusive probes usually cannot survive in the typical hypersonic engine environment, where flow velocities may be as high as  $2100 \text{ m/sec}$  and temperatures may range from cryogenic ( $\sim 170 \text{ K}$ ) to  $\sim 2800 \text{ K}$ . Hypersonic flow diagnostics must have high temporal (1 to 10 nsec) and spatial (0.1 to 1.0 mm) resolution to resolve flow features, such as eddies and swirls, that tend to be small and short lived.

Computer models are used to simulate hypersonic propulsion system fluid dynamics. These simulation codes must be validated so that the user has confidence in the simulation over the whole flow field and for all flow regimes. Therefore, validation experiments must yield two- and even three-dimensional results. Test times as short as  $300 \mu\text{sec}$  leave no time for scanning and make necessary simultaneous measurement at many points.

NASA Lewis has developed a multipoint, multiparameter (MPMP) measurement system for hypersonic flow diagnostics in the National Aerospace Plane Program. The system includes two lasers, two cameras, and a dual data acquisition system for doing planar laser-induced-fluorescence measurements and a Raman scattering sub-





Planar laser-induced-fluorescence measurements of OH concentration in scramjet combustors: (a) short combustor; (b) long combustor (showing more uniform fuel mixing).

system for measuring the concentration of major species at a point. The two lasers and several detectors allow the system to be used in several different configurations.

Two lasers and two cameras can be used to simultaneously measure two different species (e.g., OH and NO). Each laser beam is formed into a sheet at a wavelength appropriate for one species. The laser sheets are aimed to cut through the flow, and the cameras are aligned with their optical axes perpendicular to the laser sheet planes. Camera 1 is triggered when laser 1 fires, and camera 2 is triggered when laser 2 fires. Camera images are stored as arrays of numbers (pixels); each number corresponds to the fluorescence intensity at a particular location in the laser sheet. With background subtracted and other corrections made, the pixel values are directly proportional to the species number density.

Flow temperature is measured by setting each laser to a different absorption wavelength in the same species (e.g., OH). The images from the cameras are combined by dividing one by the other. Because the fluorescence intensity ratio at two appropriately selected wavelengths will vary with temperature, the combined image yields a temperature map.

In using the Raman subsystem, one laser is focused to a point in the flow that is observed through a spectrometer with a charge-coupled-device detector array. Analyzing the system output can yield simultaneously the concentrations at the detection points of major species ( $H_2$ ,  $H_2O$ ,  $N_2$ , and  $O_2$ ). In this case the second laser and one of the cameras may be used to make planar laser-induced-fluorescence measurements at the same time as the Raman measurements.

The MPMP system can take data at 1 frame/sec or may be triggered to take just one frame. It is being used to support NASP hypersonic propulsion system test programs.

**Lewis contact:** Robert C. Anderson, (216) 433-3643  
**Headquarters program office:** OAST

### Alignment of Optical Measurement Systems Automated

Optical methods are valuable for making nonintrusive measurements of the properties of aerospace flows and structures. They are used for inspection, testing, monitoring, and model verification. One defect of optical measurement systems is the need for skilled human operators to do alignment and operations. Aerospace measurement environments are often too remote, harsh, or dangerous for human operators; hence, it is important to learn to automate optical alignment.

Neural networks were tested for their ability to learn optical alignment procedures. An artificial neural network is an array of nonlinear processors called nodes or neurons that are interconnected with weighted connections called synapses. Neural networks can learn to map or transform patterns of sensor information at their inputs into patterns of alignment control information at their outputs. In principle, a neural network can learn by example to perform an optical alignment function, just like a human operator. The examples are called a training set.



Commercial neural-network packages were used to learn and direct the alignment of a spatial filter. Spatial filters are used to remove pattern noise from laser beams or for optical signal isolation. Spatial filters are simple yet require a sensitive, pattern-based alignment procedure; their alignment is a good test. The alignment procedure was encoded in training sets generated from actual alignments by a technician. The training set design was a special case of a more general alignment paradigm that should be useful for alignment and operations in general. An input pattern consisted of the control action at the previous alignment step, the XY position of the beam bright spot, the beam pattern class, and the logarithm of average beam intensity. The output control pattern consisted of the control action, the new XY position of the beam, and an estimate of the new logarithm of intensity.

The tests of neural-network-directed alignment of the spatial filter were successful, indicating that artificial neural networks can learn to perform pattern-based optical alignment. Neural networks should be a good step toward automating the alignment of optical measurement systems for aerospace applications.

## Bibliography

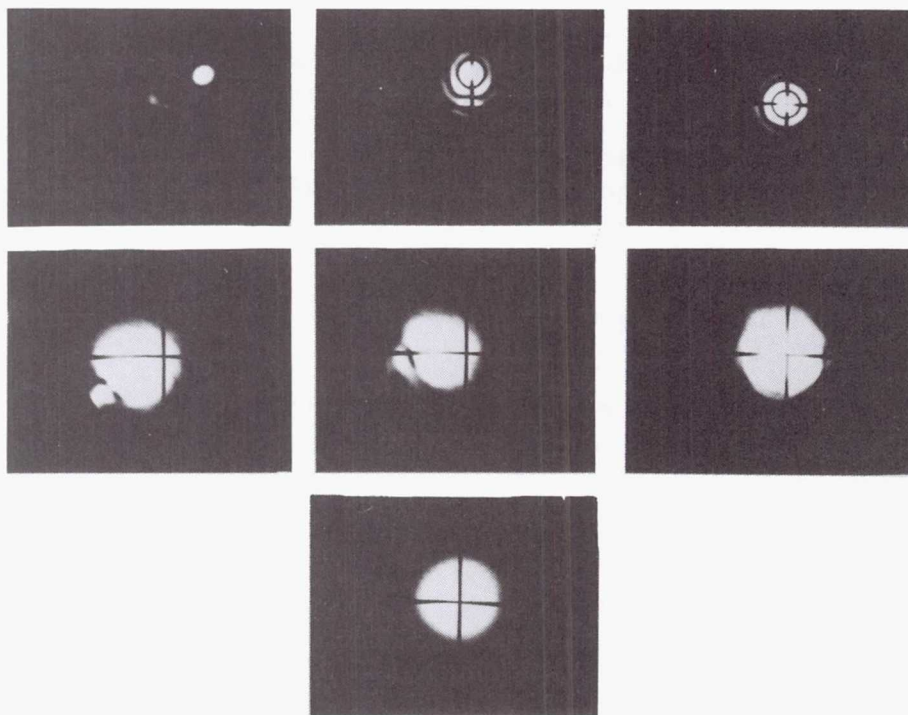
Decker, A.J.; and Krasowski, M.J.: Neural Nets for Aligning Optical Components in Harsh Environments—Beam Smoothing Spatial Filter as an Example. *Structural Integrity and Durability of Reusable Space Propulsion Systems*, NASA CP-10064, 1991, pp. 29-38.

Decker, A.J.: Self-Aligning Optical Measurement Systems. Submitted to *Applied Optics*, 1991.

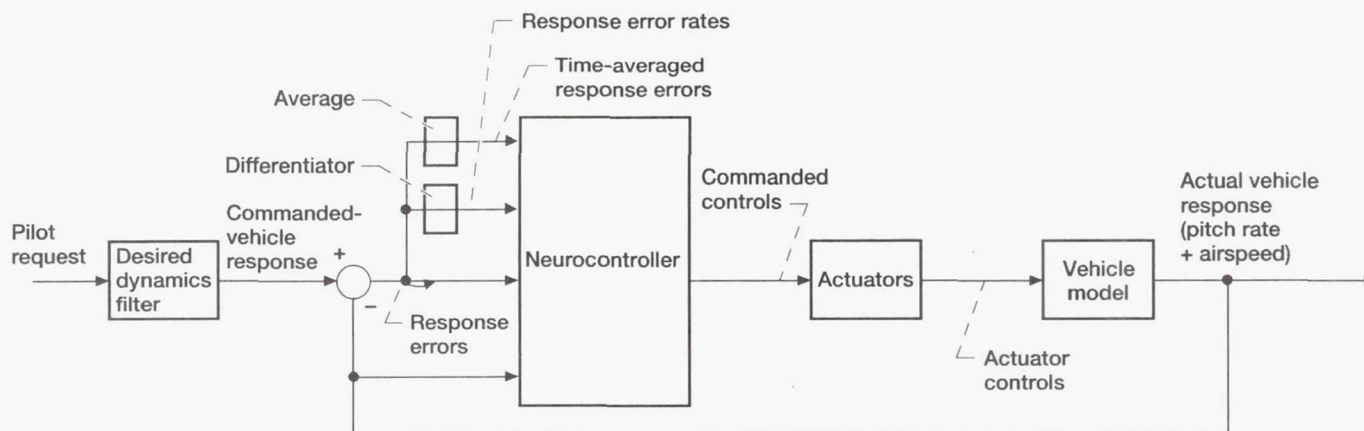
**Lewis contact: Dr. Arthur J. Decker, (216) 433-3639**  
**Headquarters program office: OAST**

## Neural-Network-Based Control Designed

The past few years have seen an increasing interest by the control community in exploiting the promise of artificial neural networks to solve difficult control problems. NASA Lewis has investigated the feasibility of using artificial neural networks as control systems for modern, complex aerospace vehicles. An example study considered the problem of designing an integrated airframe/propulsion controller for a longitudinal dynamics model of a modern fighter aircraft. The object



Beam patterns during neural-network-directed alignment of spatial filter:  
 bottom pattern is aligned state.



Evaluation architecture of closed-loop neurocontroller.

was to independently control pitch rate and airspeed responses to pilot commands.

By using the model of the desired dynamics as a command generator, a multilayer feedforward neural network has been trained to control the vehicle model within the physical limitations of the actuator dynamics. This was achieved by backpropagating through the neural network an objective function that is a weighted sum of tracking errors, control input commands, and control input rates.

The information passed to the input layer of the neurocontroller consists of controlled outputs, errors, error rates, and time-averaged error rates in both pitch rate and velocity responses. After neural information processing through two hidden layers, the neurons of the output layer provide the normalized values of the engine fuel flow rate and the nozzle thrust vectoring angle. These two commanded controls are then applied to the position- and rate-limited actuators that will provide the desired pitch rate and velocity responses. A satisfactory tradeoff between tracking performance and control effort has been achieved by an appropriate selection of the weights of the objective function.

The neurocontroller shows better performance than a baseline controller designed for the same command tracking problem. Yet it is less robust to phase variations than the baseline controller. The possibility of enhancing neurocontroller robustness through simulation of modeling uncertainties during training was considered, and a technique for improving the phase stability of the closed-loop system was demonstrated.

Future areas of research would be the synthesis of robust neurocontrollers and the innovation of tools to analyze their robustness.

**Lewis contacts:** Dr. Terry Troudet, (216) 433-8524; Dr. Sanjay Garg, (216) 433-2355; Dr. Walter C. Merrill, (216) 433-6328

**Headquarters program office:** OAST

### Sensor Validated by Autoassociative Neural Networks

In order to ensure reliable operation, a complex dynamic system, such as a spacecraft or an aircraft, may use redundant sensors for measuring critical variables. This redundancy makes it possible to validate measured data, to identify a sensor failure, and to recover the failed measurement. This can be accomplished by using an advanced neural network called an autoassociative neural network.

An autoassociative network is trained to produce an output vector that is equal to its original input vector. The operation of the autoassociative network is based on the principle of dimensionality reduction: The input information is compressed (dimension reduction), and then the output information is regenerated. The redundant sensor information is compressed, mixed, and reorganized in the first part of the network. By compression the sensor information is encoded into a significantly smaller representation. The compressed information is then used to regenerate the original redundant data at the output.



Because of the information mixture, if a sensor fails, other sensor data can still provide enough information to regenerate a good estimate for the faulty measurement. Because of its parallel-processing capability the neural network can process real-time data for time-critical applications. Also, because it learns by example, the neural network does not require a detailed system model for sensor validation, as is often required.

In the network training phase a group of analytically redundant measurements is identified. Correct sensor data as well as simulated failed-sensor data are used as input patterns. The target output is set to the correct sensor data; that is, with or without the sensor failure the network is trained to estimate all the correct sensor outputs by using the given measurement set. During operation, if a sensor signal is significantly different from the corresponding estimated value, the sensor signal is considered incorrect and the sensor is identified as failed. The failed-sensor reading is isolated by feeding the neural network with its previous estimated value. The isolation of a failed sensor enables the neural network to detect subsequent sensor failures.

An autoassociative network has been tested for a group of nine related sensors on the fuel side of a Space Shuttle main engine. This sensor group represents a redundant measurement set. Measurements of the system during engine start were used to train the neural network; then the trained autoassociative neural network was tested for its ability to detect failed sensors and to recover faulty data during the subsequent operation for

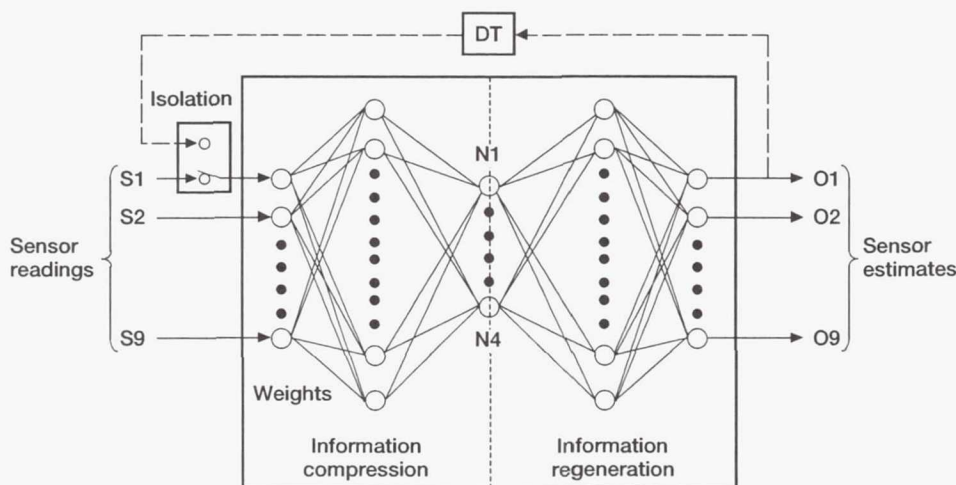
rated power and reduced power throttling. The trained neural network correctly identified five failed sensors and provided accurate estimates for those sensors.

**Lewis contact:** Dr. Ten-Huei Guo, (216) 433-3734  
**Headquarters program office:** OAST

### Design Methodology Developed for Integrated Flight/Propulsion Control Systems

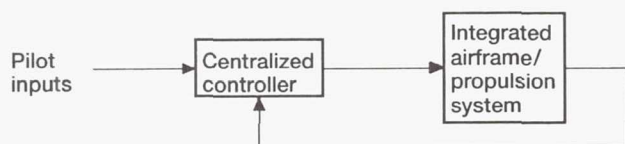
The designs of many future military fighter and tactical aircraft will incorporate enhanced maneuver capabilities, such as short takeoff and vertical landing (STOVL) and high-angle-of-attack performance. Such capabilities are achieved by using the forces and moments generated by the propulsion system to augment those generated by the flight control surfaces. The resulting coupling between the propulsion system and the airframe is significant enough that the traditional approach of designing the propulsion control system and the flight control system separately and then putting them together in an ad-hoc manner is no longer adequate. An integrated approach to flight/propulsion control system design is required to obtain an overall system with optimum performance and minimal pilot workload.

The NASA Lewis Integrated Flight/Propulsion Control (IFPC) Program has completed preliminary conceptual development of an IFPC design

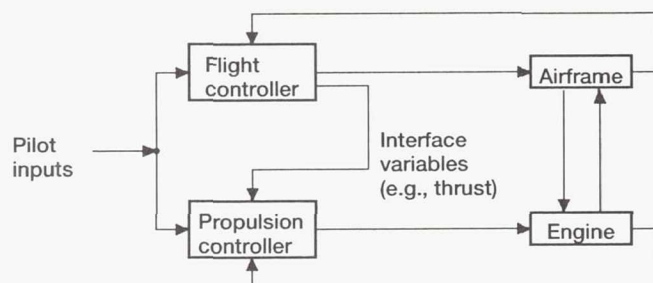


Autoassociative neural network for Space Shuttle main engine sensor validation. Dashed line shows feedback path for isolation when a sensor failure is identified.





Centralized integrated flight propulsion control (IFPC) design.



Decentralized, hierarchical IFPC implementation.

methodology. It has the potential to improve system performance over the existing integrated control design methodologies but with simple control law synthesis and implementation. The detailed aspects of the methodology are currently being developed, and the methodology is being demonstrated by application to a supersonic STOVL fighter aircraft. The NASA Lewis IFPC design methodology is referred to as IMPAC, integrated methodology for propulsion and airframe control.

Under IMPAC a centralized controller is first designed by considering the airframe and propulsion systems as one integrated system. In the second step the complex centralized controller is partitioned into a decentralized, hierarchical design. The partitioned design consists of two or more simpler subcontrollers with intercoupling. The essential design requirements of the partitioned design are (1) that the closed-loop system response with the partitioned subcontrollers closely approximate the closed-loop system behavior with the centralized controller and (2) that the partitioned subcontrollers satisfy the structural constraints from implementation issues. The centralized control design accounts for all the subsystem interactions in the design stage, and the partitioning results in easy-to-implement subcontrollers that allow for independent subsystem validation.

The IMPAC methodology is being applied to IFPC design for the E-7D STOVL aircraft, which is

powered by a high-bypass-ratio turbofan engine and is equipped with ejectors on the wing to provide propulsive lift at low speeds and hover. Preliminary results from applying the IMPAC methodology to the E-7D aircraft are encouraging. Initial fixed-base piloted simulation evaluation of the IMPAC E-7D control design will be done with the NASA Lewis integrated propulsion and flight control simulator.

#### Bibliography

Garg, S.; and Mattern, D.L.: Application of an Integrated Flight/Propulsion Control Design Methodology to a STOVL Aircraft. AIAA Paper 91-2792, Aug. 1991. (Also, NASA TM-105254.)

Garg, S., et al.: IMPAC—An Integrated Methodology for Propulsion and Airframe Control. Presented at the American Control Conference, Boston, MA, June 1991. (Also, NASA TM-103805.)

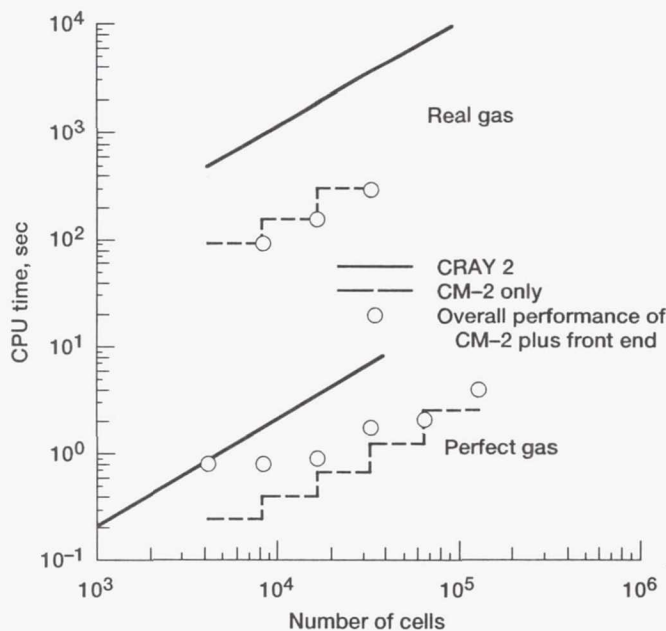
**Lewis contact:** Dr. Sanjay Garg, (216) 433-2355  
**Headquarters program office:** OAST

## Internal Fluid Mechanics

### Parallel Computation Uses Lagrangian Formulation

The future of high-speed aviation programs, such as the National Aerospace Plane (NASP) and High Speed Research (HSR), is heavily dependent on the ability to do accurate, reasonably fast numerical simulations of complex flows. Many simulations currently require impractical amounts of computer time. Parallel computers offer hope of achieving reasonable run times for these simulations. However, new mathematical models that can readily exploit parallel architectures must be devised. A mathematical model of supersonic and hypersonic flow using a Lagrangian formulation has been developed. The inherent parallelism in this model is ideally suited to massively parallel computers, such as the Thinking Machines Corporation CM-2.

One of the critical issues in implementing flow models on parallel computers is the minimization of communication time between processors. The



Computational efficiency of Lagrangian formulation.

Lagrangian formulation computes flow streamlines, with the only communication between streamlines (and processors) being pressure. This compares to Eulerian formulations, in which mass, momentum, and total enthalpy must be transferred between processors. The Lagrangian approach also results in a more accurate resolution of shocks than its Eulerian counterpart.

The suitability of the Lagrangian formulation for parallel computation was demonstrated by implementing it on the CM-2. Results show that the scheme is both accurate and efficient. Both perfect-gas and real-gas effects were modeled. The CM-2 results were obtained faster, in both cases, than they were on a traditional supercomputer, the Cray 2. Performance improved as the number of computational "cells" increased. In some cases the CM-2 implementation was up to six times faster than on the Cray. Future work will include investigating the performance of this algorithm on other parallel computers.

#### Bibliography

Liou, M.F.; and Loh, C.Y.: Parallel Computing Using a Lagrangian Formulation. NASA TM-104446, 1991.

**Lewis contact:** May-Fun Liou, (216) 433-3600  
**Headquarters program office:** OAST

#### Progress Made Toward Developing Parallel Turbomachinery Code

TURBO is a computer code that is used to simulate the flows through multistage turbomachinery. TURBO was developed at Mississippi State University and is expected to play a key role in the development of propulsion system models for NASA Lewis' Numerical Propulsion System Simulator (NPSS). TURBO is a computationally intensive code, requiring hours of Cray time. This becomes especially significant when it is combined with simulations of other propulsion system components, such as inlets and combustors. The time it takes to run the TURBO code can potentially be reduced by using parallel computers. A version of TURBO that can run on parallel computers is being developed under a grant to Mississippi State University. This work is being supported as part of the Federal High Performance Computing and Communication Program (HPCCP).

The original TURBO code uses an implicit lower-upper factorization algorithm to solve the Euler equations. Grid blocking is used to simplify the representation of complex geometries and to allow large problems to be run efficiently in main memory. The parallel version of TURBO takes advantage of the blocked-grid structure by mapping blocks to individual processors on a parallel computer. The original implicit coupling between blocks in the original algorithm is relaxed to allow parallel computation of the individual blocks. The major issue is how this decoupling affects the accuracy and convergence of the parallel code.

A parallel version of TURBO is currently running on several parallel computing systems. These include networked workstations, an SGI power Iris, and an Intel iPSC/860. A portable, parallel programming environment called object-oriented Fortran was used to facilitate porting between parallel machines. Performance statistics for several cases are given in the table. Statistics are shown for both single-processor and five-processor cases. Note that in the five-processor Sparcstation 2 case about 14 percent of the performance of a single-processor Cray Y/MP is obtained. An error analysis was done to compare the decoupled parallel code with the serial code. The worst-case error was found to be  $\pm 3$  percent for the test cases run. No test cases were run where shocks were present. It is anticipated that the accuracy will be reduced in these cases.



PERFORMANCE OF TURBO CODE ON VARIOUS  
PARALLEL COMPUTING SYSTEMS

System	Sustained megaflops
1 SGI personal Iris	1.9
SGI power Iris (1 processor)	3.5
Intel iPSC/860 (1 node)	4.0
1 Sparcstation 2	4.7
5 SGI personal Irises	11.1
Intel iPSC/860 (5 nodes)	18.0
SGI power Iris (5 processors)	18.8
5 Sparcstation 2's	23.5
Cray Y/MP (1 processor)	172.0

Plans include investigating algorithm modifications to improve the accuracy of the parallel code, as well as adding additional blocking so that large numbers of processors can be used. Modeling viscous effects will be added. The code will also be ported to other parallel machines, such as the Intel Delta machine and the NCUBE-2.

#### Bibliography

Henley, G.J.; and Janus, J.M.: Parallelization and Convergence of a 3-D, Implicit, Unsteady, Turbomachinery Flow Code. Fifth SIAM Conference on Parallel Processing for Scientific Computing, March 1991.

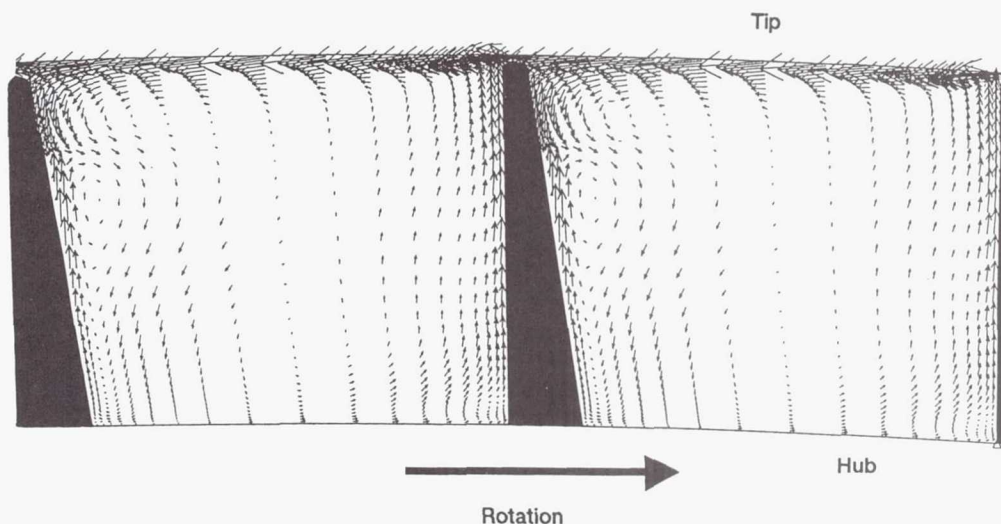
**Lewis contact: Richard A. Blech, (216) 433-3657**  
**Headquarters program office: OAST**

### Centrifugal Compressor Flow Physics Studied

Centrifugal compressors are used in relatively small propulsion systems for vehicles such as helicopters and small business jets. These compressors are attractive in small engines because of their potential for high performance, greater reliability, and lower initial cost than small axial compressors. However, centrifugal compressors generally have lower efficiency than axial compressors. Research is currently under way that is aimed at improving the efficiency levels of centrifugal compressors.

The flow field within centrifugal compressors is extremely complex and includes flow features such as thick blade surface, hub, and casing boundary layers, strong secondary and tip leakage flows, shock waves in the inducer region of high-speed compressors, and strong unsteady flow interactions between the rotating impeller blades and the stationary diffuser vanes. These flow features currently limit the efficiency of centrifugal compressors. Successful management of these features is the key to improved centrifugal compressor performance.

Centrifugal compressor flow fields are being studied at NASA Lewis through a tightly coupled experimental and numerical research analysis program in order to develop insight that can be used to improve the design of new centrifugal compressors. Experiments are being performed in small, high-speed compressors and in a large,



Numerical prediction of flow field near exit of large, low-speed centrifugal compressor as viewed looking downstream.



low-speed compressor. Numerical analysis tools that solve the full three-dimensional, viscous Navier-Stokes equations are also being used to predict the measured flow fields. These predictions are being used to guide the experimental measurements. The measurements are then compared with the numerical results, and the differences between the two are used to develop improved models for those flow features that are not accurately modeled by the numerical analysis codes. These improved codes can then be used to guide the design of new compressor hardware.

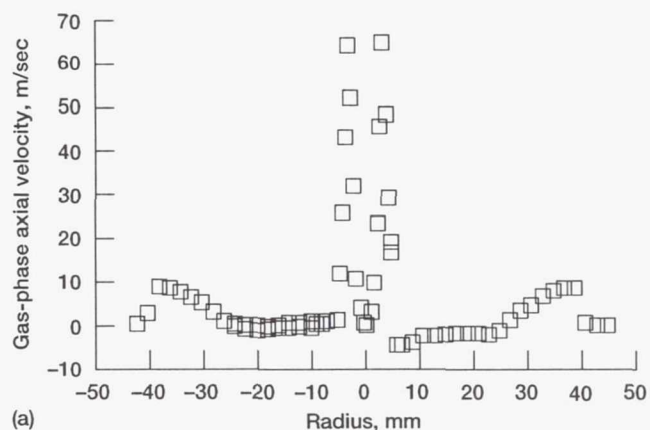
Laser-based instrumentation is currently being used to study the three-dimensional flow field in the large, low-speed centrifugal compressor. The inlet diameter of the impeller is about 3 ft and the exit diameter is 5 ft. The rotor blade height varies from about 9 in. at the inlet to about 6 in. at the exit. This large size allows detailed measurements of all three velocity components within the blade passage. Viscous flow effects, which are confined to thin regions near the blade surfaces, have also been successfully measured for the first time in this unique facility. Preliminary comparison of the measured and numerically predicted flow fields indicates that the numerical predictions of the complex flows within the blade passage are quite accurate. Experimental research in the large, low-speed compressor will continue until December 1991. Laser-based measurements in a small, high-speed centrifugal compressor will begin in October 1991.

**Lewis contact:** Dr. Michael Hathaway, (216) 433-6250  
**Headquarters program office:** OAST

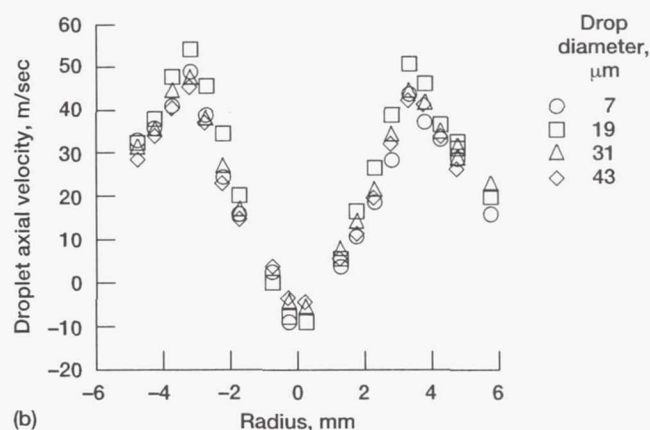
### Progress Made Toward Evaluating Multiphase-Flow Computer Codes

In order to demonstrate greater fuel efficiency and higher thrust-to-weight ratios, future engines will be required to operate at higher pressure ratios than current engines. As a result the injection of liquid fuel into a very dense environment and its subsequent combustion will be a key technology. Computer codes that can accurately simulate this process will be important design tools.

As a step toward validating multiphase computer models, NASA Lewis has begun a study of an



(a)



(b)

*Experimental measurements of mean axial velocity of gas phase and droplets in swirl-stabilized, combustng spray, 2.5 mm downstream of spray nozzle.*

unconfined, swirl-stabilized combustng spray. Nonintrusive measurements of droplet size and velocity as well as gas-phase velocity are being obtained for liquid fuel sprayed from an air-assist nozzle. The fuel currently used for the experiments is n-heptane. The figure presents data obtained 2.5 mm downstream of the spray nozzle. Radial profiles of gas-phase mean axial velocity and axial velocities for 7-, 19-, 31-, and 43- $\mu$ m-diameter droplets are presented. The measurements obtained include all three mean and fluctuating components of velocity for both phases. The complete set of measurements will be used to evaluate current multiphase-flow computer models and to identify areas for improvement. Comparison of the data with a current multiphase-flow code is being performed under grant by The University of Illinois at Chicago.

## Bibliography

Bulzan, D.L., et al.: Measurements and Predictions of a Liquid Spray From an Air-Assist Nozzle. AIAA Paper 91-0962, Jan. 1991. (Also, NASA TM-103640.)

**Lewis contact:** Dr. Daniel L. Bulzan, (216) 433-5848  
**Headquarters program office:** OAST

## Hot-Gas Ingestion Calculated for STOVL Aircraft Model

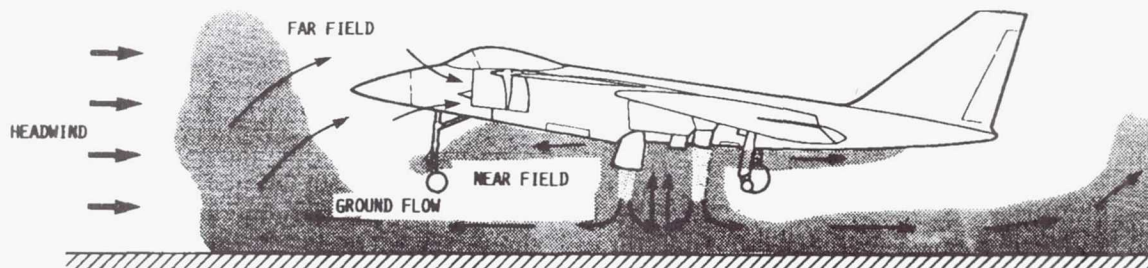
Hot-gas ingestion can cause significant problems for short-takeoff, vertical-landing (STOVL) aircraft, such as reduced thrust and compressor stalls. These problems involve many hazards for the pilots, including very hard landings. During the design of a STOVL aircraft hot-gas ingestion problems are typically approached with empirical methods and experience. Given the power of today's supercomputers and workstations, numerical methods employing efficient algorithms are becoming a viable engineering tool for analysis and design. Previous work at NASA Lewis proved the feasibility of computational fluid dynamics (CFD) analysis for hot-gas ingestion. A follow-on effort is exploring the practicality of using an efficient numerical method for solving the problem of hot-gas ingestion. A simple model of a STOVL aircraft with four lift jets was studied at various heights, headwind speeds, and thrust splay angles in a modest parametric study. This work is continuing with a new version of the CFD code that allows more realistic aircraft geometries and operational modes.

Ingestion of hot gases generates problems in two ways: An average temperature rise results in a loss of engine thrust, and a temperature distortion may cause the engine to stall. Engine

exhaust gases may be ingested by far-field mechanisms, near-field mechanisms, or both. Far-field ingestion results from the exhaust gases impinging on the ground and forming radial wall jets that flow forward, separate, and mix with the headwind. Near-field ingestion occurs with multiple-jet configurations. Wall jets flowing out from the lift jets meet and create an upflow, or fountain. This fountain flow can impinge on the aircraft's underside, flow along the fuselage to the engine inlets, and be ingested. The gases ingested by this near-field mechanism tend to be hotter, giving greater temperature distortion than those ingested by the far-field mechanism.

In this study the hot-gas environment around a STOVL aircraft was modeled as four choked jets in a uniform crossflow with inlet suction matching the mass ejected by the lift jets. A CFD code solved the Cartesian-based Navier-Stokes equations and the  $k-\epsilon$  turbulence equations in three dimensions by using a multigrid technique to calculate this complex flow field. This CFD code was obtained under a grant to the University of Illinois at Urbana-Champaign. The requirements of the CFD code are met by placing the aircraft model in a confined flow (i.e., a wind tunnel). Also, the aircraft model has no angle of attack owing to the use of a Cartesian-grid-based flow solver.

The parametric study conducted with this model varied the aircraft altitude, the headwind speed, and the splay angle of the lift jets. It proved the practicality of using efficient algorithms on simple configurations. The test cases calculated with the multigrid CFD code were solved within a day, as compared with months in the previous study. The project is now moving to calculating more realistic configurations. A curvilinear version of the multigrid CFD code will be directly compared with experimental data obtained under a grant to



Hot-gas ingestion mechanisms.



Purdue University. This phase will test the practicality of using CFD in analyzing the hot-gas ingestion problems of STOVL aircraft, as well as impact other fluid dynamics problems with turbulent, three-dimensional flow fields.

### Bibliography

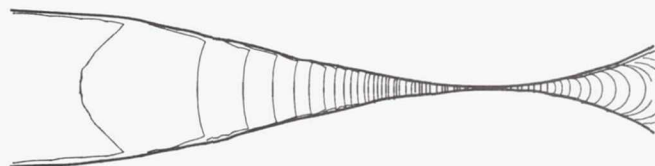
Fricker, D.M.; Holdeman, J.; and Vanka, S.: Calculations of Hot Gas Ingestion for a STOVL Aircraft Model. AIAA Paper 92-0385, Jan. 1992.

**Lewis contact: David M. Fricker, (216) 433-5960**  
**Headquarters program office: OAST**

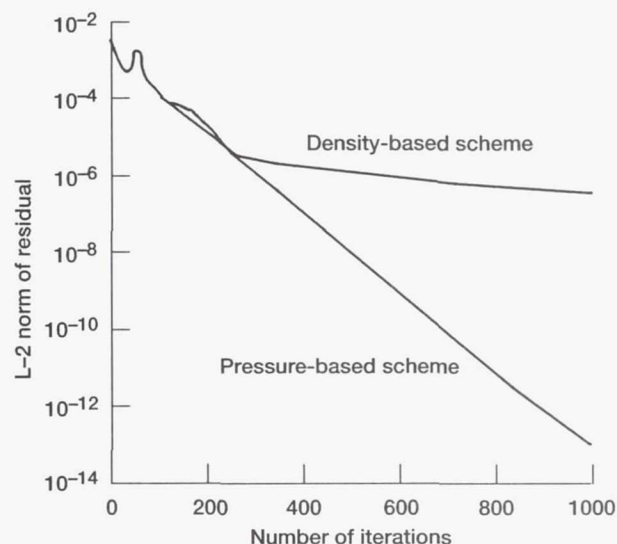
### All-Speed Reacting Flow Code Developed for Engine Simulations

Even with the advent of supercomputers a realistic simulation of chemically reacting flows in a gas turbine combustor or a rocket motor still poses a formidable challenge. One of the difficulties is the inefficiency of the existing numerical algorithms for reacting flows, especially for flows with the wide variation in Mach number found in aeropropulsion systems. To address this problem, NASA Lewis has started an in-house project to develop a new numerical algorithm and computer code. This code can calculate flows with several orders of magnitude variation in Mach number yet still offers a large increase in computational speed and improved accuracy over most existing reacting flow codes.

The new code is based on a unified procedure for solving the unsteady Navier-Stokes equations at all Mach numbers, ranging from molecular diffusion velocities to hypersonic speeds. Nonequilibrium chemistry and real-gas thermophysical properties are considered. The code is written in general curvilinear coordinates so that it can handle complex geometries common to propulsion engines. A two-dimensional code and an axisymmetric code have been developed. The two-dimensional code has been tested for large-area-ratio converging-diverging nozzle flows, backward-facing step flows, and driven cavity flows. Results have shown good accuracy and fast convergence for all test cases over a wide range of Mach numbers.



*Mach number contours of converging-diverging nozzle flow.*



*Convergence histories of converging-diverging nozzle flow calculations.*

Development of the all-speed code is continuing at Lewis. The code will be extended to three dimensions, and the addition of a liquid fuel spray model, a turbulence-combustion closure model, and a thermal radiation model is planned.

### Bibliography

Whithington, J.P.; Yang, V.; and Shuen, J.S.: A Time Accurate, Implicit Method for Chemically Reacting Flows at All Mach Numbers. AIAA Paper 91-0581, Jan. 1991.

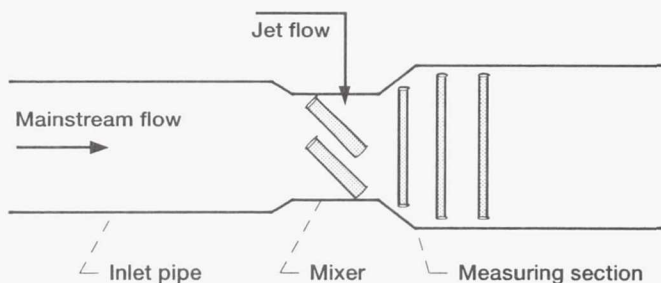
**Lewis contacts: Dr. Jian-Shun Shuen, (216) 826-2262;**  
**Dr. Edward Mularz, (216) 433-5850**  
**Headquarters program office: OAST**

## Enhanced Mixing Tested and Modeled

Rapid mixing is a prerequisite to the success of several proposed low-emissions combustor concepts, among which is the mixing region of a rich burn/quick mix/lean burn (RQL) combustor. Nonreacting and reacting flow experiments and calculations are being performed to identify methods for rapid mixing of two gas streams. Schemes currently being investigated include wall (orifice) injection and lobed (corrugated shear layer) mixers. The former scheme is being studied in both cylindrical and rectangular geometries. Investigations of the latter scheme are currently planned in only the rectangular duct.

Experiments in a cylindrical duct at the United Technologies Research Center are described in reference 1. These results show that above a certain ratio between the dynamic pressures of the two streams (the momentum flux ratio) mixing is faster with slanted-slot injectors than with circular holes. This may be due to the asymmetric vortex pattern characteristic of slanted slots. At representative momentum flux ratios and optimum orifice spacing, low levels of unmixedness are attainable in one mixing passage height downstream from the injector. The unmixedness is nearly independent of orifice size and hence of the mass flow ratio.

Both the experimental results and computational studies at CFD Research Corporation (refs. 2 and 3) suggest that there is an optimum momentum flux ratio for a given number of orifices (and conversely an optimum number of orifices for a given momentum flux ratio). The computational studies further suggest that although convergence and size do not have a noticeable effect on the mixing, they may significantly affect  $\text{NO}_x$  emissions (ref. 3).



*Schematic of apparatus for enhanced mixing studies.*

## References

1. Vranos, A., et al.: Experimental Study of Cross-Stream Mixing in a Cylindrical Duct. AIAA Paper 91-2459 June 1991. (Also, NASA TM-105180.)
2. Talpallikar, M.V., et al.: CFD Analysis of Jet Mixing in Low  $\text{NO}_x$  Flametube Combustors. ASME Paper 91-GT-217, June 1991. (Also, NASA TM-104466.)
3. Smith, C.E.; Talpallikar, M.V.; and Holdeman, J.D.: A CFD Study of Jet Mixing in Reduced Flow Areas for Lower Combustor Emissions. AIAA Paper 91-2460, June 1991. (Also, NASA TM-104411.)

**Lewis contact:** Dr. James D. Holdeman, (216) 433-5846  
**Headquarters program office:** OAST

## Jet Mixing Increased by Using Tabs

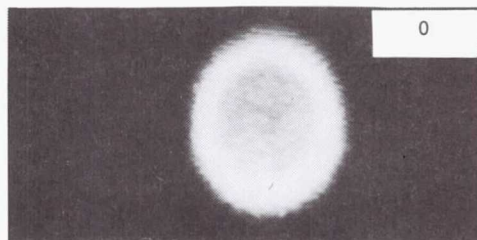
Effective mixing of flow streams is necessary for the efficient operation of several propulsion system components. Examples include mixing of a hot engine exhaust jet with the surrounding cooler air for exhaust temperature reduction, mixing of the fuel and air within a combustor, and mixing of turbine exhaust and ambient air within an ejector nozzle. In each case it is desirable to achieve the required mixing in as short a length as possible in order to minimize both the surface area and weight of the mixing hardware.

A research program at NASA Lewis is investigating methods for enhancing the mixing process and thereby reducing the mixing length between two flow streams. One method being considered involves inserting small protrusions, called tabs, in one of the flow streams at the point where the two streams meet. The tabs have the effect of producing vortices within the flow streams that considerably alter the nature of the interaction between the two streams.

Experimental results have demonstrated that the use of tabs leads to significant increases in mixing effectiveness for round jets exiting into ambient air. Initial experiments involved obtaining both flow visualization and quantitative data for configurations consisting of one, two, and four tabs equally spaced about the circumference at the jet exit. Each tab blocked about 1.5 percent of the jet exit area. The experiments were conducted over a jet exit Mach number range from



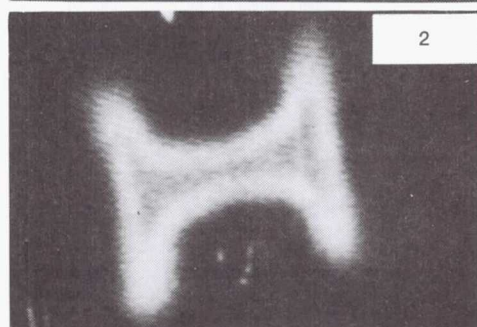
Number of  
tabs



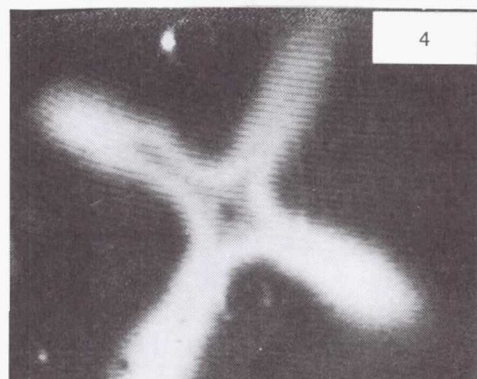
0



1



2



4

*Effect of tabs on round supersonic jet.*

0.3 to 1.8. The results showed that the tabs provided a significant increase in mixing effectiveness over the full range of Mach numbers.

More recent experiments have investigated the effects of tab shape and size on mixing effectiveness. Future work will focus on developing a more detailed understanding of the flow physics

at work in this promising technique for increasing the mixing between two flow streams.

#### Bibliography

Samimy, M.; Reeder, M.; and Zaman, K.B.M.Q.: Supersonic Jet Mixing Enhancement by Vortex Generators. AIAA Paper 91-2263, June 1991.

Zaman, K.B.M.Q.; Samimy, M.; and Reeder, M.F.: Effect of Tabs on the Evolution of an Axisymmetric Jet. NASA TM-104472, 1991.

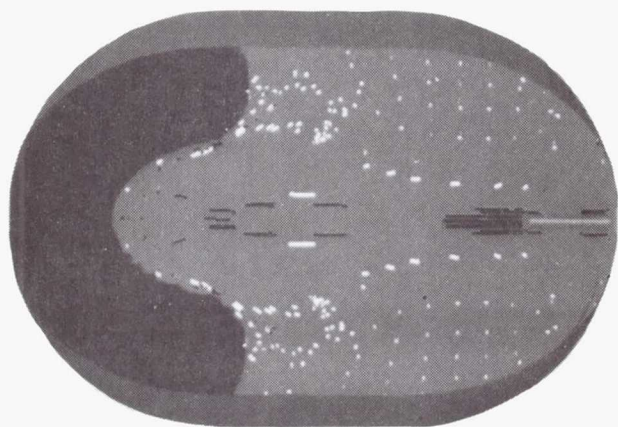
**Lewis contact: Dr. Khairul Zaman, (216) 433-5888**  
**Headquarters program office: OAST**

#### Microgravity Fluid Mechanics Studied With CFD

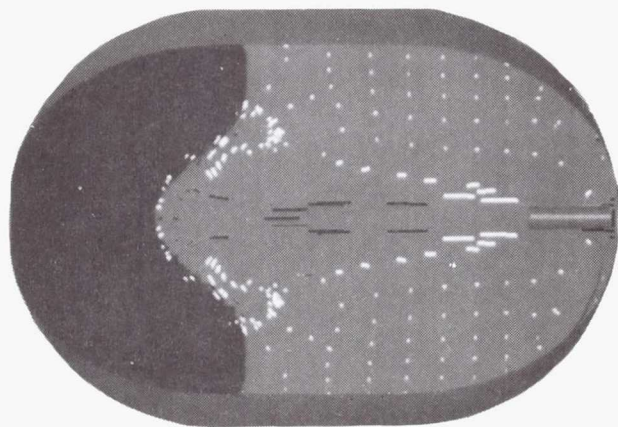
Fluids can behave quite differently in the microgravity environment of near Earth orbit than they do on Earth. In orbit, for example, surface tension forces can be much greater than gravitational forces; on the Earth's surface the opposite is usually true. Routine operations, such as boiling water or filling a tank, can become a complex process in space because of microgravity fluid mechanics.

To better understand fluid mechanics in microgravity, one could conduct experiments in orbit or in special test facilities, such as the drop towers or zero-gravity aircraft. This method of testing is quite expensive and often has limited test time and instrumentation. Researchers at NASA Lewis are now using computational fluid dynamics (CFD) to study these phenomena with high-power computers. Using this technique, one can easily vary the conditions of numerical experiments to gain increased understanding of complex flow problems at a fraction of the cost. With the vast amount of information available from a numerical experiment, one can design better flight experiments.

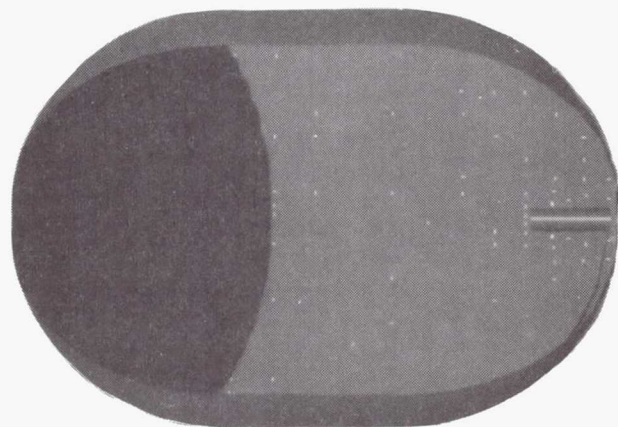
The figure shows time-dependent computer predictions of tank filling in microgravity. Fluid is injected from the right and, for this set of conditions, is confined by the surface tension at the boundary between the liquid and its vapor. Numerical simulations have been performed at higher injection velocity and show the flow breaking through this surface to the opposite wall. The



$T = 10.0$



$T = 5.0$



$T = 0.0$

*Microgravity fluid injection predicted by CFD.*

computer program used in this simulation was developed under contract to NASA Lewis by John Hochstein at Washington University, St. Louis, and is available on the NASA Lewis Cray Y/MP. It is currently being used to study similar microgravity fluid problems.

**Lewis contact:** Thomas J. Benson, (216) 433-5920  
**Headquarters program office:** OAST

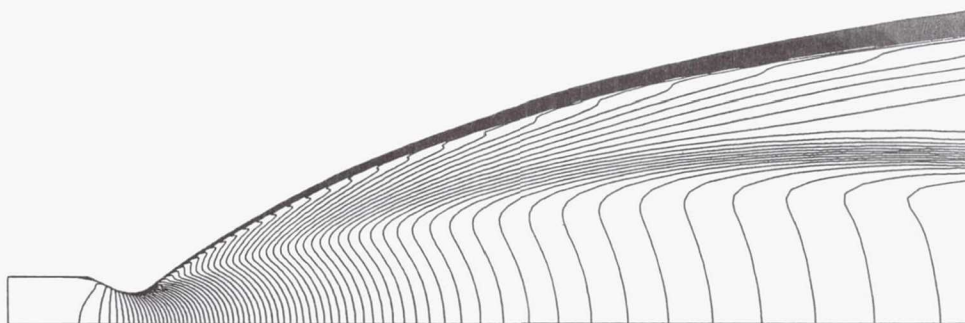
### Computational Fluid Dynamics Simulations Performed for Space Propulsion Rockets

The design of a high-performance rocket for space propulsion requires that the performance of rockets with various configurations be accurately predicted. With recent advancements in computational fluid dynamics and the availability of supercomputers, it is now possible to simulate the complex, chemically reacting rocket flow fields numerically by solving the full Navier-Stokes equations and the species equations simultaneously. The RPLUS code, which was developed at NASA Lewis, has been used to calculate the flow fields and to predict the performances of various space propulsion rockets such as the resistojet thruster, a hydrogen/oxygen 25-lbf thruster for Space Station auxiliary propulsion, a nuclear thermal rocket for a Mars mission, and the hydrogen/oxygen 500-lbf orbital transfer vehicle. The predicted performance values from the RPLUS code are in good agreement with the performance measured in experiments. With further development and improvement the RPLUS code can be a valuable tool for the analysis and design of space propulsion rockets for a variety of missions.

### Bibliography

- Kim, S.C.; and VanOverbeke, T.J.: Performance and Flow Calculations for a Gaseous  $H_2/O_2$  Thruster, *J. Spacecraft Rockets*, vol. 28, no. 4, 1991, pp. 433-438.
- Kim, S.C.: Numerical Study of High-Area-Ratio  $H_2/O_2$  Rocket Nozzles. AIAA Paper 91-2434, June 1991.
- Stubbs, R.M.; Kim, S.C.; and Benson, T.J.: Computational Fluid Dynamics Studies of Nuclear Rocket Performance. AIAA Paper 91-3577, 1991.





*Mach number contours for nuclear thermal rocket.*

**Lewis contacts:** Dr. Suk C. Kim, (216) 826-6670;  
 Dr. Robert M. Stubbs, (216) 433-6303  
 Headquarters program office: OAST

## Propulsion Systems

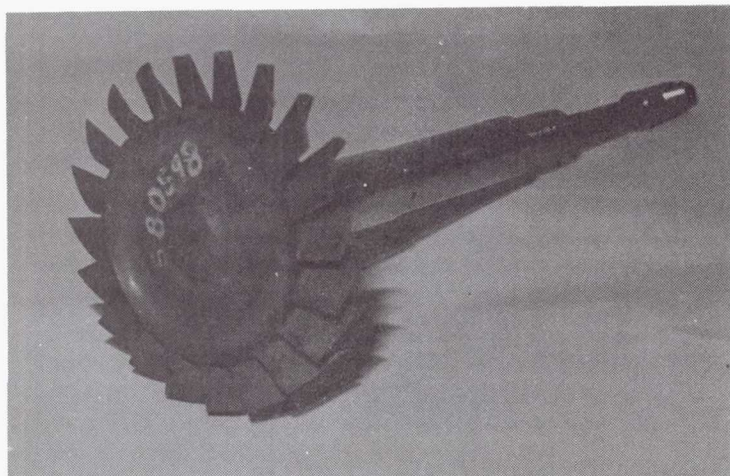
### **Ceramic Components for Gas Turbine Engines Tested to 2500 °F**

In order to exploit the high-temperature performance potential of the gas turbine engine without using strategic materials or exotic hot-section cooling techniques, NASA Lewis is working to develop a ceramic component technology base. As part of the U.S. Department of Energy's Automotive Gas Turbine Program, the Advanced Turbine Technology Applications Project (ATTAP) is developing structural ceramic hot-flow-path component technology for advanced small gas turbine engines. These engines, designed to operate at temperatures to 2500 °F, have the potential for significantly less fuel consumption than either metal turbine engines or conventional piston engines. In addition, the turbine engines operate with reduced emission levels that meet the current and proposed Federal standards.

Technology development contracts are in place with the Allison Gas Turbine Division of General Motors Corporation and with the Garrett Auxiliary Power Division of the Allied-Signal Aerospace Company. Each contract relies on the strong support of the U.S. ceramics industry for component development.

During the past year hot-rig testing of U.S.-manufactured ceramic components was begun. The test rig, based on engine hardware, duplicates actual engine startup, steady-state, and transient operating conditions. A silicon nitride turbine rotor (Norton/TRW Company) has been successfully proof-tested for 211 hr at temperatures up to 2200 °F and design speed with no indication of damage. Peak temperature for the single ceramic component test was limited to 2200 °F by the metal static components. The Norton/TRW monolithic silicon nitride material has demonstrated flexural strength characteristics significantly higher than those of Japanese materials on the basis of test bars cut from turbine rotors. Hot proof testing of a ceramic turbine scroll and vane assembly is under way. The ceramic static parts have operated for just over 6 hr with a brief excursion to 2500 °F and have passed post-test inspection.

Testing of an all-ceramic turbine stage, including the proof-tested rotor and static parts to 2500 °F, is scheduled for early next year.



Norton/TRW rotor after 211 hr of hot-rig testing.

#### Bibliography

Carruthers, W.D.; and Smyth, J.R.: Advanced Ceramic Engine Technology for Gas Turbines. ASME Paper 91-GT-368, June 1991.

Haley, P.J.: Advanced Turbine Technology Applications Project (ATTAP)—Overview and Ceramic Component Technology Status. ASME Paper 91-GT-367, June 1991.

**Lewis contact:** Paul T. Kerwin, (216) 433-3409  
**Headquarters program office:** OAST

#### Low- $\text{NO}_x$ Combustor Concepts Reach Goal

Control of oxides of nitrogen ( $\text{NO}_x$ ) produced by aircraft flying in the stratosphere has been identified as the top priority in High Speed Research (HSR) studies conducted at NASA Lewis, Boeing, and McDonnell Douglas. In the stratosphere, at altitudes of approximately 50,000 ft and above,  $\text{NO}_x$  acts as a catalyst to destroy ozone. In order to build an environmentally acceptable High Speed Civil Transport (HSCT),  $\text{NO}_x$  emissions must be reduced. The goal  $\text{NO}_x$  levels (3 to 8 grams of  $\text{NO}_x$  per kilogram of fuel consumed) represent approximately 90-percent reductions of the  $\text{NO}_x$  levels produced by conventional combustion systems. These goal  $\text{NO}_x$  levels were achieved by two combustor concepts described here.

An extensive program to reduce  $\text{NO}_x$  in gas turbine combustors is under way at Lewis. In-house experiments have successfully provided evidence of the feasibility of two promising combustor concepts: lean premixed prevaporized (LPP) combustion and rich burn/quick quench/lean burn (RQL) combustion.

The LPP concept is based on burning at a lean fuel/air ratio, where the mixture has less fuel than at the stoichiometric fuel/air ratio (when fuel and air are in "perfect balance" so that all the fuel burns with all the oxygen in the air). A lean mixture burns at a lower flame temperature and produces lower  $\text{NO}_x$  emissions. The LPP combustion flame tube rig is currently in operation. Low  $\text{NO}_x$  levels within the HSR goal range have been obtained. Detailed studies of the fuel injection system and combustion chemistry (using laser diagnostics) will follow.

The RQL concept uses the principle that both rich (higher fuel/air ratio than stoichiometric) and lean mixtures produce lower  $\text{NO}_x$ . Rich combustion is more stable but uses more fuel than necessary. Therefore, a staged combustor concept is envisioned where the stable rich zone is followed by a "quick quench" zone to pass quickly through the stoichiometric condition to a lean-burning chamber, which completes the burning process. The RQL combustion flame tube successfully achieved  $\text{NO}_x$  levels within the HSR goal. Further



studies will follow to optimize the rich, quench, and lean zones and subcomponent hardware as a guide for future combustor design criteria.

Contracted work is also being done to develop these concepts into actual combustors for use in the future HSCT. General Electric is concentrating on the LPP combustor concept, and Pratt & Whitney is focusing on the RQL combustor. Results from the flame tube experiments are being applied to combustor subcomponent development currently at General Electric and Pratt & Whitney. Many university grants complement the overall program. Some grants are providing analytical support that assists in the prediction of combustion processes at the HSR conditions. Some university grants are developing laser diagnostic capabilities for making nonintrusive measurements in the LPP and RQL combustion test rigs.

#### Bibliography

Nguyen, H.L.; Bittker, D.A.; and Niedzwiecki, R.W.: Investigation of Low  $\text{NO}_x$  Staged Combustor Concept in High-Speed Civil Transport Engines. AIAA Paper 89-2942, July 1989. (Also, NASA TM-101977.)

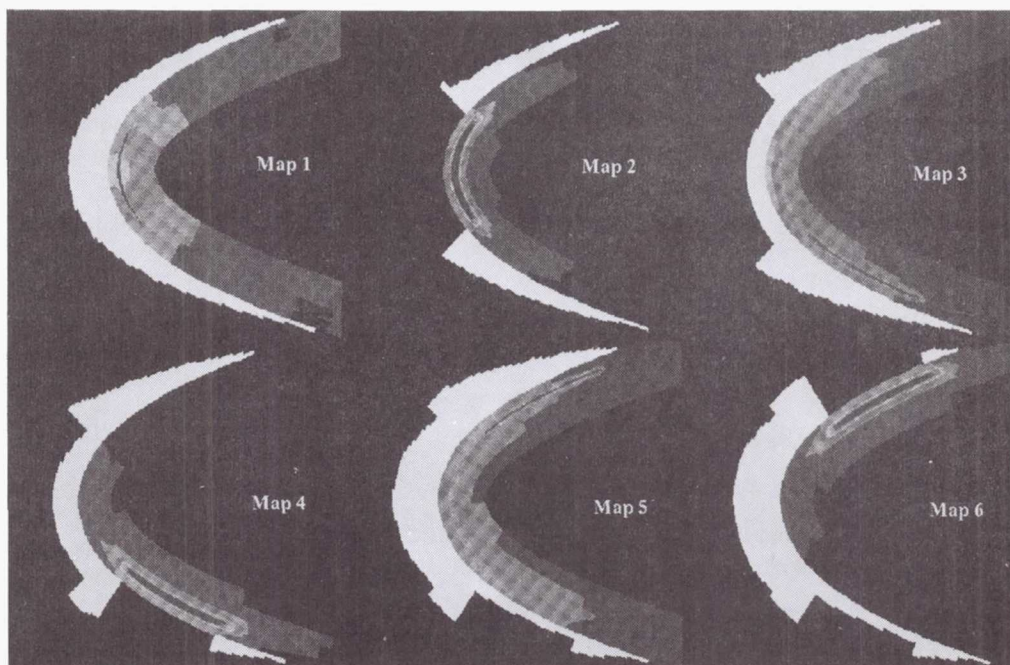
Tacina, R.R.: Combustor Technology for Future Aircraft. AIAA Paper 90-2400, July 1990. (Also, NASA TM-103268.)

**Lewis contact:** Richard W. Niedzwiecki, (216) 433-3407  
**Headquarters program office:** OAST

#### Code Numerically Simulates Icing, Deicing, and Shedding

The NASA Lewis aircraft icing group has combined two of its most popular computer codes into a single code that numerically simulates the growth, melting, and shedding of ice on airfoils moving through supercooled icing clouds while being protected by electrothermal deicing or anti-icing ice protection systems. The code also predicts the transient temperatures within the airfoil and heater structure. This new computer code is useful both for designing deicers and analyzing their operation and for setting the heater power levels and on/off times for various cloud conditions and outside air temperatures. This capability offers the potential for significantly reducing the amount of expensive and high-risk icing flight testing required to determine the heater control laws that produce acceptable aerodynamic penalties and prevent water from running back and freezing beyond the heaters.

This code, entitled LEWICE, predicts the growth and shape of ice on the leading edge of two-dimensional airfoils. LEWICE includes an inviscid panel flow code that predicts the flow field around an airfoil, a droplet trajectory code that predicts the flux of supercooled cloud water droplets impinging on the airfoil, and an energy balance/heat transfer code that predicts where the



*Sequence of temperature contour maps and ice profiles that illustrates cyclic deicer operation.*

water freezes and what the ice shape will be. In LEWICE the airfoil surface is treated as being either adiabatic or having a constant heat flux. LEWICE is widely used by industry and government.

NASA Lewis, through grants to the University of Toledo, has also supported the development of a series of computer codes that combine conduction, convection, and phase-change heat transfer to predict the transient operation of electrothermal deicers. Deicers employ electrical heater strips embedded in a heater mat that is affixed to, or made integral with, the leading edge of the airfoil. These codes predict temperatures throughout the airfoil leading edge and heater structure and also predict melting of the ice above the heaters. These deicer codes are also widely used by industry and government.

Recently, the University of Toledo enhanced LEWICE by combining it with their electrothermal deicer code. The enhanced LEWICE can be run in three modes: the original mode, where the airfoil surface is modeled as being adiabatic or having a constant heat flux; a mode where the heaters are unpowered but the initiation of icing causes transient temperatures within the icing and wing structure; and a deicing or anti-icing mode, where the heaters are powered, with subsequent possibilities of ice melt, ice shedding, water runback, and water freezing beyond the heaters. A simple ice shedding model is included as a subroutine in the second and third modes, but the subroutine could be replaced by other shedding models.

The enhanced LEWICE is set up to model spanwise heater strips. The user may specify any number of heaters, any chordwise heater width, any heater gap width, and any number of material layers in the airfoil and heater structure. The heaters may be cycled on and off in unison or with periods independent of each other, and each heater may have a different power level. Thus, the enhanced LEWICE has maximum flexibility in modeling virtually any electrothermal deicer installed into any two-dimensional airfoil.

This code is particularly suited for modeling electrothermal deicer operation on helicopter main rotor blades. As an illustration a simplified deicer system was modeled and the code was used to analyze it for a particular on/off cycle. The deicer

consists of three spanwise heater strips embedded in the leading edge of an airfoil. (In practice, more than three heater strips would be used, and heater cycling times would be different.) The accompanying figure shows a sequence of temperature contour maps and ice profiles that illustrates one cycle of operation for the three heater elements. After a layer of ice (shown in white) accretes on the leading edge, the center heater is turned on for 20 sec (map 1), enough time to melt the ice at the ice-surface interface and induce a shed (map 2). The heater is then shut off for 1 min and ice continues to accumulate on the airfoil. Next, the lower heater is actuated for 20 sec (map 3), and the ice at the interface melts and induces a shed (map 4). The heaters are turned off for 1 min and ice continues to accumulate. Finally, the upper heater is actuated for 20 sec (map 5), and again the ice at the interface melts and induces a shed (map 6).

#### Bibliography

Ruff, G.A.; and Berkowitz, B.M.: Users Manual for the NASA Lewis Ice Accretion Prediction Code (LEWICE). NASA CR-185129, 1990.

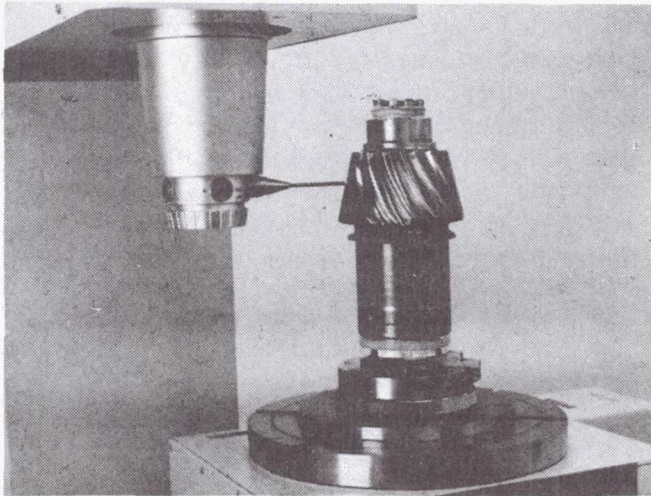
Wright, W.B.; Keith, T.G.; and DeWitt, K.J.: Numerical Simulation of Icing, Deicing, and Shedding. AIAA Paper 91-0665, Jan. 1991.

**Lewis contacts:** John J. Reinmann, (216) 433-3900;  
William D. Wright, (216) 433-4030  
**Headquarters program office:** OAST

#### Automated Spiral Bevel Gear Grinding and Inspection Enhanced

The final step in the manufacture of an aerospace-quality spiral bevel gear is grinding the tooth surfaces. This final grinding process is a very precise machining operation that requires complex machinery and highly skilled operators. The spiral bevel gear grinding process has been improved dramatically in recent years by the introduction of two new technologies: computer numerical control for grinding machines and computer-controlled coordinate measuring machines for inspection. An enhanced automated inspection technique, recently developed and successfully demonstrated, further improves the grinding process. In this technique, tooth profiles of production parts are measured with a





*Inspection of spiral bevel gear using coordinate measuring machine.*

coordinate measuring machine and then compared with those of a reference master gear. The optimal grinding machine settings are determined automatically from the inspection data. Case studies have shown that using the new technique reduces costs and improves quality.

The project to develop the enhanced automated inspection technology was done under a NASA contract funded by the U.S. Army Aviation Systems Command. Sikorsky Aircraft was the prime contractor with The Gleason Works as the major subcontractor. The enhanced inspection technology has been developed, implemented, and demonstrated. While previously only first-order grinding machine settings could be determined from inspection data, now both first- and second-order setting adjustments are determined automatically. The number and types of machine setting adjustments specified are now optimized. Also, gears can now be measured as they were ground, either single sided or spread blade. The enhanced inspection technique can be used with either computer numerically controlled grinders or the still more common manual grinders. When used with the new full computer numerically controlled grinders, production parts are now ground to near-master-gear quality. A case study was done to evaluate the new inspection technique. The quality of the production parts improved while final grinding time and cost were

reduced by 58 percent. The technology for a true closed-loop spiral bevel gear grinding process has now been developed and demonstrated.

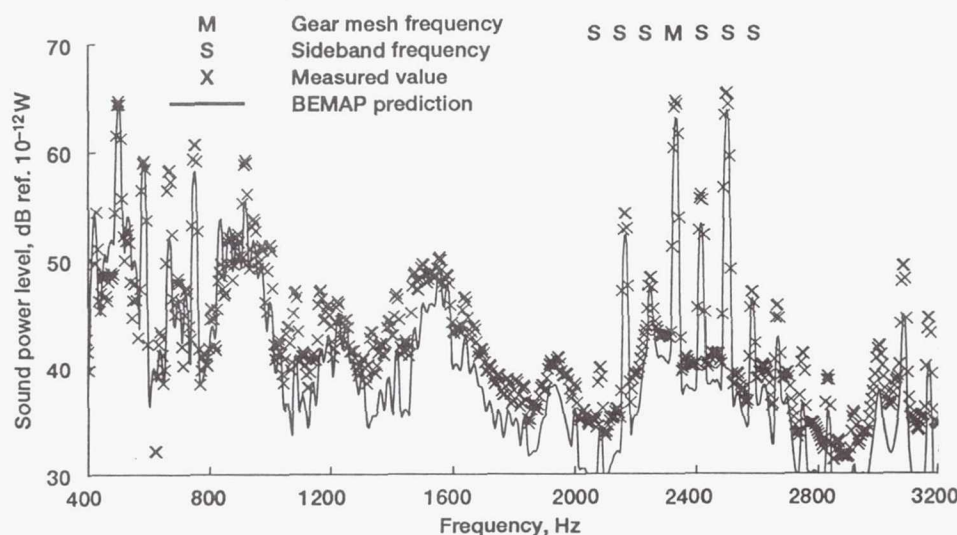
**Lewis contact:** Timothy L. Krantz, (216) 433-3580  
**Headquarters program office:** OAST

### **Gearbox Acoustic Code Validated**

Reduction of helicopter cabin noise (which has been measured at over 100-dB sound pressure level) is a NASA and U.S. Army goal. A major source of this noise is the gearbox. A requirement for the Advanced Rotorcraft Transmission Project is a 10-dB noise reduction relative to current designs. A combined analytical and experimental effort is under way to study the effects of design parameters on noise production. An important part of the project is performing experiments in the NASA Lewis gear noise rig to verify analytical codes.

Vibration spectra were measured on the top surface of an instrumented gearbox in the gear noise rig. These vibration data were input to the acoustics code BEMAP to predict the acoustic field around the gearbox. The code is based on the boundary element method (BEM), which models the gearbox top as a plate in an infinite baffle. Under identical operating conditions, the sound intensity was measured just above the same grid points. Sound power spectra were generated from both analytical and measured data. Analytical and experimental results for sound power were compared for speeds of 3000, 4000, 5000, and 6000 rpm over the frequency range 400 to 3200 Hz. The sound power at gearbox frequencies is typically 3 dB greater than the predicted value. The predicted sound power curve closely follows the measured values. The results validate the BEMAP sound power predictions made from gearbox vibration data.

BEMAP can be used after a finite-element structural vibration analysis of a gear housing, where BEMAP establishes the link between the finite-element results and noise radiation. BEMAP provides designers with a valuable tool for investigating methods of controlling helicopter gearbox noise. Experiments continue to find new tools for reducing this noise.



Comparison of measured sound power with BEMAP predictions.

#### Bibliography

Oswald, Fred B., et al.: Comparison of Analysis and Experiment for Gearbox Noise. NASA TM-105330 (AVSCOM TR-9-C-030), 1992.

**Lewis contact:** Fred B. Oswald, (216) 433-3957  
**Headquarters program office:** OAST

#### Transonic Performance of NASP Nozzle Evaluated in Wind Tunnel Tests

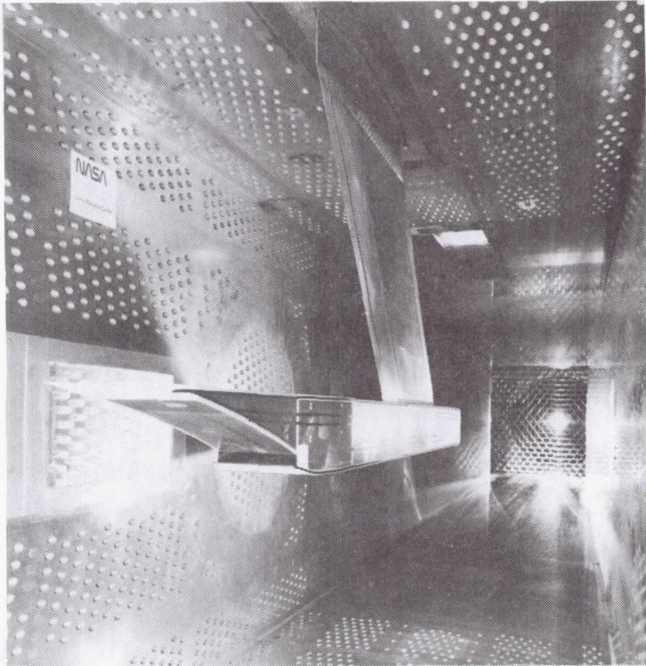
The air-breathing propulsion system on the National Aerospace Plane (NASP) must operate over an unprecedented range of flight conditions from takeoff to hypersonic speeds at extreme altitudes. The large nozzle area required for efficient operation at high speeds and altitudes becomes a liability at lower speeds, where the engine exhaust gases do not fill the large nozzle area. During acceleration through the transonic speed regime, the propulsion system and especially the nozzle experience a critical transonic drag rise due to off-design operation, which must be understood and controlled. Recent tests of a generic NASP nozzle configuration in the NASA Lewis 8- by 6-Foot Transonic Wind Tunnel provided valuable information on the performance and operability of such nozzles from Mach 0.6 to 2. Proper simulation of the exhaust gas properties was assured by using an actual hydrogen-air combustor upstream of the nozzle test article.

Transonic drag was successfully reduced by using external burning.

The water-cooled NASP nozzle test article was mounted to the jet-exit rig, which was developed specifically for nozzle testing with hot combustion products by the North American Aircraft Division of Rockwell International under contract to NASA Lewis. The jet-exit rig houses hydrogen- and airflow-measuring systems, a six-component flowthrough force balance, and the water-cooled hydrogen-air combustor that is used to produce the proper test gas composition for the nozzle. The combustor is capable of delivering gas temperatures of 3500° R, at pressures to 100 psia. A separate hydrogen line serves the external burning system, which consists of a control valve, a row of sonic injectors, and a series of interchangeable flameholders. Infrared flow visualization of the hot nozzle exhaust and the external burning plume was used to verify combustor operation and external burning flame stability.

External burning succeeded in reducing nozzle drag and increasing normal forces over a range of transonic speeds from Mach 0.8 to 1.8. The external burning plume was ignited by the hot exhaust jet and did not require a separate ignition source. Data obtained during these initial tests of the generic nozzle configuration were supplied to the NASP contractor team for inclusion in the nozzle performance data base. Nozzle design and operational information is being





NASP nozzle in wind tunnel.

incorporated into a follow-on test under NASP Government Work Package 58, in which the specific NASP nozzle geometry and external burning system will be used. These follow-on tests, scheduled to begin in April 1992, will be conducted at Lewis in both the 8- by 6-Foot and 10- by 10-Foot Wind Tunnels over a range of Mach numbers from 0.6 to 3.0.

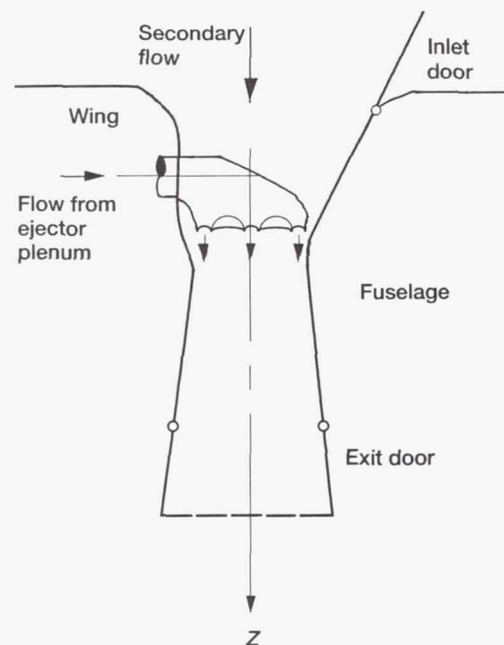
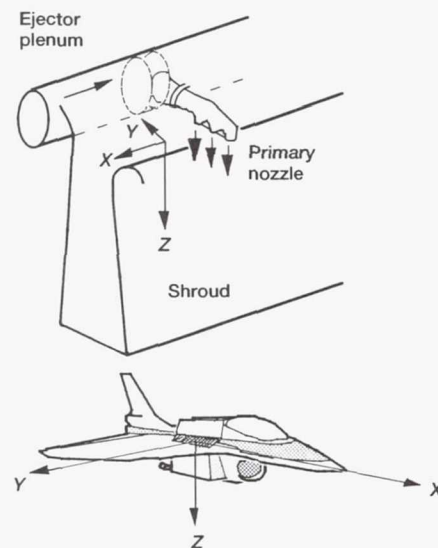
**Lewis contact:** Charles J. Trefny, (216) 433-2162  
**Headquarters program office:** OAST

### Data Base Compiled for Thrust-Augmenting Ejector

Short-takeoff-and-vertical-landing (STOVL) aircraft are potential candidates for future high-performance aircraft. Successful STOVL designs depend heavily on propulsion system development whereby both vertical lift and forward thrust must be attained without drastically increasing the aircraft's weight or cross-sectional area. One method of achieving STOVL capability in an aircraft is through the use of thrust-augmenting ejectors. Basically, an ejector is a pumping device through which large amounts of air are drawn from the atmosphere by the

entrainment action of the primary nozzle jet shear layer. Thrust augmentation results when the entrained secondary air mixes with the primary flow, increasing total mass flow and thus the vertical thrust.

The design and development of thrust-augmenting STOVL ejectors has typically been based on trial and error. As part of STOVL component research NASA Lewis, in conjunction with Boeing Military Airplanes and Boeing



Typical STOVL ejector configuration.

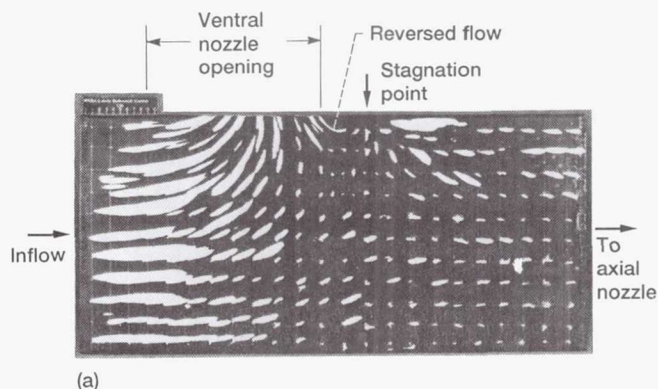
deHavilland, completed a series of tests on a full-scale ejector with primary nozzle flow up to 1100 °F. This unique ejector testing was performed in house at the Powered Lift Facility and signifies the first design-point (both temperature and pressure) testing of a full-scale, thrust-augmenting ejector. In cold-flow tests using ambient air, several modifications were made to decrease inlet losses, to enhance the shear layer mixing, and to improve the ejector performance. Hot-flow testing was then performed with a similar configuration; only slight changes were made to allow for thermal expansion of the ejector duct.

An extensive data base was obtained from the ejector testing. As expected from theory, the cold-flow tests resulted in a higher overall augmentation than the hot flow. Ejector exit plane surveys showed a more uniform profile for the hot flow (the design condition) than for the cold flow—indicative of better mixing of the primary and secondary streams. However, this mixing was less than expected. This could be attributed to the mixing length for the primary and secondary streams being shorter than optimum to keep the ejector a reasonable size. This data base can be used to verify ejector design technology and to calibrate computer codes for evaluating ejector performance in future STOVL aircraft.

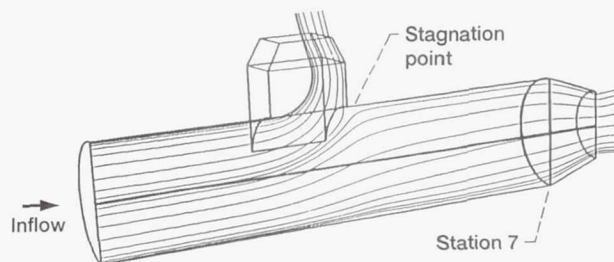
**Lewis contact:** Wendy S. Barankiewicz, (216) 433-8706  
**Headquarters program office:** OAST

### Analytical Tool Developed for Ventral/Cruise Exhaust Nozzles

Improved short-takeoff-and-vertical-landing (STOVL) aircraft are planned for possible future development. For these aircraft the same propulsion system will provide power for lift and hover as well as for supersonic horizontal flight. When the STOVL propulsion system is operating in the transition mode (i.e., converting from lift and hover to forward flight), the rear jet (or cruise) nozzle will be open, and valves will be opened to duct engine exhaust gases to two or more thrust-ers directed downward. In many proposed configurations one of the lift thrust-ers will be a ventral nozzle located in the bottom of the aircraft fuselage. NASA Lewis has an on-going, in-house effort to develop the required technology for these



(a)



(b)

*Tailpipe plane-of-symmetry flow visualization: (a) experimental results; (b) analytical particle traces.*

aircraft. We are establishing aerodynamic design principles and a data base for key components through experimental testing and computational fluid dynamics (CFD) analyses.

Experimental and analytical flow studies of a generic model tailpipe with cruise and ventral nozzles flowing have recently been completed. The model was about one-third of full size. The analytical work was done by using PARC3D, a full Navier-Stokes CFD code, to predict the internal flow patterns and the overall system performance. The results of the PARC3D computational fluid dynamics code compared well with the experimental results. The analytical studies indicated that the boundary layer was nearly completely drawn off by the ventral nozzle. The boundary layer started to reform on the ventral duct side of the tailpipe downstream of the ventral duct. On the opposite side of the tailpipe downstream of the ventral duct, the flow dispersed to be distorted at the entrance to the cruise nozzle. The studies also indicated that the flow separated from the front wall of the ventral duct and that large vortices were formed in this region. This behavior resulted in a low-pressure region that



caused the ventral nozzle airflow to overturn back toward the inlet to the tailpipe and create a significant reverse thrust component. This reverse thrust component adversely affected the horizontal thrust of the cruise nozzle and resulted in a low net horizontal thrust component for the overall propulsion system. As a result of this work another calibrated CFD analytical tool is available to assist in the design of STOVL propulsion nozzles.

**Lewis contact:** Barbara S. Esker, (216) 433-8707  
**Headquarters program office:** OAST

## Radial Rotor Cooling Studied

Most if not all radial turbines in use today are uncooled and limited by material properties to about 1800 °F inlet temperature. Going significantly beyond this temperature limit requires that either nonmetallic materials (e.g., ceramics) or radial rotor cooling technology must be developed. Research programs for both approaches are under way. This article highlights the cooled radial rotor technology program at Lewis. This cooling research consists of both experiments and the application of advanced aerothermodynamic analysis.

The aerodynamic and cooling design of a research turbine to operate at 2500 °F inlet temperature was performed by the Allison Gas Turbine Division of General Motors Corporation in collaboration with NASA Lewis engineers (ref. 1). Two rotors, an uncooled version and a cast cooled version, are being used in the experimental part of the program. Aerodynamic performance tests of the uncooled rotor are complete. Rotor blade surface pressures were measured during this test



*Cooling flow study of internal passages of cooled radial rotor (view from suction side); compressible solution; blade rotating at 21,596 rpm; cooling air temperature.*

and compared with computational fluid dynamics calculations for two streamlines (70 percent and 20 percent). The comparison was generally good except for the inducer part of the blade for the 20-percent streamline. This discrepancy is believed to be caused by the flow in the clearance space between the rotor and the backface, which is not modeled. Additional details of these experimental results and the calculated hot-side flow field are contained in reference 2.

An extensive effort is also under way to develop accurate coolant-side flow analysis methods. Current computational efforts include an improved one-dimensional coolant design code and the development of three-dimensional viscous coolant codes. The development of a grid-generating code, which is required to calculate the flow field, was reviewed in the 1989 annual report (ref. 3). An example of the calculated coolant flow inside the radial rotor blade was obtained with Adapco's three-dimensional viscous STARCD code. These analytical results will be compared with data from both stationary and low-speed simulated blade tests as well as the high-speed experiments with the cooled radial rotor. Results obtained from this cooling technology program will be applicable to axial as well as radial turbines.

#### References

1. Snyder, P.H.; and Roelke, R.J.: The Design of an Air-Cooled Metallic High-Temperature Radial Turbine. *J. Propulsion Power*, vol. 6, no. 3, May-June 1990, pp. 283-288.
2. Tirres, L.: A Comparison of the Analytical and Experimental Performance of the Solid Version of a Cooled Radial Rotor. *AIAA Paper 91-2133*, June 1991. (Also, NASA CR-187195.)
3. Annual Report 1989—NASA Lewis Research Center, NASA TM-102296, 1991.

**Lewis contact: Richard J. Roelke, (216) 433-3403**  
**Headquarters program office: OAST**

#### Viscous Three-Dimensional Codes Predict Transonic Fan Performance

One goal of computational fluid dynamics for turbomachinery is the prediction of component

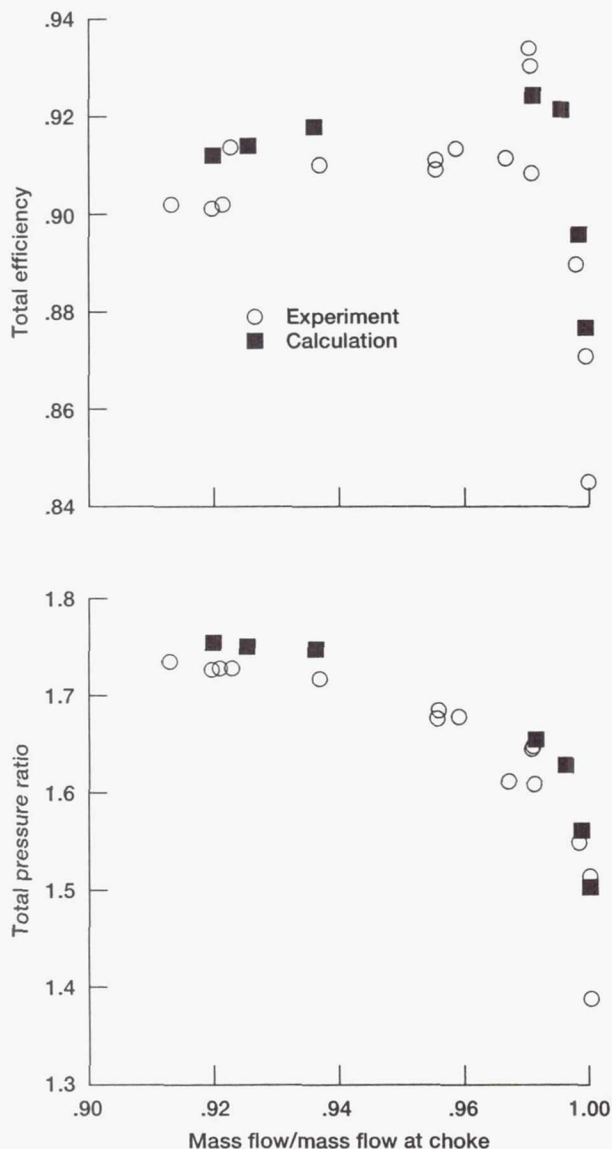
performance, for example, fan pressure ratio and efficiency. Because a small improvement in fan efficiency can amount to a large savings in yearly fuel costs for a fleet of commercial aircraft, turbomachinery designers are extremely interested in tools that give good quantitative prediction of turbomachinery performance. To that end, three-dimensional grid generation and viscous flow analysis codes have been developed for turbomachinery at NASA Lewis. The grid code, called TCGRID (Turbomachinery C-Grid), generates elliptic grids about arbitrary isolated blade rows. The flow analysis code, called RVC3D (Rotor Viscous Code 3-D), is an explicit finite difference code with an algebraic turbulence model.

In order to validate these codes, the design-speed operating line of a transonic fan rotor has been computed, and the results have been compared with experimental data. The fan (designated NASA rotor 67) has been tested experimentally at NASA Lewis by using both aerodynamic probes and laser anemometry. Maps of total pressure ratio and adiabatic efficiency have been computed and agree well with experimental maps.

Detailed comparisons between the calculations and experiment have been made at two operating points, one near peak efficiency and one near stall. Blade-to-blade contour maps show the shock structure in the fan. Comparisons made with aerodynamic survey data downstream of the fan generally show good agreement with measured total temperature and total pressure but some disagreement with measured static pressure and flow angle. Comparisons made with laser velocimeter data show that shock location and strength were predicted closely near peak efficiency but were somewhat overpredicted near stall. Predicted wake profiles had about the right location and spread but were deeper than the measured wakes, probably owing to a lack of resolution in the laser data.

Particle traces showed separated flow at the fan leading and trailing edges at both operating points. The code's ability to predict these features suggests that it could be used to guide future experimental work aimed at resolving these features or to eliminate them in future designs. Overall the code showed very good agreement with a variety of experimental data, thereby increasing confidence that the code can be used to predict the performance of other machines as well.





Comparison of computed and measured adiabatic efficiency and total pressure ratio characteristic for rotor 67 at 100-percent speed.

#### Bibliography

Chima, R.V.: Viscous Three-Dimensional Calculations of Transonic Fan Performance. Presented at the AGARD Propulsion and Energetics Symposium on Computational Fluid Mechanics for Propulsion, San Antonio, TX, May 27-31, 1991. (Also, NASA TM-103800.)

**Lewis contact:** Dr. Rodrick V. Chima, (216) 433-5919  
**Headquarters program office:** OAST

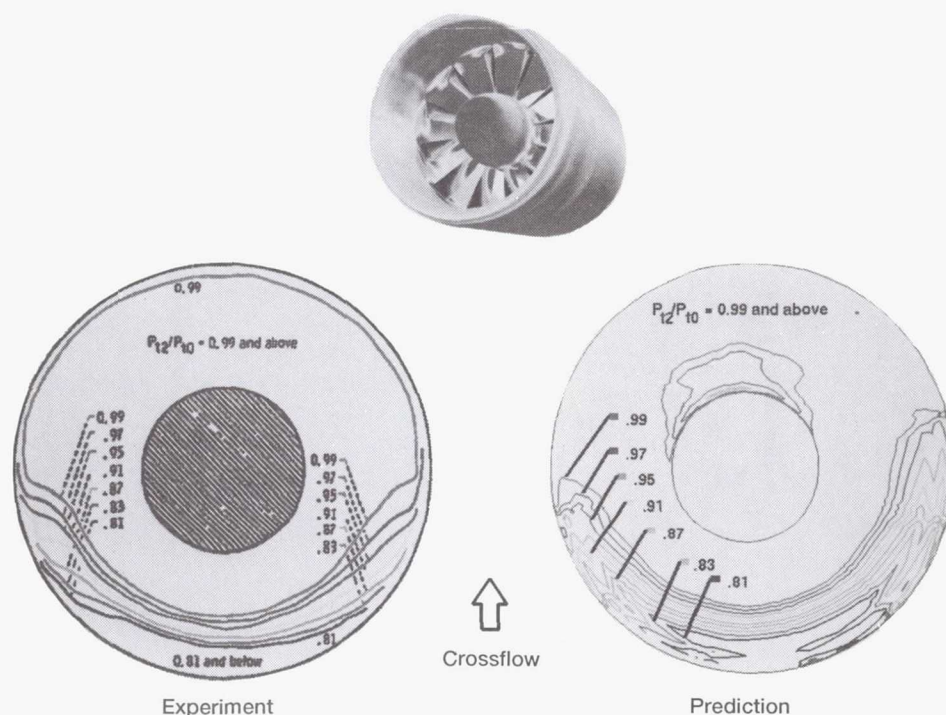
#### Euler/Navier-Stokes Code Predicts Unsteady Ducted-Propfan Aerodynamics

Advanced turbofan engines planned for future commercial aircraft will be larger in diameter and have higher thrusts than current engines. One characteristic, their much shorter cowls, creates a problem in the design process. Traditional computational fluid dynamics tools for the analysis and design of turbofan engines treat the flow outside the engine and the flow through the engine independently. Unfortunately, as the cowl length decreases, the coupling between the internal and external flows becomes stronger. For the concept engines of the future the cowl length is short enough that predicting engine performance with independent codes is difficult. A better procedure, developed at NASA, is to simultaneously compute the internal and external flows in the same calculation.

In support of the turbofan engine manufacturers, NASA Lewis has been developing, under a contract to the Allison Gas Turbine Division of General Motors Corporation, a series of three-dimensional Euler and Navier-Stokes codes for short-cowl ducted propfans. These computational codes were originally developed for internal turbomachinery flow and then modified for NASA's Advanced Propfan Project. With the shift in emphasis on ducted propellers, these codes have been extended to simultaneously solve for the flow inside and outside the cowl.

The latest development in the series of Advanced Ducted Propfan analysis codes is an unsteady single-blade-row Euler/Navier-Stokes code. One of the difficult predictions that are now possible is shown here. The code was used to predict the flow field about a NASA 1.15-pressure-ratio fan at Mach 0.2 and 40° angle of attack. At this (edge of the operating envelope) climb condition the high angle of attack leads to cowl lip separation. The experiment shows the loss in total pressure at the fan face, as measured with a pitot-static rake. Shown at one instant in time (not time averaged) after the solution has developed, the predicted total pressure at the fan face looks very similar.

The actual fan has both a rotor and a stator, but the current prediction only includes the rotor. To improve the code, Allison is currently extending it to handle multiple blade rows. Once completed,



Prediction of flow field at Mach 0.2 and 40° angle of attack.

the predictions will include both the steady and unsteady rotor-stator interactions, further improving the information available to the engine designer.

Lewis contact: Dr. Christopher J. Miller, (216) 433-6179  
Headquarters program office: OAST

### Novel Method Allows Direct Measurement of Acoustic Modes in Fan Engine

Most of the noise generated by aircraft fans is in the form of tones at the blade passing frequency (number of blades passing a fixed point in 1 sec) and its harmonics. Fan noise is transmitted through the inlet and aft duct of the engine in the form of spinning modes (rotating pressure patterns). Measuring these modes is important for the following reasons:

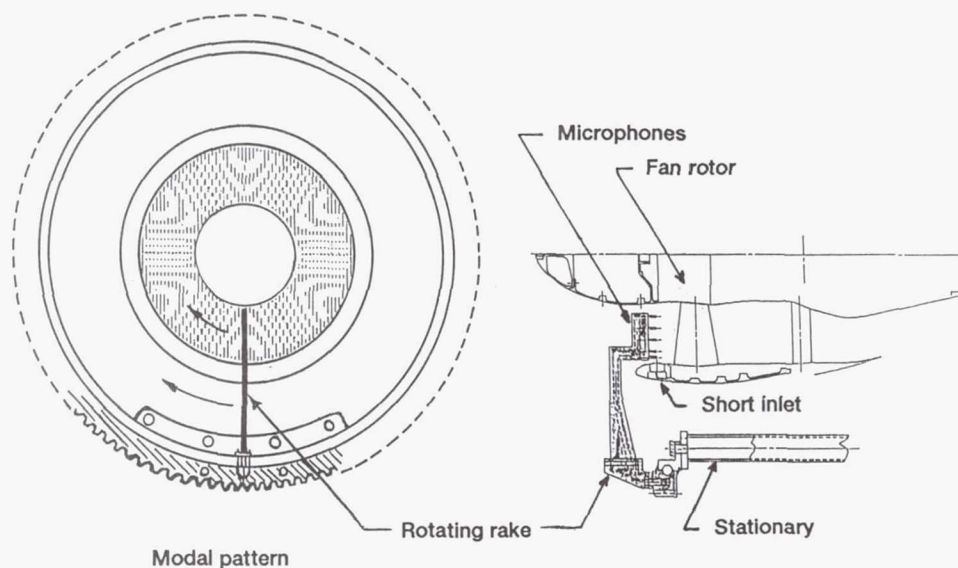
- They help identify the generating mechanism of the fan.

- They control the propagation within the duct as well as the design and effectiveness of any acoustic treatment.

- They control the direction to which the noise radiates in the far field.

One property of these modes that makes them difficult to measure is that to a fixed observer they all have the same frequency. A novel concept suggested many years ago by T.G. Sofrin at Pratt & Whitney Division of United Technologies Corporation involves rotating microphones within the fan duct to measure spinning modes. The first implementation of this concept was completed at NASA Lewis during the Advanced Ducted Propeller test program in the 9- by 15-Foot Low-Speed Wind Tunnel. The principle involved in the rotating microphone rake is basically that of Doppler shift, which separates the various circumferential mode orders into different frequencies, since each order rotates at a different speed. For a rake moving in the direction of the fan rotation, corotating modes are shifted to lower frequencies while counterrotating modes are shifted to higher frequencies. The interaction of the rake wake with the fan during inlet testing





*Ducted propfan acoustic mode measurement.*

has only minimal effect on the results because it only contaminates one frequency corresponding to the rotor locked mode (the order equal to the blade number).

The rake was attached to a large ring gear surrounding the inlet so as to minimize inflow distortion. A key element to this measurement is the control system that drives the ring gear in a synchronous fashion relative to the fan. In this case the rake makes one revolution while the fan makes 250. The rake's position is maintained to  $\pm 0.2^\circ$  relative to the fan. The radial mode order is determined from the radial profile for each circumferential order.

**Lewis contact:** Laurence J. Heidelberg, (216) 433-3859  
**Headquarters program office:** OAST

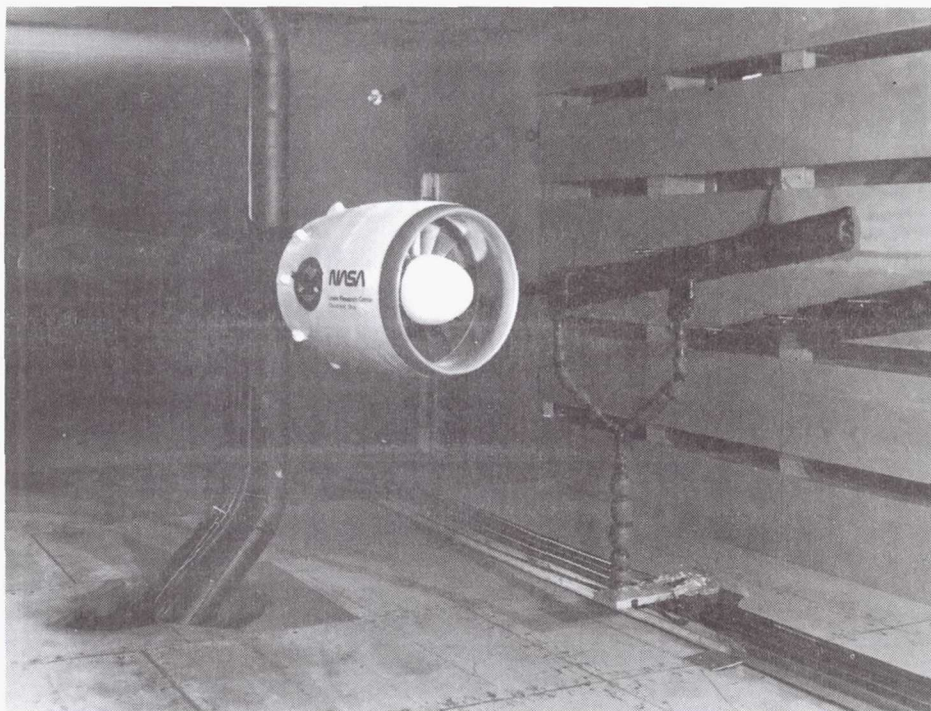
### **Takeoff Noise Tests Completed on a Model Advanced Ducted Propeller**

The advanced propeller program has successfully demonstrated significant performance improvements for single and counterrotating propellers relative to that of current turbofan engines at typical cruise conditions of Mach 0.8 and 10,668-m (35,000-ft) altitude. However, uncertainties over new propeller technologies and inherent structural and acoustic benefits

associated with propeller shrouds have directed current research toward the advanced ducted propeller, which is a marriage of the turbofan and propeller technologies. The advanced ducted propeller will typically feature a low number of rotor blades and a stator designed to satisfy the cutoff criterion. Bypass ratios of 20 or greater will be characteristic of these propellers.

A model ducted propeller, designed and built by Pratt & Whitney Division of United Technologies Corporation, was recently tested in the NASA Lewis 9- by 15-Foot Anechoic Wind Tunnel at takeoff conditions of Mach 0.2. A range of model configurations was tested to investigate the aeroacoustic effects of inlet and spinner length, blade setting angle and tip speed, and nozzle size. The model, which had 16 rotor blades, was tested with 22- and 40-vane stators to investigate the cutoff criterion of having sufficient stator vanes to prevent propagation of the fundamental rotor tone. The model was tested over a range of rotor speeds and at angles of attack up to  $30^\circ$ . Acoustic data were acquired with an array of fixed microphones located on the tunnel wall and with a translating microphone probe affixed to the tunnel floor. Results from these tests will be used to better define parameters for future quieter and more efficient ducted propellers.

**Lewis contact:** Richard P. Woodward, (216) 433-3923  
**Headquarters program office:** OAST



*Advanced ducted propeller model in wind tunnel.*

### **Stationary Blockage Devices Simulate Inlet Separation Angle of Attack in an ADP Simulator**

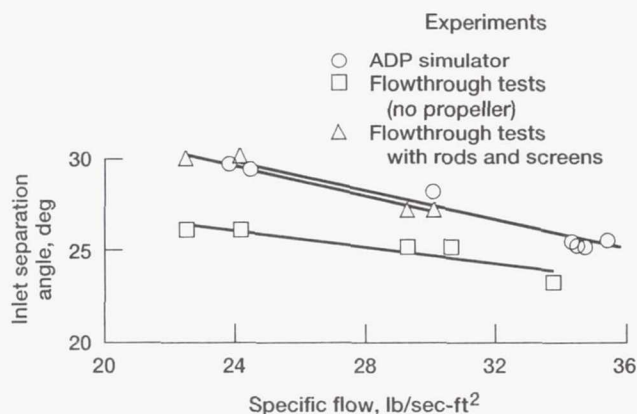
Inlet performance tests are often performed in wind tunnels with an aspirated flow to simulate the flow rates that would be pumped by a fan or ducted propeller in a powered-rig test. Recently tests were conducted with the Pratt & Whitney 17-in. Advanced Ducted Propeller (ADP) simulator in the NASA Lewis 9- by 15-Foot Low-Speed Wind Tunnel with aspirated flow (no propeller). Pratt & Whitney's comparison of the results has shown that an operating propeller delays inlet separation. Experiments with short inlets have shown that this interaction can be appreciable, especially with the aggressive designs being considered for the ADP class of ultra-high-bypass engines. In order to better understand the fan/inlet interaction problem, a joint effort between NASA Lewis and Pratt & Whitney was undertaken. Many of the problems with past experiments of this type were eliminated by using the same inlet hardware, instrumentation locations, and fine angle-of-attack settings and by the ability to match airflow rates in tests with and without a propeller.

In order to circumvent the problem of performing inlet tests without a powered propeller, and thus improve the agreement between aspirated-flow and powered-rig results, stationary flow blockage devices were installed in the inlet to replace the powered propeller. Several blockage configurations were tested, including screens and combinations of screens and rods. The best simulation of powered-rig inlet separation angle of attack was obtained with a blockage geometry comprising a combination of tapered rods and screens.

Experimental results of inlet separation angle as a function of specific flow clearly reveal the differences between powered-rig results and aspirated-flow tests. Furthermore, the experiments with the stationary blockage device showed that the separation angle was within  $1^\circ$  of the powered-rig test results.

An important ramification of these results concerns the method in which aspirated-flow inlet tests are performed. The inclusion of a stationary blockage device to replace the operating propeller can provide a better simulation of the separation angle of attack than the more traditional aspirated-flow tests without blockage.





Experimental separation angle of attack. Free-stream Mach number, 0.2; propeller area, 187.7 in.<sup>2</sup>; conventional inlet.

### Bibliography

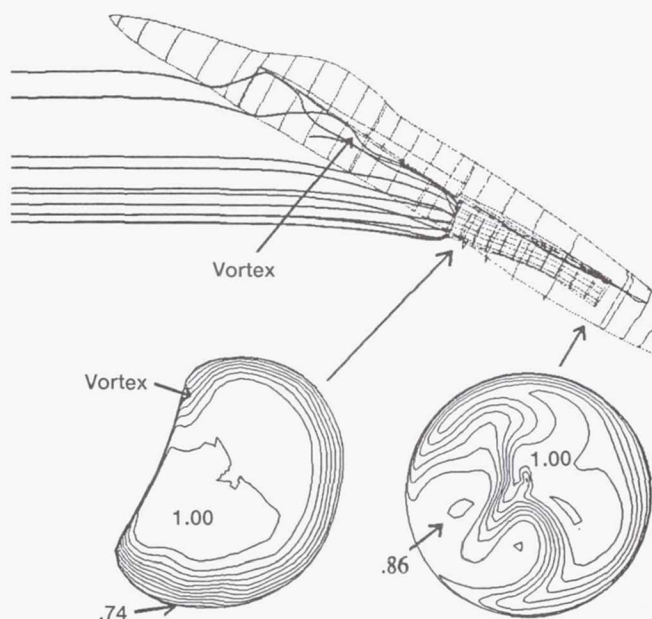
Boldman, D.R., et al.: Evaluation of Panel Code Predictions With Experimental Results of Inlet Performance for a 17-Inch Ducted Prop/Fan Simulator Operating at Mach 0.2. AIAA Paper 91-3354, June 1991. (Also, NASA TM-104428.)

**Lewis contact: Chanthy Iek, (216) 433-3897**  
**Headquarters program office: OAST**

### F-18 Inlet Flow Calculated at High Angles of Attack

NASA Lewis is currently engaged in a research effort as a team member of the High Alpha Technology Program (HATP) within NASA. This program utilizes a specially equipped F-18, the high alpha research vehicle (HARV), in an ambitious effort to improve the maneuverability of high-performance military aircraft at low-subsonic-speed, high-angle-of-attack conditions. The overall objective of the Lewis effort is to develop inlet technology that will ensure efficient airflow delivery to the engine during these maneuvers. One part of the Lewis approach utilizes computational fluid dynamics codes to predict the installed performance of inlets for these highly maneuverable aircraft.

The PARC3D code, a three-dimensional Navier-Stokes solver, is being used to calculate the flow field ahead of and inside the inlets of the HARV



Normalized F-18 total pressure contours.

and a subscale F-18 model. A sample of the preliminary computational results is presented here for a 19.78-percent scale model at 30° angle of attack. The particle trajectories indicate that a vortex shed from the forebody is deflected by the leading-edge extension and enters the inlet. The thicker contours along the lower side of the inlet entrance are the result of flow separation from the lower lip. The presence of the ingested vortex is indicated by the contour shape in the upper left-hand region of the inlet entrance. The combination of ingested vortex and lip flow separation results in the large total pressure distortion at the exit of the inlet duct (i.e., at the engine face plane).

The preliminary results demonstrate the capability of the PARC3D code to predict the extremely complex flow field near an inlet.

**Lewis contacts: Richard R. Burley, (216) 433-3605;**  
**C. Frederic Smith, (216) 826-6708**  
**Headquarters program office: OAST**

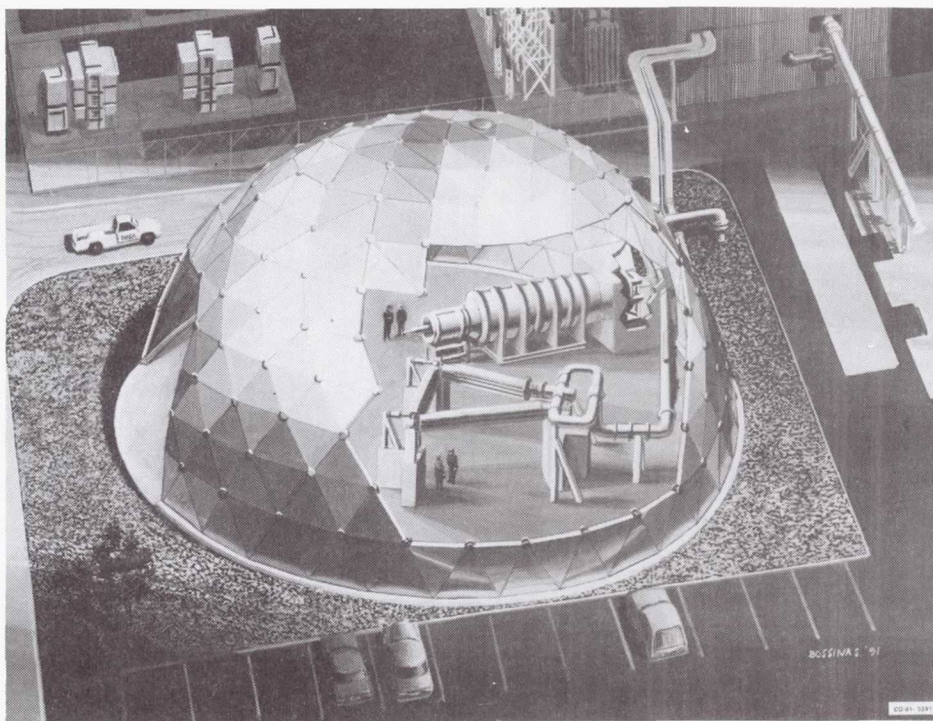
## Acoustic Dome Constructed

NASA Lewis has constructed an acoustically treated geodesic dome to enclose the Powered Lift Facility (PLF) and the Nozzle Acoustic Test Rig (NATR). Its construction will permit nearly unrestricted testing of powered-lift concepts that have application to short-takeoff-and-vertical-landing aircraft and of exhaust nozzles for High-Speed Research. The dome was constructed in response to a need to alleviate a potential source of irritation to the nearby community—the noise generated by high-velocity air from the research hardware. The dome accomplished this. The added benefit is a site in which acoustic measurements can be made in a controlled environment for nozzle concept evaluations. The dome wall is lined with acoustic material that minimizes sound reverberation within the structure, making these acoustic measurements possible.

The acoustic dome is a 130-ft-diameter geodesic dome. Anodized structural members, or struts,

form the basic triangular pattern of the dome. Starting from the inside of the dome, the triangular panels of the wall consist of a sheet of aluminum, followed by fiberglass insulation, then an air gap, another sheet of aluminum, and finally a thin, layered outer panel of aluminum. Acoustic measurements during initial tests have confirmed predictions that the untreated dome walls attenuate the noise by at least 20 dBA. Atmospheric attenuation between the dome and the nearest neighborhood accounts for additional sound suppression. Acoustic treatment, in the form of fiberglass wedges, was placed on the inside surface of the dome—with 2-in. minimum standoff from the wall. This will permit nozzle acoustic measurements to be made without sound reflections from the wall. An added benefit of the construction is that the enclosure allows year-round testing.

**Lewis contact:** Richard L. Barth, (216) 433-5686  
**Headquarters program office:** OAST



*Acoustic dome.*



# Aerospace Technology

## Materials

### Advanced High-Temperature Engine Materials Technology Continues Progress

The objective of the Advanced High-Temperature Engine Materials Technology (HITEMP) Program is to generate technology for revolutionary advances in composite materials and their structural analysis that will enable the development of 21st century civil propulsion systems with greatly increased fuel economy, improved reliability, extended life, and reduced operating costs. The primary focus is on polymer, metallic, intermetallic, and ceramic-matrix composites. These composite materials are being developed by in-house researchers and on grants and contracts for eventual use in fans, compressors, and turbines for future civil transport aircraft.

NASA considers this program to be a focused materials and structures research effort that builds upon our basic research programs and will feed results into application-oriented projects, such as the proposed NASA new initiative to develop the technology for a 21st century high-speed civil transport. HITEMP is also closely coordinated with the Department of Defense/NASA Integrated High Performance Turbine Engine Technology (IHPTET) Program, and new composite materials from HITEMP may be used in future military applications.

A Lewis-developed polymer resin has been selected to replace portions of a F110 forward fairing. Parts have been fabricated and will be engine tested in early 1992. A Lewis-developed

process of postcuring polymer composites in nitrogen gas results in composites with significantly higher use temperature capability. This process won a 1991 R&D 100 Award. Lewis researchers have developed a model to determine the high-temperature creep strength of silicon carbide ceramic fibers. Three invention disclosures have been filed recently by Lewis researchers on a process of fabricating strong, tough fiber-reinforced ceramic composites. The wire arc spray process has been used to successfully fabricate high-quality silicon-carbide-reinforced titanium aluminide intermetallic composites. Lewis researchers have shown that elastic-plastic analytical models accurately represent the experimentally observed deformation behavior of titanium alloy composites.

The fourth annual review of the HITEMP program was held October 29 and 30, 1991. Details of research accomplishments are published in a conference report, NASA CP-10082.

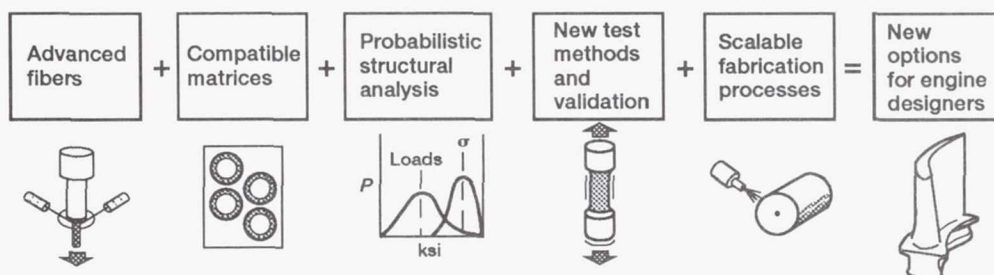
**Lewis contact:** Dr. Hugh R. Gray, (216) 433-3230  
**Headquarters program office:** OAST

### Materials Program Supports HSCT

NASA is undertaking a materials research and development program in support of the development of a high-speed (supersonic) civil transport (HSCT) for entry into commercial service by the year 2005.

The objectives of the Enabling Propulsion Materials (EPM) Program are

- To develop high-temperature advanced materials including fibers, ceramic-matrix compos-



Elements of HITEMP program.

ites, and lightweight intermetallic matrix composites/metal-matrix composites

- To establish improved processes for fabricating advanced composite components
- To enhance the development of analytical tools for composite and component design, fabrication, and life prediction
- To develop improved procedures for testing composite subcomponents
- To evaluate composite subcomponent and component reliability and durability in a rig or engine environment. The primary focus is on demonstrating the technology readiness of a combustor liner and an exhaust nozzle for an HSCT propulsion system by 1999.

EPM will be primarily a contractual effort involving the team of the two major U.S. aircraft engine manufacturers, Pratt & Whitney (P&W) and General Electric Aircraft Engines (GEAE). In addition, a broad-based subcontractor team will include other engine companies, fiber producers, composite fabricators, testing companies, and academia. Complementing this contractual effort will be an in-house program that will address risk reduction issues.

A unique feature of EPM is the establishment of integrated product development teams for the combustor liner and the exhaust nozzle. These teams will consist of representatives from P&W, GEAE, NASA, and subcontractors where appropriate. Members will be from various disciplines including engineering expertise in design, processing, materials, structures, and test operations. The major benefit of these teams will be to reduce the risk of the materials development.

The enormous challenge of developing materials for an HSCT engine required an immediate response from NASA Lewis and industry. Therefore, NASA Lewis has awarded two preliminary contracts that involve materials development for HSCT engines. A contract awarded to P&W contains guidelines for developing the materials for various HSCT engine components. An important accomplishment of this contract will be to establish a materials data base related to the physical and mechanical properties and the environmental durability of a commercial silicon-carbide (SiC)-reinforced silicon nitride (Si<sub>3</sub>N<sub>4</sub>) ceramic-matrix

composite. A second preliminary contract awarded to GEAE deals specifically with materials for HSCT combustors. A major accomplishment of the GEAE contract has been quantifying the need for using a high-thermal-conductivity CMC in an HSCT combustor liner. A materials data base is being established, in this case for an SiC-reinforced SiC ceramic-matrix composite developed by GEAE. A significant effort has been given to characterizing the thermal shock behavior of the SiC/SiC composite because thermal shock could be life limiting in a ceramic-matrix composite combustor liner.

The in-house efforts at NASA Lewis have made significant contributions to the development of materials for HSCT engines. NASA Lewis' unique ability to conduct environmental durability tests of candidate materials is critical to the overall program. The tests are performed in a high-pressure burner rig that simulates the HSCT combustor environment while thermally cycling the materials as in an actual HSCT mission. Additional in-house research includes studies of environmental degradation mechanisms, ceramic fiber and matrix development and characterization, and development of novel ceramic materials designed to alleviate the risk involved in HSCT materials development.

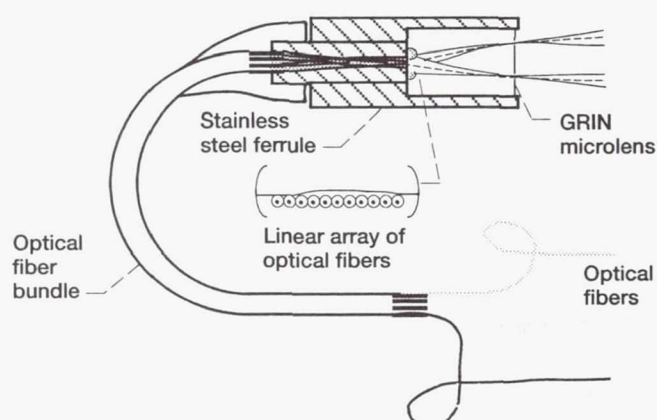
**Lewis contact:** Joseph R. Stephens, (216) 433-3195  
**Headquarters program office:** OAST

### Laser Light Scattering Opens New Frontiers

Light scattered from jostling particles suspended in a liquid reveals a wealth of information about their submicroscopic world. With recent developments in laser light scattering, we have been able to coax this display of Brownian motion into answering questions about fractal growth, oil recovery, polymers, pigments, cataracts, and crystal formation. When used in space these instrument advances will provide answers to many basic science questions.

This window into the world of macromolecules will allow space scientists to interact with their experiments as they progress, permitting experiments that have not been possible until now. Nucleation, spinodal decomposition, gelation, critical phenomena, aggregation, and diffusion, to





Multiple-fiber optic probe.

name a few, are influenced by gravity and can be better studied in outer space, free from the convective flows and sedimentation caused by gravity.

Prior to flight hardware development, the Advanced Technology Development Project in laser light scattering at NASA Lewis devised and coordinated the development of a compact, miniature, solid-state laser light scattering instrument. This reliable, low-power instrument will allow inexpensive science to be conducted in a compact space. Building on the work of R.G.W. Brown and others, we have taken an instrument that used to fill a small laboratory and fit it into a small briefcase. This modular instrument design allows us to plug miniature fiber optic probes into pocket-sized laser and photon-counting modules attached to a laptop computer, making it a complete system for rapid data acquisition and analysis. This spinoff is essentially an enhanced instrument capable of making on-line quality control measurements.

The fiber optic probes developed under a NASA grant at the State University of New York-Stonybrook by H.S. Dhadwal when pushed by in-house tests of their potential have opened new areas of research. This probe makes rapid and noninvasive measurements for the early detection of cataracts. Tests have been performed on excised bovine eye lenses and the probe awaits in-situ clinical trials for complete eye diagnostics. These probes have also proved invaluable for measuring the size of particles in concentrated (milky white) solutions, thus enabling the instrument's use as a process control monitor for both industrial and laboratory applications.

The laser light scattering technology guided by NASA's Advanced Technology Development Project has significant commercial potential. For example, our recent laser light scattering studies with DuPont have provided new insights into the structure of nylon, a 7.6-billion-pound-a-year product. When these hardware advances are introduced for quality control monitoring, they will offer U.S. companies a way to tailor their products for niche markets.

#### Bibliography

Dhadwal, H.S.; Ansari, R.R.; and Meyer, W.V.: A Fiber Optic Probe for Particle Sizing in Concentrated Suspensions. *Rev. Sci. Instrum.*, vol. 62, Dec. 1991.

Dhadwal, H.S.; and Ansari, R.R.: Multiple Fiber Optic Probe for Several Sensing Applications. *Proceedings of SPIE International Symposium on Opto-Electronics/Fibers '91*, Boston, MA, Sept. 3-6, 1991.

Meyer, W.V.; and Ansari, R.R.: A Preview of a Microgravity Laser Light Scattering Instrument. *AIAA Paper 91-0779*, Jan. 1991.

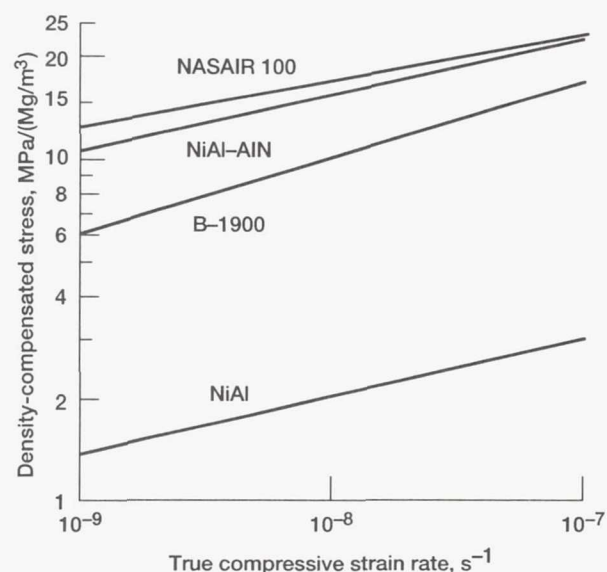
**Lewis contacts: William V. Meyer, (216) 433-5011; and Dr. Rafat R. Ansari, (216) 433-5008**  
**Headquarters program office: OSSA**

#### New High-Temperature Composite Strengthened

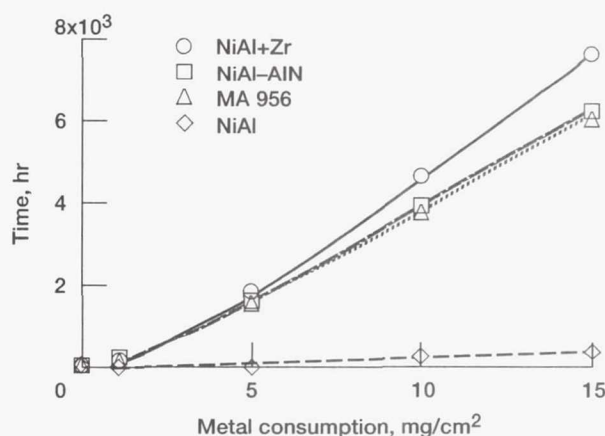
The simplest way to improve the efficiency of jet aircraft engines is to increase their operating temperature. This cannot be accomplished with existing nickel-base superalloys because they are already used at temperatures very close to their melting points. Hence, a new high-temperature structural material is needed, and the intermetallic composed of equal numbers of nickel and aluminum atoms (NiAl) has many attractive features. For example, this aluminide melts at about 1910 K (2980 °F), whereas superalloys melt at ~1600 K (2420 °F); it can form a protective oxide coating in air at high temperatures, whereas most alloys cannot; it weighs about two-thirds of an equal volume of superalloy; and finally it conducts heat four times better than nickel alloys. In spite of these properties NiAl cannot presently be employed in engines because it lacks mechanical strength at elevated temperatures. Therefore, methods to improve its strength are being investigated.

Recently, an informal joint effort by NASA Lewis, Exxon Research and Engineering Company, and the Max Planck Institut für Metallforschung has found that cryomilling (a grinding process carried out in liquid nitrogen) NiAl powder produces a high-strength, elevated-temperature composite. During cryomilling the powder particles are fractured into smaller bits, and the near surface layer of each piece becomes supersaturated with nitrogen atoms (N). When the as-cryomilled powder is consolidated by compression under high temperature and pressure conditions, the nitrogen reacts with the aluminum to form very small-diameter (~50 nm, or 0.000002 in.) AlN particles. Because the nitrogen absorbed during cryomilling is located only at near-surface regions, the composite has a unique microstructure composed of cores of pure NiAl surrounded by a thin coating of aluminide containing a very high density of small AlN particles.

Measurement of its 1300 K (1880 °F) mechanical properties has shown that the NiAl-AlN composite is about 10 times stronger than unreinforced NiAl and is much stronger than a typical nickel-base superalloy (B-1900). Furthermore, on a density-compensated basis this composite is nearly as strong as one of the newest generation of single-crystal superalloys (NASAIR 100). In addition, cyclic oxidation testing found that the behavior of NiAl-AlN was nearly equivalent to that of the best third-element-doped aluminide (NiAl+Zr), which is as good as the most oxidation-resistant, commercially available alloy (MA 956). All three of these



Density-compensated 1300 K (1880 °F) creep strength of several high-temperature materials as a function of strain rate.



Time for calculated metal consumption by oxidation for several high-temperature alloys at 1473 K (2200 °F).

materials have better oxidation properties than NiAl.

Several technical papers outlining the properties of NiAl-AlN have been published, and work is currently being undertaken at all three laboratories to understand the cryomilling process, the reproducibility of the technique, and the reasons for the high-temperature strength and oxidation resistance of the composite. NiAl-AlN is under consideration for use as a structural material and is also being studied as a potential matrix for fiber-reinforced composites.

#### Bibliography

Lowell, C.E.; Barrett, C.A.; and Whittenberger, J.D.: Cyclic Oxidation Resistance of a Reaction Milled NiAl-AlN Composite. *Intermetallic Matrix Composites*, MRS Symp. Proc. Vol. 194, D.L. Anton, et al., eds., Materials Research Society, Pittsburgh, PA, 1990, pp. 355-360.

Whittenberger, J.D.; Arzt, E.; and Luton, M.J.: 1300 K Compressive Properties of a Reaction Milled NiAl-AlN Composite. *J. Mater. Res.*, vol. 5, 1990, pp. 2819-2827.

**Lewis contact: Dr. J. Daniel Whittenberger,**  
(216) 433-3196  
**Headquarters program office: OAST**



*The 1991 Lewis Research Center Distinguished Publication Award*

**$\gamma'$  Coarsening in High Volume Fraction Nickel-Base Alloys**

The 1991 Lewis Research Center Distinguished Publication Award was presented to Dr. Rebecca A. MacKay and Dr. Michael V. Nathal in recognition of the excellence and value of their publication entitled, " $\gamma'$  Coarsening in High Volume Fraction Nickel-Base Alloys." The distinguished paper was published in the June 1990 issue of *Acta Metallurgica et Materialia*. This paper documents a comprehensive experimental research project that contributes to the theoretical understanding of nickel-base alloys and also has a very practical effect on alloy design.

The gas turbine engine industry has been concerned for over 40 years with the long-time, high-temperature stability of nickel-base superalloys, which are used extensively in the hot section of gas turbine engines. Superalloy microstructures consist of  $\gamma'$  particles in a matrix of  $\gamma$  phase; the  $\gamma'$  particles provide these superalloys with much of their high-temperature strength. However, as the  $\gamma'$  particles coarsen, or grow, with time at high temperatures, the load-carrying capability of the alloy degrades, limiting both life and maximum load.

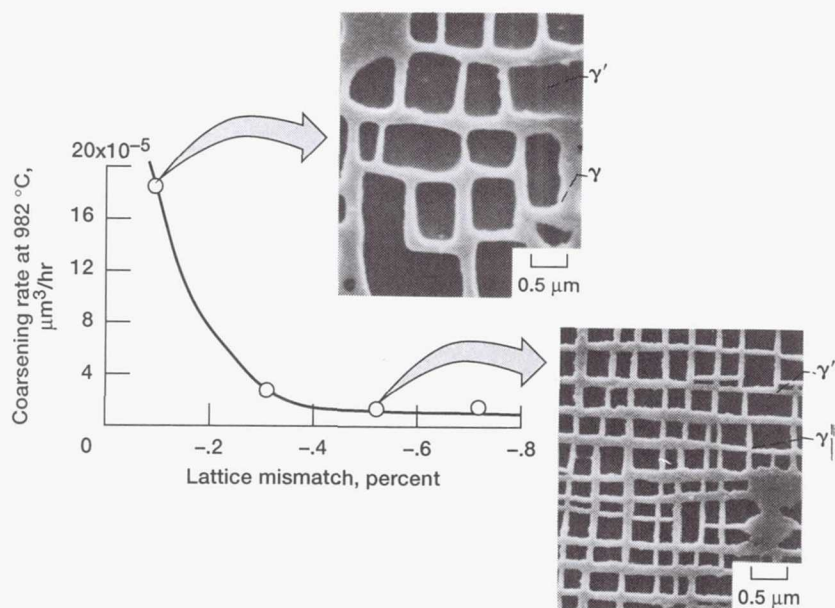
This study addressed the issue of  $\gamma'$  coarsening. Specifically, it examined the  $\gamma'$  coarsening behavior in a systematic series of alloys having different magnitudes of  $\gamma$ - $\gamma'$  lattice mismatch. Lattice mismatch refers to the difference in the lattice spacing between the atoms in the  $\gamma$  and  $\gamma'$  phases. This study determined that current theories neither adequately explain nor predict  $\gamma'$  coarsening because elastic coherency strains and lattice mismatch were not incorporated in these theories. Additionally, the study concluded that increasing the magnitude of the lattice mismatch actually leads to a more stable  $\gamma'$  that is far less susceptible to coarsening. This is contrary to the accepted practice for the past 45 years in which alloy developers have attempted to minimize this difference in atomic spacing. This new concept will alter the direction of alloy development and will lead to dramatically improved and more stable gas turbine alloys.

**Bibliography**

MacKay, R.A.; and Nathal, M.V.:  $\gamma'$  Coarsening in High Volume Fraction Nickel-Base Alloys. *Acta Metall. Mater.*, vol. 38, no. 6, 1990, pp. 993-1005.

MacKay, R.A.; Nathal, M.V.; and Pearson, D.D.: Influence of Molybdenum on the Creep Properties of Nickel-Base Superalloy Single Crystals. *Metall. Trans. A*, vol. 21A, 1990, pp. 381-388.

**Lewis contacts: Dr. Rebecca A. MacKay, (216) 433-3269;  
Dr. Michael V. Nathal, (216) 433-3197  
Headquarters program office: OAST**



Coarsening rate at 982 °C as function of lattice mismatch. Photographs after 200 hr.

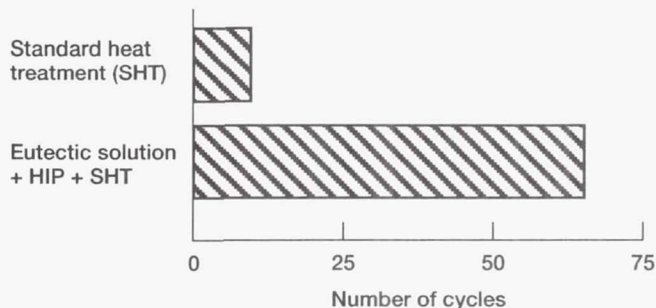
## Processing Improved for Single-Crystal Turbine Blades

Among the components that limit the lives of the Space Shuttle main engine (SSME) high-pressure turbopumps are the turbine blades. The blades are subject to fatigue cracking, which is caused by both a high-frequency flutter and the lower number of larger strain cycles associated with engine starts, stops, and changes in power level. The hydrogen-rich environment in the turbine also contributes to the problem. Laboratory tests have shown that the presence of hydrogen degrades the behavior of alloys relative to that in air or inert gas environments. Because of this hydrogen-aggravated fatigue problem the service life of the SSME blades is limited to a specified number of seconds of operation to assure flight safety of the vehicle.

One approach being considered for extending the service life of the blades is to change to a carbon-free single-crystal alloy. The directionally solidified nickel-base alloy currently specified as bill of materiel contains carbides and has a columnar polycrystalline structure. Carbon-free single crystals have been shown to extend fatigue life because they lack both the boundaries between crystals and the carbides that may act as fatigue crack initiation sites. More recently, Carnegie Mellon University, working under a grant, demonstrated that the tensile ductility of single-crystal nickel-base superalloys charged with hydrogen can be improved by using thermomechanical treatments that remove two microstructural features, microporosity and eutectic  $\gamma/\gamma'$  nodules. These eutectic nodules represent a poor distribution of the strengthening  $\gamma'$  phase. The thermomechanical treatments consisted of a long, high-temperature heat treatment to dissolve the eutectic  $\gamma/\gamma'$  nodules, followed by hot isostatic pressing (HIPing) to close the porosity, and then the standard heat treatment to properly distribute the  $\gamma'$ .

Recent work performed at NASA Lewis has shown directly that these same thermomechanical processes are beneficial in increasing the low-cycle fatigue life of PWA 1480, a hydrogen-charged, nickel-base, single-crystal alloy.

Hydrogen charging of standard PWA 1480, which contains the normal levels of porosity and eutectic  $\gamma/\gamma'$ , reduces the room-temperature, strain-controlled fatigue life by more than one order of



Room-temperature fatigue life at 2-percent strain range.

magnitude. Fatigue initiation sites in hydrogen-charged standard PWA 1480 are easily identified by large flat facets on the fracture surface. At the center of each facet a large pore, a  $\gamma/\gamma'$  eutectic, or both could be found at high magnification. Substantially longer fatigue life after hydrogen charging was measured for PWA 1480 that had been given the eutectic solution treatment plus HIPing. Porosity and eutectic content were significantly lower than that for standard PWA 1480. Furthermore, the degree of facet formation on the fracture surface of tested specimens was also greatly reduced. The reduction in porosity level achieved by this duplex thermomechanical treatment suggests that closure of porosity is more readily achieved if eutectic content is minimized before HIPing.

It is indicated that using single crystals given the improved thermomechanical treatment would improve the durability of SSME turbine blades and thus may reduce launch costs.

**Lewis contacts:** Dr. Robert Dreshfield, (216) 433-3267; Dr. John Gayda, (216) 433-3273  
Headquarters program office: OAST

## Engineered Interface Eliminates Thermal Ratcheting in Graphite-Fiber-Reinforced Copper-Matrix Composites

Many applications require materials that combine high strength, stiffness, and conductivity with low-to-moderate density. Among the applications of interest to NASA Lewis are heat exchangers for the National Aerospace Plane (NASP) and other hypersonic vehicles and for space power system radiator fins. Work is currently focused on graphite-fiber-reinforced copper matrix (Gr/Cu) composites. Densities range from 4.5 to 5.5 g/cm<sup>3</sup> for the fiber volume fractions of inter-



est. Ultra-high-modulus, pitch-based fibers have up to three times the conductivity of copper, and high-strength polyacrylonitrile-based fibers can have ultimate tensile strengths approaching 1 million psi. Pitch-based fibers, such as Amoco P-100, are favored to increase the stiffness and in-plane thermal conductivity of space radiator fins. Heat exchangers for the NASP combustor section utilize high-strength fibers to increase the in-plane strength of the facesheets. Good through-thickness conductivity for all Gr/Cu composites comes from the copper matrix.

Graphite and copper are noted for their lack of wetting, reaction, and solubility with one another. This combination of properties leads to only a weak mechanical bond across the Gr/Cu composite interface. Voids form in the composite at elevated temperatures because copper migrates away from the graphite fibers. The transverse strength of these composites is also very low. In order to improve these properties, an engineered interface must be introduced to promote wetting and bonding between the copper matrix and the graphite fibers. An extensive wetting study has shown several potential copper alloys that can wet graphite fibers. The wetting study and prior work with copper-matrix composites has also indicated several refractory metals that can be used as fiber coatings to promote good bonding. Work is ongoing to produce and evaluate the effects of adding an engineered interface to Gr/Cu composites.

Traditionally Gr/Cu composites have been produced by hot pressing copper-coated graphite fiber preforms. A more economical production

method currently being pursued is pressure infiltration casting. Liquid copper or copper alloy is forced into a fiber preform to form the composite. Complex net shape parts can be produced easily.

The thermal expansion of Gr/Cu composites is of particular interest because of the need to minimize the mismatch in coefficient of thermal expansion (CTE) between the composite plates and other structures, such as heat pipes and manifolds. Excessive CTE mismatch will lead to thermal stresses that can fail the joint between the composite and other structure. Varying the architecture and the volume fraction is being examined as a way to minimize CTE mismatch.

Preliminary testing of composites without an engineered interface revealed a large hysteresis in the thermal expansion curves. This hysteresis is a permanent deformation of the sample to a strain of 0.5 percent. Repeated thermal cycling could therefore build up considerable deformation in the composite, a process called thermal ratcheting. Adding chromium to a pressure-infiltrated copper matrix resulted in the formation of a thin chromium carbide layer around the graphite fibers. This bar showed no signs of damage after undergoing the same thermal cycle as the cast bar. Furthermore, there was no hysteresis in its thermal expansion curves. Samples prepared by pressure infiltrating pure copper into fibers coated with titanium and tungsten showed the same beneficial effects. The low alloying content or thin fiber coating should not significantly reduce the thermal conductivity of the material. The transverse strength of the composites is also expected to improve because load can be transferred across the interface and into the fiber.

The results from these first tests strongly indicate that the use of an engineered interface can greatly improve the properties of Gr/Cu composites and overcome problems such as thermal ratcheting.

**Lewis contact: Dr. David Ellis, (216) 433-8736**  
**Headquarters program office: OAST**



(a)



1 cm



(b)



1 cm

Bars after one thermal cycle from room temperature to 800 °C (1472 °F): (a) cast bar showing macroscopic shear bands and cracking of the copper matrix; (b) bar produced by pressure infiltration casting with matrix of copper-0.1 wt% chromium alloy instead of pure copper, showing no damage.

## Stability of Ceramics in Hydrogen Evaluated

Ceramic materials in the form of matrices, fibers, and coatings are considered enabling for many advanced aerospace propulsion systems. In some applications such as the National Aerospace Plane and rocket propulsion, the ceramics must be stable in hot hydrogen environments.

Using thermodynamic predictions is one way to gain an understanding of the thermal stability of a material in hydrogen-containing atmospheres. With the aid of a state-of-the-art computerized thermodynamic prediction program called SOLGASMIX-PV, the hydrogen compatibility of a variety of potentially useful ceramic materials was evaluated.

In order to validate the thermodynamic predictions, a number of ceramic materials were exposed to wet hydrogen at temperatures to 1400 °C. Postexposure evaluation provided information on the validity of the thermodynamic predictions and an insight into the morphology of hydrogen attack, if any. By using a stability criterion of  $\leq 1$  ppm of reaction product species in the vapor phase, it was found that thermodynamics offers a good guide to identifying promising materials in hot hydrogen environments.

Experimental results verified the predicted stability of selected ceramics: silicon carbide and silicon nitride are stable to approximately 1100 °C in dry hydrogen and to higher temperatures in wet hydrogen; alumina is stable to 1350 °C in dry hydrogen and to over 1800 °C in wet hydrogen; mullite is unstable at or above 1100 °C, even in wet hydrogen; and titanium diboride is unstable in hydrogen at all moisture levels.

## Bibliography

Herbell, T.P.; Eckel, A.J.; and Misra, A.K.: Effect of Hydrogen on the Strength and Microstructure of Selected Ceramics. *Environmental Effects on Advanced Materials*, Russell H. Jones and Richard E. Ricker, eds., The Minerals, Metals and Materials Society, 1991, pp. 159-172.

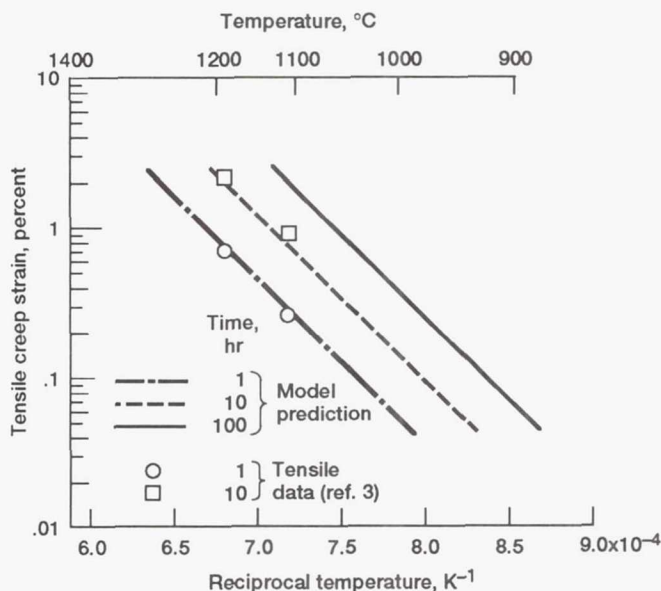
**Lewis contacts:** Dr. Thomas P. Herbell, (216) 433-3246; Andrew J. Eckel, (216) 433-8185  
Headquarters program office: OAST

## Creep Modeled for Polycrystalline Ceramic Fibers

Before a structural ceramic composite material can be applied in an advanced aerospace component, the composite's high-temperature deformation must be understood as a function of such key service conditions as stress, time, and temperature. Because creep of the fiber reinforcement controls this deformation, a recent in-house study at Lewis has focused on measuring and modeling creep behavior for a variety of currently available polycrystalline ceramic fibers (ref. 1).

For constant stress and temperature conditions it is assumed that the tensile creep of all polycrystalline fibers can be analytically modeled by a simple relation containing four empirically determined parameters. The Lewis-developed bend stress relaxation (BSR) test, which is much simpler and more convenient than a typical tensile creep test (ref. 2), was used to measure the creep parameters for silicon-carbide-based fibers (SCS-6 and Nicalon) and alumina-based fibers (FP and PRD-166). Excellent agreement was found between the model-predicted creep strain and actual tensile creep strain data reported in the literature.

The results of this study confirm both the predictive capability of the creep model and the use of the BSR test as a simple method for determining polycrystalline ceramic fiber parameters. Given information on component application conditions



Comparison of predicted and actual creep for Nicalon fiber at stress of 0.5 GPa.



and creep design limits, the model can now be used to estimate optimum service times, temperatures, or both for potential fiber-reinforced ceramic composites. This insight is being employed to determine whether current fibers are suitable for NASA's advanced engine programs or whether new fibers with improved creep resistance need to be developed.

#### References

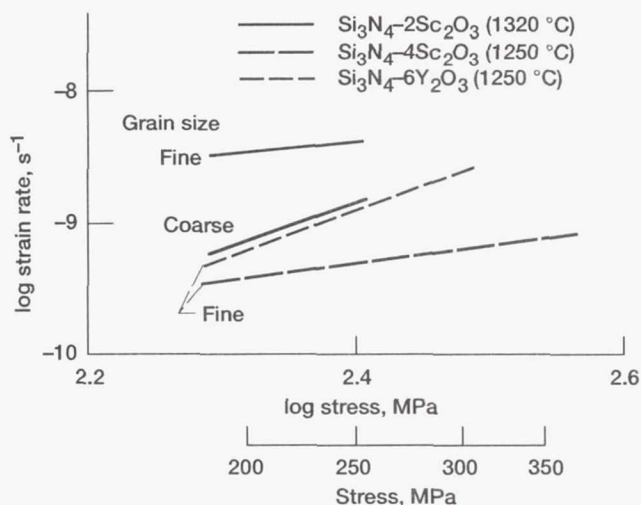
1. Morscher, G.N.; and DiCarlo, J.A.: A Simple Test for Thermomechanical Evaluation of Ceramic Fibers. NASA TM-103767, 1991.
2. Jia, N.; Bodet, R.; and Tressler, R.E.: Creep and Creep Rupture Behavior of Si-C-O and Si-N-C-O Based Continuous Fibers, Presented at 93rd Annual Mtg. of Amer. Ceram. Soc., Cincinnati, OH, 1991.

**Lewis contacts:** Dr. James A. DiCarlo, (216) 433-5514;  
Gregory N. Morscher, (216) 433-8675  
**Headquarters program office:** OAST

### Processing Optimization Improves Flexural Creep Resistance of Sintered Silicon Nitride

The high-temperature creep resistance of sintered silicon nitride is of primary importance in the application of this material in a monolithic component or as the matrix in a ceramic-matrix composite component for advanced heat engines. The additives required to densify silicon nitride ( $\text{Si}_3\text{N}_4$ ) and processing parameters such as powder grinding time and sintering and heat treatment times and temperatures have been studied at NASA Lewis to improve creep resistance. Improvements have been realized by processing refinements.

The creep resistance of silicon nitride has been improved by introducing a previously untried densification aid, scandium oxide ( $\text{Sc}_2\text{O}_3$ ). The use of this more refractory oxide in relatively small amounts resulted in full densification of silicon nitride by conventional sintering for 4 hr at 2140 °C under 25-atm nitrogen pressure. Neither hot pressing nor hot isostatic pressing were required for full densification. The scandium oxide combines with the inherent or intentionally added silica to form a liquid phase for sintering. The scandia-silica liquid phase is unique in that it readily crystallizes on cooling after sintering and results in a stronger, more deformation-



Improved flexural creep of sintered silicon nitride matrices.

resistant grain boundary phase. This is in contrast to other oxide additives, such as yttrium oxide ( $\text{Y}_2\text{O}_3$ ), where the second phase in the as-sintered silicon nitride remains glassy and causes the material to creep. Although analyses by transmission electron microscopy and x-ray diffraction indicate a preponderance of crystalline silicate grain boundary phase in the silicon nitride-scandia materials, heat treatment may promote further crystallization. Creep resistance has also been found to depend strongly on the grain size and morphology of the silicon nitride-scandia materials. Coarse structures and acicular grain shapes have been found to contribute to deformation resistance. A coarse-grain 2-wt%  $\text{Sc}_2\text{O}_3$  material showed nearly a 120 deg C advantage over a 6-wt%  $\text{Y}_2\text{O}_3$  material. Efforts are ongoing to develop microstructures for further improvements in creep resistance.

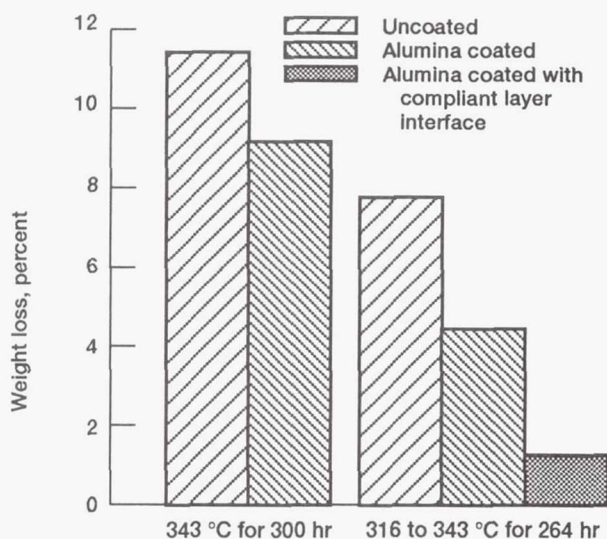
**Lewis contact:** William A. Sanders, (216) 433-3297  
**Headquarters program office:** OAST

### Oxidation-Resistant Coatings Tested on High-Temperature Polymer Composites

The potential to replace current aerospace materials with less expensive and easier-to-manufacture lightweight polymer composites is presently limited by the maximum temperature the polymer composite can endure. At elevated temperatures polymer matrix composites (PMC's) experience oxidation-induced decomposition and a loss of

mechanical strength. However, a category of polymer material (polyimide, PMR-II) that meets almost all the required specifications has recently been developed (ref. 1). It is nonflammable and easy to cast, has a threefold higher specific strength than titanium, and can be utilized up to 370 °C. This temperature is 55 deg C lower than the target temperature of 425 °C, which would permit the widespread incorporation of this polymer composite into jet engines and related structural supports. The material remains vulnerable to oxidation at temperatures greater than 370 °C. Therein lies the rationale for developing an oxidation-resistant coating that would encapsulate the PMC and prevent oxygen from contacting it and reacting with it.

Depositing an adherent, oxidation-resistant impermeable ceramic, or metallic, barrier on a material with a significantly different thermal expansion behavior is a unique problem. Special attention must be given to the stresses imposed on the coating by the dimensional changes that occur over the temperature gradient (~400 deg C) encountered. Additionally, the complex shapes and comparatively low temperature tolerance of the PMC restrict the coating techniques available. Currently, metal-organic chemical vapor deposition, plasma-enhanced chemical vapor deposition, and physical vapor deposition are used to deposit alumina, diamond-like carbon, and metallic coatings, respectively.



Oxidation results for PMR-15 coated by chemical vapor deposition.

Tests of alumina coatings on PMR-15, a predecessor of the still experimental PMR-II that is currently used in jet engines, demonstrate that the oxidation-induced weight loss of PMR-15 can be significantly reduced. However, the degree of protection afforded depends upon the adhesion of the coating and the microstructure of the coating material. Furthermore, the adhesion of the coating depends upon the coating thickness, the use of a compliant interfacial layer, the bond strength at the coating/substrate interface, and the thermal expansion coefficients of the substrate and the coating. Diamond-like carbon coatings exhibited excellent adhesion to the polymer substrate, possibly because of the chemical compatibility of the coating and the negligible oxidation at 370 °C. Adherent metallic coatings (NiTiB<sub>3</sub>, AuPd, Al, and NiCrAlY) have been achieved, but little improvement in oxidation resistance at high temperatures (>315 °C) has been realized.

Continuing research is aimed at developing the techniques to effect the low-temperature deposition of oxidation-resistant materials that can accommodate the temperature-induced stresses and deposit a material which is both resistant to oxidation and impermeable to oxygen diffusion.

#### Reference

1. Vannucci, R.D.; and Cifani, D.: 700 °F Properties of Autoclave Cured PMR-II Composites. *Materials Processes: The Intercept Point*, C. Prosen and D. Meth, eds., SAMPE, 1988, pp. 562-575.

Lewis contact: Dr. David R. Harding, (216) 433-6175  
Headquarters program office: OAST

#### Beryllium Oxide Identified as an Effective Reaction Barrier for NiAl/Nb<sub>2</sub>Be<sub>17</sub> Composite to 1373 K

Alloys based on the ordered B2 nickel aluminum (NiAl) phase are being considered as potential high-temperature structural materials. One drawback of this material, its lack of high-temperature strength, can be overcome by reinforcing the alloy with high-strength continuous fibers. As for any other composite system, a suitable reinforcement material for the NiAl matrix must have a matching coefficient of thermal expansion (CTE) with the matrix in addition to high-temperature

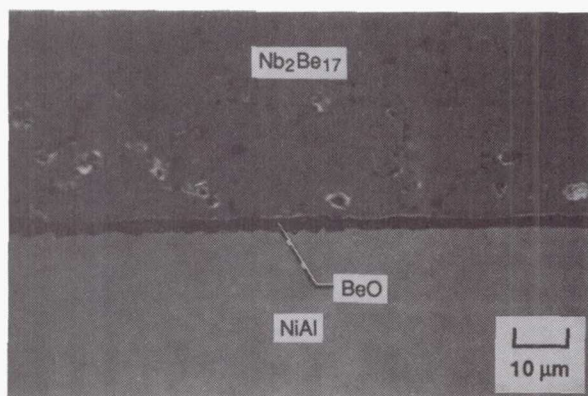


strength and chemical compatibility with the matrix. The CTE's for the currently available fibers, silicon carbide and alumina, are much lower than that of NiAl ( $\sim 16 \times 10^{-6} \text{ K}^{-1}$ ). Although many other high-melting-point ceramic materials are chemically stable in the NiAl matrix, none have CTE's as high as that of NiAl. Thus, there is a need to develop high-CTE fibers for the NiAl matrix.

One group of materials with CTE's matching that of NiAl are the beryllium-rich intermetallic compounds, called beryllides, of formula  $\text{M}_2\text{Be}_{17}$ ,  $\text{M}_2\text{Be}_{13}$ , or  $\text{M}_2\text{Be}_{12}$ , where M stands for tantalum, niobium, titanium, zirconium, or hafnium. Matching CTE's along with low density and good high-temperature strength makes the beryllides attractive as reinforcement materials for the NiAl matrix.

One of the beryllides,  $\text{Nb}_2\text{Be}_{17}$ , is currently being considered as a potential reinforcement material for NiAl. Reaction studies show extensive reaction between NiAl and  $\text{Nb}_2\text{Be}_{17}$  at both 1373 and 1473 K, with the reaction product being molten at 1473 K. Thus, the success of a  $\text{Nb}_2\text{Be}_{17}$ -reinforced NiAl composite depends on the development of suitable interfacial reaction barriers.

Preliminary thermodynamic calculations indicated that beryllium oxide (BeO) can be a potential reaction barrier between NiAl and  $\text{Nb}_2\text{Be}_{17}$ . Experiments were conducted to examine this. A 2- to 3- $\mu\text{m}$  interfacial BeO layer was formed by preoxidizing  $\text{Nb}_2\text{Be}_{17}$  at 1473 K. Diffusion couple experiments indicated that it was effective as a reaction barrier after hot pressing for 2 hr at 1373 K and after subsequent annealing at this



*NiAl/ $\text{Nb}_2\text{Be}_{17}$  sandwich with interfacial BeO layer after hot pressing at 1373 K.*

temperature for 100 hr. However, it was not effective as a reaction barrier at 1473 K.

Work is in progress to identify the failure mechanisms of the interfacial BeO reaction barrier layer at 1473 K. In addition, alternative interfacial barrier coatings are being identified.

**Lewis contact: Dr. Ajay K. Misra, (216) 433-5497**  
**Headquarters program office: OAST**

### **Persian Gulf Sand Deposits on Helicopter Turbine Vanes Analyzed**

Operations Desert Shield and Desert Storm required the extensive use of turbine-powered helicopters in the Persian Gulf region. Sand ingestion was recognized early on as the cause of serious compressor erosion and loss of efficiency. However state-side engine teardown also revealed that thick deposits formed on high-temperature turbine vanes. A concern was that these deposits, presumably a result of sand flowing through the combustion path, could lead to a serious hot-corrosion problem. At the request of the Army Propulsion Office at NASA Lewis, a program was begun to analyze deposit and sand chemistry in order to assess the potential for hot corrosion.

Sand samples were obtained from various field operations in Saudi Arabia, including Dhahran and King Fahd International Airport. Deposits on aluminide-coated X-40 vanes were obtained from four T700 turbine engines used on Black Hawk personnel carrier helicopters. Fine powders found in the cooling passages of these engines were also provided for analysis.

The major components of the samples are listed in the following table. The values were normalized to 100 percent by weight and are presented as oxide components. The sand sample from Dhahran was primarily  $\text{SiO}_2$  (quartz) with only

Sample	Content, percent						
	$\text{SiO}_2$	CaO	$\text{Al}_2\text{O}_3$	$\text{Fe}_2\text{O}_3$	MgO	C	S
Sand	90.8	1.5	2.5	0.8	0.5	1.5	0.6
Stones	12.3	25.9	5.2	.9	15.6	10.7	4.3
Powders	50.2	4.1	16.4	15.1	2.1	1.0	.5
Deposits	43.4	17.7	11.7	11.4	5.8	.1	2.3

small amounts of other oxides. Finer sand particles, sieved from these samples, showed considerably higher levels of the other oxides. Also, pebbles or stones from a nearby river bed had very high calcium, magnesium, and carbon contents in the form of  $\text{CaCO}_3$  (limestone) and  $(\text{Ca,Mg})\text{CO}_3$  (dolomite).

The engine deposits also contained  $\text{SiO}_2$  at a lower level, with higher amounts of Ca, Al, Fe, and Mg. This is due in part to the higher secondary metal content in the fine sand particles, which are more likely to bypass the particle separator filtration systems. Metallic particles from erosion of stainless steel and titanium compressor hardware were also present in these deposits. Similar results, listed under "powders," were obtained for the fine talc-like powder collected from turbine disk cooling passages.

The deposits were 1/4-in.-thick crusts at the base of the vanes. Much of the deposit was a glassy oxide with numerous gas bubbles. It also contained diopside crystals, a complex Ca-Mg-Al-Fe silicate. The inner portion of the deposit was  $\text{CaSO}_4$ . The latter phase resulted from calcium in the sand reacting with sulfur in the fuel as it passed through the combustor:



The  $\text{CaSO}_4$  can in turn react with the impacted quartz particles:



The  $\text{SO}_2$  gas liberated by this process may account for the gas bubbles observed in the glassy deposits.

The melting point of  $\text{CaSO}_4$  (1540 °C) is well above the metal use temperature. Classic molten sulfate hot corrosion is therefore not expected. The 1070 °C eutectic in the  $\text{CaO-FeO-Al}_2\text{O}_3\text{-SiO}_2$  system could account for the molten glassy deposits, but its corrosive ability is not known.

Laboratory corrosion tests of the cooling passage powder on NiAl did not exhibit any corrosion, but  $\text{CaCO}_3$  and  $\text{CaSO}_4$  powders did cause accelerated oxidation at 1200 °C. This type of attack on actual helicopter vanes has yet to be seen. The major problem appears to be cooling hole plugging and associated overheating. The current use of external inlet filter bags is expected to consid-



SEM micrograph of glassy silicate deposit on helicopter turbine vanes (200×).

erably reduce sand ingestion, erosion, and deposition.

#### Bibliography

Smialek, J.L.: The Chemistry of Saudi Arabian Sand: A Deposition Problem on Helicopter Turbine Airfoils. NASA TM-105234, 1991.

Kandebo, S.W.: Sand Ingestion Problems Prompt U.S. Army To Modify Transport/Utility Helicopters. *Aviat. Week Space Technol.*, vol. 134, no. 10, Mar. 11, 1991, pp. 21-22.

**Lewis contact: Dr. James L. Smialek, (216) 433-5500**  
**Headquarters program office: OAST**

#### Approach Defined for Modeling Continuous-Fiber Chemical Vapor Deposition Processes

Structural fibers are currently being considered for the reinforcement of both ceramic and inter-metallic material matrices to improve their mechanical reliability and high-temperature strength for aeropropulsion applications. Currently only a few commercially available fibers can be considered for this purpose. These and newly developed fibers will probably require specific coatings to make them compatible with the matrix and thus allow optimum composite material performance.

Chemical vapor deposition (CVD) is an excellent technique for fabricating new and novel materials. However, the control and scaleup of continuous CVD processes require a sufficient understanding of the complex physicochemical phenomena involved in CVD and their effects on



the resulting coating's properties. Fundamental thermodynamic and kinetic information is necessary to develop high-fidelity mathematical models that can guide further experimental efforts and provide predictive capabilities important to producing a useful coated fiber.

An effort is under way at NASA Lewis to model a continuous-fiber CVD process. A computational fluid dynamics code, FLUENT, was adopted to initially simulate the batch (short fiber lengths) CVD reactor built in house. This model is based on silicon deposition from silane in a hydrogen carrier gas because this system is much better studied in terms of its gas and surface chemical reaction mechanisms and rates. Also, correct analysis of this system is essential to subsequent CVD studies of other silicon-based materials that are of current interest to NASA.

The model can predict measured absolute CVD rates and trends within experimental accuracy. Two major findings are crucial to modeling fiber CVD processes: (1) gas phase transport by Soret diffusion is extremely important and may greatly alter predicted deposition rates, and (2) chemical kinetic parameters must be known as accurately as possible because small differences in values dramatically alter model predictions. These findings apply to both batch and continuous modes of fiber coating. Their importance increases as the substrate fiber diameter gets smaller. The model also predicts nonuniform growth rates along the fiber length with respect to temperature and fiber diameter as they would change in a continuous process. The axial nonuniformity of

the growth rate for the batch process implies radial nonuniformity in the continuous process.

The model will be extended to a continuous-fiber CVD process by linking the series of batch runs describing the evolution of temperature and diameter along the fiber. It can then be utilized for the in-situ control of CVD process to achieve controlled deposition rates for desired microstructures. Such models are invaluable tools for developing efficient and reliable methods of growing and coating fibers for advanced composite systems.

#### Bibliography

Gokoglu, S.A.: Chemical Vapor Deposition Modeling—An Assessment of Current Status. *Chemical Vapor Deposition XI*, K.E. Spear and G.W. Cullen, eds., The Electrochemical Society, 1990, pp. 1-9. (Also, NASA CR-185301.)

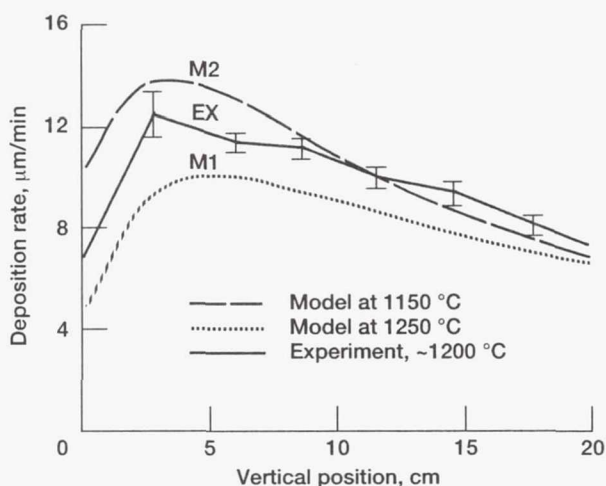
Gokoglu, S.A., et al.: A Numerical and Experimental Analysis of Reactor Performance and Deposition Rates for CVD on Monofilaments. *Chemical Vapor Deposition XI*, K.E. Spear and G.W. Cullen, eds., Electrochemical Society, 1990, pp. 31-37. (Also, NASA TM-103631.)

Gokoglu, S.A., et al.: Prediction of Chemical Vapor Deposition Rates on Monofilaments and Its Implications on Fiber Properties. Submitted to *J. Mater. Res.*, 1991.

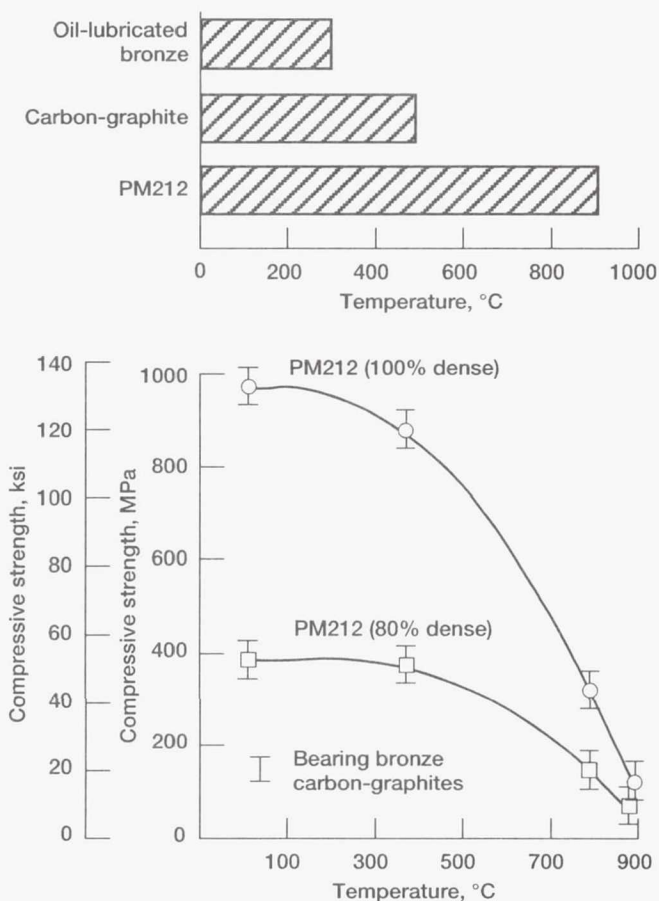
**Lewis contact: Dr. Suleyman A. Gokoglu, (216) 433-5499**  
**Headquarters program office: OAST**

#### Application-Critical Engineering Properties Determined for PM212, Self-Lubricating High-Temperature Composite

Engine efficiency can be improved by operating at higher temperatures. Higher operating temperatures, however, may preclude the use of conventional liquid and solid lubricants. Therefore, high-temperature solid lubricants are needed for advanced space and aeronautics applications where temperatures can greatly exceed the capabilities of current lubricants and bearing materials such as oils, graphite, and polytetrafluoroethylene (Teflon). Potential applications include seals for hypersonic vehicles (NASP), face seals and variable stator vane bushings for advanced gas turbine engines, and cylinder wall/piston ring lubrication for space power and terrestrial-based Stirling engines. In order to address these needs, a new high-temperature



Comparison of CVD model predictions with experimental measurements for silicon deposition rates.



Maximum service temperature and compressive strength of PM212.

solid lubricating composite material, PM212, is being developed.

PM212 is a composite material made by powder metallurgy techniques that contains a hard, wear-resistant chromium carbide matrix with silver and fluoride eutectic solid-lubricant additions. PM212 has been shown to provide low friction and wear from 25 to 900 °C in both reducing and oxidizing environments. Before it can be used as a component of an advanced engine or other application, however, its engineering properties, such as compressive strength, thermal expansion coefficient, and elastic modulus, must be known.

A study to determine these and other critical engineering properties of PM212 has been recently conducted at NASA. In addition to the properties previously mentioned, PM212's tensile strength, thermal conductivity, specific heat, and thermal diffusivity were also measured.

In terms of mechanical strength, PM212 at temperatures to about 500 °C is approximately two to five times as strong as other comparable solid lubricating materials, such as porous bronze or graphite. Even at 750 °C, where these conventional materials degrade and are no longer useful, PM212 retains sufficient strength for many bearing and seal applications. The results of the thermal properties evaluation indicate that PM212 is a practical engineering material. Its thermal expansion coefficient is similar to that of some stainless steels, and its thermal conductivity is higher than that of many ceramics.

This unique combination of adequate mechanical strength, good thermophysical properties, and high-temperature capabilities along with low friction and wear makes PM212 a viable candidate material for a wide variety of high-temperature bearing and seal applications.

#### Bibliography

DellaCorte, C.; Sliney, H.E.; and Bogdanski, M.S.: Tribological and Mechanical Comparison of Sintered and HIPped PM212: High Temperature Self-Lubricating Composites. Submitted to STLE, 1991.

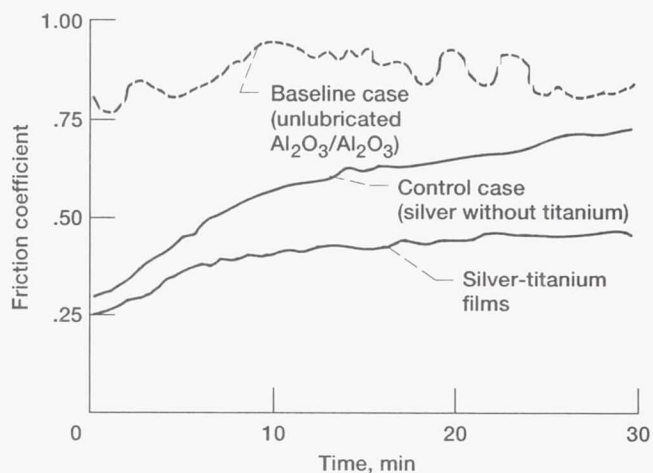
**Lewis contacts:** Harold E. Sliney, (216) 433-6055;  
Dr. Christopher DellaCorte, (216) 433-6056  
**Headquarters program office:** OAST

#### Techniques Developed To Lubricate Ceramics With Solid-Lubricant Films

Current research efforts related to hypersonics (NASP), advanced heat engines, and space power generation have emphasized the need for lightweight, high-temperature materials. Ceramics show promise for fulfilling many of these needs because of their low density, high hardness, and relatively high degree of thermal and chemical stability. However, many anticipated applications for ceramics include rubbing or sliding contacts. Recent research indicates that the friction and wear performance of unlubricated ceramics is poor. Therefore, the lubrication of ceramics is critical to their successful implementation in these advanced applications.

Coating the ceramic surface with a thin solid-lubricant film, such as silver, is a proven technique for reducing friction and wear. However,





Friction coefficients for silver and silver-titanium films.

achieving sufficient adhesion and coverage of the film to the ceramic surface is a challenge. Two techniques are being developed at NASA Lewis to apply adherent solid-lubricant films of silver to aluminum oxide (Al<sub>2</sub>O<sub>3</sub>) ceramic surfaces.

One technique involves applying an active bond layer of metal film (titanium) between the ceramic and the silver. The titanium bond layer aggressively adheres to the ceramic surface and also bonds well to the silver. The films are deposited by conventional sputtering techniques. Using these techniques without the bond layer results in a film that exhibits poor adhesion and friction-and-wear performance. The silver films deposited on top of the titanium films, however, display remarkably good friction-and-wear behavior. The titanium layer also prevents the silver film from dewetting, or "balling up," on the aluminum oxide surface at elevated temperatures.

Another technique being developed produces adherent films without the bond layer. Screen cage ion plating (SCIP) is a modification of ion plating (evaporative coating). The specimen to be coated is placed into a silver screen that is electrically coupled to the coating source. During coating, the silver atoms are electrically accelerated toward the screen. Many of these atoms pass through the screen and impinge on the ceramic substrate, where they become strongly adhered. The SCIP technique has the additional benefit of coating the entire substrate surface, including the side not facing the coating source. The technique's high throwing power produces three-directional coverage that allows the coating of intricate shapes and geometries.

These two techniques produce solid-lubricant films that significantly reduce friction and wear. The development of lubricating methods for ceramics may make it possible to include them in future engineering applications. Future work in this area may include combining the benefits of the SCIP process with the bond layer concept to produce adherent, long-life, solid-lubricant films on ceramics.

#### Bibliography

DellaCorte, C.; Pepper, S.V.; and Honey, F.S.: Tribological Properties of Ag/Ti Films on Al<sub>2</sub>O<sub>3</sub> Ceramic Substrates. NASA TM-103784, 1991. (To appear in Surface Coatings and Technology.)

Slincy, H.E.; and Spalvins, T.: The Effect of Screen Cage Ion Plated Silver and Sliding Friction on Tensile Stress Induced Cracking in Aluminum Oxide. Submitted to STLE, 1991.

**Lewis contacts:** Dr. Christopher DellaCorte, (216) 433-6056; Talivaldis Spalvins, (216) 433-6060  
Headquarters program office: OAST

#### R&D 100 Award

#### High-Temperature Nitrogen Postcure Developed for Polymer Matrix Composites

A major goal of aeronautics research is to improve the performance and operating efficiency of aircraft engines. A greater reliance on lightweight, high-strength materials is necessary to achieve this goal. Where possible, the use of fiber-reinforced, high-temperature, polymer-matrix composites has resulted in substantial weight savings in aircraft turbine engines. However, the use of these materials is limited by thermal-oxidative stability and glass transition temperature to operating temperatures no higher than 290 °C (600 °F). Current research in the development of new high-temperature polymers, such as NASA Lewis' PMR-II-50 and V-CAP polyimides, has led to improvements in the thermal-oxidative stability of these materials to the point where they can operate for thousands of hours at temperatures as high as 371 °C with minimal weight loss. However, these improvements in thermal-oxidative stability have been achieved at the expense of glass transition temperature. The glass transition temperature of a polymer is the temperature at which it transforms from a glassy to a rubbery state and loses mechanical integrity.

Design requirements for the use of polymer-matrix composites in any load-bearing application call for a glass transition temperature at least 25 deg C (50 deg F) higher than the intended upper use temperature. A new postcure treatment recently developed at Lewis raises the glass transition temperature of these polymers and fiber-reinforced composites prepared with them. This postcure treatment received a 1991 R&D 100 Award from Research & Development magazine.

Typical manufacturing practices for components fabricated from high-temperature polymer-matrix composites require that after fabrication the parts be baked (postcured) in an oven in air at temperatures above the glass transition temperature. This postcure is intended to completely react any groups that have not been polymerized during the

initial fabrication procedure. As these groups react or crosslink, the glass transition temperature of the polymer, the composite, or both should increase. However, because these postcures are performed in air at high temperatures, the polymer chain often undergoes some amount of oxidative degradation, which can lower the glass transition temperature.

The NASA Lewis treatment performs these postcures in nitrogen rather than in air. In the absence of oxygen, oxidative degradation is no longer a problem, and the maximum glass transition temperature for these systems can now be achieved. For example, the glass transition temperature of Celion-6000-reinforced PMR-15 laminates can be increased from 310 °C upon fabrication to 500 °C with a 16-hr postcure in nitrogen at 427 °C. Air postcures of the same laminates produced glass transition temperatures of only 365 °C. These increases in glass transition temperature are accompanied by better high-temperature mechanical properties (e.g., flexural strength). A 371 °C nitrogen postcure of a Celion-6000-reinforced PMR-15 laminate produced a flexural strength nearly 2.5 times higher than that of the same laminate postcured at 371 °C in air.

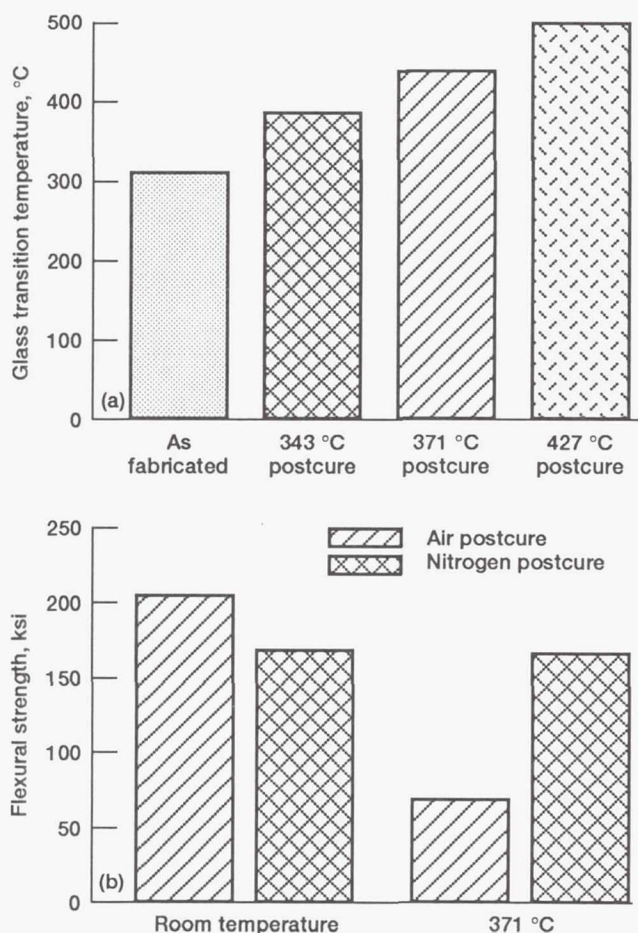
Ongoing research is aimed at optimizing this process for other high-temperature polymers and composites.

#### Bibliography

Bowles, K.J.: A Thermally Modified Polymer Matrix Composite Material With Structural Integrity to 371 °C. *Materials Processes: The Intercept Point*, H.L. Chess, et al., eds., SAMPE, 1988, pp. 552-561. (Also, NASA TM-100922.)

Bowles, K.J.: Nitrogen Aging of Graphite Fiber Reinforced Polyimide Composites. *HITEMP Review 1989*, NASA CP-10039, 1989, pp. 16-1 to 16-8.

**Lewis contact: Kenneth J. Bowles, (216) 433-3201**  
**Headquarters program office: OAST**



Effects of high-temperature nitrogen postcure on graphite/PMR-15 composites: (a) higher glass transition temperature; (b) better high-temperature flexural strength.



# Structures

## New Equations Show Oil Filtration Effect on Bearing Life

Particles found in lubricating oil reduce bearing life when they enter the contact area between the rolling elements and the raceway. The number, size, and material properties of these particles determine their relative effect. Typical particle size distributions vary in different mechanical systems.

In general, rolling-element bearing life increases with improved oil filtration. However, the industry's standard methods of calculating estimated bearing life do not consider the effect of oil filtration. The results of NASA research and an independent investigation were used to develop a method of adjusting bearing-life estimates based upon oil filter ratings. From these test results, equations were developed for calculating life factors (LF) that account for oil filtration effects on the fatigue life of both roller and ball bearings. For roller bearings

$$LF = 3.5 (FR)^{-0.55}$$

where FR is the filter rating in micrometers. For ball bearings

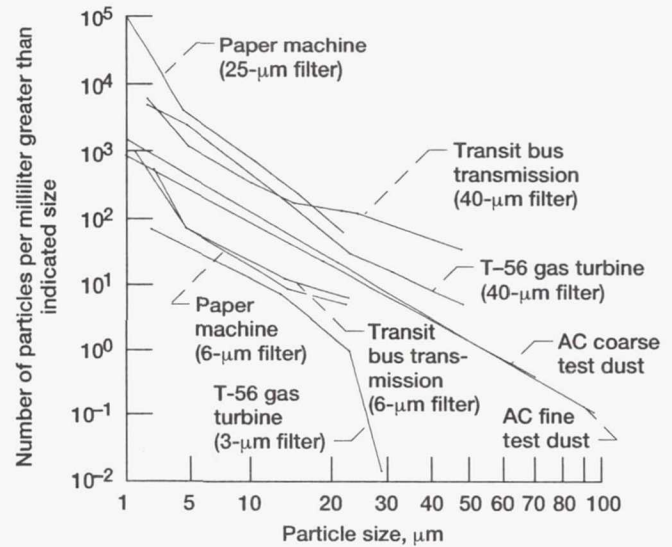
$$LF = 1.8 (FR)^{-0.25}$$

These life factors can be used to adjust the calculated bearing  $L_{10}$  (or catalog) life for the degree of filtration.

LIFE ADJUSTMENT FACTOR BASED ON FILTER RATING

Filter rating, FR	Life factor, LF	
	Roller bearing	Ball bearing
3	1.9	1.4
6	1.3	1.2
8	1.1	1.1
10	1.0	1.0
12	.9	1.0
25	.6	.8
40	.5	.7
49 <sup>a</sup>	.4	.7
60 <sup>a</sup>	.4	.6
105 <sup>a</sup>	.3	.6

<sup>a</sup>For filter ratings exceeding 40  $\mu\text{m}$  or with no filtration, it is not recommended to use a life adjustments factor less than 0.5.



Effect of oil filtration on particle contamination for mechanical systems.

## Bibliography

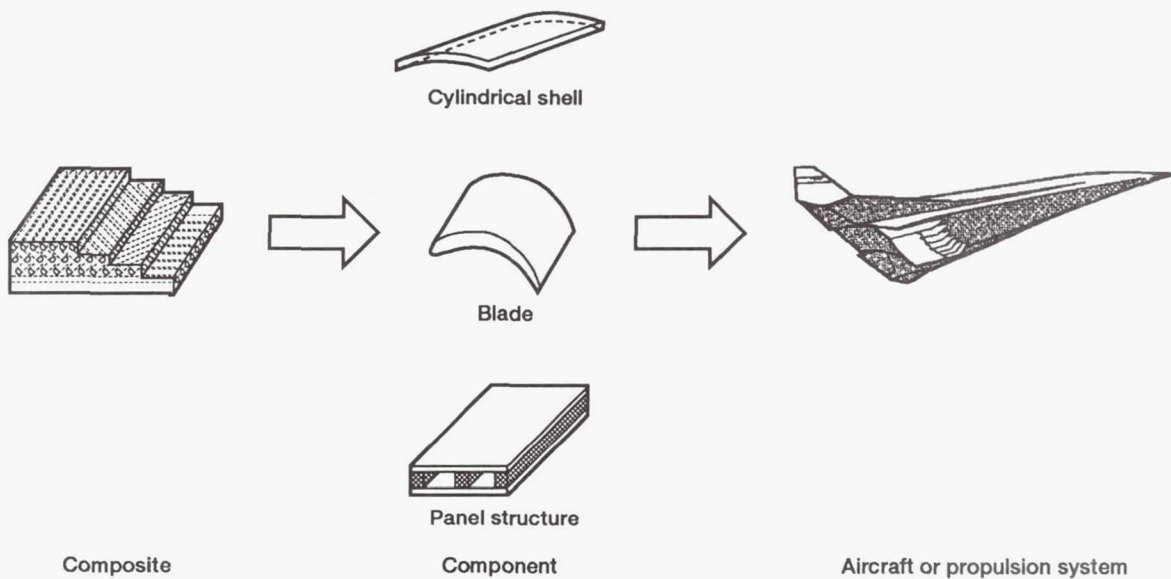
Needelman, W.M.; and Zaretsky, E.V.: Quantifying Oil Filtration Effects on Bearing Life. NASA TM-104350, 1991.

**Lewis contact:** Erwin V. Zaretsky, (216) 433-3241  
**Headquarters program office:** OAST

## Hot Composites Assessed for Adverse Thermal and Structural Loads

In the pursuit of efficient use of materials, technology must develop material combinations that are light and strong, yet able to survive in adverse environments. Research has over the years led to such materials. Innovative ways are necessary to keep these materials cool at elevated temperatures. Therefore, there is a need to assess the high-temperature endurance of these materials. Intricate computer codes are required to appropriately model the complex behavior of such materials.

Over the past two decades NASA Lewis researchers have developed HITCAN (High Temperature Composite ANalysis). With a focus on aggressive environments this computer code analyzes and designs structures made of advanced composite materials. HITCAN is a general-purpose code that predicts the global structural and local stress-strain response of hot multilayered metal-



*HITCAN analyzes complex components for future propulsion systems.*

matrix structures both at the constituent (fiber, matrix, and interphase) and the structure level, including the fabrication process effects. The thermomechanical properties of the constituents are considered to be nonlinearly dependent on several parameters including temperature, stress, and stress rate. The code's computational procedure is based on an incremental iterative nonlinear approach utilizing a multifactor interaction model.

The code has been used to analyze several typical aerospace components including actively cooled hot composite structures. The many features and analysis capabilities embedded in HITCAN make it a powerful tool for analyzing aerospace structures.

#### Bibliography

Chamis, C.C., et al.: HITCAN for Actively Cooled Hot-Composite Thermostructural Analysis. NASA TM-103750, 1991.

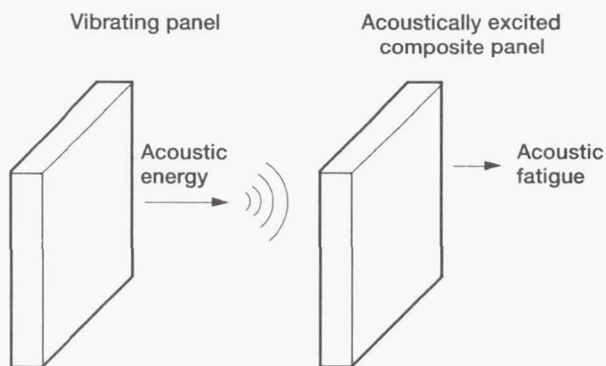
**Lewis contact: Dr. Christos C. Chamis, (216) 433-3252**  
**Headquarters program office: OAST**

#### Acoustic Fatigue of Hot Composite Structures Simulated

High-pitched noise has been known to break glass bottles. Noise can similarly damage structures made of ductile materials. Noise capable of causing damage in an aircraft's structural material emanates from the components of aircraft engines. The repeated exposure of aircraft structures to this noise can lead to fatigue cracks. The aircraft engine structures must then be designed to avoid the problem of acoustic fatigue. Acoustic fatigue becomes even more important in future, high-speed transport systems involving high-intensity acoustic excitation from engine combustion processes and complex thermomechanical loads due to hypersonic flow as well as high-temperature composites. Normal human conversation is at 70 dB, a truck horn sounds at 110 dB, an airplane propeller is at 120 dB, and the noise in scramjet engines can reach 185 dB.

The experimental study of acoustic fatigue is generally expensive; therefore, computer codes for simulating acoustic fatigue are needed. A multidisciplinary approach toward developing the appropriate codes is required to account for the complex composite material behavior, the effect of the environment, and physical modeling of acoustic noise. Over the past two decades NASA Lewis has been developing methods and multidisciplinary computer codes for computationally simulating the structural behavior of composite





Schematic of acoustic fatigue simulation.

structures subjected to hygrothermomechanical loadings. Select NASA codes from various disciplines were integrated for simulating the acoustic fatigue response and resistance of hot polymer-matrix composite structures excited by the acoustic noise generated from an adjacent vibrating component, including a propulsion environment.

The integrated simulation was demonstrated for a hot composite panel acoustically excited by an adjacent vibrating panel. A substantial increase in acoustic fatigue life was obtained (1) by keeping the off-axis plies on the outer surface of the laminate; (2) by adding moisture and increasing the use temperature of the excited panel; and (3) by increasing the temperature of the vibrating panel.

The simulation methods and codes developed for assessing the acoustic fatigue life of hot propulsion components provide information useful in designing structurally sound aircraft. Other considerations will, of course, be necessary for an all-inclusive design.

#### Bibliography

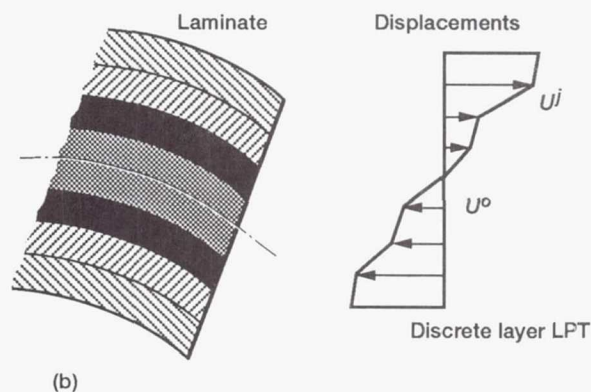
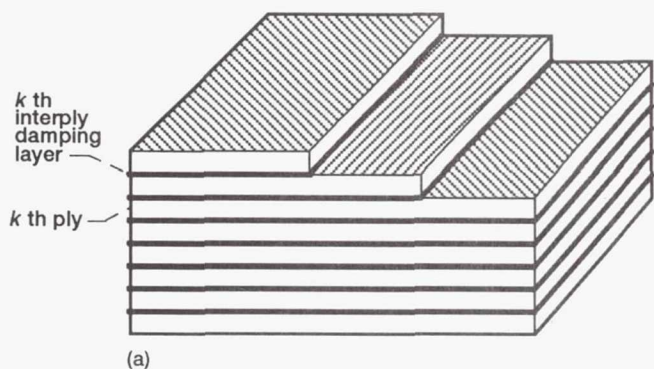
Singhal, S.N., et al.: Computational Simulation of Acoustic Fatigue for Hot Composite Structures. *32nd Structures, Structural Dynamics, and Materials Conference*, AIAA, 1991, Pt. 4, pp. 2709-2719. (Also, NASA TM-104379.)

**Lewis contact: Dr. Christos C. Chamis, (216) 433-3252**  
**Headquarters program office: OAST**

### Effects of Interply Damping Layers Simulated on Dynamic Response of Composite Structures

Static damping is the capacity built into a mechanical object or device to prevent unwanted vibration and instability caused by oscillatory conditions. In aerospace applications mechanical damping is a useful parameter for controlling vibration and noise, for accurate positioning, and for fatigue endurance and impact resistance. Many structural applications require physical damping. For example, large space stations require it for dynamic stability and accurate positioning. Jet engine blades require high fatigue resistance and thus excessive vibrations must be controlled. A further consideration for aerospace damping is that such applications require light weight and high dynamic performance; therefore, passive damping should add minimal weight and should be compatible with the structural configuration.

NASA Lewis researchers have developed integrated damping mechanics for composite laminates with constrained interlaminar layers of polymer damping materials. These mechanics



Laminates with interlaminar damping layers: (a) typical laminate configuration; (b) kinematic assumptions of discrete layer laminate theory.

include discrete layer damping for composite laminates with damping layers, combined with a semianalytical method for predicting the modal damping in simply supported specialty composite plates.

Damping predictions using these methods demonstrate that graphite-epoxy composite plates of various laminations have the potential for higher damping than geometrically equivalent aluminum plates. These predictions are made by investigating the effects of thickness aspect ratio, damping layer thickness, composite fiber volume ratio, and similar factors on the dynamic response (i.e., modal damping, natural frequency, and static deflection).

Research into the damping mechanics of composite laminates and structures has shown that composite damping is anisotropic and highly tailorable and depends on an array of micromechanical, laminate, and structural parameters. It has been further demonstrated that optimal tailoring may significantly improve the damped dynamic performance of composite structures.

#### Bibliography

Saravanos, D.A.; and Chamis, C.C.: The Effects of Interply Damping Layers on the Dynamic Response of Composite Structures. *32nd Structures, Structural Dynamics, and Materials Conference*, AIAA, 1991, Pt. 3, pp. 2363-2370. (Also, NASA TM-104497.)

**Lewis contact:** Dr. Christos C. Chamis, (216) 433-3252  
**Headquarters program office:** OAST

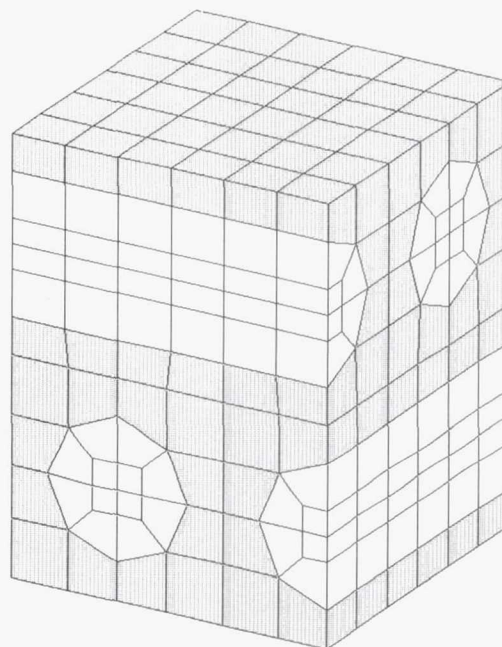
#### Nonlinear Finite Element Analysis Proves Viable for Investigating Composite Materials Behavior

The interest in applying metal-matrix composite materials in engines increases the importance of understanding their behavior on a micromechanical (constituent) scale. One approach recently demonstrated at NASA Lewis for investigating damage mechanisms in composites is a three-dimensional, nonlinear, finite element analysis.

A finite element model of laminated (cross-ply) silicon-carbide-fiber-reinforced, titanium-matrix (SiC/Ti) composite was used to correlate nonlinear finite element analyses with experimental observations of this composite's stress-strain

behavior (ref. 1). In tensile tests conducted on the SiC/Ti laminates, the observed stress-strain behavior could not be rationalized. Photomicrographs of the test specimens revealed localized damage (plastic slip) zones in the titanium matrix. The experimental evidence of matrix plasticity inspired the idea of performing nonlinear finite element analyses to establish its feasibility for simulating composite micromechanical behavior.

In conducting the finite element analyses the silicon carbide fibers were presented as elastic material and the titanium matrix as elastic-plastic material. The weak fiber-to-matrix interface that forms during the composite fabrication process was modeled with "gap" finite elements to transmit only compressive loads. Thermal and mechanical boundary conditions were imposed to represent the fabrication process and the test conditions. The information obtained from the finite element analyses demonstrated behavior nearly identical to that observed in the tensile tests. Areas in the titanium matrix where localized damage was revealed in the photomicrographs corresponded to areas in the finite element model where maximum shear strains (a plastic damage mechanism) were computed.



*Finite element model of laminated composite.*



The study established credibility in using nonlinear finite element analyses for investigating composite micromechanical behavior. Additional studies are under way to examine the effects of ply orientation for the same SiC/Ti composites. Similar studies are planned to investigate the plasticity and creep behavior of tungsten-fiber-reinforced copper composites. To facilitate future studies, a computer program has been created (ref. 2) that automatically generates intricate finite element models of laminated fiber composites. The program, which rapidly generates models from a basic set of user-specified parameters, will substantially shorten the time required in the overall process.

#### References

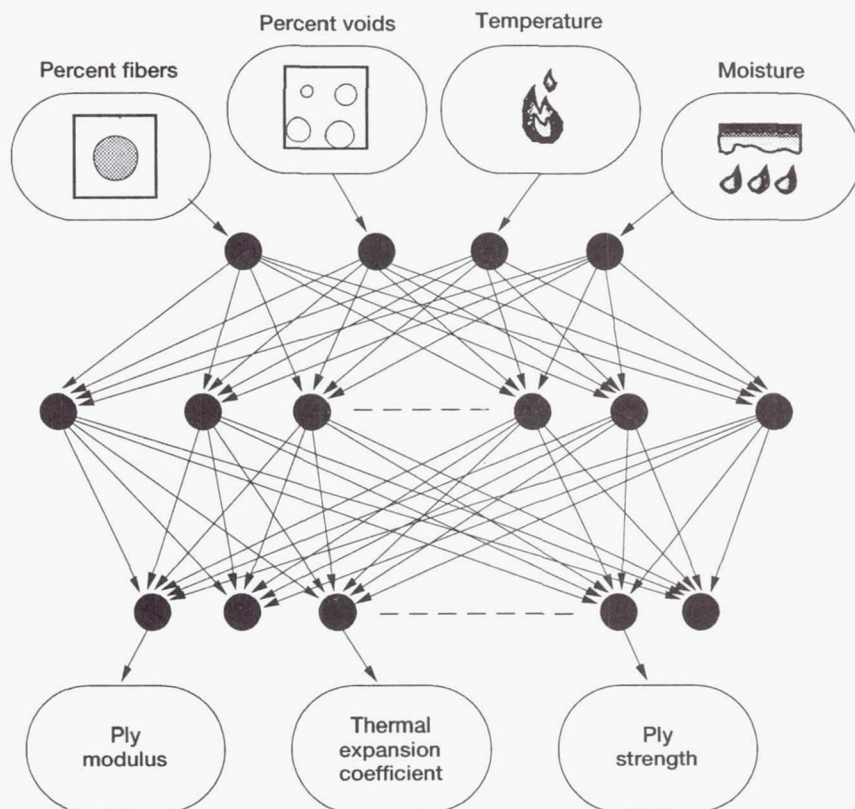
1. Melis, M.E.: COMGEN—A Computer Program for Generating Finite Element Models of Composite Materials at the Micro Level. NASA TM-102556, 1990.
2. Lerch, B.A.; Melis, M.E.; and Tong, M.: Experimental and Analytical Analysis of the Stress-Strain Behavior in a  $[90/0]_{2S}$  SiC/Ti-15-3 Laminate. NASA TM-104470, 1991.

**Lewis contact:** Matthew E. Melis, (216) 433-3322  
**Headquarters program office:** OAST

#### Artificial Neural Networks Simulate Composite Hygrothermal Properties

Artificial neural networks can improve computational efficiency relative to existing methods when algorithmic description of functional relationships is either totally unavailable or complex. The amount of computational effort (CPU time) saved is naturally a function of the complexity of the relationships between the various input and output variables of interest in a given problem. Significant reductions in elapsed computation time are possible. These concepts are currently being investigated at NASA Lewis for material characterization, which includes both the nonlinear hysteretic response of conventional high-performance materials and advanced polymer-matrix composites operating in an adverse hygrothermal environment.

The artificial neural network program selected for this study was NETS 2.0, which was developed at NASA Johnson Space Center. This program was modified at NASA Lewis under a summer faculty fellowship program and now resides on NASA's Cray X/MP, VAX, Sun Micro, and IBM PC/AT systems. The significant modifications to the code include automatic scaling of input and



Artificial neural network for predicting composite hygrothermal behavior.

output variables, a capability that permits creation of neural networks that work with real user-supplied data. The resulting code has been shared with NASA Johnson. The future release of the NETS code will incorporate these modifications.

The program chosen for providing the composite mechanics data is ICAN (Integrated Composite ANalyzer). ICAN is an in-house-developed computer code that performs dedicated composite mechanics analysis of polymer-based composites. Three different composite systems were selected for the study: S-glass fiber with an epoxy matrix; graphite fiber with a low-modulus, low-strength matrix; and P-75 fiber with a high-modulus, high-strength matrix. The input variables are the use temperature, moisture content, fiber volume ratio, and void volume ratio. The output consists of 37 ply-level properties (ply moduli, Poisson's ratios, strengths, etc.) Most of the properties are predicted within 1 percent of the target values.

These methods are innovative and have a high potential for reducing computational time when used in conjunction with other nonlinear structural analyses programs that require the computation of material properties repeatedly because of the iterations involved in the analyses.

#### Bibliography

Brown, D.A.; Murthy, P.L.N.; and Berke, L.: Application of Artificial Neural Networks to Composite Ply Micromechanics. NASA TM-104365, 1991.

Murthy, P.L.N.; and Chamis, C.C.: Integrated Composite Analyzer (ICAN): Users and Programmers Manual. NASA TP-2515, 1986.

**Lewis contact:** Pappu L.N. Murthy, (216) 433-3332  
**Headquarters program office:** OAST

#### Structural NDE Approach Used in Health-Monitoring System

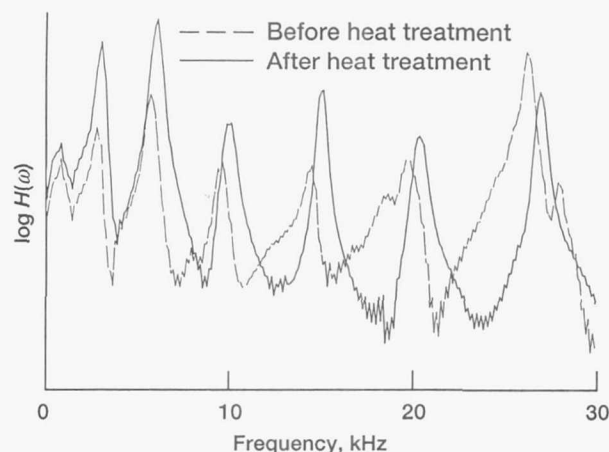
Thermal and mechanical loading introduce damage into metal-matrix composites that can eventually lead to the failure of composite structures. Extensive research has been aimed at developing noninvasive techniques to detect damage-induced changes in a material's microstructure. An alternative to these traditional *local* nondestructive evaluation (NDE) techniques is to measure

changes in the *global* structural response that result from changes in the material's properties.

NASA Lewis researchers have developed a sensitive technique for detecting small changes in material properties, such as those caused by damage from thermomechanical loading. This technique requires accurate measurements of the vibration frequencies from an instrumented test specimen (ref. 1). Recently, this approach was extended to determine how damping properties of SiC/Ti-15-3 composites are affected by heat treatment.

Changes in matrix microstructure caused by heat treatment stiffen the composite and reduce its damping capacity. Heat treatment temperature and exposure time determine the extent to which these changes occur (ref. 2). Damping was found to be more sensitive than stiffness to changes in microstructure. These results indicate that both frequency and damping measurements can be used to nondestructively detect microstructural changes in SiC/Ti-15-3 composites.

This approach is being used in a NASA-sponsored Small Business Innovation Research contract (ref. 3) to develop an artificial-intelligence-based health-monitoring system for an actual aerospace structural component. Results of this work show that a pattern recognition algorithm can be "trained" to recognize certain characteristic changes in structural frequency response and to infer from those changes the extent of damage in the structure.



Heat treatment shifts frequency response.



## References

1. Grady, J.E.; and Lerch, B.A.: Evaluation of Thermomechanical Damage in Silicon Carbide/Titanium Composites. *AIAA J.* vol. 29, no. 6, 1991, pp. 992-997.
2. Grady, J.E.; and Lerch, B.A.: Effects of Heat Treatment on Stiffness and Damping of Unidirectional SiC/Ti-15-3. *HITEMP Review* —1991, NASA CP-10082, 1991.
3. Tang, S.S.; Chen, K.L.; Riccardella, P.C.; and Kuo, A.Y.: On-Line Monitoring of Material Degradation of Composite Materials. Structural Integrity Associates, Inc., Report SIR-91-043, 1991.

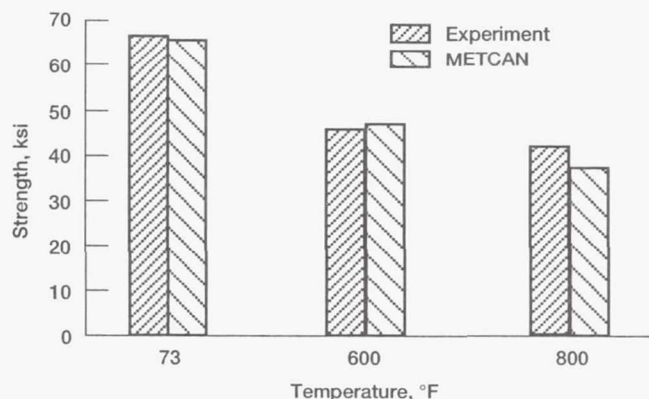
**Lewis contact:** Dr. Joseph E. Grady, (216) 433-6728  
**Headquarters program office:** OAST

## Computational Simulation of Metal-Matrix Composites Verified

High-temperature metal-matrix composites (HTMMC) have great potential for advanced aerospace structural applications. The realization of this goal, however, requires concurrent developments in fabrication techniques, experimental measurement techniques, and computational methods. In the development of HTMMC it is beneficial to first simulate the composite's behavior through computational methods. Besides providing an initial assessment of the HTMMC, this method helps to minimize the costly and time-consuming experimental effort that would otherwise be required.

NASA Lewis research into computational methods for simulating HTMMC's nonlinear behavior has led to the development of the METCAN (Metal Matrix Composite ANalyzer) computer code. METCAN incorporates various levels of composite mechanics models along with a nonlinear constitutive material model to perform a comprehensive point analysis of composite behavior. The development and verification (comparisons with experimental data) of METCAN are ongoing.

The latest METCAN verification activity indicates that the code can be used with confidence to predict the nonlinear behavior of HTMMC. Two composites (SiC/Ti-15-3 and SiC/Ti-6-4) from the Advanced High Temperature Engine Materials Technology Program (HITEMP) were studied at room and high temperatures. The verification included comparisons of elastic modulus,



Typical results from METCAN verification: transverse strengths of SiC/Ti-6-4 at room and high temperatures; fiber volume ratio, 34 percent.

Poisson's ratio, strength, and stress-strain behavior. For all cases examined, METCAN predictions are in excellent agreement with experimental data.

## Bibliography

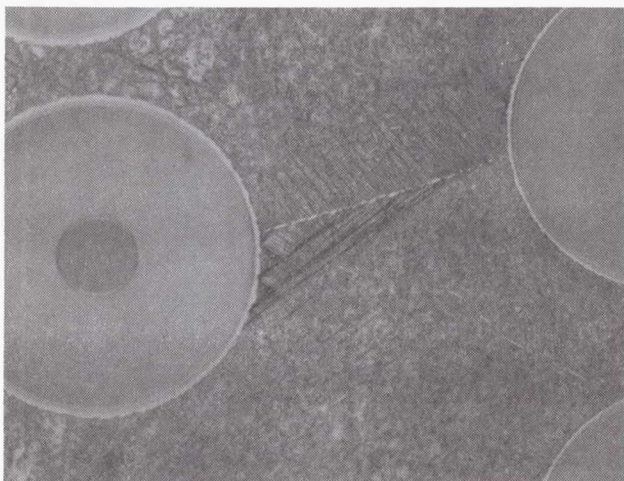
Lee, H.-J.; Murthy, P.L.N.; and Chamis, C.C.: METCAN Updates for High Temperature Composite Behavior: Simulation/Verification. NASA TM-103682, 1991.

**Lewis contact:** Ho-Jun Lee, (216) 433-3316  
**Headquarters program office:** OAST

## Method Developed for Observing Matrix Plasticity in Metal-Matrix Composites

Before metal-matrix composites can be used in critical applications, their deformation behavior must be thoroughly understood and accurately modeled. Knowing the behavior of each constituent may not be sufficient because the constituents may behave differently in the composite, especially the matrix material. The matrix may exhibit plastic flow in the unreinforced state, but because of the fibers in the composite, the matrix may experience constrained flow or be incapable of deforming plastically.

Testing of SiC/Ti composite specimens at NASA Lewis has shown behavior that could be explained by plastic flow in the matrix. For instance, during unloading the stress-strain behavior does not follow that of the loading portion of the curve but traces a new path. Upon



Slip bands in matrix of SiC/Ti composite.

reaching zero load there remains a permanent strain offset. During tension-tension fatigue open hysteresis loops, strain ratchetting, and a decrease in the secant modulus are evidence of irreversible deformation. This nonlinear and irreversible deformation could be attributed to several damage mechanisms, such as cracking of the fiber, the matrix, or both, debonding, or matrix plasticity. Therefore, detailed investigations have been performed to determine which damage mechanism or combinations of mechanisms are operative.

Until now, conclusive metallographic evidence of plastic deformation in the Ti matrix has been unattainable. Chemical etchants fail to reveal slip bands—indicators of plastic flow. NASA Lewis has developed a method to reveal slip bands in the composite matrix. The method uses a post-test heat treatment to precipitate fine particles on slip bands. The particles are subsequently revealed by a chemical etchant that preferentially attacks this phase, thus highlighting the slip bands. This method is used to investigate deformation and damage development on composite specimens of various SiC/Ti-15-3 system laminates.

Matrix slip bands were observed in specimens of various layups that were strained until nonlinear behavior was observed. The specimens were then unloaded and examined by the aforementioned technique. No fiber breakage was observed in the specimens; therefore, the matrix can plastically deform before the fibers crack. In a  $[90/0]_{2s}$  layup, the occurrence of slip bands spawned a

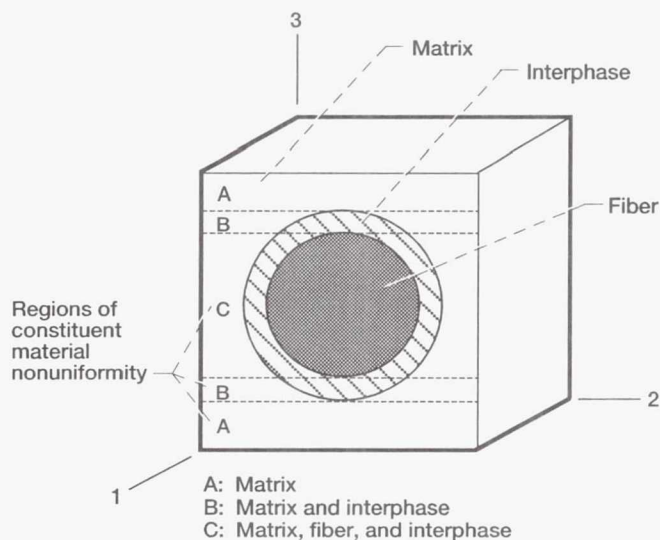
numerical analysis of deformation using a finite element approach. Good agreement was observed between the slip patterns predicted in the finite element approach and those observed in metallographic sections. Work in using the finite element method to predict the deformation response of other layups continues.

**Lewis contact:** Dr. Bradley A. Lerch, (216) 433-5522  
**Headquarters program office:** OAST

### Interphase Layer of Metal-Matrix Composites Tailored With Fabrication Considerations

The aerospace industry's demand for advanced, lightweight composites is increasing. However, combining various composite materials to produce the required performance characteristics is not always possible because incompatible combinations often result in adverse effects. To yield a cost-effective material while ensuring maximum performance, compliant layers (interphase) must be used and a suitable fabrication process must be determined.

NASA Lewis researchers have developed a methodology for reducing the matrix microstresses in metal-matrix composites by concurrently tailoring the interphase characteristics and the fabrication process. Results indicate that these methods produce significant reductions in the matrix's residual stresses. The most important design parameters are the interphase thermal-expansion



Material microregions in typical metal-matrix composite cell.



coefficient and the fabrication consolidation pressure. They must be concurrently optimized to further reduce the microstresses to more desirable magnitudes.

The simulation methods and codes developed for tailoring the interphase and fabrication processes of metal-matrix composites will help in designing composite structures with minimum residual stresses, thereby extending their life.

#### Bibliography

Morel, M.; Saravanos, D.A.; and Chamis, C.C.: Interphase Layer Optimization for Metal Matrix Composites With Fabrication Considerations. NASA TM-105166, 1991.

**Lewis contact:** Dr. Christos C. Chamis, (216) 433-3252  
**Headquarters program office:** OAST

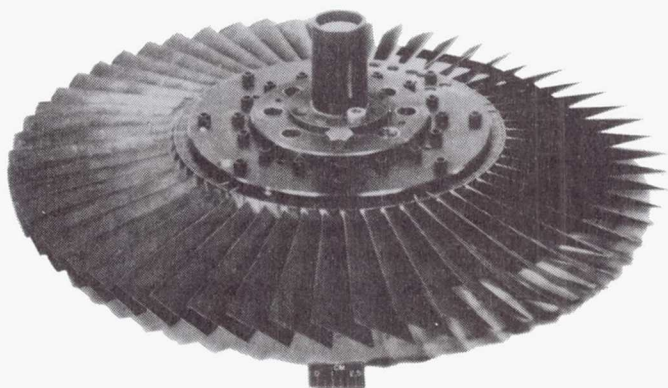
### Aeroelastic Vibration of Rogue Blades in Turbomachinery Demonstrated

In real turbomachinery rotors all the blades are not identical. Differences caused by manufacturing, material imperfections, or both disrupt the symmetry of each blade's structural properties. This phenomenon is known as mistuning.

Mistuning can markedly increase the size and cost of the aeroelastic analysis of engine and fan blade assemblies. To reduce computational costs, it is frequently assumed that all blades are identical. This assumption allows the equations of motion to be uncoupled, thereby reducing the problem size to that of only one blade. The difficulty with this is that the response of the real rotor may be qualitatively different, leading to unanticipated blade failures. Even small mistuning can lead to very high, localized stress on the blades. This phenomenon is known as mode localization.

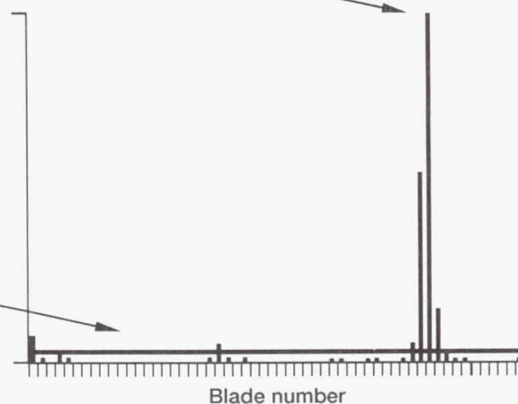
NASA Lewis has conducted a study to demonstrate analytically that mode localization can occur in turbomachinery rotors because of aerodynamic coupling and to develop analytical models that clarify the effect of mistuning, which can produce large vibrations in a small number of blades. The approach was to model a representative rotor as an assembly of 56 beams with random imperfections and then subject it to unsteady aerodynamic forces.

The study showed that changes in aeroelastic vibration modes can result from small imperfections in blade properties and that the vibration energy tends to be localized to very few blades on the rotor. This is the first time that an analytical



In tuned analysis, blades vibrate with equal amplitudes and share the excitation energy

Real system has all the vibration energy confined to 3 rogue blades out of 56



*Aeroelastic vibration of rogue blades in turbomachinery.*

demonstration has shown that aeroelastic vibration can cause high stresses and severe blade fatigue. This analytical model will help prevent catastrophic turbomachinery blade failures.

**Lewis contacts:** Durbha V. Murthy, (216) 433-6714;  
George L. Stefko, (216) 433-3920  
**Headquarters program office:** OAST

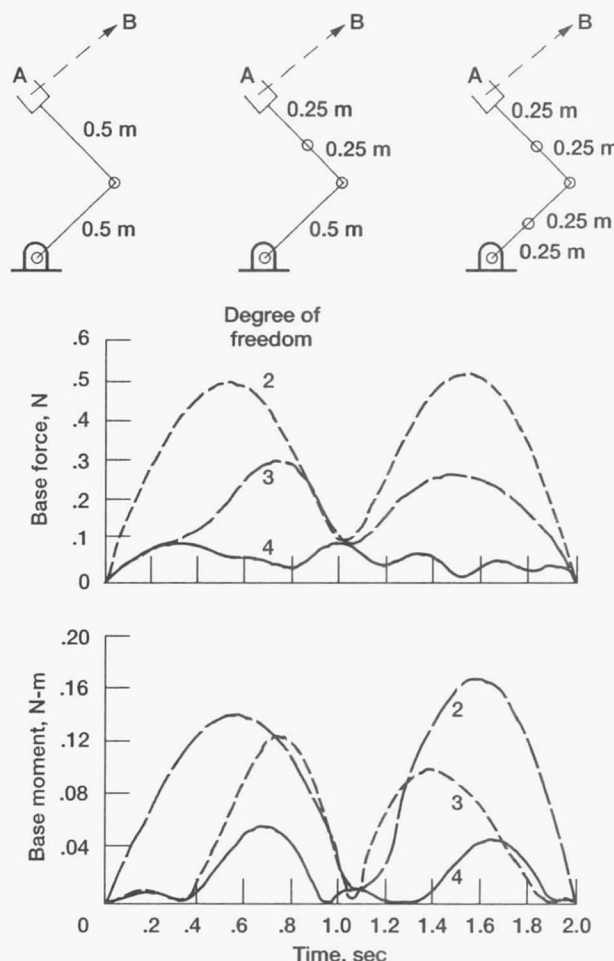
### Unified Motion Planning Approach Developed for Redundant Manipulators

Traditionally, motion planning refers to the process of generating a trajectory to accomplish a desired manipulation motion. In many studies the motion-planning problem has been solved purely from the kinematics viewpoint. However, this approach has major drawbacks. Besides its difficulty in dealing with actuator constraints, it does not provide any information regarding the actual performance of a manipulator when a closed-loop controller is used to execute the trajectory.

NASA Lewis has developed a unified motion-planning strategy for generating optimal (e.g., minimal time, minimal base reactions) trajectories for kinematically redundant and nonredundant robots. The approach was to couple the robot kinematics, dynamics, and controls to form an integrated dynamic optimization problem. Multicriterion optimization was then used to determine optimal end effector and joint trajectories.

The unified-trajectory-planning approach was developed for both redundant and nonredundant manipulators. Both motion planning and controller synthesis were addressed simultaneously. Multiple optimization criteria, such as minimal trajectory time, minimal base reaction, and actuator torque constraints, were included in the framework. By using an original definition of kinematic redundancy, the superior performance of redundant manipulators was demonstrated.

The study was the first methodology to employ multiple objective criteria and actuator constraints. As a result robot planning can be accomplished in an integrated fashion. The methodology is being integrated into the matrix control design module (Integrated Systems Inc.), a widely used controls software package.



Base reactions of two-, three-, and four-degree-of-freedom planar manipulators.

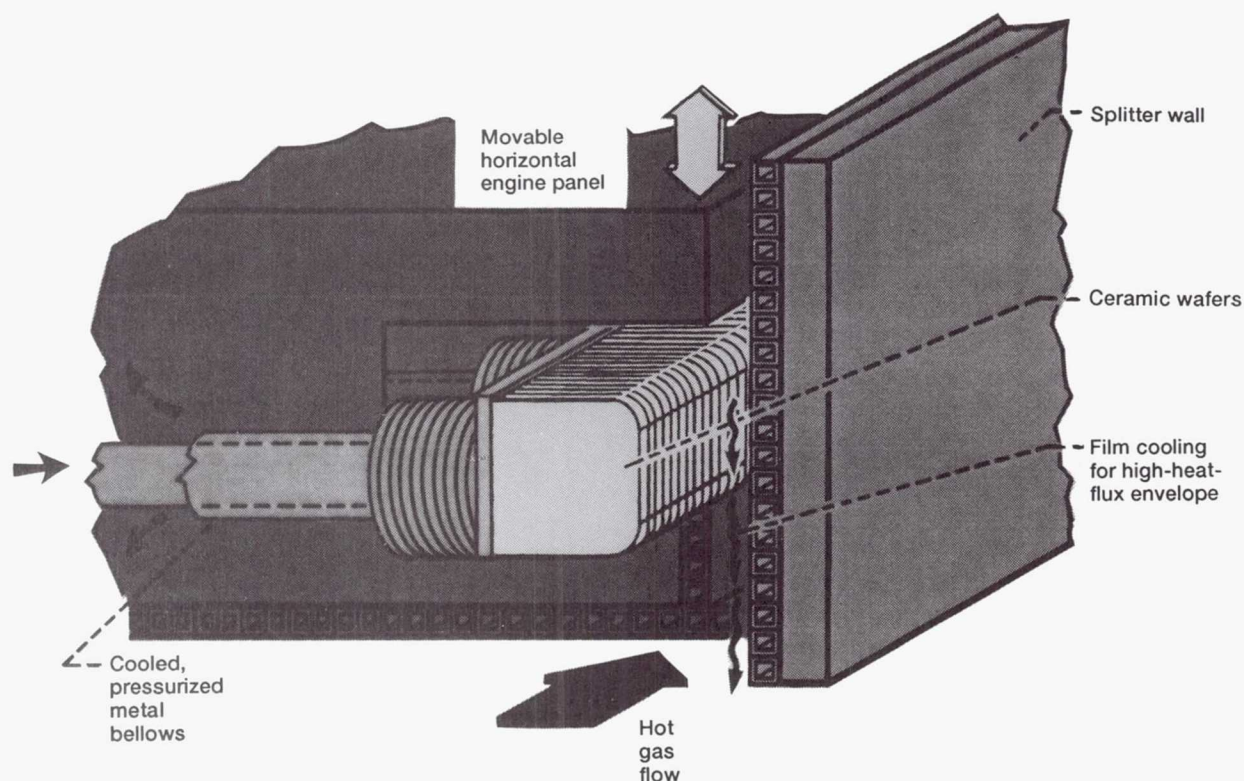
**Lewis contact:** Dr. Charles Lawrence, (216) 433-6048  
**Headquarters program office:** OAST

### High-Temperature Ceramic-Wafer Seal Leakage Assessed

High-temperature, flexible seals are required to seal the many feet of sliding, structural-panel interfaces of the National Aerospace Plane (NASP) engine. The seals are needed to form an effective barrier against leakage of the superheated ( $>4000^\circ\text{F}$ ), pressurized (up to 100 psi) flow path gases and thus prevent catastrophic burn-through of back-side articulation systems.

To solve this problem, NASA Lewis has developed a high-temperature, flexible, ceramic-wafer seal.





*Isometric of high-temperature, flexible, ceramic-wafer NASP engine seal.*

The seal will be used between the movable horizontal engine panel and the adjacent splitter wall. The seal uses a series of preloaded seal wafers mounted in a channel in the movable engine panel. Flexibility of the wafer stack is achieved through relative sliding between adjacent wafers. The wafers are preloaded against the adjacent splitter wall by using a series of pressurized Inconel metal bellows. The wafers can be made of any of the high-temperature, engineered ceramics including silicon carbide (SiC), silicon nitride ( $\text{Si}_3\text{N}_4$ ), or aluminum oxide ( $\text{Al}_2\text{O}_3$ ). Making the wafers out of high-conductivity silicon carbide ceramic will reduce the active coolant requirements, saving considerable weight and minimizing demands on engine coolant resources that are already stretched to their limits. But to demonstrate this concept in a timely manner, initial tests used wafers made of aluminum oxide ceramic, which is relatively inexpensive and easily obtained.

Leakage measurements were made by using a unique NASA Lewis panel-edge seal test fixture. Key parameters, such as temperature, pressure, wall condition, and preloads, were controlled and varied. Ceramic wafer seal leakage rates were measured at temperatures up to 1350 °F (the

typical temperature 1 to 2 in. forward of the combustor) and at pressures up to 100 psi (the maximum normal engine pressure). By using interchangeable front walls, the seal's ability to conform to and seal against both flat and engine-simulated distorted wall conditions was assessed.

The seal performed exceptionally well. Leakage rates were below the tentative limit (established by the NASP engine seal community) for the full range of engine pressures. Seal leakage repeatability was also demonstrated.

**Lewis contact: Dr. Bruce M. Steinetz, (216) 433-3302**  
**Headquarters program office: OAST**

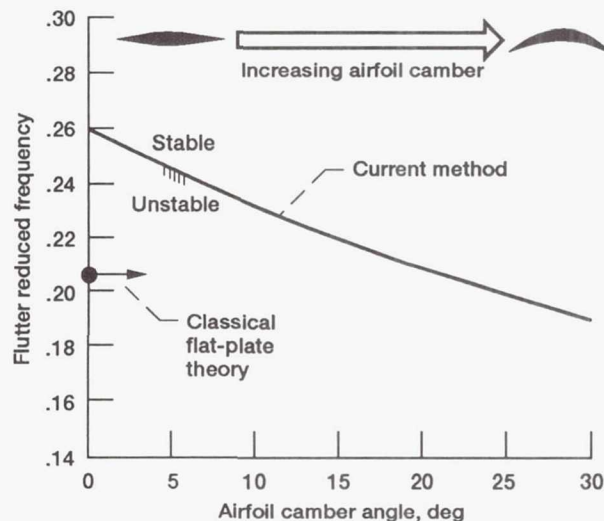
## Efficient Flutter Analysis Developed for Cambered Compressor and Turbine Blades

Designers of turbomachinery for aircraft and propulsion systems rely heavily on simplified flutter analysis methods. These methods are most commonly based on simple unsteady aerodynamic theories that disregard the effect of real airfoil shape and off-design flow conditions. A considerable data base of empirical correlations has been compiled in order to adjust designs to achieve aeroelastic stability. The primary motive for using these empirical design systems is that they are cost effective (in computer resources and time) and fairly accurate for design analysis.

Research at NASA Lewis is focused on developing advanced unsteady aerodynamic and aeroelastic models to specifically address the flutter problem. One of the tools that has been developed for NASA Lewis is a linearized, unsteady aerodynamic code (LINFLO) for calculating two-dimensional flows due to airfoil oscillation and wake passing in turbomachinery cascades. This code has been developed under contract to NASA Lewis by United Technologies Research Center. The code is applied to airfoils having large thickness and high camber and flow turning and operating within subsonic to transonic flow regimes. A distinct advantage of LINFLO is that it assumes harmonic airfoil oscillations, so that the unsteady solution is performed in the frequency domain. Subsonic flutter inception has been found experimentally to be fully linear and to occur at a discrete single frequency. The frequency domain approach results in computation times that offer several orders of magnitude reduction relative to comparable CFD time domain methods.

A flutter prediction code has been developed that uses LINFLO to compute unsteady aerodynamic loads. The aeroelastic code is based on a classical two-degree-of-freedom, lumped-parameter structural model that represents a "typical section" of a full three-dimensional blade. An iterative flutter search technique based on Newton's method is used to pinpoint the conditions under which a flutter instability may occur.

The method has been demonstrated by analyzing a compressor cascade operating under subsonic flows. The compressor blade was modeled as a flat plate, and an NACA 0006 thickness distribution was applied over circular-arc mean camber lines of various camber levels. In addition, a



Efficient flutter analysis developed for cambered compressor and turbine blades at Mach 0.6.

single airfoil case was analyzed over a range of Mach numbers and steady flow incidence angles.

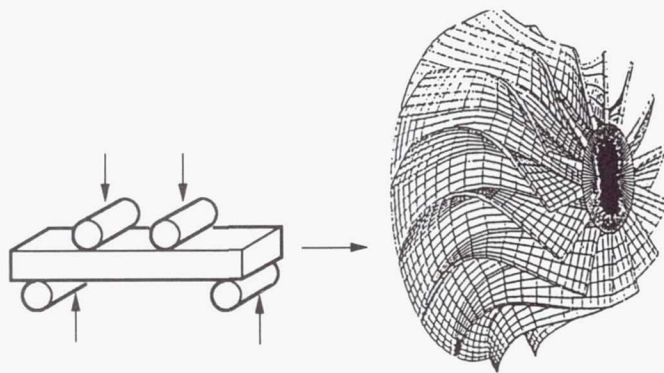
The results indicate that increasing the airfoil camber stabilizes the rotor when considering classical bending-torsion flutter. These results also demonstrate the sensitivity and susceptibility of a cascade to airfoil shape, and in particular to the airfoil camber. The same sensitivity has been shown for variations in the inlet flow incidence angle into the cascade. Neglecting the effect of steady aerodynamic loading due to either airfoil shape (thickness and camber) or steady flow incidence can cause misleading estimates of turbomachinery flutter behavior.

**Lewis contact:** George L. Stefko, (216) 433-3920  
**Headquarters program office:** OAST

## Integrated Design Program Predicts Life of Monolithic Ceramic Components

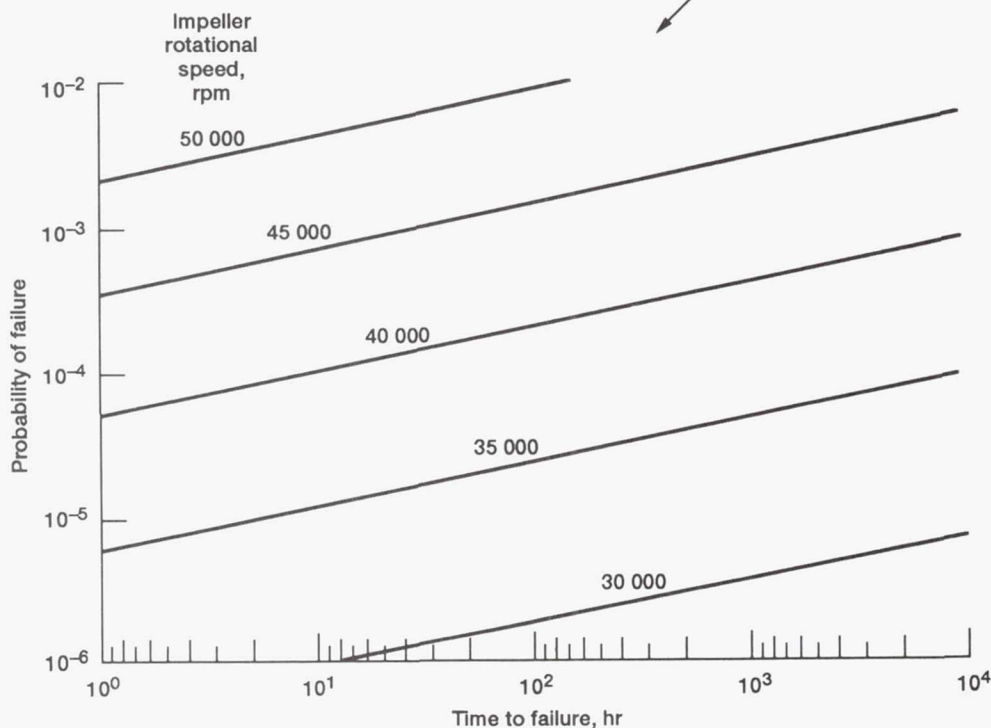
Ceramics are candidate materials for advanced heat engine applications because of their ability to sustain load at high temperatures and their relatively low density. However, ceramics are brittle and ceramic components fail because of the unavoidable presence of preexisting flaws. Designing with these materials requires knowledge of the probabilistic nature of these flaws as





Simple tests

Complex predictions



Typical usage of CARES/LIFE code.

well as the physics of crack growth. The Ceramics Analysis and Reliability Evaluation of Structures Life Prediction (CARES/LIFE) computer program, which is being developed at NASA Lewis, characterizes this behavior to predict the probability of a monolithic ceramic component's failure versus its service life. CARES/LIFE couples commercially available finite element programs, such as NASTRAN, ANSYS, and ABAQUS, to probabilistic design methodologies.

CARES/LIFE is the time-dependent extension of the CARES code, which predicts fast-fracture reliability of ceramic components. Fast-fracture

refers to uncontrolled crack growth from preexisting flaws. Slow (subcritical) crack growth refers to controlled growth until a critical crack size is reached so that fast-fracture ensues. These phenomena are accounted for by using fracture mechanics relationships and Weibull statistics. CARES/LIFE is the successor code to CARES and includes new, user-friendly features and personal computer capability.

CARES has been distributed to many companies and research organizations worldwide. Applications include design of gas turbine rotors and stationary parts, internal combustion engine

exhaust valves, bearings, laser windows on test rigs, radomes, spacecraft activation valves, cathode ray tubes, rocket launcher tubes, and microchip substrates. Engineers and material scientists also use CARES to reduce data from specimen tests to the fundamental statistical parameters for a material. In this way a comparison of materials is achieved that is independent of the specimen geometry and loading.

#### Bibliography

Nemeth, N.N.; Manderscheid, J.M.; and Gyekenyesi, J.P.: *Ceramics Analysis and Reliability Evaluation of Structures (CARES) Users and Programmers Manual*. NASA TP-2916, 1990.

**Lewis contacts:** Noel N. Nemeth, (216) 433-3215;

Lynn M. Powers, (216) 433-8374

Headquarters program office: OAST

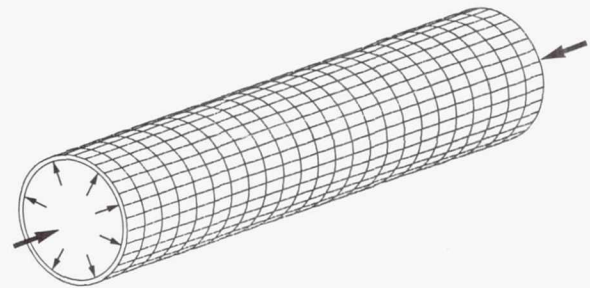
#### Reliability Evaluated for Laminated CMC Components

Structural components fabricated from laminated ceramic-matrix composite (CMC) materials are being considered for a broad range of aerospace and industrial applications, specifically those involving high-temperature environments. Although CMC-material systems exhibit potentially critical properties, such as strength retention at high temperatures, chemical inertness, and low density, the general variability in strength (especially in directions transverse to the fiber reinforcement) requires a rethinking of design concepts. Traditional factor-of-safety design procedures that are rooted in deterministic engineering mechanics and commonly used for metal alloys must be abandoned. Use of this class of engineered materials will be aided by probabilistic design methods that are under development.

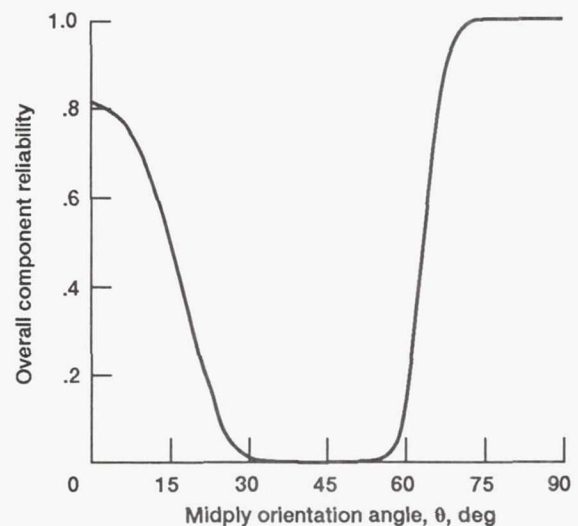
In order to help establish this new philosophy, the integrated design program C/CARES (Composite Ceramics Analysis and Reliability of Structures) was developed with funding from the Advanced High Temperature Engine Materials Technology Program (HITEMP). This ongoing project for developing probabilistic design methods is supported by personnel at NASA Lewis working under a cooperative agreement with Cleveland State University. The goal is to provide design engineers with a computer program that predicts reliability bounds for structural compo-

nents fabricated from laminated CMC-material systems. Component stress fields obtained from finite element analyses are fundamental in predicting component reliability. The C/CARES program is interfaced with two commercial finite element codes, MSC/NASTRAN and MARC. In general, the program uses a formatted neutral data base, which allows C/CARES to be coupled to any general-purpose finite element program that supports laminated composite analysis.

A major advantage of designing components with laminated CMC materials is the ability to tailor the high-strength direction of plies in order to maximize component reliability. Ply orientation has a decided effect on a component's structural integrity. Through the use of C/CARES the design engineer can optimize component reliability by exploring multiple ply layups and orientations for a given component.



Three-ply laminate ( $90^\circ/\theta/90^\circ$  layup) where  $\theta$  is measured relative to longitudinal axis



Reliability of thin-wall tube subjected to intensive pressure (4.25 MPa) and axial compressive load (87.5 MPa).



## Bibliography

Duffy, S.F.; Palko, J.L.; and Gyekenyesi, J.P.: Structural Reliability Analysis of Laminated CMC Components. NASA TM-103685, 1991.

Starlinger, A.; et al.: Reliability Analysis of Laminated CMC by Applying Shell Subelement Techniques. To be presented at AIAA/ASME/ASCE/AHS/ASC 33rd Structures, Structural Dynamics, and Materials Conference, Dallas, TX, Apr. 1992.

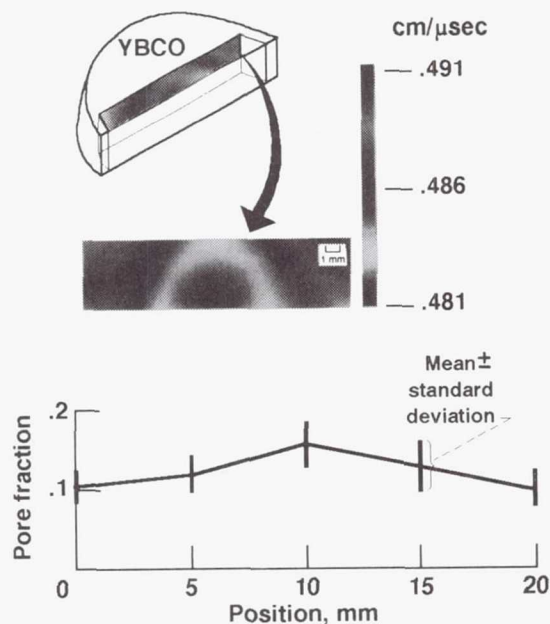
**Lewis contacts:** Joseph L. Palko, (216) 433-5587; Dr. Alois Starlinger, (216) 433-6510; Dr. Steve Duffy, (216) 433-5626

Headquarters program office: OAST

## Ultrasonic Test Determines Superconductivity Variations Caused by Porosity Gradient

The last several years have seen the remarkable development of a new class of ceramics that exhibit superconductivity to unprecedentedly high temperatures. The subject of work at NASA Lewis is the yttrium-barium-copper-oxide (YBCO) superconductor. Microstructural and compositional variations have resulted in significant electrical and magnetic property variations in YBCO. Previous observations of ceramics show that such microstructural and property variations may be present *within* individual YBCO parts. Knowledge and minimization of such spatial variation is critical both to quantitative analysis (predictability) of the superconductor's behavior and to attempts at optimizing properties, such as normal-to-superconducting transition temperature and critical current density.

In this study spatial variations in microstructure and properties were investigated for YBCO specimens from 75 to 90 percent of theoretical density. The study comprised two experiments. In the first, alternating current susceptibility measurements were used to examine superconducting behavior at edge and center locations of specimens without prior knowledge of microstructural or compositional differences at these locations. In the second, an ultrasonic scan technique was employed to locate within-sample microstructural nonuniformity in a YBCO disk. Susceptibility measurements were made at locations that ultrasonic images indicated as nonuniform. Microstructural analysis was performed on several sample sections to determine the microstructural



Ultrasonic test determines superconductivity variations caused by porosity gradient.

feature or features responsible for the variability observed in ultrasonic images.

First, it was observed that the densest samples (90 percent) exhibited significant differences in superconducting transition temperature and transition width at edge and center locations. Second, an ultrasonic velocity image constructed from measurements at 1-mm increments on a typical sample revealed microstructural nonuniformity from edge to center. The microstructural nonuniformity was not optically apparent on the intact sample. However, the nonuniformity was revealed to be a pore fraction gradient from edge to center after cutting open the sample and performing optical image analysis measurements. Thus, the velocity image revealed microstructural variations that correlated with variations in superconductor behavior. The ramifications of this are that a *room-temperature*, noninvasive technique (ultrasonic velocity imaging) exhibited the ability to predict spatial variation in *cryogenic* behavior of superconductors. Such a tool can prove invaluable in process control by reducing the need to test these materials at cryogenic temperatures. Future testing in this area will study spatial variations in these materials in greater detail than just at edge and center locations. An additional observation was that less dense samples (75 to 85 percent) did not exhibit significant property or microstructural nonuniformity at edge and center locations.

## Bibliography

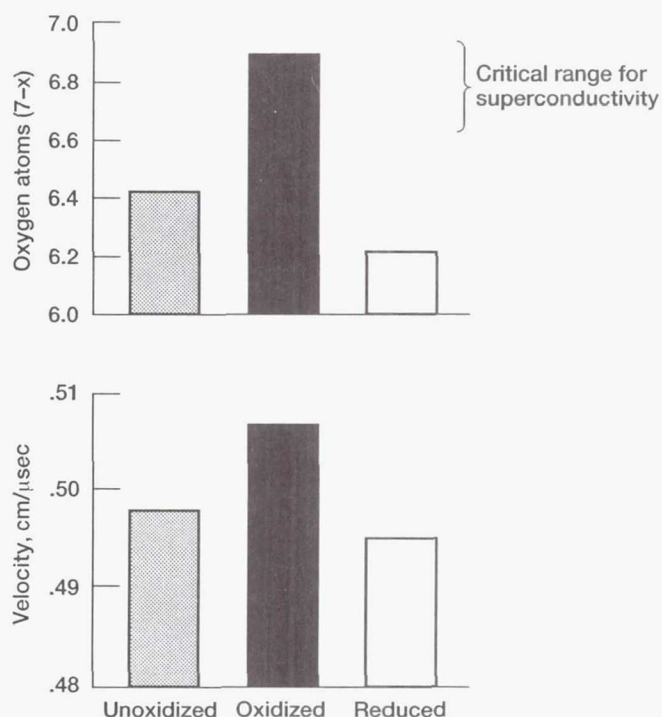
Roth, D.J., et al.: Spatial Variations in ac Susceptibility and Microstructure for the  $\text{YBa}_2\text{Cu}_3\text{O}_{(7-x)}$  Superconductor and Their Correlation With Room-Temperature Ultrasonic Measurements. NASA TM-103787, 1991.

**Lewis contact: Dr. Don J. Roth, (216) 433-6017**  
**Headquarters program office: OAST**

## Processing Changes in $\text{YBa}_2\text{Cu}_3\text{O}_{7-x}$ Ultrasonically Evaluated

NASA Lewis is studying the yttrium-barium-copper-oxide (YBCO) superconductor, one of a remarkable new class of ceramics that exhibit superconductivity to unprecedentedly high temperatures. Oxidation (immersing the sample in pure oxygen gas at elevated temperatures) is the final and, arguably, the most important processing step in the manufacture of YBCO. This step increases oxygen content from the sintered state, making the material superconducting. Loss of oxygen (reduction) diminishes superconductivity and can result from the chemical reaction between YBCO and water. In addition to oxygen content changes during oxidation and reduction, microstructural changes occur that can further affect YBCO's superconducting and mechanical behavior. (Mechanical behavior becomes an issue if these materials are to be used in magnets that will experience large stresses.) In its study NASA Lewis evaluated changes in the oxygen content, bulk density, stiffness, and microstructure of YBCO occurring during oxidation and reduction. The primary focus of this work was the use of a nondestructive measurement, ultrasonic velocity, as a means of evaluating the observed material and property changes. More specifically, changes in ultrasonic velocity were correlated with oxygen content, density, and microstructural change and used to calculate stiffness changes in order to assess the feasibility of using velocity measurements as a process control. YBCO samples ranging from 70 to 90 percent of theoretical density underwent oxidation and reduction treatments.

Qualitative agreement was obtained between changes in velocity and changes in oxygen content and density. The ultrasonic velocity, bulk density, and Young's modulus generally increased with oxygen content upon oxidation; this behavior



*Ultrasonic velocity proves feasible for monitoring oxygen content in YBCO ceramic superconductor.*

was reversible upon reduction. From previous experience concerning the strong density effect on velocity, it is likely that during oxidation and reduction the velocity changes were most strongly influenced by the density changes accompanying the oxygen content changes. Thus, oxygen content changes may be interpreted, at least qualitatively, in terms of density and velocity changes. The ramifications of this are that ultrasonic velocity measurements can help control oxidation during processing and can help monitor oxygen loss during service. In future tests NASA Lewis hopes to improve the understanding of the relation between oxygen content and velocity by working with single crystals to eliminate bulk material effects.

Ultrasonic velocity images of a YBCO sample were similar after oxidation and reduction treatments, although the velocity value at any given point on the sample was different after the treatments. The unchanging velocity pattern correlated with destructive measurements which showed that the spatial pore distribution (fraction and size) was not measurably altered after the treatments. It also suggested that extended oxidation times were sufficient for uniform oxygenation of high-density samples.



## Bibliography

Roth, D.J., et al.: Ultrasonic Evaluation of Oxidation and Reduction Effects on the Elastic Behavior and Global Microstructure of  $\text{YbA}_2\text{Cu}_3\text{O}_{(7-x)}$ . NASA TM-104529, 1991.

**Lewis contact:** Dr. Don J. Roth, (216) 433-6017

**Headquarters program office:** OAST

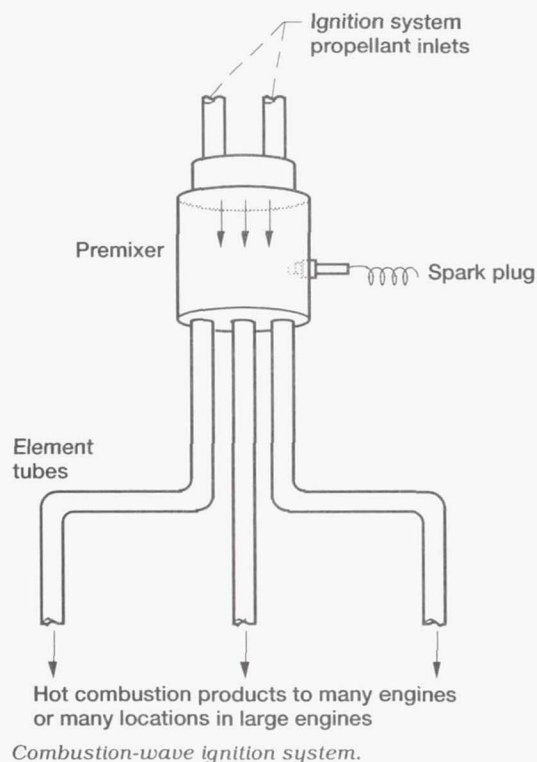
## Space Propulsion Technology

### Combustion-Wave Ignition Demonstrated for Multiple Engines

A combustion-wave ignition system is a device that can be used to initiate ignition simultaneously in many rocket engines or, alternatively, in many locations in a large engine. Tests of a subscale prototype show excellent results.

The ignition system consists of a premixer and a varying number of element tubes. The propellants are mixed in the premixer and ignited by electrical sparks. The element tubes allow the flame to propagate to those locations requiring ignition. The system is unique because it requires only a few weak sparks to generate the combustion wave, and once generated, the combustion wave propagates through the tubes and transforms into a powerful detonation that carries energetic combustion products for ignition. A complete set of tests have been performed on a prototype system to demonstrate the theory of combustion-wave ignition.

In the tests two propellant combinations were used: oxygen/hydrogen and oxygen/methane, both in the gaseous state. Straight and bent tubes of various lengths and diameters were tested in combination. In addition, a test engine was installed to confirm the ignition system's capability. For each of these apparatus configurations the propellant mixture ratio was varied to identify the conditions required for ignition and their associated ignition timing. The test results show that ignition is attainable over a wide range of mixture ratios, that the ignition delay for all apparatus configurations used is consistently



well under 10 msec, and that the ignition delay difference across the tubes is below 1 msec.

In summary, the test results have shown that the combustion-wave ignition system offers many attractive characteristics that can be used to simultaneously ignite multiple engines, such as the clustered engines proposed for the National Launch System.

**Lewis contact:** Larry C. Liou, (216) 977-7433

**Headquarters program office:** OAST

### Atomic Implants Investigated for Spectroscopic Wear Detection

A common failure mode for the internal components of liquid-propellant rocket engines is wear. A technique utilizing "tracer" atoms is being investigated for real-time detection of maximum allowable component wear. This technique involves implanting an atomic species into the structure of a component and then making spectroscopic measurements of the engine plume.

The tracer species is implanted into the structure to a predetermined depth that is based on the

maximum allowable wear of the component. As the component wears, the implanted species surfaces and begins to erode. The eroded particulates are carried by the propellants into the combustion chamber, where they are thermally excited and emit their characteristic spectrum. By spectroscopically monitoring the contents of the plume, it is possible to identify the presence of the implanted atomic species by its emissions. Detection of the implanted species in the plume indicates that the component has worn down to the maximum allowable level.

Implementing this technique requires that the implanted species is not normally found in any of the components in the propulsion system and is spectrally observable upon thermal excitation. In addition, it has to be metallurgically compatible with the materials of the structure to be monitored for wear.

Several implantation techniques have been identified. Implantation can be accomplished by accelerating the atoms in a particle accelerator and allowing them to impact the component. The depth of the penetration depends on the energy gained by the atoms in the accelerator. An alternative approach is to sputter or evaporate the species onto the structure and "implant" this layer by coating it with a layer of the structure material.

NASA Lewis is pursuing the development of this technology for rocket engine wear detection. Initial experiments have been performed with tantalum implanted into the cathode of a magnetoplasmadynamic engine. Further work is planned with different material implanted into components of hydrogen/oxygen-fueled engines.

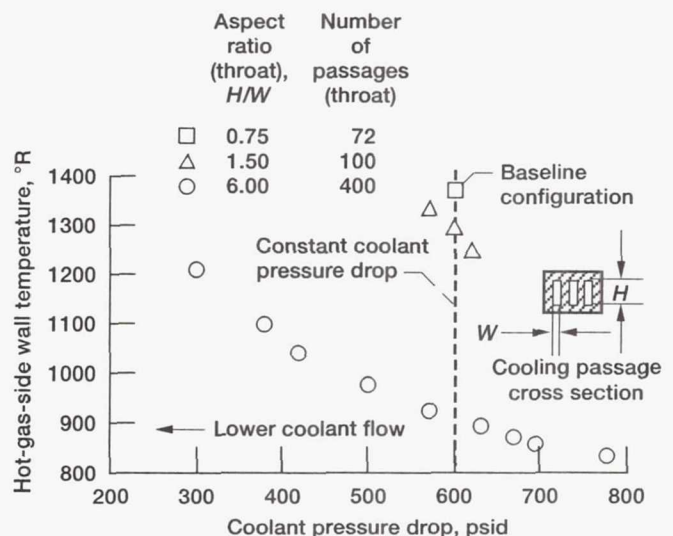
Lewis contact: George C. Madzsar, (216) 977-7434  
Headquarters program office: OAST

## Rocket Engine Advanced Cooling Techniques Evaluated

High-pressure, reusable rocket engines, such as the Space Shuttle main engine (SSME), are life limited by cracks that form in the wall of the combustion-chamber cooling jacket. During engine operation the hot-gas-side wall tries to expand but is constrained by the relatively cool structural jacket. The resulting high plastic strain in the hot-gas-side wall causes a progressive thinning and roughening of the wall with each thermal cycle, known as thermal ratcheting. After repeated thermal cycles, cracks develop.

One way to reduce the strain and extend chamber life is to lower the hot-gas-side wall temperature. Analyses have shown that this can be done by substantially increasing the coolant-side surface area relative to the hot-gas-side surface area. Increasing the number of cooling passages, for a given total coolant flow area, requires the use of high-aspect-ratio cooling passages (height/width). The net result is an increase in the fin effect of the cooling passage ribs.

In order to evaluate this concept, three subscale rocket chambers were tested, all having the same total coolant flow area, but each with a different number of cooling passages and different aspect ratios. The 72-cooling-passage chamber represents the baseline configuration (i.e., the maximum allowable hot-gas-side wall temperature). The 400-cooling-passage chamber represents a high-aspect-ratio configuration.



Hot-gas-side wall temperature at throat versus coolant pressure drop.



The experimental results show that the hot-gas-side wall temperature can be substantially lowered for a given coolant pressure drop as the aspect ratio increases. Furthermore, the data show that the pressure drop for the high-aspect-ratio configuration can be reduced, while still achieving a significant drop in wall temperature, by decreasing the coolant weight flow.

The use of high-aspect-ratio cooling passages in the design of high-pressure rocket thrust chambers has the potential of significantly extending chamber life and, because of the lower pressure drop requirements, reducing the load on the turbomachinery.

The tests were performed on subscale rocket chambers with straight cooling passages. The work will be extended to investigate the effectiveness of high-aspect-ratio cooling passages in the throat region of contoured chambers. There secondary flow effects in the fluid going through the curved cooling passages may change the magnitude of the temperature reduction achieved in straight cooling passages.

**Lewis contacts:** Julie A. Carlile, (216) 977-7432;

Richard J. Quentmeyer, (216) 977-7471

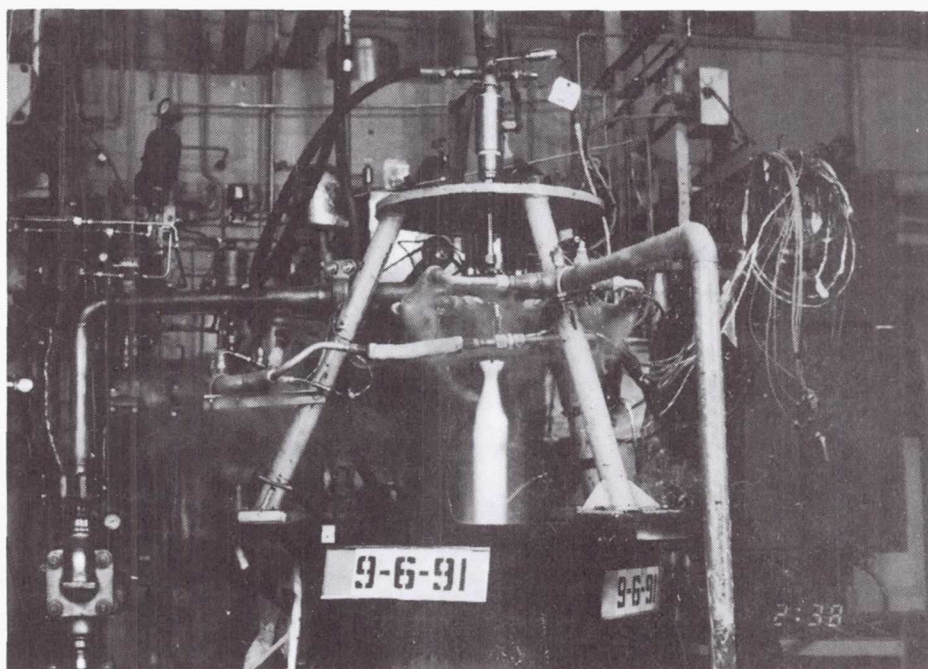
**Headquarters program office:** OAST

### **Tubular Copper Thrust Chamber Fabricated and Tested**

An ongoing focused-technology study in support of the Space Chemical Engine Technology Program has evolved into fabrication and hot-fire testing of candidate tubular copper thrust chamber configurations. Analysis of a tube bundle configuration fabricated by electroform bonding of the tubes has shown significant potential.

The thermal analysis showed that the tubular thrust chamber configuration promised a 18- to 40-percent additional enthalpy extraction with a coolant pressure drop approximately the same as that for the state-of-the-art (Space Shuttle main engine) channel chamber configuration.

Fatigue life analysis has shown a strain decrease of 25 percent for a tube bundle configuration, which results in a 100-percent increase in fatigue life over an equivalent "milled liner" configuration. In order to confirm these advantages, several candidate configurations have been fabricated by a cost-efficient electroform bonding procedure and successfully leak tested at twice the design pressure without failures or leaks. These configurations are presently being hot-fire tested to verify the fatigue life and heat transfer advantages predicted by the analysis. Preliminary



*Hot-fire testing of tubular copper thrust chamber.*

results appear to confirm the analysis predictions. Further testing will provide conclusive evidence.

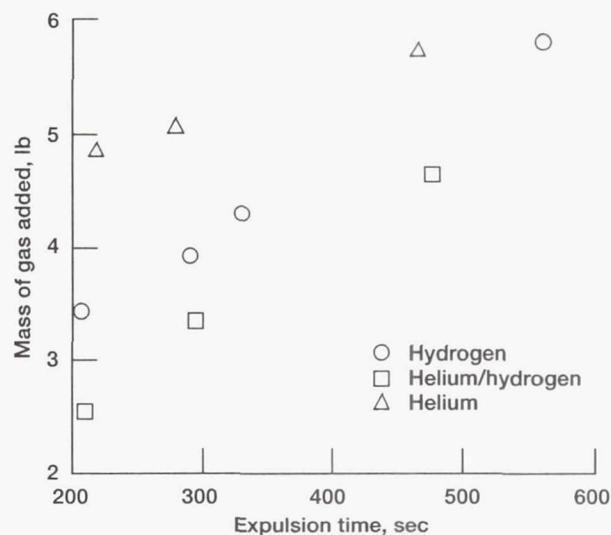
**Lewis contacts:** John M. Kazaroff, (216) 433-2473; Robert S. Jankovsky, (216) 433-2471; Albert J. Pavli, (216) 433-2470  
**Headquarters program office:** OAST

### Slush Hydrogen Experiments Conducted at K-Site Facility

Slush hydrogen (SLH<sub>2</sub>), a mixture of solid and liquid hydrogen, has been selected to fuel the National Aerospace Plane (NASP) (ref. 1). The SLH<sub>2</sub> is denser and has a higher heat capacity than normal-boiling-point liquid hydrogen (NBPH<sub>2</sub>), thus potentially reducing the vehicle size and weight. Previous testing (refs. 2 to 4) at the K-Site facility provided the first large-scale production and handling experience with SLH<sub>2</sub>. The current test series was developed to address specific NASP issues, such as tank pressure control.

Slush hydrogen is produced and exists as a mixture of solid and liquid hydrogen at 24.8 °R and 1.02 psia. Thus, sudden sharp decreases in tank ullage pressure can occur with fluid motion, such as mixing or sloshing. These decreases in tank pressure could result in failure of a propellant tank. The NASP SLH<sub>2</sub> technology program is therefore investigating tank operation and specifically tank pressure control.

The SLH<sub>2</sub> testing was conducted at the K-Site facility, which is located at NASA Lewis' Plum Brook Station. The testing included large-scale production and transfer operations, as well as specific tank pressure control testing. Pressurized expulsion tests were conducted by ullage injection, through the main pressurant line, of gaseous helium (GHe) and gaseous hydrogen (GH<sub>2</sub>), or GHe during pressurization followed by GH<sub>2</sub> during the expulsion. Recirculation tests were also conducted with GH<sub>2</sub> injected into the SLH<sub>2</sub> through a submerged recirculation tube. Tank pressures were 35 and 50 psia, with the pressurant at 540 and 250 °R. Most of the tests included in-tank mixing of the propellant.



Effect of pressurant gas type on mass of gas added. Tank pressure, 35 psia; gas temperature, 520 °R.

During the test series 75 batches of SLH<sub>2</sub> with greater than 50-percent solid fraction (greater than 5.11 lb/ft<sup>3</sup>), totaling approximately 48,000 gal, were produced. The average batch size was 640 gal. After production and prior to SLH<sub>2</sub> transfer, the 1.5-in.-diameter transfer line and the test tank were prechilled by using NBPH<sub>2</sub>. The SLH<sub>2</sub> was pressure transferred from the generator to the 5-ft-diameter spherical test tank, which was located inside a 25-ft-diameter vacuum chamber. Output from the transfer tests included flow-rate-versus-pressure-drop characteristics as well as solid fraction loss during transfer.

Preliminary results from the pressurized expulsion tests show that pressurant gas type significantly affected the pressurant gas requirements during the expulsion process. The mass of gas added was highest for the helium cases and lowest for the helium/hydrogen cases. Initial pressurization with helium may reduce the condensation, and hence pressurant gas requirements, during expulsion.

### References

1. Kandebo, S.W.: NASP Team Narrows Its Options as First Design Cycle Nears Completion. *Aviat. Week Space Technol.*, vol. 134, no. 13, Apr. 1, 1990, p. 80.
2. Whalen, M.V., et al.: Preliminary Data of Slush Hydrogen Propellant Tank Studies at NASA K-Site Facility. NASP TM-1131, 1991.



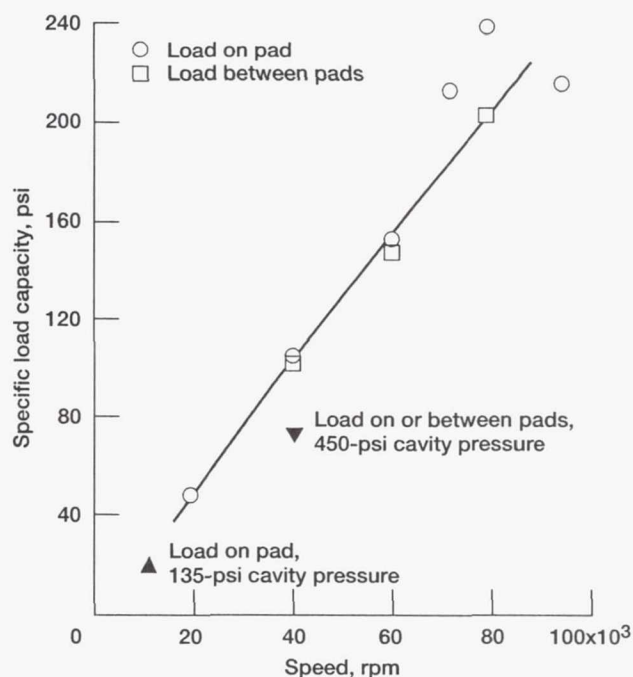
3. Hardy, T.L., et al.: Transfer of Slush Hydrogen Through the K-Site Facility Cryogenic Flow System. NASP TM-1136, 1991.
4. Whalen, M.V., et al.: Pressurized Expulsion Studies of Slush Hydrogen Using Hydrogen Pressurant Gas. NASP TM-1143, 1991.

**Lewis contacts:** Terry L. Hardy, (216) 977-7517; Margaret V. Whalen, (216) 977-7530  
**Headquarters program office:** OAST

### Performance Characteristics of Liquid Hydrogen Foil Bearing Demonstrated

NASA Lewis and AiResearch Division of Allied-Signal Aerospace Company have jointly conducted a test program to demonstrate the load-carrying capacity and other performance characteristics of a bending-dominated foil journal bearing in liquid hydrogen. Foil bearings are candidates for use in small, high-speed cryogenic turbopumps, offering the potential benefits of long life and reliability. They have an admirable service record in aircraft auxiliary power units and in Earth-based machines. In those applications the bearing lives are on the order of 10,000 hours and they sustain many start-stop cycles. But the radial bearing loads in those machines range from only 10 to 40 psi (based on projected bearing area). Space transfer vehicle bearings require larger load capacities, ranging from 40 to 200 psi. The problem was to develop a small, high-speed bearing that could support these loads via the hydrodynamic principle when using an extremely low-viscosity fluid, liquid hydrogen.

AiResearch developed a high-performance foil bearing with a predicted load capacity of 280 psi at 80,000 rpm. The 1.75-in.-diameter bearing consists of five overlapping foils, each foil supported by an underspring optimized for load capacity and stiffness. Foil coatings aid in accommodating the journal's starts and stops. Teflon-S and polyimide-bonded graphite fluoride (PBGF) were tested in the program. The bearing was tested in a liquid hydrogen test facility at NASA Lewis' Cryogenic Components Laboratory. The tester was driven by a gaseous hydrogen turbine. Radial loads were placed on the test shaft by a pneumatic loader, and a dynamometer measured the frictional drag in the test bearing.



Load capacity of high-performance foil journal bearing. Cavity pressure, 800 psi; diameter, 1.75 in.

Experimental results were very encouraging. Load capacity was proportional to speed. At 80,000 rpm it was 240 psi—a 600-percent increase over air bearing load capacity. At 80,000 rpm the bearing power loss was 2.2 hp, at one-tenth of the flow for a similar size rolling-element bearing. The Teflon-S foil coating sustained 130 start-stop cycles. The PBGF foil coating sustained 170 start-stop cycles. No wear was detected in either coating. A minimum of 100 start-stop cycles is required for space transfer vehicle turbopumps. The fluid film was stable throughout the speed range of 10,000 to 97,000 rpm, showing very low subsynchronous response.

The remaining technical issues to be determined for this bearing in liquid hydrogen are separated rotordynamic coefficients and performance in turbopump configurations.

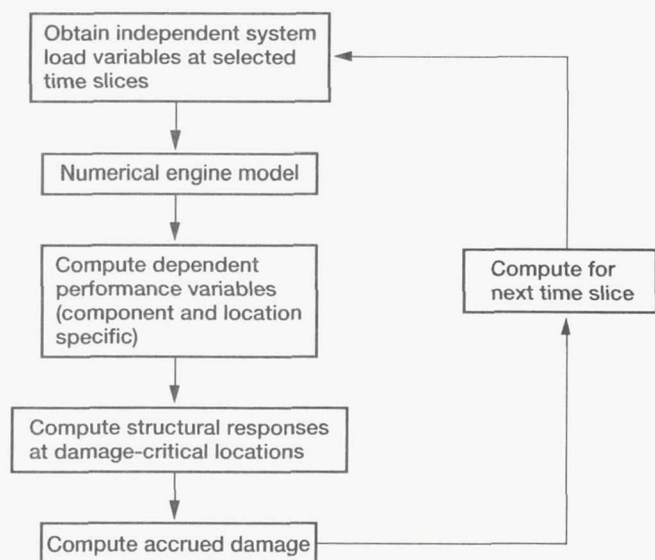
### Bibliography

Saville, M.; Capaldi, R.; and Gu, A.: Liquid Hydrogen Turbopump Foil Bearing. AIAA Paper 91-2108, June 1991.

**Lewis contact:** Russell J. Capaldi, (216) 433-6676  
**Headquarters program office:** OAST

## Advanced Method Tracks Evolution of Fatigue Damage in Reusable Space Propulsion Systems

A general method has been developed for tracking the evolution of fatigue damage at preselected locations in reusable space propulsion system components. The method is suitable for use in advanced diagnostic or prognostic health-monitoring systems. The fatigue damage accrued is calculated by using a state-of-the-art nonlinear damage accumulation method. The accumulated damage is a function of propulsion system performance variables, some of which are measured routinely to monitor system performance. The proposed methodology computes the accumulated damage in a three-step process. In the first step the boundary conditions and the hot gas and coolant characteristics are computed by using a numerical engine model together with actual measurements. In the second step detailed structural response quantities of interest, such as effective (Von Mises) stress, effective strain, and plastic strain, are computed by using quick influence coefficient models. The coefficients for the influence coefficient model are obtained from state-of-the-art finite difference and finite element detailed thermal and structural models. This one-time effort need not be repeated for mission-to-mission tracking. As a third step the detailed damage computation module is used to compute the accrued damage for a variety of options. The entire procedure is in the form of two computer codes for efficiently tracking the condition of the



Overview of methodology linking performance variables to damage.

hardware after each test or flight. Furthermore, with this method future engine operations can be better planned so that the maximum damage accumulated does not violate allowable criteria.

**Lewis contact:** Michael A. McGaw, (216) 433-3308  
**Headquarters program office:** OAST

## Brush Seals for Cryogenic Turbopumps Studied

Engineers at NASA Lewis are studying the application of brush seals in cryogenic turbopumps for rocket engine systems. Labyrinth seals in many aircraft gas turbine engines are being replaced by brush seals because brush seals are compliant, reliable, and cost competitive. They have been shown to leak less and to enhance rotor stability. Hence, in cryogenic turbopumps, where long-life, low-leakage, reliable seals are essential, brush seals may be a good candidate.

A brush seal is simply a ring of wire bristles sandwiched between a front and back washer. The bristles usually have a 5- to 10-mil interference fit with the shaft and are installed at a 30° to 60° angle to the radius so that the bristles can bend as cantilever beams during shaft perturbations. The back washer is on the low-pressure side of the seal and has an inside diameter just slightly larger than the bristle bore diameter. It supports the bristles, preventing them from blowing downstream, and acts as a fixed clearance seal should the bristles fail.

In a cryogenic turbopump brush seals may be used to seal either liquid hydrogen or liquid oxygen at locations near the pump or the bearings, or they may be used to seal hot gaseous hydrogen, warm gaseous oxygen, or helium at locations near the turbine or purge seals. In this environment large temperature gradients, oxygen compatibility, and hydrogen embrittlement are concerns. Also, the shaft speeds attained in cryogenic turbopumps for rocket engine systems are high, up to 200,000 rpm for a liquid hydrogen turbopump. Since brush seals are contact seals, their wear rate under these conditions is important.

In order to study these issues, a tester has been fabricated to test brush seals in liquid nitrogen





*Brush seal.*

and liquid hydrogen at the Cryogenic Components Laboratory. As many as five 2-in.-inside-diameter brush seals can be tested at one time at pressures to 150 psi per brush. Shaft speeds to 40,000 rpm, and with further modifications to 63,000 rpm, will be attained. After brush seal performance has been demonstrated in liquid nitrogen and hydrogen, several configurations will be tested to measure the effect of bristle and runner material combinations, brush and bristle geometry, and staging on leakage rate, wear rate, life, power loss, and stability. The data will also be used to calibrate and update an analytical computer code developed at NASA Lewis that models brush seal performance.

**Lewis contacts:** Margaret P. Proctor, (216) 977-7526;  
Julie A. Carlile, (216) 977-7432  
**Headquarters program office:** OAST

### **Advanced Concepts Program Studies High-Energy-Density Propellants**

A possible way to increase the performance of chemical rocket engines is by using higher energy propellants. Some of the most energetic chemical compounds and atoms, however, are unstable and have very short life. Atomic hydrogen is an example of this type of atom. Upon recombining, atomic hydrogen atoms release tremendous energy. Studies have shown the great promise of this atom as a rocket propellant. A specific impulse of 1.5 to 4 times that of the highest-performing chemical propellants may be attainable (ref. 1). However, creating, storing, and using these atoms efficiently is not easy. NASA Lewis is seeking ways to control these atoms for useful rocket propulsion.

Ongoing theoretical and experimental work of the Advanced Concepts Program is directed toward basic research on methods of using atomic hydrogen and other highly energetic materials for launch vehicle and upper stage propulsion. Research continued this year at a university and work began with two Department of Energy laboratories. In-house studies of the rocket engines and propellant storage systems are also continuing.

At the Lawrence Livermore National Laboratory the basic properties of atomic hydrogen were

studied. This research seeks to improve the storage density of atomic hydrogen to a level that is useful for rocket propulsion. By using a small glass microsphere of a hydrogen and tritium mixture, the forming and recombining of hydrogen atoms was scrutinized. These experiments were conducted at temperatures as low as 2 K ( $-456^{\circ}\text{F}$ ). Both heat and light energy is released when the atoms recombine. The different energy levels of this light and heat are being analyzed to discover the basic nature of these atoms. Computer modeling of atomic hydrogen in a solid molecular hydrogen storage medium is also under way at the University of Hawaii. Comparing the experimental results with current theories shows a marked difference between the density predicted with two different measurements. These discrepant estimates are under investigation.

Other activities are a study of the engine performance at NASA Lewis and work on powerful magnets for the storage and propellant transfer of atomic hydrogen and other free-radical propellants at the Oak Ridge National Laboratory.

#### Reference

1. Palaszewski, B.A.: Atomic Hydrogen as a Launch Vehicle Propellant. AIAA Paper 90-0715, Jan. 1990. (Also, NASA TM-102459.)

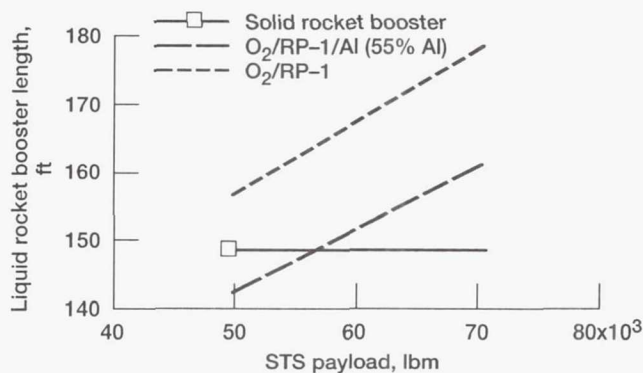
**Lewis contact:** Bryan Palaszewski, (216) 433-2439  
**Headquarters program office:** OAST

### Metallized Propellant Program Develops New Technologies

In the Metallized Propellant Program the technologies for using metal additives in gelled liquid fuels are being developed. These additives increase the engine specific impulse, or the propellant density, or both, and thus can increase a space vehicle's payload. Propellant handling is also safer with gelled propellants. Fuel spills are smaller with gelled liquids and the propellant is less likely to combust during an accidental release. Typically, aluminum particles are suspended in gelled fuels such as hydrogen, RP-1, or monomethyl hydrazine. Ongoing research will quantify vehicle and engine performance, propellant chemistry, and production.

Over the last year a series of vehicle systems analyses and experimental programs were conducted to identify the best applications for metallized propellants and to demonstrate the technologies of propellant formulation and combustion. Both the Space Shuttle and the Titan 4 were studied. It was shown that the payload, packaging, and safety of Earth-to-orbit vehicles can be improved with metallized propellants (refs. 1 and 2). With high-density RP-1/aluminum fuel a liquid rocket booster fit into a smaller volume than the current solid rocket booster for the Space Shuttle. To send a 49,664-lbm payload into orbit, the metallized booster need only be 142 ft long, whereas the solid booster length is 149 ft. Further payload increases are possible with a metallized booster that is as long as the solid booster: up to 56,600 lbm, or a 14-percent increase. Alternatively, increasing the booster diameter by only 1 ft raises the payload by 42 percent to 70,500 lbm.

Other propellant combinations that were considered were nitrogen tetroxide/monomethyl hydrazine/aluminum (NTO/MMH/Al) and oxygen/hydrogen/aluminum ( $\text{O}_2/\text{H}_2/\text{Al}$ ). Even better packaging of the liquid booster was possible with the NTO/MMH/Al system. This booster need only be 134 ft long. The maximum payload that can be flown while staying within the length of the solid rocket booster is 67,200 lbm, a 35-percent increase. A Shuttle external tank using  $\text{O}_2/\text{H}_2/\text{Al}$  propellants was also analyzed. The volume of the tank increases significantly with metallized  $\text{H}_2/\text{Al}$  propellants. Although  $\text{O}_2/\text{H}_2/\text{Al}$  in the external tank does not appear beneficial for the Space Shuttle, future Earth-to-orbit vehicles with different volume limits will be able to benefit greatly from metallized propellants.



Space Shuttle performance with metallized  $\text{O}_2/\text{RP-1}/\text{Al}$ .



A Titan 4 vehicle using metallized NTO/MMH/Al can increase its payload by 11 to 12 percent. In this example, only the liquid stages use metallized propellants. If the solid rocket boosters were also modified to metallized propellants, even larger payloads to orbit would be possible.

Other related work is ongoing at the Pennsylvania State University and TRW. Penn State is determining the "best" operating conditions for a rocket engine using RP-1/Al fuel. This research will allow the most complete combustion of all of the metallized propellant. At TRW cryogenic gellants are being made to gel hydrogen. Aluminum particles will be suspended in it to make a metallized fuel.

#### References

1. Palaszewski, B.; and Powell, R.: Launch Vehicle Performance Using Metallized Propellants. NASA TM-104456, 1991. (Also, AIAA Paper 91-2050.)
2. Palaszewski, B.; and Rapp, D.: Design Issues for Propulsion Systems Using Metallized Propellants. NASA TM-105190, 1991. (Also, AIAA Paper 91-3484.)

**Lewis contact:** Bryan Palaszewski, (216) 433-2439  
**Headquarters program office:** OAST

#### Lunar Indigenous Monopropellants Formulated and Characterized

The Space Exploration Initiative calls for the exploration and eventual settlement of the solar system. The production of propellants from the resources available at the Moon and Mars has been shown to offer significant mission benefits, including lower launch costs, shorter trip times to Mars, and larger payload capability. Although the samples returned from the Moon were greater than 40 wt % oxygen, traditional liquid propellant fuel elements, such as hydrogen and carbon, were not present to any appreciable extent. However, metals such as aluminum, silicon, iron, titanium, and magnesium do exist on the Moon in quantities ranging from 3 to 20 wt %. If these metals could be used as rocket fuels, it would eliminate the need to transport fuel from Earth for near-lunar operations.

NASA Lewis has begun a technology program to investigate the feasibility of using a powdered

metal/liquid oxygen monopropellant for rocket combustion. The initial objectives of the program are to evaluate potential hazards involved with formulating and handling such a monopropellant, to determine the proper formulation, and to investigate the physical and chemical characteristics of the monopropellant.

Two phases of the hazards evaluation have been completed by NASA White Sands Test Facility. Mixing tests in which small amounts of the powdered metals were combined with liquid oxygen and stirred at speeds up to 900 rpm resulted in no reactions in any of the 63 tests. Mechanical impact tests were also performed, and the results from the monopropellants were compared with data for pentaerythritol tetranitrate (PETN), which is a known division I, class I, explosive. A titanium powder mixture reacted when the weight was dropped from the lowest height on the test apparatus and is considered too sensitive for formulation work to continue. Aluminum, silicon, and iron powder mixtures did not react when weights were dropped from the highest height and are considered safe to handle in the quantities and manners necessary to begin formulation and characterization of the monopropellant.

Preliminary formulation work has been completed by Wickman Spacecraft and Propulsion. The formulation experiments indicate that aluminum and silicon can be stably suspended in liquid oxygen with only 1 to 2 wt % gellant (amorphous fumed silica). With this amount of gellant, very little settling of the metal powder was observed during the first 24-hr period, yet the measurements indicate a satisfactory viscosity. The monopropellant appears thick at rest and will hold a shape, yet becomes fluid when subjected to a shear force.

#### Bibliography

LOX/Metal Gel Mechanical Impact Test, Special Test Data Report. WSTF 90-24223-28, 90-24490-91, 91-25136.

Wickman, J.H.: Liquid Oxygen/Metal Gelled Monopropellants. NASA CR-187193, 1991.

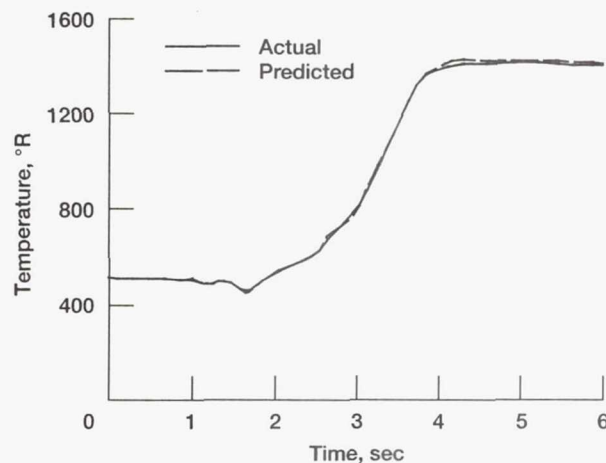
**Lewis contact:** Diane L. Linne, (216) 977-7512  
**Headquarters program office:** OAST

## Neural Networks Predict Critical Parameters During SSME Startup Transient

Recent rocket engine condition monitoring activities at NASA Lewis have focused on both real-time safety monitoring and post-test diagnostics. These efforts have demonstrated the ability of advanced algorithms to provide improved failure detection capability during ground test firings, thus reducing engine and test stand damage, and to facilitate the post-test diagnostic process. Efforts in advanced safety systems for the Space Shuttle main engines (SSME) have emphasized main-stage failure detection. Startup is difficult to monitor because of the highly complex and nonlinear nature of the SSME dynamics. Accurate models of parameters during startup would provide improved engine and sensor failure detection capability during the first 6 sec of engine operation. The models would also provide additional information for fault detection and isolation when used as part of an automated engine diagnostic system. For both applications the residuals between the actual and predicted values must be analyzed to detect an anomalous engine condition or to identify an engine or sensor failure.

Feed-forward neural networks can uniformly approximate any continuous function and are well suited for problems in which the exact relationships between sensor measurements are complex or unknown. Neural networks with a single hidden layer were used to accurately model three critical parameters during the first 6 sec of SSME operation. The three parameters modeled were the main combustion chamber pressure, a controlled variable; the high-pressure oxidizer turbine discharge temperature, a redlined parameter; and the high-pressure fuel pump discharge pressure, a parameter cited in failure investigation summaries for providing early failure indications. Each parameter was modeled separately; network inputs consisted of time windows of data from nonredundant highly correlated engine measurements.

A back-propagation algorithm was used to train the feed-forward networks on SSME data from two nominal ground test firings. Model prediction accuracy was achieved by constructing the training sets to reflect important system conditions, such as the prime times of the three combustion chambers and the transition to complete closed-loop control. Data from four additional nominal



Actual and neural-network-predicted high-pressure oxidizer turbine discharge temperature for a validation test firing.

firings were used to validate the trained networks. The maximum errors on the validation sets were all less than 5 percent. Furthermore, the neural network predicted values that all fell within the nominal two-standard-deviation envelopes currently used in SSME post-test data reviews.

Anomalous SSME data are being acquired to test the trained networks on sensor and engine failures. Also, the modeling interval is being extended to include main-stage operation and power level transitions.

### Bibliography

Meyer, C.M.; and Maul, W.A.: The Application of Neural Networks to the SSME Startup Transient. AIAA Paper 91-2530, June 1991. (Also, NASA CR-187138.)

**Lewis contact:** Claudia M. Meyer, (216) 433-8545  
**Headquarters program office:** OAST

## Expert System Analyzes Chemical and Nuclear Rocket Nozzle Performance

NASA Lewis' Rocket Engine Design Expert System (REDES) is an interactive computer application that uses a commercially available expert system shell. It was developed to evaluate and design liquid chemical rocket engines by using state-of-the-art computational tools and heuristic design methods. By automating the in-house expertise for performing a comprehensive rocket engine



analysis and design, REDES encourages proper use of computer codes and maintains the availability of design expertise.

Recently, capabilities within REDES were developed to analyze the nozzle performance of chemical and nuclear rocket engines. Using an iterative solution function that holds user-selected geometric parameters constant while varying others, REDES sizes a rocket nozzle to deliver a specified level of thrust. It then predicts rocket nozzle performance by using standardized Joint Army-Navy-NASA-Air Force (JANNAF) methodologies.

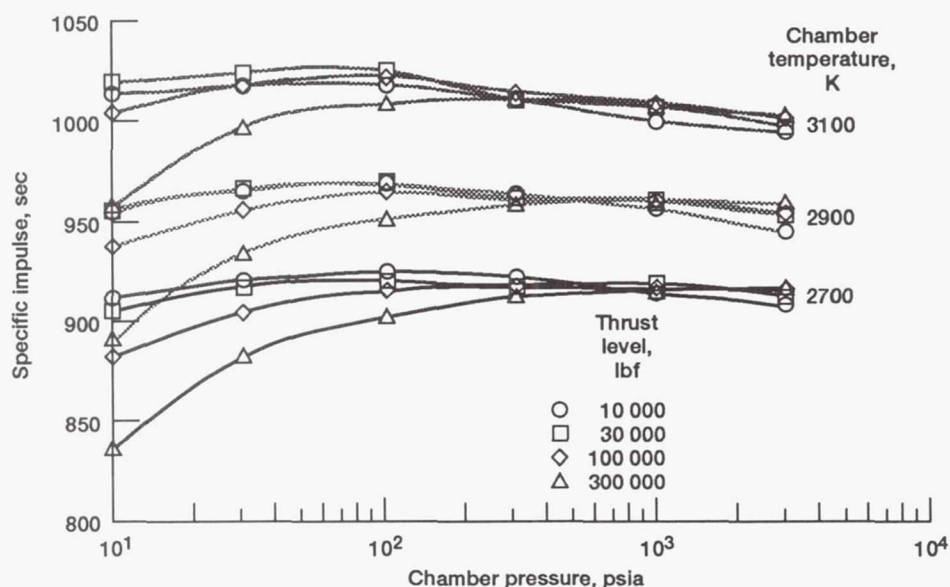
A parametric study of liquid chemical rocket engines was performed to determine the specific impulse efficiency factors that represent the two-dimensional losses, kinetic chemistry effects, and boundary layer losses encountered in a real liquid hydrogen/liquid oxygen rocket engine. Results from this study are of general interest as engineering tools because they can be used to provide quick estimates of real rocket engine performance based on ideal specific impulse values and cover a wide range of thrust levels, chamber pressures, mixture ratios, area ratios, and nozzle lengths. Engine geometry and operating conditions not varied by the test matrix were based on the RL10 liquid rocket engine.

Results of the nuclear rocket engine study conclude that although the performance of the nuclear thermal rocket, based on infinite reaction rates, looks promising at low chamber pressures, finite-rate chemical reactions will cause the actual performance to be considerably lower. Parameters that have a major influence on the delivered specific impulse value include the chamber temperature and the chamber pressures in the high-thrust domain. Other parameters, such as two-dimensional and boundary layer effects, kinetic rates, and number of nozzles, affect the deliverable performance of a nuclear thermal rocket nozzle to a lesser degree. For a single nozzle, maximum performance of 930 and 1030 sec occurs at chamber temperatures of 2700 and 3100 K, respectively.

#### Bibliography

Davidian, K.O.; and Kacynski, K.J.: Analytical Study of Nozzle Performance for Nuclear Thermal Rockets. AIAA Paper 91-3578, Sept. 1991. (Also, NASA TM-105251.)

**Lewis contact: Kenneth J. Davidian, (216) 433-7495**  
**Headquarters program office: OAST**



Delivered nuclear thermal rocket nozzle performance for all chamber temperatures, chamber pressures, and thrust levels investigated in the REDES study.

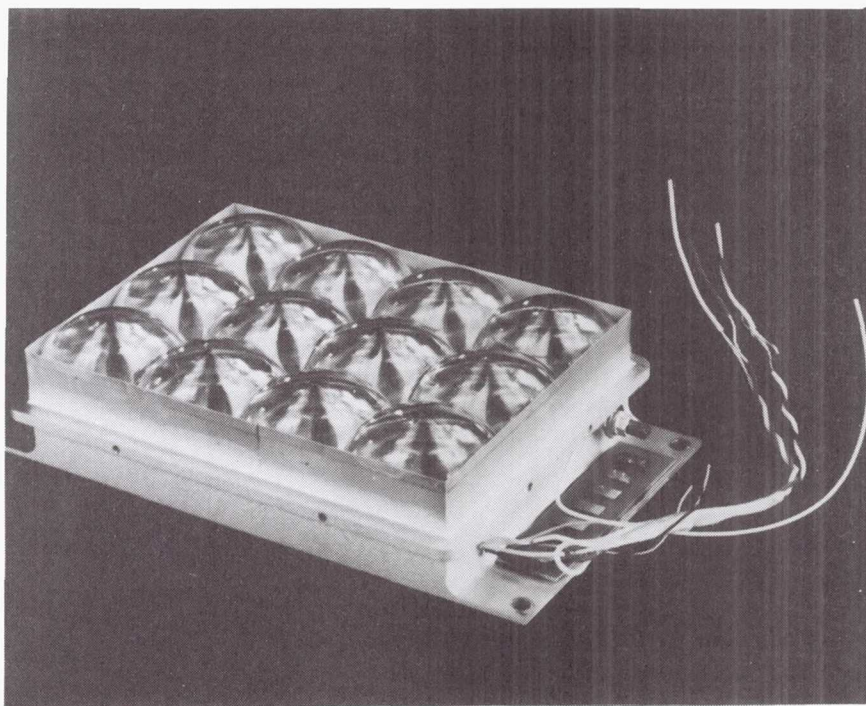
## Power Technology

### Flight Hardware Developed for Mini-Dome Fresnel Lens Photovoltaic Concentrator Array

Space power system designers are constantly searching for ways to improve the performance of photovoltaic arrays. Photovoltaic concentrator systems offer the potential to significantly and cost-effectively reduce the area and weight of current arrays. They allow smaller photovoltaic devices to be operated at much higher efficiencies. By replacing large areas of photovoltaic cells with lower cost concentrator lenses (reducing cell area by a factor of 50 to 100), cell cost can be dramatically reduced. This attribute makes the use of new tandem photovoltaic cell structures (multijunction photovoltaic devices that respond to different portions of the spectrum to make more efficient use of the incoming light) feasible and cost-effective alternatives to planar solar cells. The mini-dome Fresnel lens concentrator is a unique high-efficiency, lightweight photovoltaic concept that significantly improves the performance of space power systems.

The mini-dome Fresnel lens concentrator is a point-focus refractive lens that was developed

under a Small Business Innovative Research (SBIR) contract by Entech, Inc. of Dallas, Texas. The concentrator lens has a smooth outer surface with individually tailored Fresnel facets along the inside of the domed surface. The combination of the domed shape and the Fresnel facets provides a unique geometry that minimizes reflection from each Fresnel prism, thereby providing maximal sunlight transmittance through the lens. During the past year the SBIR portion of this program, which emphasized concept demonstration, was completed. A six-by-six prototype panel that integrates a number of high-efficiency photovoltaic concepts, was delivered to NASA Lewis. The panel includes gallium arsenide (GaAs) concentrator cells with prismatic cell covers. These covers eliminate reflection losses from the top gridlines by refracting the light to the exposed cell areas. The concentrator lenses were made from a flexible silicone that was then bonded to a domed, ceria-doped microglass superstrate. This lens design was selected as a preliminary attempt to fabricate a lens that would survive the space environment and is expected to be fully space qualifiable. The lenses and cells were integrated into an improved honeycomb structure with increased stiffness and lighter weight.



12-Element mini-dome Fresnel lens photovoltaic concentrator with Boeing GaAs/GaSb cells (PASP PLUS flight hardware).



Under the current program NASA Lewis, Entech, and Boeing Defense & Space Group have been cooperating on an informal basis to continue work on this concept. Boeing has integrated the mini-dome concentrator concept with a gallium arsenide/gallium antimonide (GaAs/GaSb) tandem cell developed at the Boeing High Tech Center. This new tandem cell has demonstrated an efficiency higher than 30 percent (air mass zero). Using this cell, a concentrator array with a performance of over 300 W/m<sup>2</sup> (100 W/kg) could be achieved in the near term—a significant improvement over current photovoltaic arrays. As the work on this concept continues, more emphasis is being placed on lens manufacturability, the integration of advanced photovoltaic devices, and the durability and qualification of the array within the space environment.

The mini-dome concentrator, with glass-domed lenses and GaAs/GaSb cells, is one of the photovoltaic technologies that will be tested in the PASP PLUS flight experiment. PASP PLUS, an Air Force spaceflight experiment that is primarily designed to study high-voltage plasma interaction effects and radiation damage on advanced and existing array technologies, is scheduled on a Pegasus launch vehicle in late 1992. A 12-element flight module, built by Boeing, was delivered to Lewis in July for integration and testing. This first flight of the mini-dome Fresnel lens concentrator and GaAs/GaSb cell technologies will also test the applicability of the concept for high-voltage array designs.

The mini-dome Fresnel lens photovoltaic concentrator technology has progressed from an initial concept to flight hardware in a few short years. With its distinction of integrating high-efficiency components into a relatively lightweight structure, it has the potential to significantly impact future civil and military space power systems. The PASP PLUS flight experiment, in addition to continued ground testing, will yield valuable information and help verify the expected performance of this technology.

**Lewis contact:** Michael F. Piszczor, Jr., (216) 433-2237  
**Headquarters program offices:** OCR and OAST

## **Mars Insolation Model Expanded**

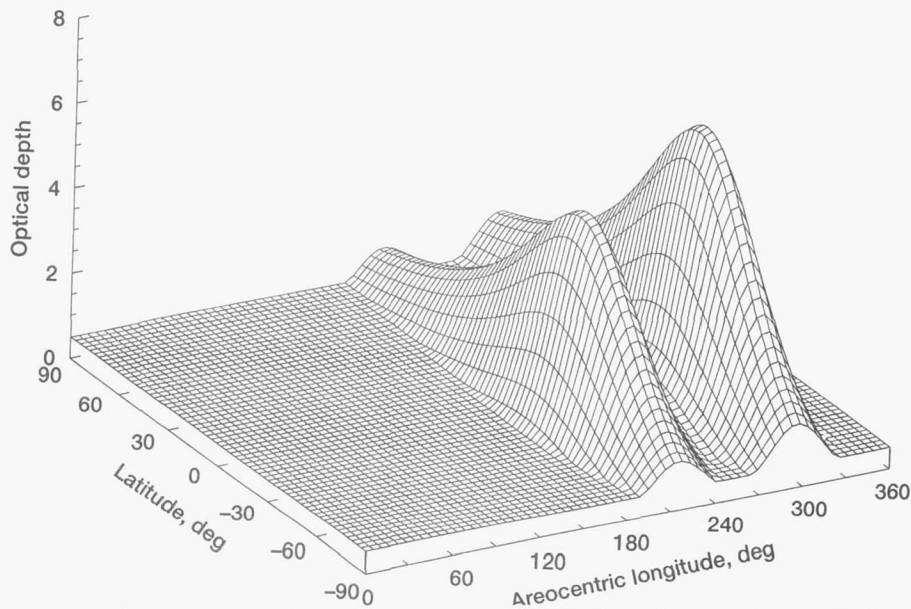
Missions to the Martian surface and activities there will require electric power. Of the several possibilities, photovoltaics can offer many advantages, including a high power-to-weight ratio, modularity, and a long history of successful application in space—if the solar energy incident on the Martian surface is sufficiently intense. Mars is not only farther from the Sun than Earth but is also known to have occasional intense dust storms. As a result, there has been some skepticism about the potential of photovoltaics for application on Mars.

NASA Lewis is attempting to quantify the insolation, including the effects of dust storms, at the surface of Mars so that planners of Mars missions can accurately determine if photovoltaics is a viable power option. Diurnal and daily variations of the global, direct-beam, and diffuse insolation on a Martian surface were calculated from data measured by the Viking Landers (VL1 and VL2) for the sites visited. The global insolation was derived from the normalized net solar flux function; the direct-beam component was determined by using Beer's law, which relates the insolation to the optical depth of the atmosphere; and the diffuse component was obtained from the difference between the global and direct-beam insulations.

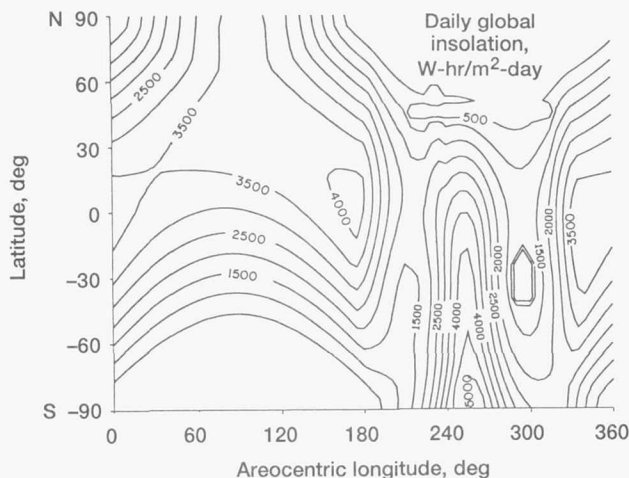
The Mars insolation model has been expanded and refined by using the available data from the Viking Landers, and the model is now applicable to a wider range of latitudes and to local as well as global variation in atmospheric opacity caused by storms. The analysis shows that there is sufficient insolation, primarily from a large diffuse component, to usefully operate a photovoltaic system on the surface of Mars.

During the spring and summer the insolation on a horizontal Martian surface at the two Viking Lander locations is relatively high, varying from about 2 to 4 kW-hr/m<sup>2</sup>-day because of the low optical depth of the Martian atmosphere. During autumn and winter, when dust storms typically take place, the insolation is lower.

This Mars surface insolation model is being used in Martian mission studies. For example, AeroVironment, Inc., designer and builder of the SunRaycer solar-powered car, has used this



Variation of optical depths of Mars atmosphere with latitude and areocentric longitude.



Variation of daily global insolation with latitude and areocentric longitude on a horizontal surface of Mars.

model to estimate the output of a flat-plate solar array for a solar-powered Mars vehicle. This model is also being used by the Jet Propulsion Laboratory, NASA Lewis' Power Technology Division and Advanced Space Analysis Office, and others.

The research is performed partly in house and partly under NASA contract at Tel Aviv University. This work, which has established the feasibility of using solar power on the surface of Mars, is expected to substantially affect the result of Martian missions. The model will enable more accurate

engineering studies and estimates of solar array size and performance than have heretofore been possible.

#### Bibliography

Appelbaum, J.; and Flood, D.J.: The Mars Climate for Photovoltaic System Operation. *Space Power*, vol. 8, no. 3, 1989, pp. 307-317.

Appelbaum, J.; and Flood, D.J.: Photovoltaic Power System Operation in the Mars Environment. *Proceedings of 24th IECEC, IEEE*, 1989, vol. 2, pp. 841-848.

Appelbaum, J.; and Flood, D.J.: Solar Radiation on Mars, *Solar Energy*, vol. 45, no. 6, 1990, pp. 353-363.

Appelbaum, J.; and Landis, G.A.: Solar Radiation on Mars—Update 1991. Submitted to *Solar Energy Journal*.

**Lewis contact: Dr. Joseph Appelbaum, (216) 433-8401**  
**Headquarters program office: OAST**

#### Advanced Induction Motor Developed

An advanced induction motor has been built under a National Launch System (NLS) task managed by NASA Lewis. General Dynamics' Space Systems Division is the prime contractor; Sundstrand Corporation is the subcontractor. The motor is designed to meet the thrust-vector-



control actuation requirements for gimbaling the main engines of the NLS vehicle. NASA Lewis identified the need to design an advanced induction motor, one that takes advantage of the induction motor's inherent strengths, has a different method of control, and is specific to this particular application. The induction motor has a high peak-torque-to-current ratio, is capable of high-temperature operation, and has a rugged design that safely handles faults. With the recent advances in power electronics the induction motor is well suited for actuation applications because it can be easily controlled as a servomotor through field-oriented control techniques.

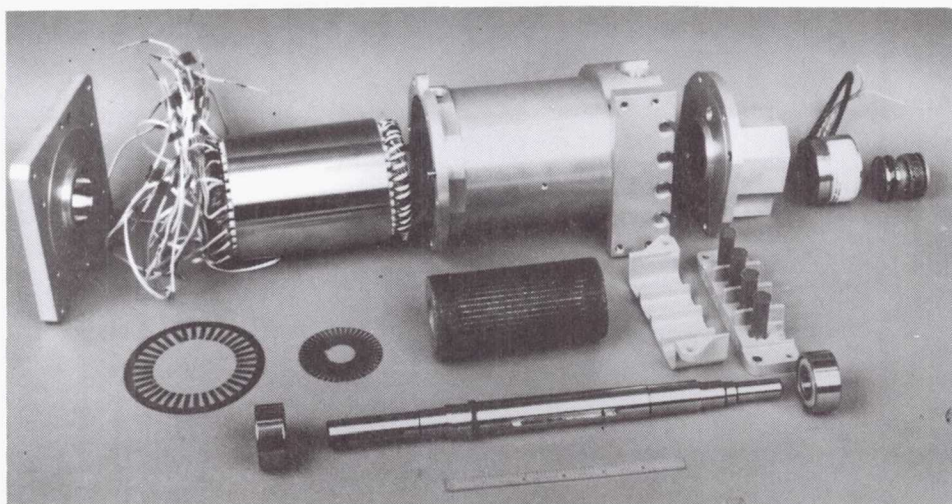
To meet the thrust-vector-control requirements of the NLS vehicle, the new motor must deliver high peak torques for short periods of time (seconds) during a launch duty cycle. Servocontrol of the new induction motor through field-oriented control techniques is required to meet the thrust-oriented-control actuation performance specifications. Field-oriented control permits operation of the motor at any torque and speed (motoring or generating) at or near peak efficiency.

The current limitation of the power electronics and the peak power requirements were the major drivers in determining critical design characteristics. A low-resistance rotor for efficiency, a high-flux-density magnetic material for power density, a low-inertia rotor for acceleration, and high-temperature capability were selected as key design issues.

The motor can deliver 70 hp peak (300 in.-lb of torque at 14,600 rpm) at 2.6-percent slip, 86.3-percent efficiency, 120 V (line to neutral), and 750 Hz. The electromagnet weighs 11 lb; the total weight including the housing is less than 20 lb. The rotor outer diameter is 2.25 in., the stator outer diameter is 3.75 in., and the rotor length is 5.75 in. The rotor inertia is 0.02764 lb-ft<sup>2</sup>. Hyperco-50 was used for both the rotor and stator laminations.

The new motor, integrated with a General Dynamics-built 40-hp pulse population motor driver, is currently under test. The advanced induction motor and driver will then be tested in a complete electromechanical actuation (EMA) system during 1992. This motor is critical to the success of the NASA EMA demonstrations to be completed under the NLS Program and the EMA Technology Bridging Program. The objective of these demonstrations is to show that EMA systems are a better alternative to the hydraulic actuation systems used in today's launch vehicles and aircraft. This type of motor is suitable for any thrust-vector-control or flight-control surface electric actuators for launch vehicles, aircraft, electric or hybrid automobiles, and adjustable speed drives for heating, ventilation, and cooling systems.

**Lewis contact:** Mary Ellen Roth, (216) 433-8061  
**Headquarters program office:** OAST



*Advanced induction motor.*

## R&amp;D 100 Award

**Fiber-Optic Sensor Measures Electrical Current**

NASA Lewis has received an R&D 100 Award from Research & Development magazine for developing a sensor that can measure electric current through optical fibers.

Because the sensor system uses only (nonconducting) optical fibers and light, it has excellent isolation, which means that it is possible to measure current at one location and report the measurement to another location when each location is at a significantly different voltage. For example, the current being measured may be flowing through wires at hundreds or thousands of volts, and the monitoring station has equipment generally near ground potential.

The current sensor is also immune to electromagnetic interference, such as electrical noise from discharges in spacecraft, lightning flashes, or nearby operating electrical machinery.

For Lewis aerospace applications the sensor was developed to operate over the broad temperature range of  $-65$  to  $125^{\circ}\text{C}$ . Frequencies that can be

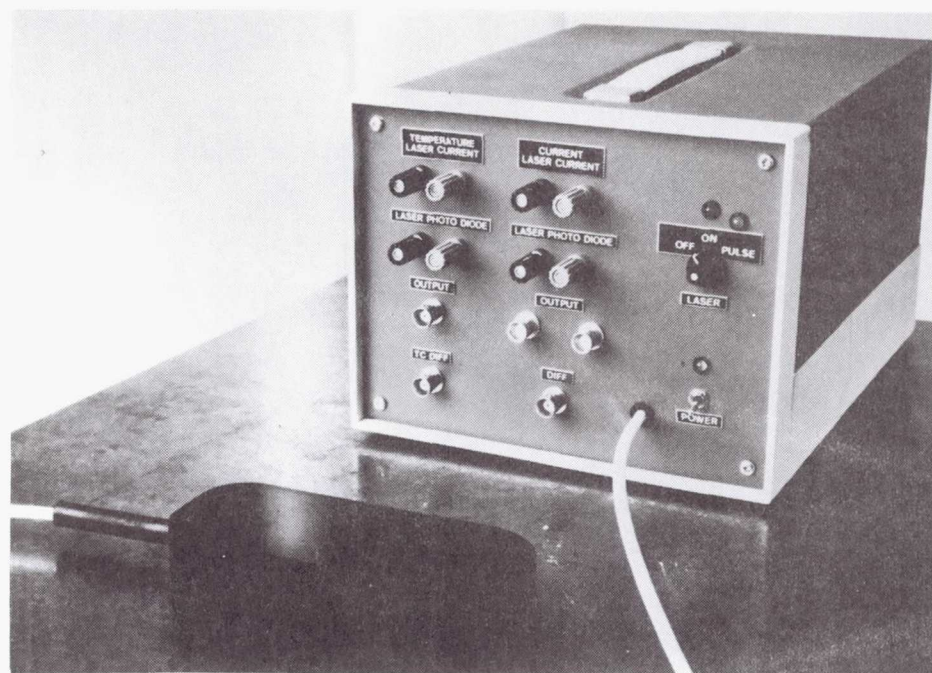
covered are 60 Hz for terrestrial use, 400 Hz for aircraft, and 20 kHz for high-frequency aerospace power.

Sharing in the award are the National Institute of Standards and Technology at Boulder, Colorado, where the major portion of the aerospace sensor was developed under contract to Lewis; the U.S. Navy, which is developing the sensor for ship-board use; and the 3M Corporation, which is developing the sensor for commercial use by the electric utility industry.

**Lewis contact:** Richard L. Patterson, (216) 433-8166  
**Headquarters program office:** OAST

**Photovoltaic Power System Planned for Use in Antarctica**

The remote and hostile nature of the Antarctic environment presents NASA with an opportunity to test and verify proposed approaches to planetary surface systems and operational techniques for future planetary missions. The U.S. Antarctic Program, run by the National Science Foundation, could, in turn, benefit from NASA systems



*Aerospace version of fiber-optic current sensor*



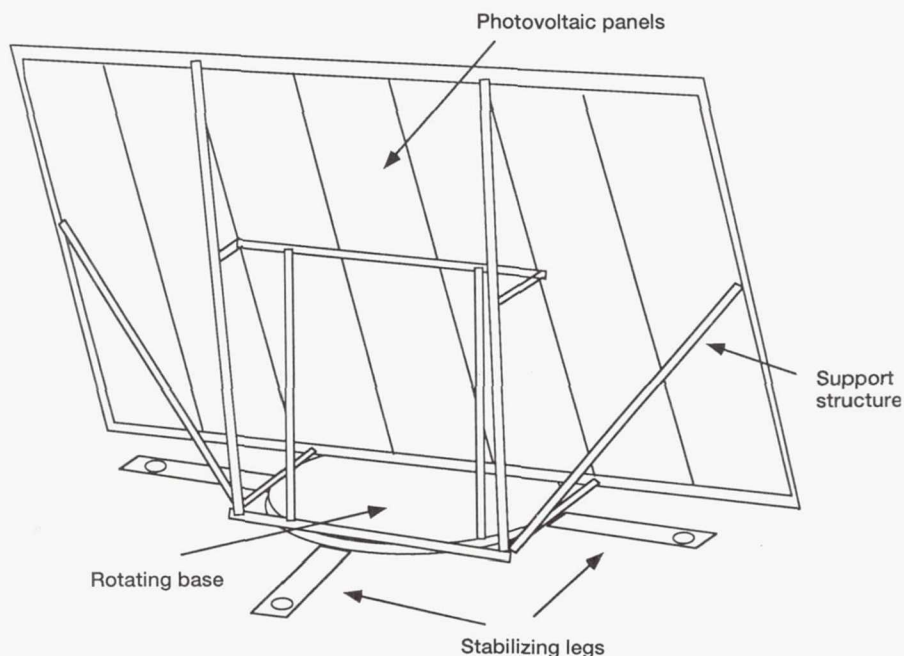
that would increase efficiency, reduce cost, and minimize environmental impact.

In support of the Antarctic Space Analog Program, begun in December 1990, NASA Lewis is currently involved in the design and construction of a photovoltaic/battery power system for use at a remote site camp in the Dry Valley region of Antarctica. Research at this site is focused on the study of life forms under the ice of Lake Hoare through the use of a remotely operated vehicle (ROV), a small submersible vehicle that moves through the water collecting data which are relayed back to the researchers on the surface. Both the ROV and the camp are currently powered by gasoline generators. Under the NASA Lewis plan, silicon photovoltaic arrays will be installed at the base camp to provide 1.5 kWe for laboratory equipment operation. The arrays will be modularized for ease of deployment and handling by the research team. Each array will be mounted on a turntable to provide Sun-tracking capability. Portable battery modules will supply approximately 3 kW-hr of power to the ROV. Fully charged batteries will be taken daily from the camp to the research site on the ice and returned for recharging at the camp during laboratory off-hours. Silver-zinc cells were chosen for this application because of their low mass and compactness.

The Antarctic power system will provide NASA with important data on system-level deployment and operation in a remote location by a minimally trained crew as well as validate initial integration concepts. The system will also serve as a precursor demonstration for large-scale base power augmentation, which would offload diesel fuel consumption, resulting in significant fuel delivery savings and a lessening of the environmental impact associated with diesel fuels.

System development, design, assembly, and integration is being done in house at NASA Lewis with delivery to the Antarctic scheduled for October 1992.

**Lewis contact: Lisa Kohout, (216) 433-8004**  
**Headquarters program offices: OAST and OSSA**



*Antarctic photovoltaic array.*

## Small Free-Piston Stirling DIPS Being Designed for Robotic Space Missions

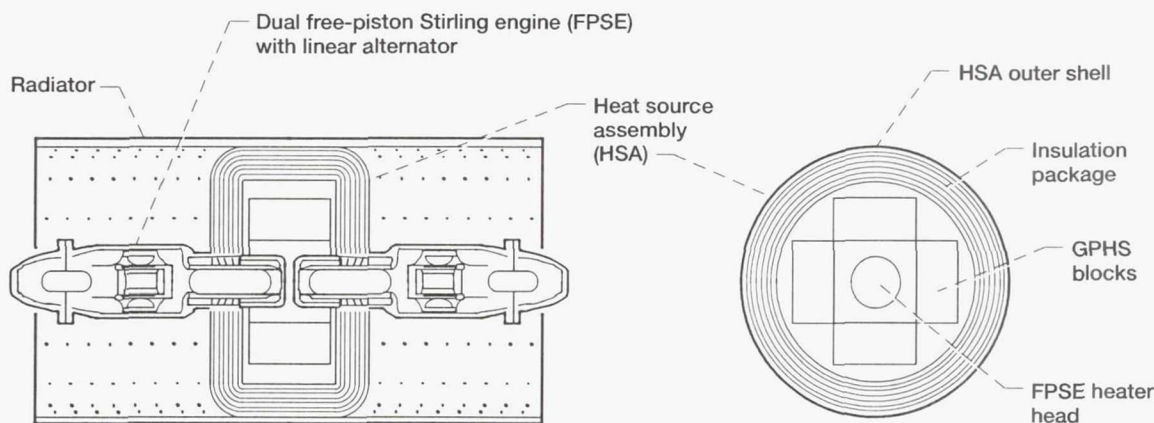
Design of a multihundred-watt dynamic isotope power system (DIPS) is being pursued as a potential low-cost alternative to radioisotope thermoelectric generators. The DIPS is based on the U.S. Department of Energy (DOE) general-purpose heat source (GPHS) and small (multihundredwatt) free-piston Stirling engine with linear alternator. The design is targeted at the power needs of future unmanned deep space and planetary surface exploration missions ranging from scientific probes to robotic precursor missions. Power levels for these missions are considerably less than a kilowatt. The incentive for any dynamic system is that it can save fuel, reducing cost and radiological hazard.

Unlike a conventional DIPS based on turbomachinery conversion, this small Stirling DIPS can be advantageously scaled to multihundred-watt unit size while preserving size and mass competitiveness with radioisotope thermoelectric generators (RTG's). Stirling conversion extends the range where dynamic systems are competitive to hundreds of watts—a power range not previously considered for these systems. The challenge for

Stirling will be to demonstrate reliability similar to that experienced with RTG's.

Previous work focused on the feasibility of directly integrating the general-purpose heat source (GPHS) with the Stirling heater head. Thermal modeling of various radiatively coupled heat source/heater head geometries using data furnished by the developers of the free-piston Stirling engine and the GPHS indicated that, for the 1050 K heater head configurations considered, GPHS fuel clad temperatures will remain within safe operating limits under all conditions, including shutdown of one engine on a twin-engine unit. Subsequent characterization of this unit, at multihundred-watt size, indicated that the GPHS/small Stirling DIPS would be roughly equivalent to the Mod RTG in size and mass but require one-third the heat source or less.

Effort is currently under way to produce a reference conceptual design. The design addresses system-level issues, such as mission environment, user vehicle integration, and launch and transit for a typical planetary spacecraft, in addition to basic requirements associated with launch safety, assembly and loading, ground handling, and storage. Mission and user vehicle



250-W Unit Comparison

	Power source mass, kg	Power source envelope		Radiator temperature, K	Number of GPHS blocks required	Isotope fuel required, kg
		Diameter, cm	Length, cm			
GPHS RTG	45.3	42	110	540	18	11
MOD RTG	31.2	38	70	598	12	7.3
Small Stirling DIPS	33.8	27	100	375	4	2.44

Small Stirling DIPS.



requirements are furnished by the Jet Propulsion Laboratory. Design of the integrated heat source/heater head assembly containing GPHS modules is being carried out in collaboration with DOE's Mound Laboratory (a GPHS developer). Present efforts at Lewis are focusing on engine configuration and the thermal, mechanical, and electrical integration of the free-piston Stirling engine with linear alternator to other subsystems.

The emerging design will be the basis for showing how mission and user vehicle requirements will be met, will permit further specification of components, and will enable potential users to independently evaluate small Stirling DIPS as a low-cost alternative to RTG's.

#### Bibliography

Bents, D., et al.: Design of Multihundred-Watt Dynamic Isotope Power System for Robotic Space Missions, *Proceedings of 26th IECEC*, American Nuclear Society, vol. 2, 1991, pp. 204-209.

Bents, D.: Small Stirling Dynamic Isotope Power System for Multihundred-Watt Robotic Missions. NASA TM-104460, 1991.

McComas, T.; and Dugan, E.: Thermal Analysis of a Conceptual Design for a 250 We GPHS/FPSE Space Power System, *Proceedings of 26th IECEC*, American Nuclear Society, vol. 2, 1991, pp. 228-233.

**Lewis contact:** David J. Bents, (216) 433-6135  
**Headquarters program office:** OAST

#### Free-Piston Stirling Space Power Research Engine Demonstrates Highly Efficient Linear Alternator

Free-piston Stirling power converters for space require low-mass, high-efficiency electromechanical conversion devices that can function for 7 to 15 years at relatively high temperatures (525 K). One technology with the potential to meet these criteria is the permanent magnet (PM) linear alternator using  $\text{Sm}_2\text{Co}_{17}$  magnets. Early attempts to integrate PM linear alternators in 12.5-kWe free-piston Stirling machines with magnetic support structures yielded disappointing alternator efficiencies of about 72 percent. Subsequent development of system design codes with supporting testing on a linear dynamometer identi-

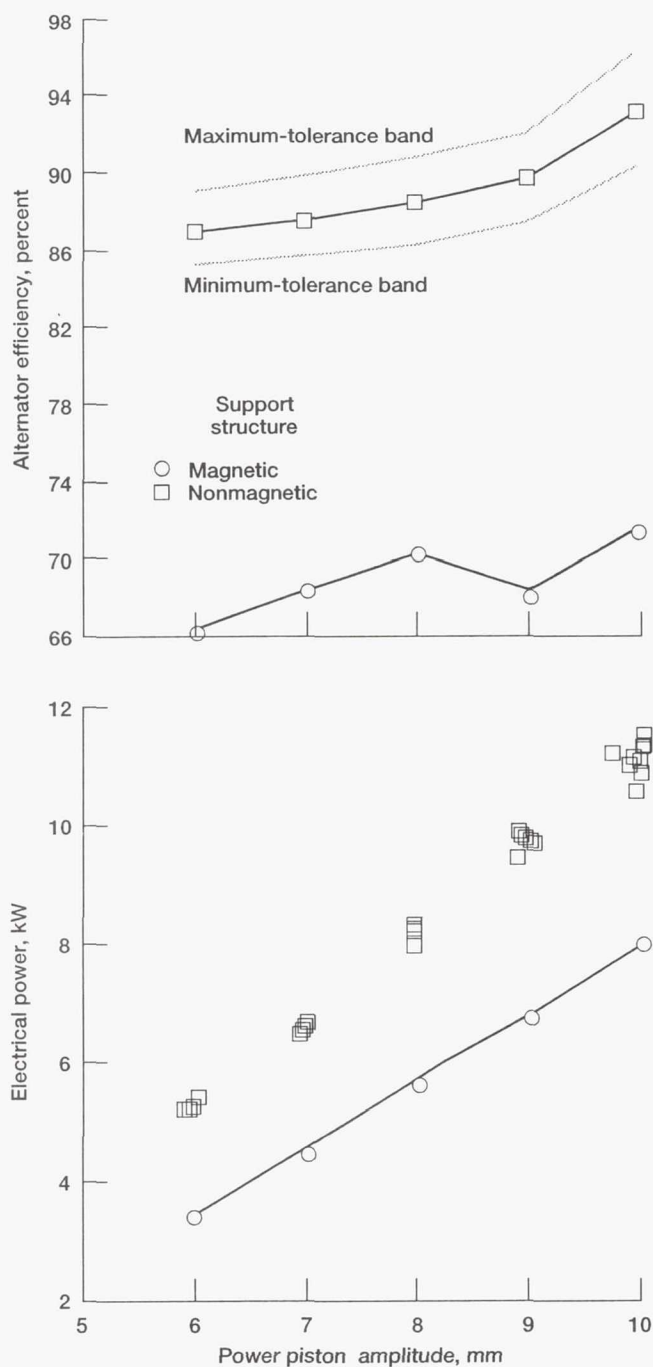
fied the areas of high loss. New alternator designs with nonmagnetic alternator support structures that have evolved from this process are yielding efficiencies greater than 90 percent at operating temperatures of 350 K. Early results from the development of a 525 K alternator indicate that a 90-percent-efficient alternator is achievable even at these temperatures.

The following configurational changes were made to transform the alternator structure of the Stirling space power research engine (SPRE) from magnetic to nonmagnetic:

- The power piston cylinder material was changed from 4140 steel to beryllium.
- The joining ring and pressure vessel material was changed from PH13-8Mo stainless steel to Inconel 718.

The alternator efficiency of greater than 90 percent measured in SPRE tests at 150-bar pressure, approximately 350 K temperature, a temperature ratio of 2, and 10-mm piston amplitude correlated well with a linear alternator computer code and agreed closely with prior static measurements made with the SPRE alternator. The static measurements had been performed by applying alternating voltage and current to the alternator coil while fixing the plunger magnet holder to prevent its movement. Magnetic flux measurements were made to ensure that the magnetic field produced by the applied alternating voltage was similar to that produced by the moving magnets during engine operation. Power consumed under these conditions is a measure of alternator power loss. By measuring the difference in power consumed as various elements of the alternator support system are changed, the loss associated with each element is measured.

A new, high-temperature alternator has been designed and fabricated for the component test power converter (CTPC). The CTPC is being used to develop components for the next generation of power converters, and the alternator is designed to operate at temperatures up to 525 K. Static measurements have been performed in a similar manner as for the SPRE. However, in this case all nonmagnetic structural elements have already been incorporated into the CTPC. Beginning with the stator and the coil the difference in power consumed was measured as the various elements of the alternator (stator, power piston cylinder,



SPRE alternator test.

engine structure, etc.) were added. The measured power losses resulting from these static tests correlated well with linear alternator code calculations. On the basis of these loss measurements, a CTPC alternator efficiency of greater than 90 percent is predicted.

Development of the new high-temperature alternator is an important step toward completion of

the Stirling space power converter. The converter is being developed under contract by Mechanical Technology Incorporated and is scheduled for completion in 1993.

**Lewis contact:** Donald L. Alger, (216) 891-2927

**Headquarters program office:** OAST

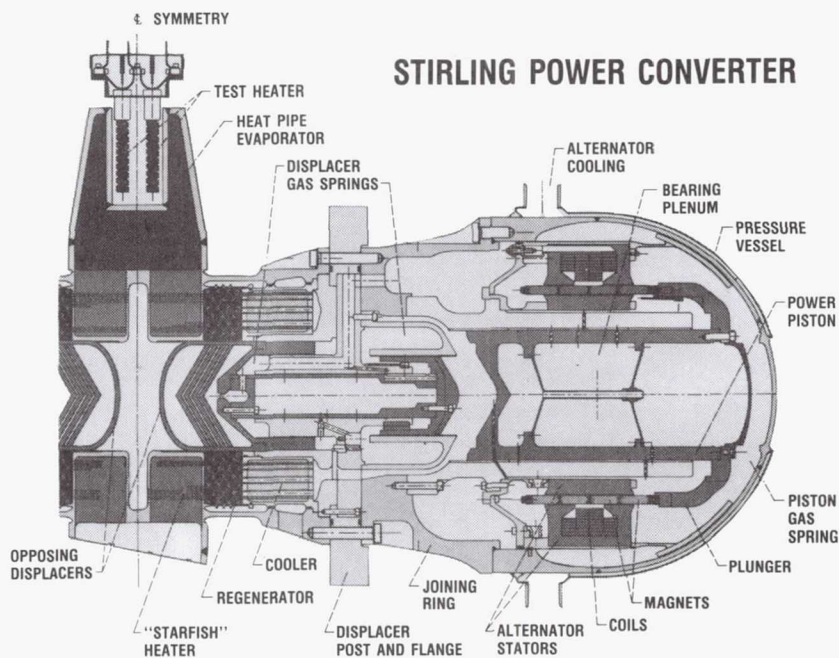
### Hydrostatic Gas Bearings Successfully Tested in Free-Piston Stirling Engine

Free-piston Stirling space power converters must rely upon noncontacting bearings to eliminate wear and thereby achieve long life. Several types of noncontacting bearings have been considered, including flexures, hydrostatic gas bearings, hydrodynamic gas bearings, and magnetic bearings. Flexures and magnetic bearings are being studied for possible application to high-power converters ( $>10\text{-kW}/\text{piston}$ ), but they are still considered developmental at these power levels. Testing at Mechanical Technology Incorporated has successfully demonstrated that hydrostatic gas bearings and hydrodynamic gas bearings are feasible for high-power converters. New hydrostatic bearing designs have been demonstrated with self-pumped operation over a power range of 50 to 100 percent with losses comparable to those for the low-loss hydrodynamic gas bearing. This technology has been demonstrated on both the power piston and the displacer piston.

Although the hydrodynamic gas bearing may have low losses, a complex electrical drive motor is required to rotate each piston, impairing the long-term reliability of the bearing system. In comparison, the new, low-loss hydrostatic gas bearing is a simple, passive system that relies upon the piston gas springs to supply gas to bearing plenums located within the pistons.

The pressure swing about the mean gas pressure in the gas spring is kept as small as possible to minimize the hysteresis power loss. Prior hydrostatic bearing systems required a pressure swing of  $\pm 10$  bar because only half of the gas spring pressure wave was used to charge the bearing supply plenum. The new hydrostatic bearing system is efficient because it uses the full gas spring pressure wave to charge both the supply and drain plenums. Because the full pressure





## STIRLING POWER CONVERTER

wave is used, the pressure in the gas spring needs to vary only  $\pm 5$  bar about the mean, with a correspondingly lower hysteresis loss. By implementing this new bearing design, hydrostatic bearing losses for a free-piston power converter with an electrical output of 12.5 kWe have been reduced from about 1700 W to 600 W.

The new hydrostatic bearing design has also incorporated other mechanical improvements. For example, bearing plenums were previously placed in the cylinder and involved tortuous flow paths that could neither be inspected nor cleaned. The new design incorporates straight-through passages that can easily be inspected and cleaned.

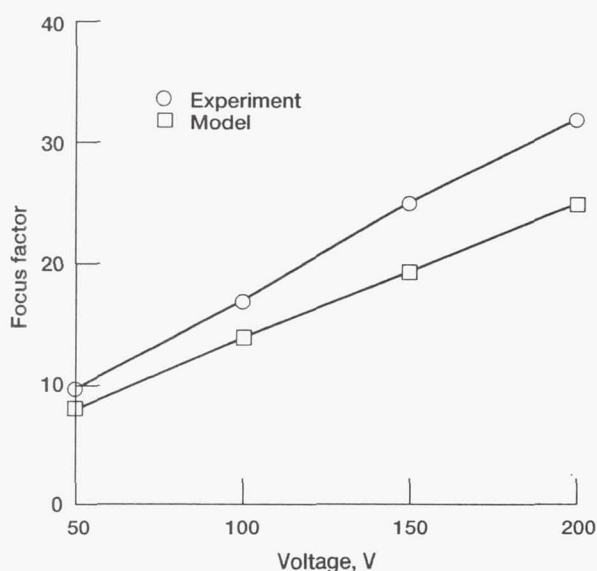
Development of the new hydrostatic bearing system is an important step toward completion of the Stirling space power converter. The converter is being developed under contract by Mechanical Technology Incorporated and is scheduled for completion in 1993.

**Lewis contact:** Donald L. Alger, (216) 891-2927  
**Headquarters program office:** OAST

## Model Predicts Focusing of Plasma Ions Into Insulation Holes

As new technologies are developed and larger, higher-power-level spacecraft are flown, interactions with the space environment will cause new problems. Space Station *Freedom* serves as an example of this. As a result of interactions between the solar arrays and the ionospheric plasma, the structure will float 100 V or more negative relative to the plasma for about one-third of its orbit. Conductive surfaces will therefore be slowly sputtered by 100-eV positive ions, and nearby surfaces will be contaminated. Tools need to be developed to assist in evaluating the contamination rate for future mission planning.

One tool that is being developed is a model to predict how ions are focused into holes and defects in the insulative coatings on the structure. The model estimates the thickness of the plasma sheath near the hole (i.e., the thickness of the region where electric fields can influence ion trajectories). It then calculates the ion trajectories to determine which ions will fall into the hole and which will harmlessly hit the insulation surface. From these trajectories the enhancement of the ion flux relative to the nominal ion flux to the hole can be calculated. Typically, ion fluxes into the hole are enhanced on the order of 16 times for space conditions and millimeter-size holes.



Measured ion currents normalized to plasma conditions (2-eV argon;  $2 \times 10^{12}/\text{m}^3$ ) and hole size (2.7-mm radius) and compared with model.

Model predictions have been compared with experimental observations obtained at Marshall Space Flight Center. The agreement is excellent—well within the uncertainty in the plasma conditions.

The model can be used to predict ion current enhancements to conductive spacecraft surfaces. These surfaces may be part of the design or created during normal operation from handling accidents, micrometeor or debris impacts, or breakdown of the thin dielectric coatings on the structure. Coupled with sputter yields, the model can be used to determine contamination source rates that are needed for evaluating possible problems.

**Lewis contacts:** David B. Snyder, (216) 433-2217;  
Joel L. Herr, (216) 433-8771  
**Headquarters program office:** OAST

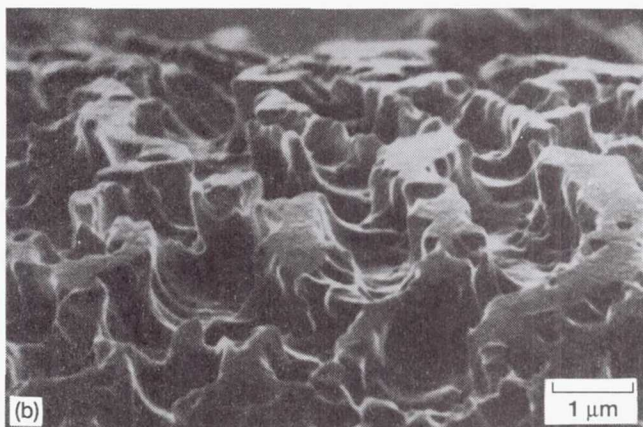
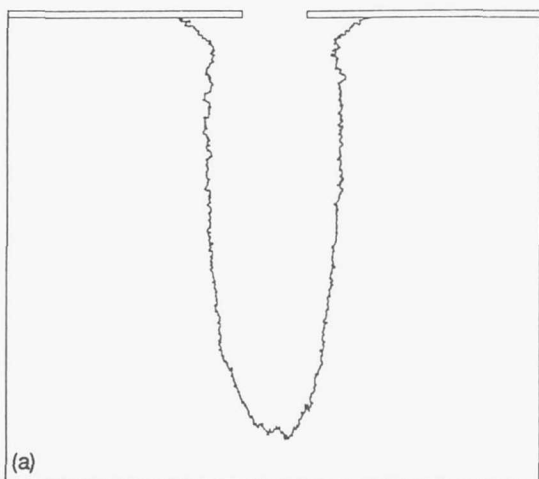
### LEO Atomic Oxygen Undercutting Documented at Protective Coating Defect Sites on LDEF

The Long Duration Exposure Facility (LDEF) exposed many types of spacecraft materials to the harsh environment of low Earth orbit (LEO) so that interactions of materials with the space environment could be characterized. Over 10,000 samples were exposed to the LEO space environment for 5.8 years. Because exact simulation of LEO atomic oxygen has not been achieved in ground-based facilities, comparisons of ground-based atomic oxygen exposure and LEO atomic oxygen exposure are greatly desired. Assessment of long-term exposure to LEO atomic oxygen can now be accomplished with the materials retrieved on LDEF.

Materials that are susceptible to oxidation must be protected when used in LEO, but protected materials are still vulnerable to atomic oxygen damage due to undercutting at protective coating defect sites. Undercutting (oxidation below the defect site that can exceed the original defect area) can occur from sweeping ram atomic oxygen exposure if the spacecraft rotates with respect to its direction of travel. Undercutting can also occur if the spacecraft is oriented with a fixed direction and receives direct ram atomic oxygen exposure. Scattering also allows the atomic oxygen to get underneath the protective coating and contributes to undercutting. The potentially devastating damage that can occur due to scattering and the thermal effects of atomic oxygen is not widely understood. Although atomic oxygen undercutting is expected to occur in LEO, it has not been observed previously and has not been documented on prior spaceflight materials.

Analysis of an aluminum-coated Kapton multi-layer insulation sample that was flown on the leading edge of LDEF has allowed documentation of atomic oxygen undercutting of oxidizable materials in LEO. After erosion of a 3-mil Kapton cover sheet (aluminized on the back side), the sample was exposed to an atomic oxygen fluence of approximately  $5.77 \times 10^{21}$  atoms/cm<sup>2</sup>. Cracks in the aluminum coating (caused by punching vent holes during fabrication) allowed atomic oxygen to attack the underlying Kapton. Undercutting of the Kapton was observed with a scanning electron microscope. The degree of atomic oxygen attack beyond the original defect site was





LEO direct ram atomic oxygen undercut profiles at protective coating defect sites: (a) Monte Carlo prediction, (b) LDEF aluminized-Kapton multilayer insulation.

extensive considering that LDEF was in a fixed orbital orientation. Undercut widths exceeded crack widths by up to 16.6 times—evidence of the potential damage atomic oxygen can cause at defect sites in protective coatings. This documentation provides evidence that atomic oxygen will scatter off spacecraft surfaces and may react with hidden unprotected oxidizable materials. Therefore, these materials should be considered for protection as well.

Many oxidizable spacecraft components, such as the photovoltaic array blanket material Kapton, will be exposed to sweeping ram atomic oxygen as the solar cells track the Sun during orbit. Sweeping ram atomic oxygen attack (the main impact direction moves across the surface in a sweeping movement, instead of impacting from one direction) will cause more severe undercutting than direct ram exposure.

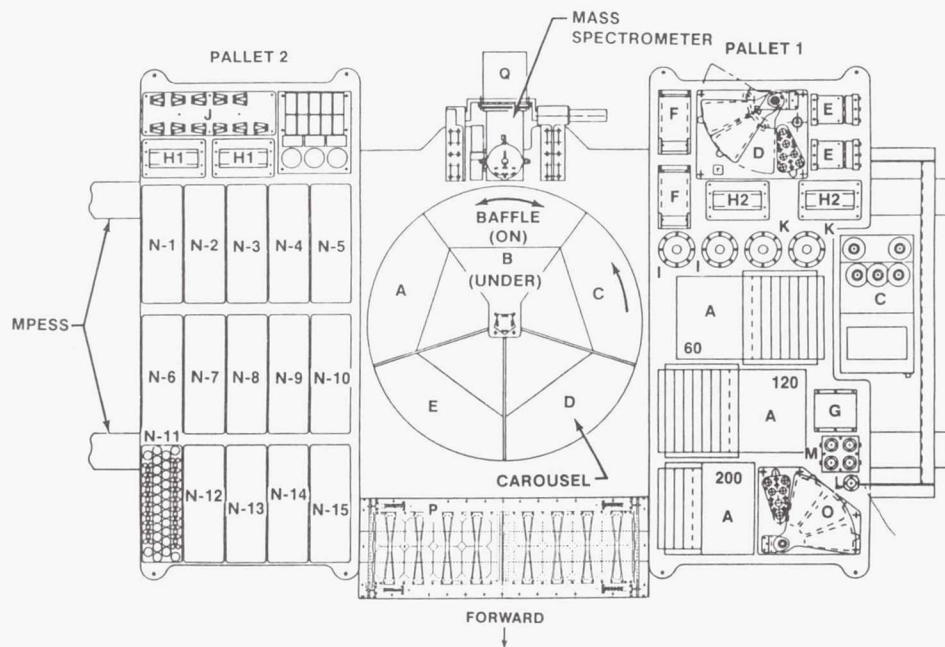
Current in-house research efforts at NASA Lewis include developing a Monte Carlo model that can predict undercutting profiles for ground-based and LEO atomic oxygen exposures. The model will be adjusted on the basis of ground exposures and further analyses of spaceflight coupons. The Monte Carlo model will be used to predict long-term LEO atomic oxygen durability of Space Station *Freedom* power system materials, such as photovoltaic array blankets.

**Lewis contacts:** Kim K. de Groh, (216) 433-2297;  
Bruce A. Banks, (216) 433-2308  
**Headquarters program office:** OAST

### Experiments Will Evaluate Oxygen-Material Interactions

The Evaluation of Oxygen Interactions with Materials Experiment (EOIM-III) is scheduled for a June 1992 launch. This experiment will expose various Space Station *Freedom* materials to ram atomic oxygen for 40 hours. The objectives of the experiment are to obtain material erosion yields, to evaluate protective coatings, and to test the durability of various materials. NASA Lewis will play a major role in determining which materials are to be exposed and how they will be evaluated. The accompanying figure shows the totality of the EOIM-III, which includes a mass spectrometer. NASA Lewis has two passive trays (92 test samples). There are also 58 samples on the heated trays, 16 samples on variable atomic oxygen exposure trays, 12 samples on controlled ultraviolet exposure trays, a pin-hole camera to measure atomic oxygen directionality, two reflectometers to measure atomic oxygen first-bounce effects on materials, 12 mechanically stressed materials to measure atomic oxygen interaction with tensile-stressed solar array blanket materials, and the Space Station *Freedom* Array Materials Erosion Experiment (SSFAME). The results will be very valuable in predicting material life and in selecting materials for Space Station *Freedom*.

**Lewis contacts:** Bruce A. Banks, (216) 433-2308;  
Michael J. Mirtich, (216) 433-5616  
**Headquarters program office:** OAST



## ATOMIC OXYGEN INTERACTION EXPERIMENTS:

- |  |  |
|--|--|
| A - HEATED PLATE (JSC), 3 EA                 | I - SCATTEROMETER (JPL), 2 EA                                |
| B - ATOM SCATTERING EXPERIMENT (UAH), 1 EA   | J - MECHANICAL STRESS FIXTURE (LeRC), 11 EA                  |
| C - ENVIRONMENT MONITOR PACKAGE (GSFC), 1 EA | K - REFLECTORMETER (LeRC), 2 EA                              |
| D - SOLAR UV EXPERIMENT (JSC), 1 EA          | L - PIN-HOLE CAMERA (LeRC), 1 EA                             |
| E - STATIC STRESS FIXTURE (MSFC), 2 EA       | M - SCATTEROMETER (AEROSPACE CORP.), 1 EA                    |
| F - UNIFORM STRESS FIXTURE (MSFC), 2 EA      | N - SAMPLE CARRIERS, 15 EA                                   |
| G - ATOMIC OXYGEN MONITOR (MSFC), 1 EA       | O - VARIABLE EXPOSURE TRAY, 1 EA                             |
| H1 - COMPOSITE STRESS FIXTURE (LeRC), 2 EA   | P - FREEDOM ARRAY MATERIALS EXPOSURE EXPERIMENT (LeRC), 1 EA |
| H2 - COMPOSITE STRESS FIXTURE (JSC), 2 EA    | Q - MASS SPECTROMETER (AFGL), 1 EA                           |

EOIM configuration.

### Fabrication Techniques Developed for All-Metal Advanced Solar Concentrators

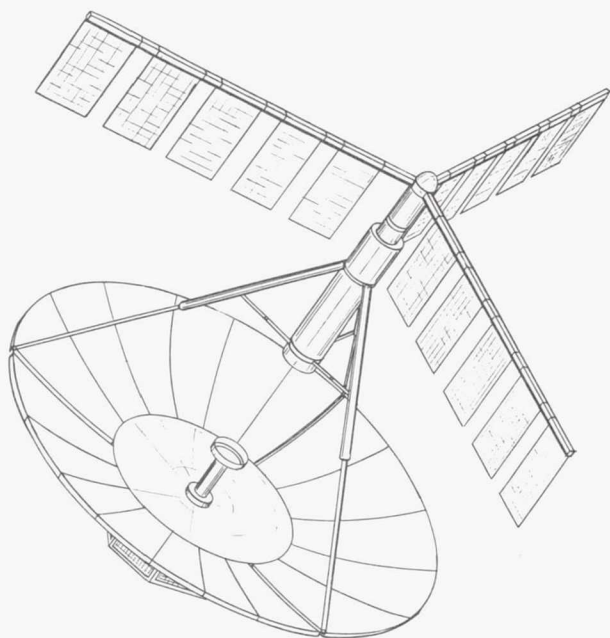
A solar dynamic power system requires a highly accurate concentrator to focus thermal energy into a heat receiver that heats the working fluid of a power conversion system (e.g., Brayton or Stirling). NASA Lewis defined the primary goal of an advanced solar concentrator panel as optical efficiency. The concentrator must be lightweight, scaleable, long lived, and survivable during launch loads and in the low-Earth-orbit environment. An all-metal concentrator resists the effects of atomic oxygen. Fabrication techniques were recently developed for a high-quality, all-metal advanced solar concentrator.

The Advanced Manufacturing Center (AMC) of Cleveland State University recently developed an all-metal panel for a 2-m-diameter concentrator. The panel is of honeycomb sandwich construction with aluminum front and back sheets and an

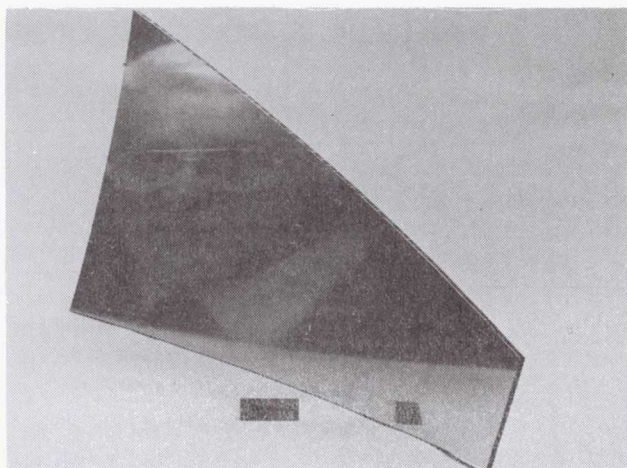
aluminum honeycomb core bonded together with a two-part epoxy fillet. Cure shrinkage and thermal contraction at the fillet can cause the facesheet to deform, resulting in panel dimpling or "print through." This effect can be reduced by increasing the facesheet thickness. The AMC panel includes a 0.25-in.-thick honeycomb sandwich between a 0.003-in.-thick back sheet and a 0.012-in.-thick front sheet. The finished panel weighs 2.2 kg/m<sup>2</sup> and has a facet slope error of 0.6 mrad. Preliminary thermal cycling of the test coupons from room temperature to 150 °C for 50 cycles shows no apparent degrading effect. The AMC is investigating two leveling polymers to produce a high-quality optical surface acceptable for further coating with vapor-deposited reflective films. The polymers include Emerson & Cuming's Eccocoat EP-3 and Shell Epon 826.

Solar Kinetics Inc. (SKI) has recently developed an all-metal aluminum honeycomb sandwich concentrator panel similar to that of the AMC. The SKI panel includes a 0.25-in.-thick





Solar concentrator.



All-metal solar concentrator panel.

honeycomb with a 0.012-in.-thick front sheet and a 0.005-in.-thick back sheet bonded by a two-part epoxy fillet, combining to produce an overall weight of  $1.8 \text{ kg/m}^2$ . A high-quality,  $3\text{-}\mu\text{m}$ -thick polyimide levelizing layer is applied by spin coating to produce a facet slope error of 0.94 mrad. A reflective layer of aluminum, including a protective layer of aluminum oxide, is then deposited on top of the polyimide coating. The overall solar-weighted reflectance within a full cone angle of 4 mrad is 85.8 percent. The completed panel was

unaffected by being thermally cycled over 4000 times from 37 to 90 °C. A thermal gravimetric analysis of the polyimide levelizing coating showed near zero weight loss up to 300 °C—well above the operating temperature of 80 °C.

Both AMC and SKI have demonstrated that an all-metal concentrator can be fabricated to be lightweight, highly reflective, accurate, scaleable, and long lived. The AMC and SKI panels that met the required goals were fabricated and delivered to NASA Lewis. The all-metal solar concentrator concept holds promise for achieving the objectives of future solar dynamic power systems for the growth of Space Station *Freedom* and other potential spacecraft missions.

**Lewis contact:** Scott W. Richter, (216) 433-6118  
**Headquarters program office:** OAST

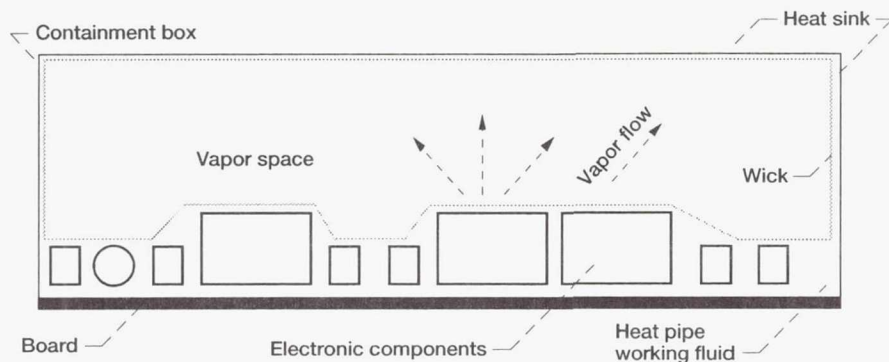
### Thermal Control Concepts Selected for Advanced Space Power Electronics

Advanced space electronics for power conditioning and control produce a significant amount of waste heat. Present state-of-the-art technology requires large radiators to transfer this heat to space. With the development at NASA Lewis of advanced electronics, which operate at high temperatures (300 to 500 K) and new thermal control techniques for these electronics, it is possible to reduce this radiator requirement by a factor of approximately 20.

Four thermal control concepts: a direct-immersion heat pipe, two micropump concepts, and a vapor-pressure-pumped-loop concept were selected for study. These concepts have the potential to significantly reduce temperature drops between electronic components and their heat sinks.

The direct-immersion heat pipe concept calls for burying the electronic components in the wick structure of a heat pipe. The working fluid of the heat pipe is dielectric. Experiments to evaluate the heat flux capability of this concept are being performed.

This work, which originated at NASA Lewis, is being pursued on research grants by the University of Kentucky and the University of California,



*Direct-immersion heat pipe concept for cooling space power electronics.*

San Diego, and on contract with Research International, Incorporated.

**Lewis contact:** Karl W. Baker, (216) 433-6162  
**Headquarters program office:** OAST

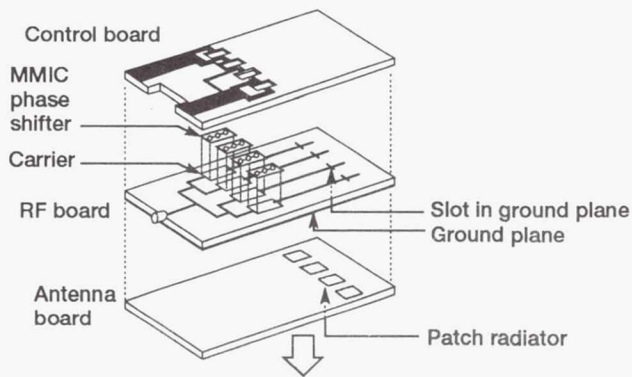
## Space Electronics

### Breadboard Testing of Ka-Band MMIC Microstrip Subarray Completed

Ka-band technology is being incorporated into new commercial and military satellite communications systems for increased channel capacity, improved security, and interference-free operation. The Advanced Communications Technology Satellite (ACTS), to be launched in 1993, represents an important commercial application of the Ka-band technology. In a recent technology assessment of alternative communications systems for NASA's Space Exploration Initiative (SEI), Ka-band communications technology has also been identified as meeting mission requirements for telecommunications, navigation, and information management. Ka-band microstrip antenna arrays with monolithic microwave integrated circuit (MMIC) amplifiers and phase shifters are particularly attractive for these applications. These planar, electronically steerable arrays, whether used as direct radiating phased arrays or as array feeds for high-gain reflector antenna systems, offer significant size and mass reduction as well as better system reliability.

NASA Lewis, under a contract with Texas Instruments, is developing a 16-element Ka-band MMIC microstrip subarray module. The contract emphasizes MMIC insertion (not MMIC device) technology development in the design and fabrication of a  $4 \times 4$  electronically steerable subarray. The 30-month contract began in March 1990. The subarray features a multilayer "tile" architecture. This approach reduces the depth of the array and exploits the performance capabilities of microstrip patch radiators. In the hybrid assembly technique individual MMIC chips are separately tested and then integrated into the microstrip beam-forming network by using wire bonds. The subarray measures 1.3 by 1.3 by 0.3 in. and consists of 16 cavity-backed circular patch elements, 16 MMIC power amplifiers, 16 MMIC phase shifters, 2 customized application-specific integrated circuit (ASIC) chips for phase shifter control, switches for remotely turning amplifiers on and off, a planar 16-way radiofrequency (RF) power divider, and 2 multilayer direct current/logic distribution boards. The patch element is excited by an aperture-coupled microstrip line, and the phase shifter is a four-bit switched line that uses





*Ka-band MMIC subarray.*

gallium arsenide P-type intrinsic N-type diodes as control elements. The subarray is designed to radiate 75 W of effective isotropic radiated power and scan over  $\pm 30^\circ$  in azimuth and elevation. The subarray has vertical polarization and is designed to operate over 5-percent bandwidth centered at 29.3 GHz.

Significant progress has been achieved this year. Breadboard testing of the RF distribution network, the radiating elements, and the mechanical test pieces has been completed. Results indicate that the radiating element provides more than 5-dB gain over 8-percent bandwidth, that the four-bit MMIC phase shifter has an insertion loss of less than 6 dB, and that amplitude variation as a function of phase state is within  $\pm 0.5$  dB. Carrier plate level testing with a new phase shifter and new amplifiers from previous contracts has demonstrated low coupling between adjacent channels and very good operational stability. Fabrication and testing of the new amplifier is in progress. The ASIC specification control drawing has been released to the vendor. After the successful completion of tasks involving the breadboarding of key components and assemblies, approval for fabrication was given at the final design review in August 1991. The current schedule shows contract completion in May 1992, four months ahead of schedule.

The contract has been augmented with funds from the ACTS Project Office to fabricate a second 16-element subarray for use in the ACTS aeroterminal experiment. Plans are proceeding for integration of both arrays into the Lewis Learjet.

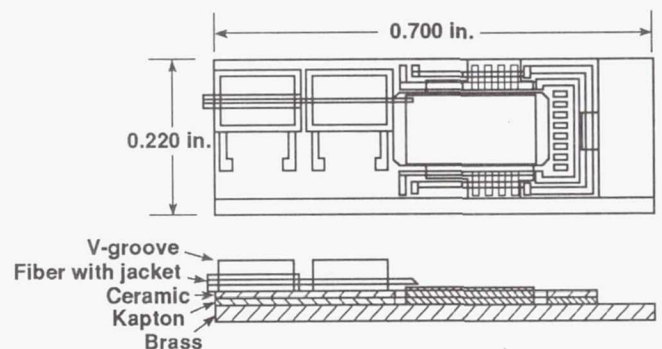
**Lewis contact:** Dr. Richard G. Lee, (216) 433-3489  
**Headquarters program office:** OAST

## Optical Control Designed for Phased-Array Antennas

Phased-array antennas are presently being developed that use monolithic microwave integrated circuit (MMIC) amplifiers and phase shifters that enable space-based communications antennas to be electronically steered and pointed. This minimizes the amount of fuel the spacecraft would require to physically position a large microwave antenna in space. At microwave frequencies in the Ka band the antennas must be larger than 10 ft in diameter in order to collect enough of the communications signal. A phased-array antenna of this size will require hundreds, perhaps thousands, of MMIC-based antenna elements. In order to coordinate the settings of the MMIC devices, a small, lightweight, low-loss control distribution network that links the antenna elements to a controller is needed. Fiber optics is being investigated for this network.

A requirement for optical control of arrays is an opto-electronic interface circuit (OEIC) that can take a serial optical input signal and demultiplex it into a parallel electrical output signal which is compatible with the MMIC digital signal inputs. Fabrication and experimental verification of OEIC devices are the objectives of a contract with Honeywell's Sensor Research Center.

The initial design and fabrication cycle produced proof-of-feasibility hybrid devices. The present cycle incorporates several additional state-of-the-art features in a fully monolithic chip. Data transmission to 300 Mbps is available with data encoding to provide built-in clock recovery. The OEIC also features on-chip addressability and on-chip diagnostics. The OEIC has been designed to meet the requirements of future advanced phased-array antenna systems and is compatible with optical local area network requirements.



*Opto-electronic interface circuit.*

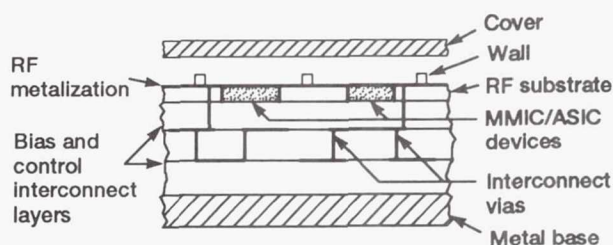
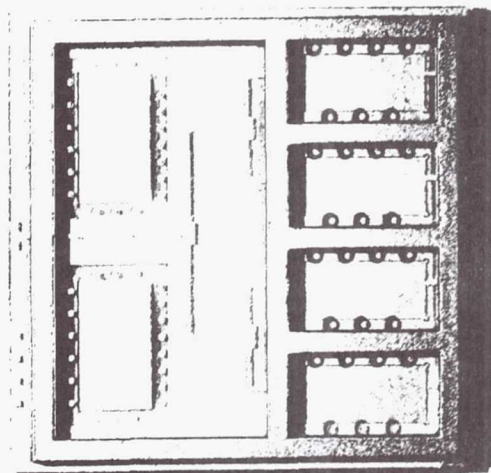
Circuit design has been completed, fabrication has begun, and delivery of OEIC devices is scheduled for January 1992.

**Lewis contact:** Richard R. Kunath, (216) 433-3490  
**Headquarters program office:** OAST

### Packaging Developed for Monolithic Microwave Integrated Circuits

The technology for packaging monolithic microwave and millimeter-wave integrated circuits (MMIC's) has not kept pace with the development of the chips themselves. Although gallium arsenide (GaAs) MMIC's can operate at frequencies higher than 40 GHz, packaging technology presently limits operation well below 25 GHz, thereby inhibiting the insertion of these devices into systems. NASA Lewis is expending much effort, particularly in the 18- to 44-GHz frequency range, to develop approaches for packaging high-performance MMIC devices. The successful development of MMIC packaging will allow the capabilities inherent in MMIC devices to be exploited in a variety of space, airborne, and terrestrial communications systems.

The Lewis packaging technology development program is supported by two industry contracts that examine various approaches to MMIC packaging. A contract with Hughes Aircraft Company deals primarily with the development of a generic, or universal, package and the attendant test fixturing that supports single MMIC chip packaging concepts. This type of package offers full hermeticity, mechanical device protection, heat removal from the device, and frequency coverage through 44 GHz. The second packaging contract, with Holz Industries, a Small Business Innovative Research (SBIR) phase II contract, specifically addresses the use of low-loss fused quartz as a substrate material. This contract has successfully demonstrated the use of fused quartz for device packaging and has examined its feasibility for multielement or multicircuit packages as they would be applied to advanced phased-array antenna systems. One such proof-of-concept package, the multielement, multilayer millimeter-wave package module, permits several radio-frequency (RF) MMIC devices to be placed in close proximity to one another in a single package to allow close spacing of radiating element in array



*Multielement, multilayer millimeter-wave packaging module.*

applications. Each MMIC is installed in an individual compartment to eliminate crosstalk between chips and to suppress electrical moding. RF signals are distributed from a single microstrip input to each of four MMIC devices by using a thin-film power divider network.

In a typical phased-array application four multi-bit phase shifters are installed into the recesses in the module. The diagram indicates how the challenging bias and control line interconnect problem is addressed. Two places are provided for application-specific integrated circuits (ASIC's) in the module to demultiplex a single serial data stream sent from a system controller. The ASIC and the RF MMIC's are interconnected through multiple layers of metalized lines printed on substrates below the RF ground plane and connected vertically by filled vias. Direct-current bias interconnection is done in a similar manner. Overall module size is approximately 1 by 1 by 1/16 in. This and other packages produced by the Holz and Hughes contracts will be fully evaluated in the Lewis MMIC characterization testbed in 1992.

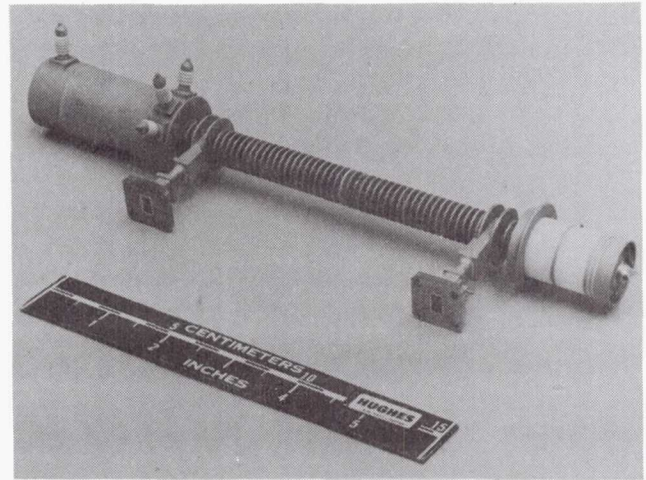
**Lewis contact:** Kurt A. Shalkhauser, (216) 433-3452  
**Headquarters program office:** OAST



## High-Efficiency Traveling Wave Tube Amplifiers Demonstrated for Deep-Space Communications

The traveling wave tube amplifier (TWTA) efficiency enhancement programs ongoing at NASA Lewis continue to provide the technologies needed for high-efficiency millimeter-wave communications amplifiers for planned NASA missions to deep space. A current objective of this effort is to develop a very high-efficiency TWTA operating in the Ka band (32 GHz) for the Cassini mission to the environment of Saturn, scheduled for launch in late 1995. This work is being conducted in contractual and cooperative effort with the Electron Dynamics Division of the Hughes Aircraft Company.

The required radiofrequency (RF) output for the Cassini traveling wave tube is 10 W; the direct-current power input to the electronic power conditioner is limited to about 30 W. Achieving this performance goal, representing a sharp increase in efficiency relative to Ka-band TWTA's now available at this power level, will permit the transmission to Earth of all the data produced in the mission. Several Lewis-developed efficiency-enhancing technologies are applied throughout the TWTA to accomplish this, including computer-aided design and experimental development efforts. A major Lewis contribution is the design of an advanced helix dynamic velocity taper (DVT) to significantly improve the interaction between the electron beam and the electromagnetic wave. Lewis also supplied the design of a spent-beam refocusing section and a multistage depressed collector (MDC) and will provide in-house treatment of the electrode surfaces to suppress secondary electron emission. All of this will enhance energy recovery in the spent electron beam. Other features intended to improve traveling wave tube performance are the reduced-interaction-section magnet period, to improve beam quality, and the more efficient cathode support assembly, to reduce required heater power. Results of tests performed recently with a development TWT having a Lewis-designed MDC and a short-pitch body magnet stack indicated a measured saturated RF output power of 9.44 W at a beam current of 13 mA and a helix voltage of 5200 V. The overall TWT efficiency at that condition was 39.5 percent. With further planned electron gun modification and other changes, the objective efficiency of 43 percent is expected to be



32-GHz Cassini traveling wave tube.

readily achieved. Importantly, the MDC design was experimentally demonstrated.

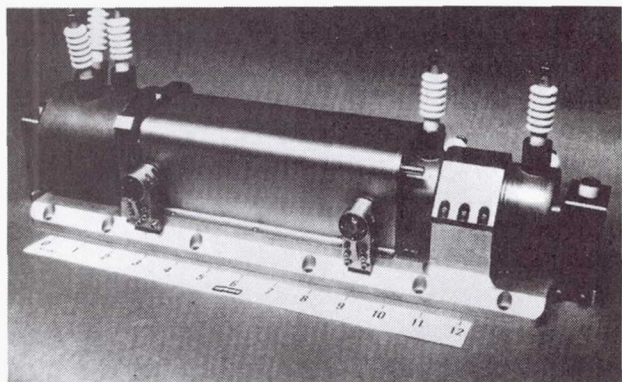
As currently planned, the program will conclude with the delivery of four fully functional engineering model TWT's along with one breadboard model electronic power conditioner integrated and tested with one of the TWT's. Coordination with the Jet Propulsion Laboratory has produced packaging and testing requirements for the hardware delivered from this research and development program to be an immediate predecessor for the development of a final flight model TWTA for the Cassini mission.

**Lewis contact:** Arthur N. Curren, (216) 433-3519  
**Headquarters program office:** OAST

## 60-GHz Traveling Wave Tube Designed for Intersatellite Communications

The frequency band near 60 GHz is ideally suited to communications between spacecraft. This frequency is strongly absorbed by the atmosphere, and therefore interference from transmitters on the ground will be minimized. However, amplifiers needed for 60-GHz transmitters tend to be inefficient and generally unsuitable for use in space. With the application of efficiency enhancement techniques developed at Lewis, a vacuum electronic device called the traveling wave tube (TWT) shows considerable promise for use in this application.





60-GHz TWT.

A dual-mode (75/30 W), 59- to 64-GHz TWT for intersatellite communications is being developed for NASA Lewis by Hughes Aircraft Company. The TWT, designated the 961 HA, employs a coupled-cavity, slow-wave structure with a two-step velocity taper and a NASA Lewis-designed isotropic graphite multistage depressed collector (MDC). Two TWT's will be fabricated and tested under the contract, with an option to purchase two more. An earlier development model (961 H) demonstrated both the high power and broad bandwidth required. The emphasis of the current effort is on achieving high overall efficiency, dual power mode capability in the required operating band, and a substantial reduction in the MDC size and weight.

The design effort has been completed with promising results. Computer modeling indicates that the radiofrequency performance of the TWT should be more than adequate. Computed MDC efficiencies in the 94-percent range indicate that the objective of a 40-percent overall TWT efficiency should be readily achievable.

Fabrication of the first of two TWT's was recently completed. A minimum saturated output power of 75 W was achieved over 4 GHz of bandwidth under low-duty operation. The estimated collector efficiency of 93.9 percent was in close agreement with the computer-predicted value of 94.3 percent. However, with an 11-percent beam interception (possibly caused by small misalignments), continuous-wave operation could not be achieved. If the beam interception design goal of 2 percent can be obtained with the second TWT, currently under fabrication, it is expected that the overall efficiency will exceed the 40-percent goal. Fabrication of the second TWT is well under way. A

third model is being purchased on the contract option.

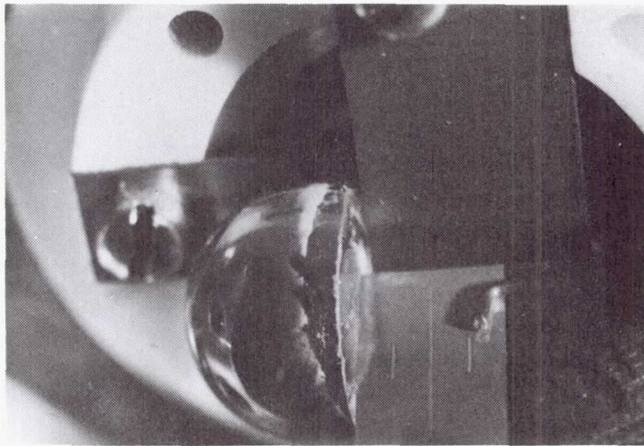
**Lewis contact:** Peter Ramins, (216) 433-3521  
**Headquarters program office:** OAST

### Submillimeter-Wavelength Backward-Wave Oscillator Designed

The submillimeter-wavelength, backward-wave oscillator is an electron beam device with potential application as a voltage-tunable local oscillator for heterodyne receiver spectrometers deployed above Earth's atmosphere. The submillimeter wavelength region is of interest to radio astronomers because it is coincident with the rotational spectra of many molecules. The backward-wave oscillator appears to be the best device for supporting this application. In addition to being voltage tunable, it can be phase locked and can provide sufficient power for almost any of the envisioned systems, including arrays of detectors for imaging and for quick data recovery. The project goal is to reach an operating frequency of 2000 GHz. A number of successful design innovations have been produced. These include a microfabricated circuit on a diamond substrate, an optical output coupler, and a high-impedance, slow-wave structure. The microfabrication technique, which was developed at MIT Lincoln Laboratory, has enabled the use of an interdigital line circuit. This fundamental backward-wave structure has a higher impedance than the vane structure that is usually used at high frequencies. The circuit is etched onto a diamond substrate to diminish the problem of passive cooling in space. Wideband operation is achieved through use of a quasi-optical output coupler. A tapered-slot line antenna, with a cover plate to confine the radiation, feeds the radiation to a sapphire lens collimator and then transmits it through a window (quartz or sapphire) in the vacuum envelope.

A lanthanum hexaboride ( $\text{LaB}_6$ ) cathode was installed into the experiment at NASA Lewis. This cathode has been cycled to operating temperature about 40 times and has been operated for nearly 300 hr without noticeable degradation in emission. The life of this cathode appears to be limited by the evaporation rate of the  $\text{LaB}_6$  crystal. The cathode is capable of the high emission densities





*Submillimeter-wavelength backward-wave oscillator.*

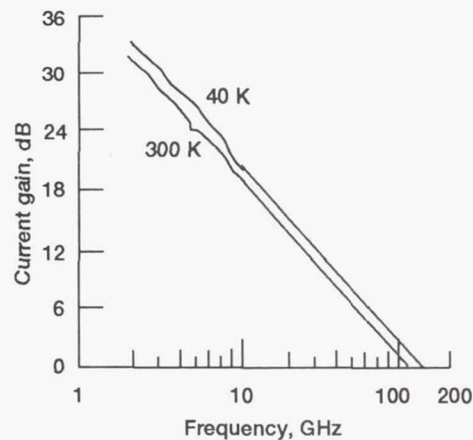
required to overcome the severe losses occurring at terahertz frequencies.

At this time the backward-wave oscillator has demonstrated a continuously tunable bandwidth of 78 percent (137 to 311.5 GHz). A measurement made at Lewis with a Golay cell detector calibrated against a carbon-dioxide-pumped far-infrared laser indicates that the output power is 21.5 mW.

**Lewis contact: Norbert Stankiewicz, (216) 433-3674**  
**Headquarters program office: OAST**

### **Cryogenic High-Electron-Mobility Transistor Studied**

Studies for future NASA missions project that communications systems will require receivers with noise figures that cannot be achieved in room-temperature electronics. Although cooling will improve the performance of most electronic systems, a device that has been optimized for operation at cryogenic temperatures promises even greater enhancements. Passive cooling in space will enable the use of these optimized devices in spacecraft without the problems encountered in active cooling. In addition, such devices would be useful in systems that contain high-temperature superconductors as these will also require more conventional semiconductor circuitry as a complementary feature. The objective of the cryogenic High-Electron-Mobility Transistor (HEMT) Program is to develop basic three-terminal devices whose structure (materials



*Current gain for 0.2-μm HEMT device.*

and geometry) has been optimized for operation at cryogenic temperatures. Improvement is measured primarily by gain as measured over frequency and temperature and the maximum frequencies of operation that are obtained from those measurements. Incorporating such devices in microwave circuitry should result in lower noise systems. The lower noise is a direct result of the higher gain and higher frequency of operation.

NASA Lewis is using an active channel of indium gallium arsenide with extremely high indium content (up to 70 percent) on indium phosphide (InP) substrates. The high indium concentration produces relatively small band gaps and therefore provides exceptionally good charge confinement when a quantum well is fabricated. During the last year, in collaboration with the University of Michigan, 0.1- and 0.2-μm gate devices were fabricated by using indium concentrations of 53 to 70 percent. S-parameters characterizing the device performance have been measured over both frequency and temperature, and equivalent circuit parameters for the devices have been extracted from these data. In conjunction with this effort, a probe-based cryogenic test station has been developed that will permit testing of devices at controllable, variable cryogenic temperatures on a wafer without bond wires. This capability is unique in the United States.

This work can be commercialized, as the main component of the device is the molecular-beam-epitaxy-grown indium gallium arsenide/indium phosphide, which can be ordered from QED, Inc. However, at the present time, only the 53 percent indium is commercially available. Field-effect transistors from the Michigan work have been

supplied for evaluation to the Princeton University research group for possible application in the Cosmic Ray Background Experiment (COBE) satellite.

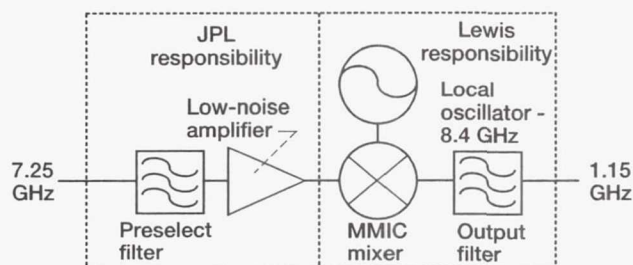
**Lewis contact:** Dr. Samuel Alterovitz, (216) 433-3517  
**Headquarters program office:** OAST

### High-Temperature Superconducting Space Experiment Begins Development

High-temperature superconductivity (HTS) offers the potential for extremely low-loss interconnects and transmission lines at frequencies below approximately 60 GHz. This in turn makes feasible the implementation of a number of components, such as filters and oscillators, in planar (microstrip or coplanar waveguide) technologies whose losses would have been prohibitive in normal metal. In addition, the reduced losses in interconnects and matching circuits have the potential for significantly lowering the losses and hence the system noise figures for ultra-low-noise communications receivers.

NASA Lewis is working to design, fabricate, evaluate, and deliver a superconducting receiver module for space testing on the Naval Research Laboratory's (NRL's) High-Temperature Superconducting Space Experiment (HTSSE-II) satellite, to be launched in 1994. NRL's host satellite will perform radiofrequency testing of a limited number of superconducting subsystems or advanced components in space for a period of approximately 6 months. The ultimate goal is the early demonstration of superconducting components that have been designed and packaged under the restrictions imposed by the space environment. In the course of fabricating the NASA module, numerous problems associated with the integration of semiconductor devices and HTS materials will be explored.

The circuits presently under development represent a joint effort of NASA Lewis and the Jet Propulsion Laboratory. The low-noise receiver to be built will accept 7.25-GHz radiofrequency input, will provide low-noise amplification, and will downconvert to 1-GHz intermediate frequency. The local oscillator will be contained within the module. Input matching and filtering circuitry will utilize HTS materials, as will the local oscilla-



*Low-noise receiver subsystem for High-Temperature Superconducting Space Experiment.*

tor. The active elements in the low-noise amplifier, the mixer, and the oscillator will all be conventional semiconductor devices.

A proposal describing the proposed experiment has been submitted to NRL and has been tentatively accepted. Responsibilities for component development have been assigned. JPL will be responsible for the input circuitry and the low-noise amplifier; Lewis will provide the mixer and the local oscillator. JPL will be responsible for module integration and space qualification.

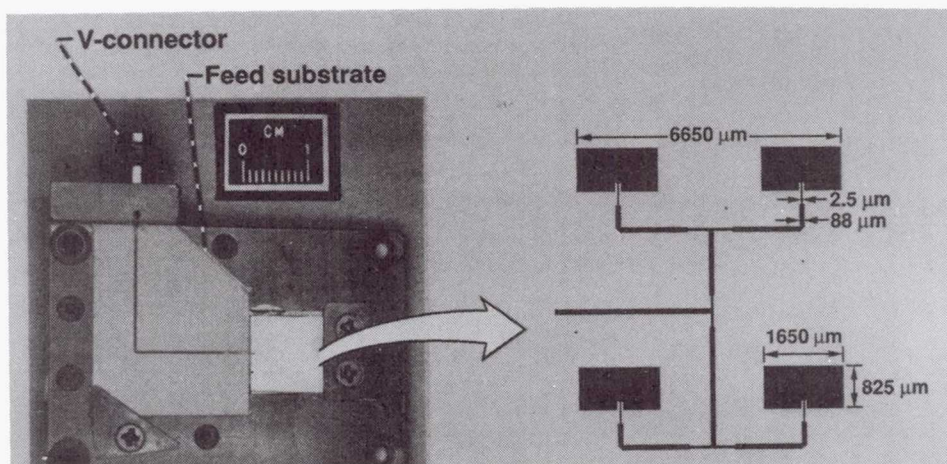
**Lewis contacts:** Dr. Kul B. Bhasin, (216) 433-3676;  
 Robert R. Romanofsky, (216) 433-3507  
**Headquarters program office:** OAST

### Four-Element Array Tested for Ka-Band Superconducting Microstrip Antenna

Phased-array antennas offer the potential for enabling large electronically steered phased arrays. Such antennas eliminate the need for large, heavy, mechanically noisy, and potentially unreliable mechanical steering devices presently used in conjunction with any highly directive antenna. The number of elements (and therefore the size) of a phased-array antenna is limited, however, by the losses incurred in the complex feed structures encountered in large arrays. Calculations indicate that at least to frequencies of 32 GHz the use of superconducting materials in the phased-array feed network will significantly reduce such losses and make higher gain antennas possible.

NASA Lewis is working to design, fabricate, and test a superconducting array antenna and to demonstrate its advantages in terms of feed network losses. This work is being carried out in





High-temperature superconducting antenna in brass test fixture.

collaboration with Ball Aerospace. Ball is actively engaged in estimating the cooling requirements of a Ka-band phased array, as well as in designing prototype antenna modules. NASA Lewis' contribution to the effort has been the fabrication and testing of a  $2 \times 2$  element array using Ball's design. As a critical part of this effort a cryogenic antenna test facility has been developed, and preliminary radiation patterns for the first four-element array have been measured. Calculations indicate that approximately 16 elements ( $4 \times 4$ ) are needed before a reduction in feed network losses can be observed.

**Lewis contact:** Dr. Kul B. Bhasin, (216) 433-3676  
**Headquarters program office:** OAST

### Flexible High-Speed Codec Designed

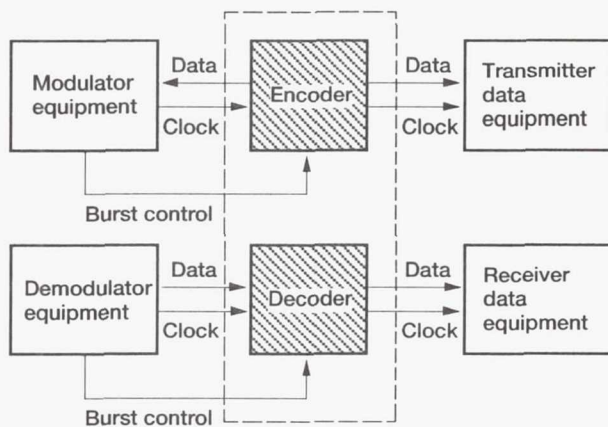
Future processing satellites with tens of gigabits per second throughput, multiple-beam time-division multiple-access/frequency-division multiple-access (TDMA/FDMA) hybrid uplinks, and multiple-beam, high-data-rate time-division-multiplexed (TDM) downlinks will require high-speed burst data encoding, decoding, and error correction. Planned NASA missions, such as the evolutionary Space Station, will require high-reliability voice, data, and video communications with several hundred megabits per second throughput. High-performance coding can reduce the transmitting power requirements and the size, weight, and costs of the antenna and radiofrequency subsystems for a given bit-error-

rate performance and bandwidth conservation requirement.

Coding may also be used to adaptively compensate for rain attenuation on a burst-by-burst basis. Further advancement of the implementation of flexible, high-speed coding technology is required to enhance the performance and efficiency of existing and future communications systems and to reduce both the development risk and the costs for Government and commercial space communications applications.

NASA Lewis has contracted the Harris Corporation to develop and demonstrate advanced high-speed coding technology that provides substantial coding gains with limited bandwidth expansion relative to the uncoded bit-error-rate performance of several common modulation techniques. The scope of the contract is to analyze, design, fabricate, test, and demonstrate advanced technology in the form of a flexible high-speed codec (FHSC) consisting of a Bose-Chaudhuri-Hocquenghem (BCH) hard-decision, complementary-metal-oxide-semiconductor, application-specific integrated circuit (CMOS ASIC) codec coupled with a Chase algorithm applique for soft decision. This advanced technology will have applications in space and ground segments of communications systems in the 1990's and beyond.

The FHSC system design and the chosen implementation provide a highly flexible architecture and components that can be applied in other systems. A stand-alone, 300-Mbps, triple-error-correcting, hard-decision BCH codec is



*FHSC soft-decision configuration.*

implemented on a single CMOS ASIC chip. This chip contains all functions necessary to operate in both burst and continuous modes. A discrete implementation of a Chase algorithm is provided to augment the hard-decision codec chip and to enhance the gain by adding soft-decision information. This feature demonstrates the first use of soft-decision information with block codes for higher coding gain.

The FHSC system is well suited for bandwidth-efficient communications systems. It provides a flexible, high-performance codec with high coding gain, high code rates, and high data rates. The FHSC provides coding gains as high as 5.3 dB at a bit error rate of  $10^{-8}$ . The FHSC can handle code rates of 7/8 to 15/16 (i.e., low band spreading) depending on block size. It can also handle data rate requirements up to 300 Mbps (uncoded) over a 200-MHz (at 3 dB) bandwidth radiofrequency channel. The FHSC also interfaces to the M-ary alphabet.

Over the past year FHSC chassis designs were completed. Checkout of the input/output formatter card was completed for the test and demonstration equipment. Also, interfaces between personal computers and the test demonstration equipment as well as noise generator card designs were completed. Wire wrap and component assembly of the BCH card cage assembly was completed. Generation of the wire wrap files for the Gardner Denver machine was completed for noise generator #1 card cage assembly. BCH ASIC chip design layout and simulation was completed. Detailed design of the FHSC soft-decision (Chase) circuits were com-

pleted. Design and simulation of the receiver formatter card for the Chase circuits were completed.

**Lewis contact:** Robert E. Jones, (216) 433-3457  
**Headquarters program office:** OAST

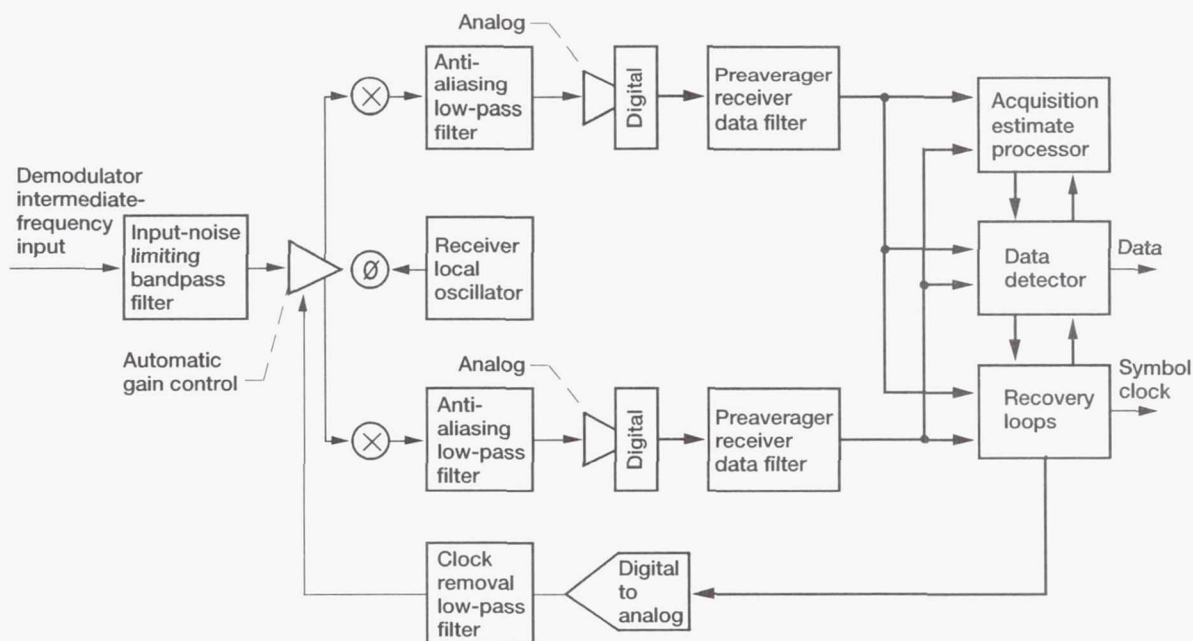
### Design of Programmable Digital Modem Nears Completion

A modulator and demodulator pair (modem) converts communications signals, such as voice, video, and computer data, into a format suitable for free-space transmission and reception. Modems are similar in function to radios and cellular telephones. NASA Lewis and Comsat Laboratories are applying advanced digital computer-like technologies to satellite modems to make significant reductions in cost and improvements in performance. Such digital modems can be easily reprogrammed to suit the needs of a variety of communications systems with no additional engineering design or hardware modification costs.

Comsat Laboratories is under contract with NASA Lewis to develop a demonstration model of a digital modem that is externally programmable for modulation technique and data rate. The programmable digital modem will support BPSK, QPSK, offset QPSK, 8-PSK, and 16-QAM modulation formats for data throughput from about 2 to 300 Mbps. The modem is designed for burst acquisition and continuous modes of operation. Comsat is sharing the cost of developing and implementing an application-specific integrated circuit (ASIC) that is critical to several functions of the demodulator. In this second year of the three-year contract, design simulation studies were completed that dictate the detailed hardware design. The detailed designs of the programmable digital modem, the preaverager ASIC, and the test demonstration equipment are near completion. A paper entitled "Programmable Digital Modem" was presented by Comsat at the NASA-sponsored Second Communications Technology Conference in November 1991.

**Lewis contact:** James M. Budinger, (216) 433-3496  
**Headquarters program office:** OAST





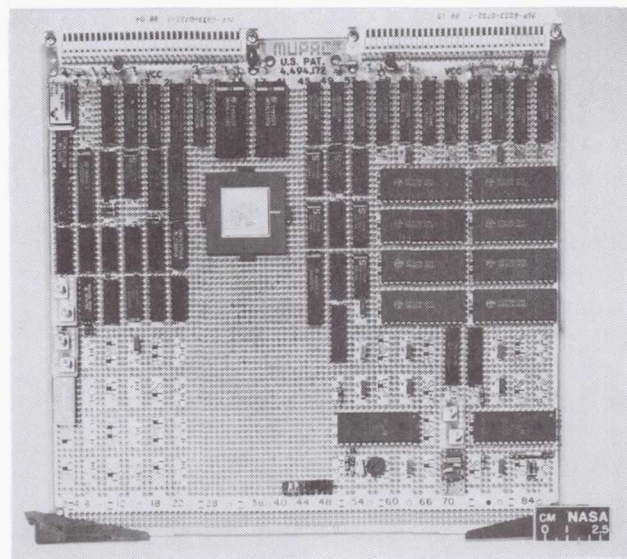
### Basic demodulator architecture.

## Flexible Trellis Modem and Codec Being Developed

Redundant information embedded in a data stream can significantly improve the chances of recovering the original data without any errors after its 44,000-mile journey through atmosphere and space. When co-designed with the modulation technique, powerful error-correcting codes can be used to reduce the amount of power and bandwidth required to convey the information. NASA Lewis, Sverdrup Technology, and Ohio University are applying state-of-the-art digital signal processing to the modulation and coding function to offer flexible operation and improved performance through combined hardware and software.

An in-house project at NASA Lewis is developing a testbed model of a digital flexible trellis modem and codec (FTMC). Its operation is based upon a pragmatic approach to trellis-coded modulation that emphasizes both power and spectral efficiency. The development incorporates programmable modulation formats, variations of trellis coding, and advanced digital signal processing techniques for baseband pulse shaping and channel precompensation.

During the past year the FTMC transmitter was built and tested. A number of modulation and coding schemes have demonstrated the soundness of flexible digital waveform synthesis. Under grant Ohio University generated the pulse-shaping data patterns necessary for programming



Digital modulator/encoder hardware

the FTMC. The application of digital channel precompensation techniques is well under way.

A paper entitled "Flexible Digital Modulation and Coding Synthesis for Satellite Communications" was presented at the NASA-sponsored Second Communications Technology Conference in November 1991.

**Lewis contacts:** James M. Budinger, (216) 433-3496;  
Mark J. Vanderaar, (216) 433-8656  
Headquarters program office: OAST

### Neurocomputing Pursued for Space Communications

Artificial neural networks are *brain-like* models for computation that attempt to capture the flexibility and power of biological information-processing systems. Applied to problems in satellite telecommunications engineering, neural networks appear to offer significant benefits in the routing, scheduling, control, and reliability of global communications traffic. As NASA's lead center for satellite communications research and development, NASA Lewis is actively pursuing the application of neural networks to satellite communications technology.

This year saw the completion of a proof-of-concept neural computer, an in-house development based on the Microdevices MD1220 neural chip and designed to run in a Sun 4/330 workstation environment. This hardware was developed for use as a flexible neural platform for two research efforts in teletraffic processing and control by satellite. The first effort addresses the use

of self-organizing neural networks to estimate and predict the statistical behavior of traffic flow through a communications satellite by combining the advantages of self-organization with those of classical stochastic control theory. The second effort is the optimization of the burst time plan for satellite-switched, time-division multiple-access traffic switching, with the goal of enhancing the efficient utilization of satellite resources.

During the past year The Ohio State University completed grant research in neural network vector quantization for video data compression and in advanced very-large-scale-integration architectures for neural computing. The New Jersey Institute of Technology completed their grant research in neural network-based control of satellite communications networks. The Ohio State University is on the verge of demonstrating a real-time hardware implementation of their neural network video compression scheme. The grants resulted in the significant publications listed in the bibliography.

### Bibliography

Ahalt, S.; et al.: Competitive Learning Algorithms for Vector Quantization. *Neural Networks*, vol. 3, no. 3, 1990.

Ansari, N.; and Liu, D.: The Performance Evaluation of a New Neural Network Based Traffic Management Scheme for a Satellite Communication Network. *Proc. IEEE GLOBECOM '91*, Phoenix, AZ, Dec. 1991.

Ansari, N.: *Managing the Traffic of a Satellite Communication Network by Neural Networks in Fuzzy, Holographic, Invariant and Parallel Intelligence*. Wiley, New York, 1992.

Krishnamurthy, A.K., et al.: Neural Networks for Vector Quantization of Speech and Images, *IEEE J. Sel. Areas Commun.*, vol. 8, no. 8, 1990.



Neurocomputing for space communications.



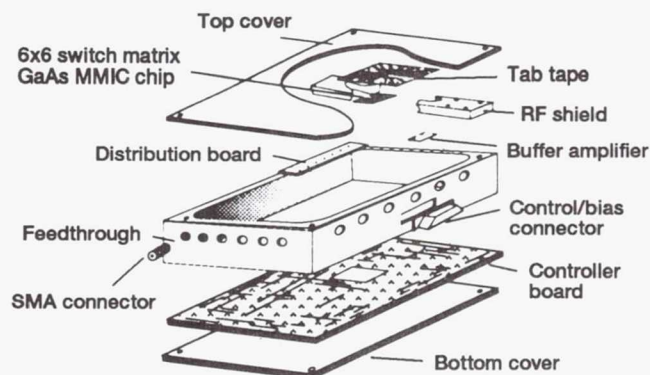
Krishnamurthy, A.K.; et al.: Video Data Compression Using Artificial Neural Network Differential Vector Quantization, *Proc. 2nd NASA Space Communications Technology Conference*, Oct. 1991.

**Lewis contact:** Eric A. Bobinsky, (216) 244-3497  
**Headquarters program office:** OAST

### Advanced GaAs Monolithic Switch Matrix Built and Tested

The monolithic implementation of the microwave switch matrix is attractive for communications satellite systems primarily for its reduced size and weight, low power consumption, and potentially lower costs. High reliability is obtainable with the ultra-large-scale-integration switching monolithic microwave integrated circuits (MMIC). The potential exists for affordable manufacturing of large switch matrices for future switching applications.

NASA Lewis has made advancements in the development of microwave switch matrix technology for use in satellite-switched, time-division, multiple-access communications systems. Present switch matrix designs rely on advanced, hybrid, microwave integrated circuit fabrication, such as the type to be flown on NASA's Advanced Communications Technology Satellite. The next generation of switch matrix technology is being developed under contract with Microwave Monolithics, Inc., of Simi Valley, California. A 6×6 (six input by six output) microwave crossbar switch matrix operating over 3 to 6 GHz is being fabricated by using gallium arsenide (GaAs) MMIC technology. High-speed switching and routing of multiple microwave signals without interference between channels is obtainable. A significant feature of the MMIC approach is the large-scale integration of many GaAs field-effect transistor switches in close proximity on a single chip while maintaining high isolation for minimal channel-to-channel crosstalk. Preliminary chip testing has resulted in isolation performance better than 60 dB. The addition of fixed-gain amplifiers around the periphery of the switch matrix chip will yield a device with an overall insertion loss of 0 dB. A modular design combined with a unique packaging concept will allow for the cascading of these zero-insertion-loss switch submodules into larger MMIC switch matrices with little or no performance degradation.



MMIC packaging layout.

All major components of the switch matrix (6×6 chip, controller, amplifiers, and housing) have been fabricated and tested. Delivery of the packaged MMIC switch matrix with fully integrated control electronics is scheduled for the first quarter of 1992.

**Lewis contact:** Gene Fujikawa, (216) 433-3495  
**Headquarters program office:** OAST

### SITE Space Communications System Simulator and Testbed Expanded

The SITE space communications system simulator and testbed provides an integrated test, evaluation, and development capability for high-frequency, space-based communications systems. The facility is used to evaluate components, systems, and networks by using real hardware integrated into a realistic communications link with computer control and monitoring. Components and subsystems, in frequency ranges up to Ka band and beyond, can be evaluated and compared. Their effect on system performance can also be evaluated in the presence of noise, interference, satellite range variation, rain attenuation at high frequencies, amplitude and phase imperfections, and other link and system effects. The SITE facility has three bursted Earth terminals operating at data rates up to 200 Mbps, allowing experimental evaluation of networking techniques and algorithms, timing and synchronization of the Earth terminals, satellite and network control, and the effects of various system perturbations on network performance.



*Ka-band multibeam three-channel transponder.*

Within the past year a third hardware channel has been added to the SITE facility. This channel allows a full  $3 \times 3$  intermediate-frequency-matrix-switched, time-division, multiple-access (TDMA) network to be simulated. The third channel also contains variable local oscillators and switchable frequency translation sections that allow components over the entire range from direct current to 22 GHz to be inserted into the SITE simulator for evaluation.

Significant progress has been made in software development for experiment and network control. The experiment control software base has been completed, and measurement sequences allowing complete measurement of bit error rates as a function of signal-to-noise ratio have been completed. These sequences allow fully automated testing, from the time the first digital data are transmitted from an Earth terminal to the time a complete bit-error-rate curve is plotted, all occurring while the satellite network simulation is functioning autonomously. Network control software has progressed to the point where acquisition of the satellite timing by the master control Earth terminal, synchronization of two Earth terminals through the satellite matrix switch in a dynamic switching environment, and the transmission of random digital data or video and audio

data have been accomplished. This will lead to the next set of experiments involving acquisition and synchronization in the presence of satellite range variation, noise, interference, and rain attenuation, followed by experiments with three Earth terminals in a dynamically switched TDMA network.

Future development of the SITE facility will include a second transponder operating in either a time-division or frequency-division uplink environment, including onboard switching and processing. An intersatellite link will connect the two transponders for investigation of component, system, and network aspects of the intersatellite link systems technology. The application of various modulation and coding techniques to space-based communications systems will also be investigated in greater detail through the development of a flexible Earth terminal.

**Lewis contact: Robert J. Kerczewski, (216) 433-3434**  
**Headquarters program office: OAST**



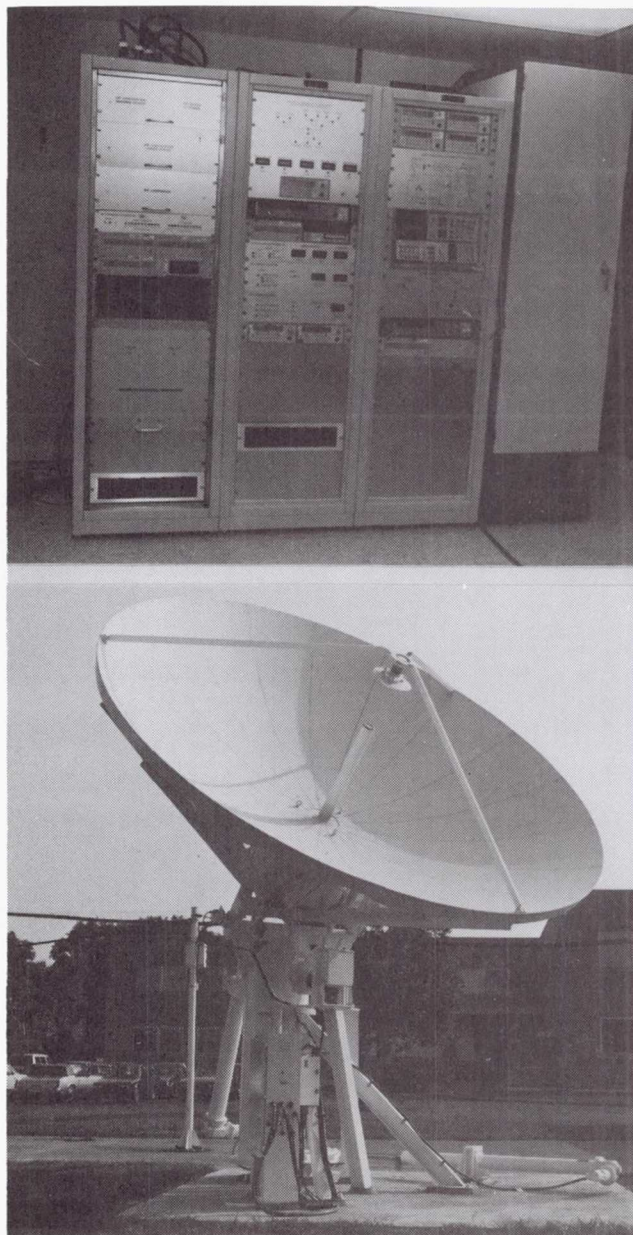
### **ACTS High-Burst-Rate Link Evaluation Terminal Being Developed**

In support of the Advanced Communications Technology Satellite (ACTS) Project, NASA Lewis is developing a high-burst-rate link evaluation terminal. This versatile and adaptable experimental test facility will support various technology experiments such as adaptive uplink radiofrequency power control and characterization of the multibeam communications package onboard the ACTS satellite.

During the past year the antenna, receiver, digital, upconverter, high-power amplifier, loopback, calibration, switching, and beacon receiver subsystems were completed and checked out on an individual basis. The subsystems were then successfully integrated to form the link evaluation terminal. The terminal is now undergoing characterization and final systems testing.

The entire terminal can be operated under computer control through IEEE 488 or RS 232 interfaces. In addition, software is being developed at NASA Lewis to assist end users. This software employs artificial intelligence techniques and will be delivered with the terminal in 1992. It will provide user-friendly assistance in operating the terminal, documentation about the terminal, and an intelligent tutor to provide initial training on the system.

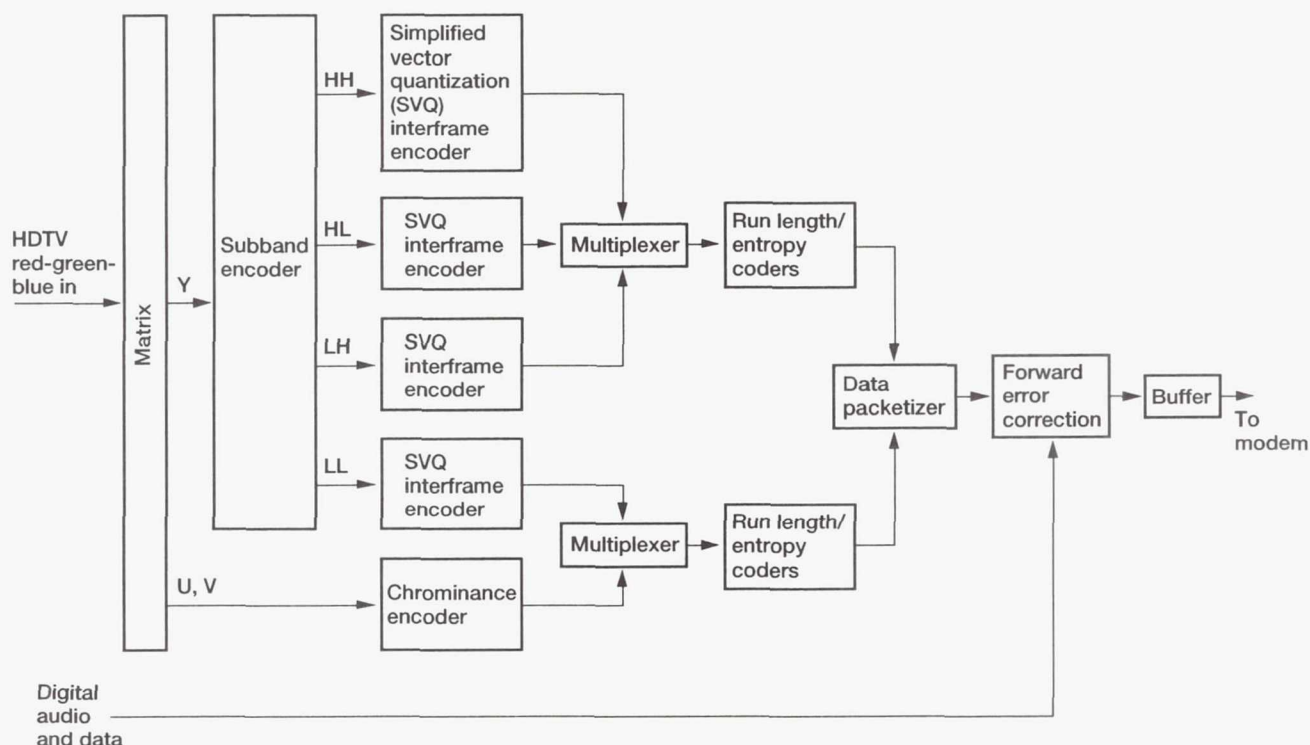
**Lewis contact: Gerald J. Chomos, (216) 433-3485**  
**Headquarters program office: OAST**



*Earth terminal and antenna for link evaluation terminal.*

### **Flexible-Rate High-Definition Television Study Completed**

In 1991, Comsat Laboratories, under a contract with NASA Lewis, completed the study phase of a flexible-rate (codec) development. The activity, funded under the Space Communications Applications Research Program, is directed toward



Block diagram of flexible-rate HDTV encoder.

digital transmission of high-definition television by satellite and thus toward maintaining the technical leadership of the United States in satellite communications technology. Because of their point-to-multipoint nature, satellites are the most cost-effective means for video distribution, including HDTV. Considering the advantages of digital transmission and the inevitable trend toward all-digital satellite communications, development of a digital HDTV codec at cost-effective data rates is very important.

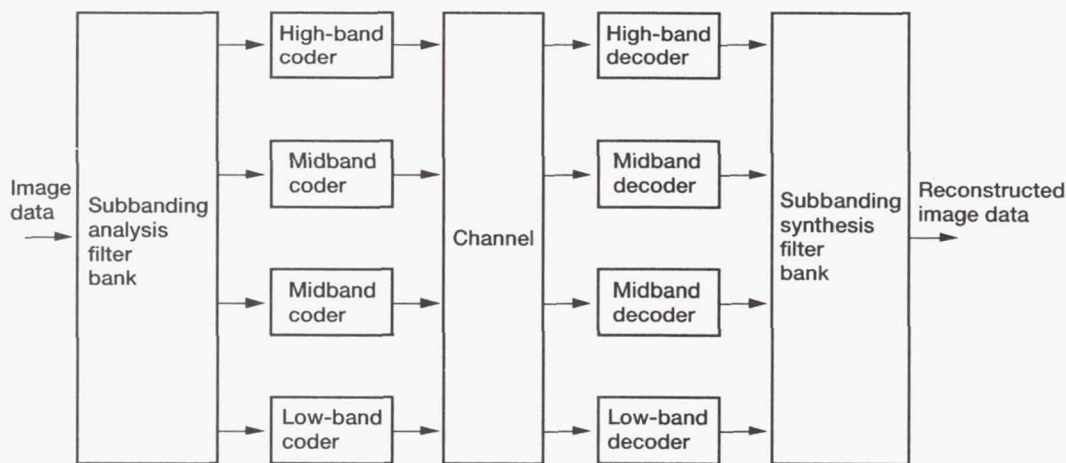
The digital HDTV codec will operate at data rates between 27 and 55 Mbps. The quality of the HDTV signal thus coded will be sufficient for distribution between studio and terrestrial broadcasting stations. Results obtained during the study phase indicate that the bit rate can be lowered to less than 20 Mbps at somewhat reduced quality. Because of its variable bit rate the digital HDTV signal may be transmitted in a wide range of satellite channels, including those for the Advanced Communications Technology Satellite and the Intelsat system. A substantial effort was made during the study phase to minimize the complexity of the digital HDTV coding algorithm so that the codec could be implemented cost effectively. As much scanning-raster flexibility as possible will be incorporated into the proto-

type hardware so that the developed technology can be adapted to the U.S. advanced television signal format, which is yet to be selected.

The next phase of the flexible-rate HDTV codec activity will focus on breadboard development of critical technology components. The subband codec and a simplified vector quantization (SVQ) codec will be implemented and integrated with motion estimation circuits.

**Lewis contact:** Wayne A. Whyte, (216) 433-3482  
**Headquarters program office:** OSSA





*Simplified block diagram of subband codec.*

### Subband Coding Improved

NASA Lewis has an ongoing research activity that is focused on developing video data compression technology for transmitting image data over space communications links in a bandwidth-efficient manner. These developments should result in greater orbit and spectrum capacity and lower space segment costs. To this end, subband coding is being investigated as a strategy for performing compression to reduce the transmitted data rate. Subband coding can be used to implement a lossless or lossy compression system.

A subbanding analysis filter bank takes a data signal and splits it into two or more subbands. These subbands can then be coded separately. A subbanding synthesis filter bank, designed in concert with the analysis bank, reconstructs the signal from the subbands in such a way that the filtering process does not distort the signal.

Subband coding is being used in a flexible-rate high-definition television coder-decoder (codec) that is currently being designed by Comsat Laboratories under contract with NASA Lewis. Compression is achieved by coarsely quantizing the high bands and by applying a simplified vector quantization code. Prof. S.C. Kwatra of the University of Toledo provides subband coding expertise as a subcontractor to Comsat. Doctoral research by University of Toledo students in subband coding is also being directly supported by NASA Lewis.

A novel hardware implementation for subbanding at video rates with simple filters is being developed in house by using computer simulation for initial investigation and refinement. A very-large-scale-integration implementation of the key parts of the system is planned. The hardware performs only subbanding and reconstruction; designers insert their own coding schemes. If no compression or lossless compression is performed, the signal can be reconstructed perfectly.

Subband coding is very promising as a data archiving tool. Because the low-frequency band is a low-resolution version of the original signal, it provides a smaller research data set for browsing. Subbanding in a tree structure (cascading stages) can also provide progressive-resolution transmission. This makes subbanding attractive for data storage and retrieval for programs such as the Earth Observing System (EOS).

**Lewis contact:** Daniel R. Glover, (216) 433-2847  
**Headquarters program office:** OAST

# Space Flight Systems

## Cryogenic Fluids Technology

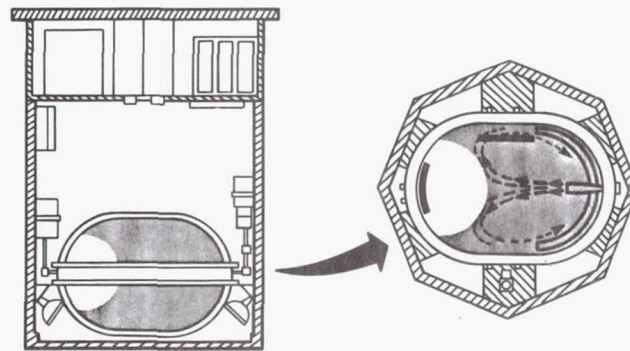
### Tank Pressure Control Experiment Flies on Shuttle

The Tank Pressure Control Experiment (TPCE), which flew aboard the Space Shuttle *Atlantis* in August 1991, was designed to provide data on the fluid dynamics and thermodynamics of jet-induced fluid mixing for controlling tank pressure in low gravity. Initial review of the results indicates that all objectives were met. It also appears that a substantial amount of data was acquired that may provide an early insight into pool-boiling mechanisms during extended low-gravity conditions.

The experiment simulated the behavior of cryogenics in a low-gravity environment by using Freon 113 at saturated conditions. Using Freon as the test fluid and fabricating the test tank out of Plexiglas allowed the low-gravity fluid dynamics of the mixing to be video taped; a dye was added to enhance the optical characteristics of the Freon.

The experiment was mounted in a Get Away Special (GAS) canister and ran for 26 hr. Prior to the first astronaut sleep period, in which disturbances would be minimized, the Shuttle *Atlantis* was maneuvered into a tail-to-wind orientation for 11 hr. The TPCE was designed so that this orientation would provide just enough acceleration to position the liquid over the mixer outlet and center the vapor at the opposite end. This fluid positioning simplified the comparisons of the flight results with analytical models.

The experiment consisted of a 0.5-ft<sup>3</sup> Plexiglas tank filled to 85 percent with Freon 113. Two separate heaters were activated alternately for specified times to create thermal gradients in the liquid and a subsequent tank pressure rise prior to mixing. Once the specified conditions had been achieved, the liquid was drawn out through a liquid acquisition device and fed to one or two pumps prior to exiting through the nozzle that



Tank Pressure Control Experiment mounted in a GAS can.

created the mixing jet. The pumps provided a range of flow rates to cover the pertinent low-gravity fluid mixing regimes established by drop-tower testing at Lewis in the 1970's. The liquid jet eliminated the thermal gradient and reduced the tank pressure.

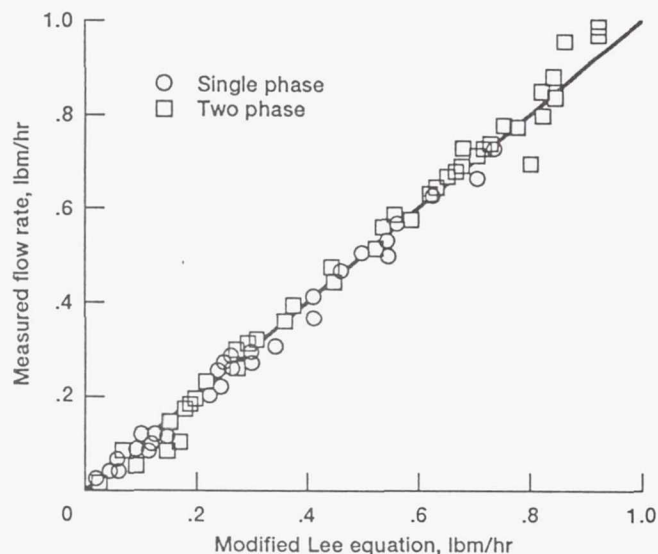
Pressure, temperature, and flow data were collected throughout the tests along with 4 hr of high-quality video data. Initial review of the video indicates that the fluid mixing patterns were similar to those predicted with developmental versions of the ECLIPSE computer code. The next step will be to compare fluid mixing times (for pressure equilibration) with those predicted from existing semiempirical correlations and then make the necessary improvements to these correlations.

**Lewis contact:** Richard H. Knoll, (216) 433-2419  
**Headquarters program office:** OAST

### Cryogenic Component Characterized With Liquid Hydrogen

Designers of space systems work to increase system reliability by minimizing the number of moving parts in system components. Program cost and risk can also be decreased by reducing component development. This second objective often can be met for cryogenic fluid systems by using components developed for noncryogenic applications and characterizing their performance with cryogenic fluids. An effort that combines both objectives was completed in a NASA Lewis facility in 1991.





Results from Visco-Jet tests with liquid hydrogen.

In the Cryogenic Components Laboratory, cell 4, a simple yet versatile rig has been developed to test components with liquid hydrogen or liquid nitrogen. The first component tested was a multiple-orifice Joule-Thomson device called a Visco-Jet. It was developed by The Lee Company for use as a hydraulic flow control component. Multiple orifices increase the minimum diameter required to achieve the desired pressure drop for flow control, reducing the risk of clogging. If the devices are found to be suitable for cryogenic applications, they would eliminate the need for low-reliability components such as needle valves and pressure regulators.

The primary objective of the test program was to characterize the mass flow rate for subcooled liquid hydrogen inlet conditions with either liquid or two-phase flow at the outlet. Inlet and outlet temperatures were varied over a range of typical operating conditions. The data were first compared with the manufacturers equation developed for hydraulic fluid flow. As anticipated, this equation was found to overpredict the flow rate for a given pressure drop across the devices: Lewis-developed modifications to the equation resulted in a data correlation that predicts single- and two-phase flow across the Visco-Jets. The first modification was a theoretical reduction of flow rate by the factor  $1-X$ , where  $X$  is the flow quality of the two-phase fluid at the outlet based on an isenthalpic expansion across the device. Next, an empirical modification was made with a 10-percent correction term. The two modifications resulted in the correlation of 90 percent of

all data points to within a  $\pm 10$ -percent scatter band.

Results indicate that Visco-Jets will be suitable for cryogenic applications. The new correlation can now be used to select the appropriate size for specific applications.

**Lewis contact:** Joseph D. Gaby, (216) 433-3852  
**Headquarters program office:** OAST

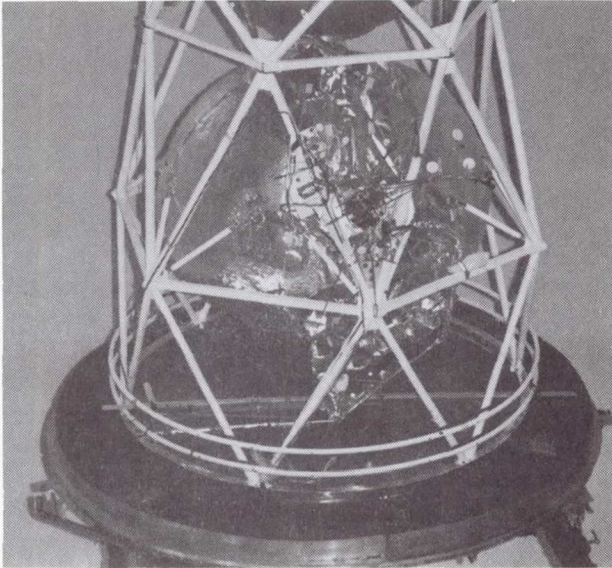
### Lunar Thermal Environment Simulated for Cryogenic Storage Tests

The ability to store cryogenic fluids for long periods of time is a major requirement for future space exploration missions. Recent mission analyses indicate that storage durations will range from 135 to 168 days for a lunar mission to more than 2 years for a Martian mission. The liquid loss due to boiloff must be limited to between 5 and 10 percent of the total propellant loading, at a rate as low as 0.03 percent per day, to ensure a vehicle's return to Earth. Higher boiloff rates will result in severe cost penalties and may preclude manned missions to Mars.

This storage capability requires a lightweight, high-performance thermal protection system. Specific designs will be mission dependent, but most vehicles will require some type of multilayer insulation (MLI) system containing between 50 and 200 layers of radiation shields with low-conducting spacers. The insulation systems for lunar or Martian missions will be subjected to warm-side boundary temperatures between 200 and 650 °R.

NASA Lewis is implementing a ground-based test program to completely characterize the performance of thick MLI systems (up to 200 layers) over warm-side boundary temperatures from 140 to 650 °R. In 1991, tests were conducted on a 34-layer MLI system applied to a 175-ft<sup>3</sup> tank in the K-Site thermal vacuum chamber at Plum Brook Station.

Steady-state thermal performance data were obtained at warm-side boundary temperatures of 150, 530, and 630 °R. The steady-state heat input results for the three boundary temperatures translate to liquid hydrogen losses of 0.2,



175-ft<sup>3</sup> tank with 34-layer MLI blanket.

1.3, and 2.3 percent per day, respectively. This same tank and insulation system was previously tested in the mid-1970's at a 530 °R warm-side boundary temperature. When the K-Site facility was deactivated after the test, the insulated tank remained within the vacuum chamber for 17 years until the facility reactivation in 1989. The present test showed only a 13-percent performance degradation of the insulation during that 17-year period. This demonstrates the durability of MLI systems under extended space vacuum conditions.

Another test was performed to characterize the insulation system as it was subjected to a warm-side temperature profile that simulated a partial lunar day from sunrise until noon, the equivalent of seven Earth days. The test used data gathered by the Surveyor mission and demonstrates K-Site's capability for conducting transient thermal control testing.

Future technology tests will characterize the effects of seams and penetrations for thick MLI systems over the required temperature range. Tests will also be performed on subscale, tank-applied MLI systems designed to meet lunar and Martian storage requirements.

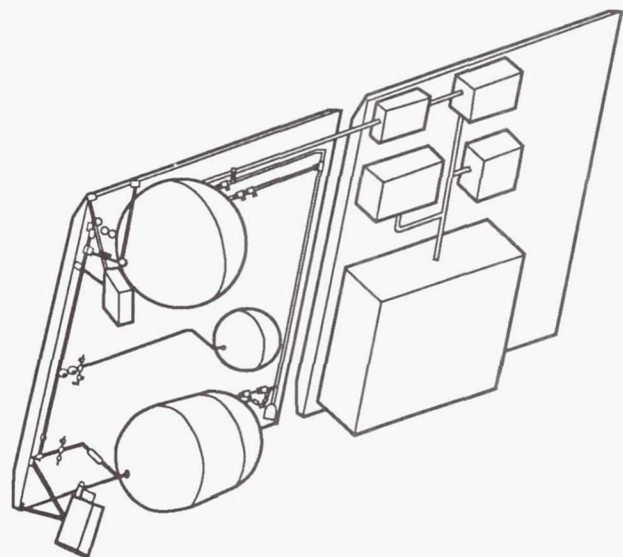
**Lewis contact:** Robert J. Stochl, (216) 433-5403  
**Headquarters program office:** OAST

## Vented-Tank Resupply Experiment Being Designed

Future space missions will require new technologies for managing fluids in the absence of gravity. Two critical operations are tank venting to reduce pressure and resupplying fluids consumed during mission operations. The state of the art for tank venting requires the operationally complex and costly procedure of propulsive settling to position the liquid away from the vent. The resupply of cryogenic fluids has never been demonstrated in space. The Vented-Tank Resupply Experiment (VTRE) currently is being designed as a Space Shuttle experiment that will provide low-gravity data critical to the development of these technologies.

The VTRE will investigate how well special devices that are designed to exploit the dominance of capillary forces in space prevent liquid loss during direct venting and vented resupply operations. It is being funded under the In-Space Technology Experiments Program (IN-STEP).

The VTRE will use Freon as the test fluid to simulate the behavior of a liquid propellant and to allow the use of transparent tanks for the collection of visual data by video cameras. Two tanks will be configured with capillary devices so that the Freon can be transferred between them in either direction. The devices will be evaluated on their ability to position the liquid in the absence



Vented-Tank Resupply Experiment mounted on a Hitchhiker-G.



of gravity, after an acceleration-induced upset, during bulk boiling, and during pressurant evolution, as well as during inflow and outflow. Key performance criteria are the conditions of acceleration, inflow and outflow rates, and vent rates at which liquid-free venting can be ensured; achievable receiver-tank liquid fill level; and fluid repositioning times.

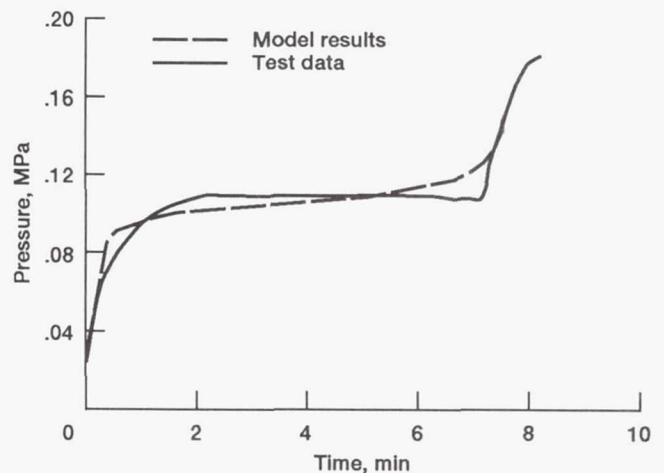
The experiment is being designed for manifesting as part of the NASA Hitchhiker Program, so that standard Shuttle services and interfaces will be provided. The use of tanks approximately 1 ft in diameter and the extended low-gravity test times will significantly add to the knowledge previously gained through low-gravity testing in drop towers and on a KC-135. The data obtained will be used to validate capillary device design criteria and low-gravity fluid dynamic correlations. This knowledge could then be used on a larger-scale, in-space experiment for designing future space systems.

**Lewis contact:** Donald L. Bresnahan, (216) 433-2844  
**Headquarters program office:** OAST

### No-Vent Fill Method Modeled for Orbital Propellant Transfer

Many future space missions call for the transfer of cryogenic propellants between tankage systems while on orbit. In the absence of gravity, venting during tank filling is likely to result in large liquid losses. Therefore, NASA Lewis is developing no-vent fill technology. The ability to model this process is critical for the design of future spacecraft because the inability to sufficiently fill a liquid propellant tank could jeopardize future missions.

We have developed and implemented an analytical model of the no-vent fill process in the NVFILL computer program. The no-vent fill process relies on condensing the vapor generated in a tank being filled rather than venting the vapor continuously as is commonly done on the ground. A simple thermodynamic model of the process based on the principles of conservation of mass and energy has been developed. The NVFILL program implements this model for a spray configuration that injects liquid droplets through the



Comparison of analytical model results and test data for 1.2-ft<sup>3</sup> tank.

vapor region to promote condensation before the droplets impinge on the walls. The program's primary outputs are the fill level of the tank, the liquid temperature, and the tank pressure.

The no-vent fill process is being investigated as part of an extensive ground test program at NASA Lewis. Tests have been performed with liquid hydrogen in receiver tanks having volumes of 1.2, 5.0, and 175 ft<sup>3</sup>. The NVFILL program has been used to model the tests conducted with the two smaller tanks at cell 7 of the Cryogenic Components Laboratory. For example, the 1.2-ft<sup>3</sup> tank, initially at 53.6 K, was filled to 98 percent (by volume) with liquid hydrogen subcooled to 19.7 K at a rate of 0.32 kg/min. The model was found to provide a good representation of the test data until the spray system became submerged in the rising liquid; this is a known limitation of the code.

Efforts to validate the model will continue when the model results are compared with test data from the 175-ft<sup>3</sup> tank at Plum Brook's K-Site facility. The model also will be revised to accommodate alternative liquid injection configurations and low-gravity effects on the liquid-to-vapor heat and mass transfer. Additional ground testing will include larger-scale tank-to-tank liquid transfer with greater control of fluid conditions and higher transfer rates.

**Lewis contact:** William J. Taylor, (216) 433-6568  
**Headquarters program office:** OAST

### Tank Chillover Demonstrated at K-Site Facility

Space-based cryogenic fluid systems will play a critical role in future NASA missions for space propulsion and life support systems. The necessary technologies to support these missions are under development at NASA Lewis. Tank chillover will be required for many applications in which a warm cryogenic tank is to be filled when venting is neither possible nor desired. The combination of tank chillover and nonvented fill minimizes the risk of liquid loss during venting operations in a low-gravity environment when the fluid position is not controlled.

The charge-hold-vent (CHV) tank chillover technique has been proposed because of its synergistic use of tank filling components and its efficient use of cryogenics. A large-scale, normal-gravity test of this technique was conducted at Plum Brook's K-Site facility in February 1991. A lightweight, 175-ft<sup>3</sup> tank was used in the large vacuum chamber, which simulates a near-Earth space environment.

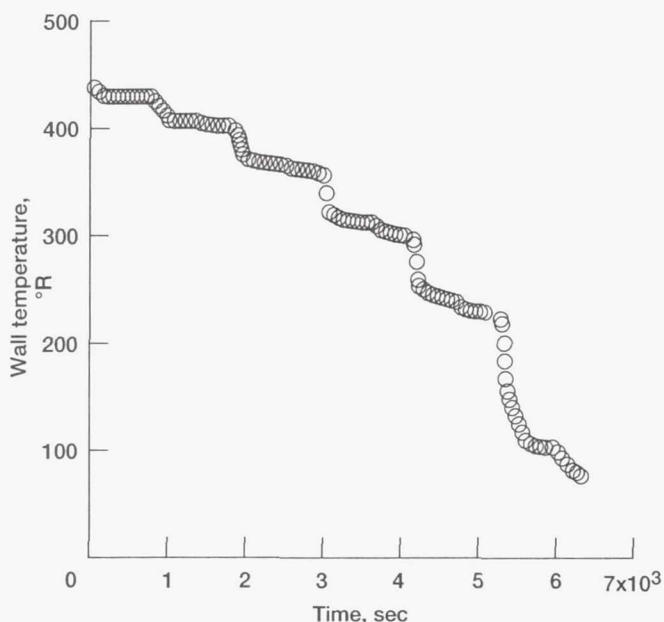
An unmetered "charge" of liquid hydrogen was injected into a warm (440 °R) tank through top and bottom sprays with all vents closed. During this phase the liquid hydrogen impinged on the tank wall and evaporated, causing partial tank wall cooling. In the hold phase the resulting vapor continued to provide cooling by natural

convection. When the vapor warmed and approached thermal equilibrium with the tank wall, the vents were opened to remove the warm vapor and allow for the next liquid charge. During venting, additional cooling was realized as the remaining vapor expanded and cooled. Six CHV cycles were run in succession until the tank was chilled to 60 °R.

The results of this test are being compared with portions of the analysis done for the CRYOCHIL computer model developed at Lewis in the late 1980's. The model predicts the transient profiles for tank pressure, tank wall temperatures, and vapor temperatures.

Further testing will be required before the model can be fully validated for normal-gravity cases. Because there will be little or no free convection in space, new ground tests will be required in which the liquid injection method creates a forced-convection field that dominates the natural convection. Ultimately, in-space experimentation with a cryogenic fluid will be required.

**Lewis contact:** Naseem H. Saiyed, (216) 433-8350  
**Headquarters program office:** OAST

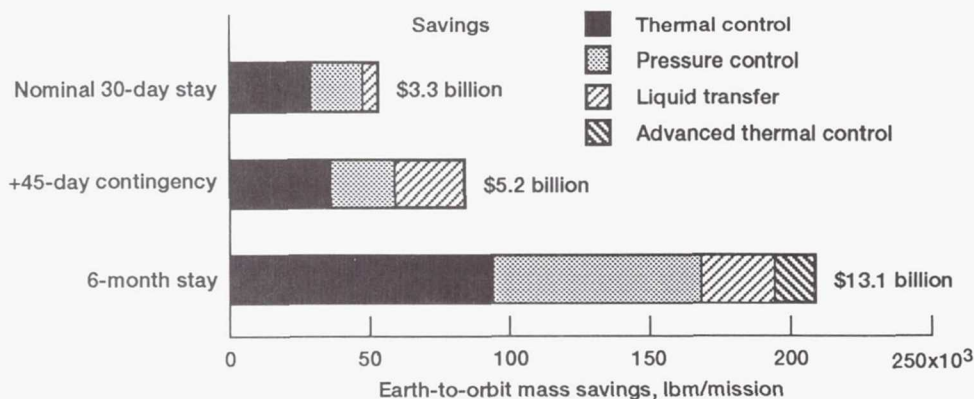


Tank wall temperature data (mass averaged).

### Cryogenic Fluid Management Technology Benefits Quantified for Lunar Transfer Vehicles

The performance and cost advantages of hydrogen/oxygen chemical propulsion and hydrogen-propelled nuclear thermal rockets dictate their use for most future space missions including the proposed Space Exploration Initiative (SEI). Therefore, an aggressive program for developing cryogenic fluid management (CFM) technologies has been established as a priority for NASA. CFM technology is enhancing or enabling to all known, viable transportation scenarios for the SEI. Cryogenics also will play critical roles for life support and as reactants and coolants.





Results of cryogenic fluid management technology benefits assessment.

The current state of the art for CFM technology is based on Centaur and Saturn upper-stage technology, which is already 15 to 20 years old. Continued use of existing state-of-the-art technology imposes prohibitive cost and performance penalties on future missions. In 1991, the magnitude of these penalties was assessed for a typical lunar transfer vehicle (LTV) concept.

A typical LTV concept, developed by Martin Marietta, was selected to demonstrate the benefits of advanced CFM technology. Baseline system characteristics and operations were compared with technology advancements in the areas of thermal control, pressure control, and liquid transfer (tank toff and complete tank fueling). Mass savings were then calculated by using Earth-to-orbit mass multipliers to account for net changes in total propellant and tankage mass. Cost savings were calculated by assuming a \$2500 per pound Earth-to-orbit launch cost and were then projected over 25 missions.

The analysis included a nominal 30-day stay on the lunar surface, an additional 45-day hold contingency prior to departure from low Earth orbit, and an extended 6-month lunar stay. The results of this analysis indicate that the development of advanced thermal control technology is required for current LTV concepts and operating scenarios. Similar results were found for advanced pressure control technology, both providing significant reduction in Earth-to-orbit mass transportation requirements. When liquid transfer technology was included to enable space basing of LTV's, the total estimated cost benefits were \$13.1 billion plus \$10 billion for reusability.

This represents approximately 25 percent of projected LTV life-cycle costs.

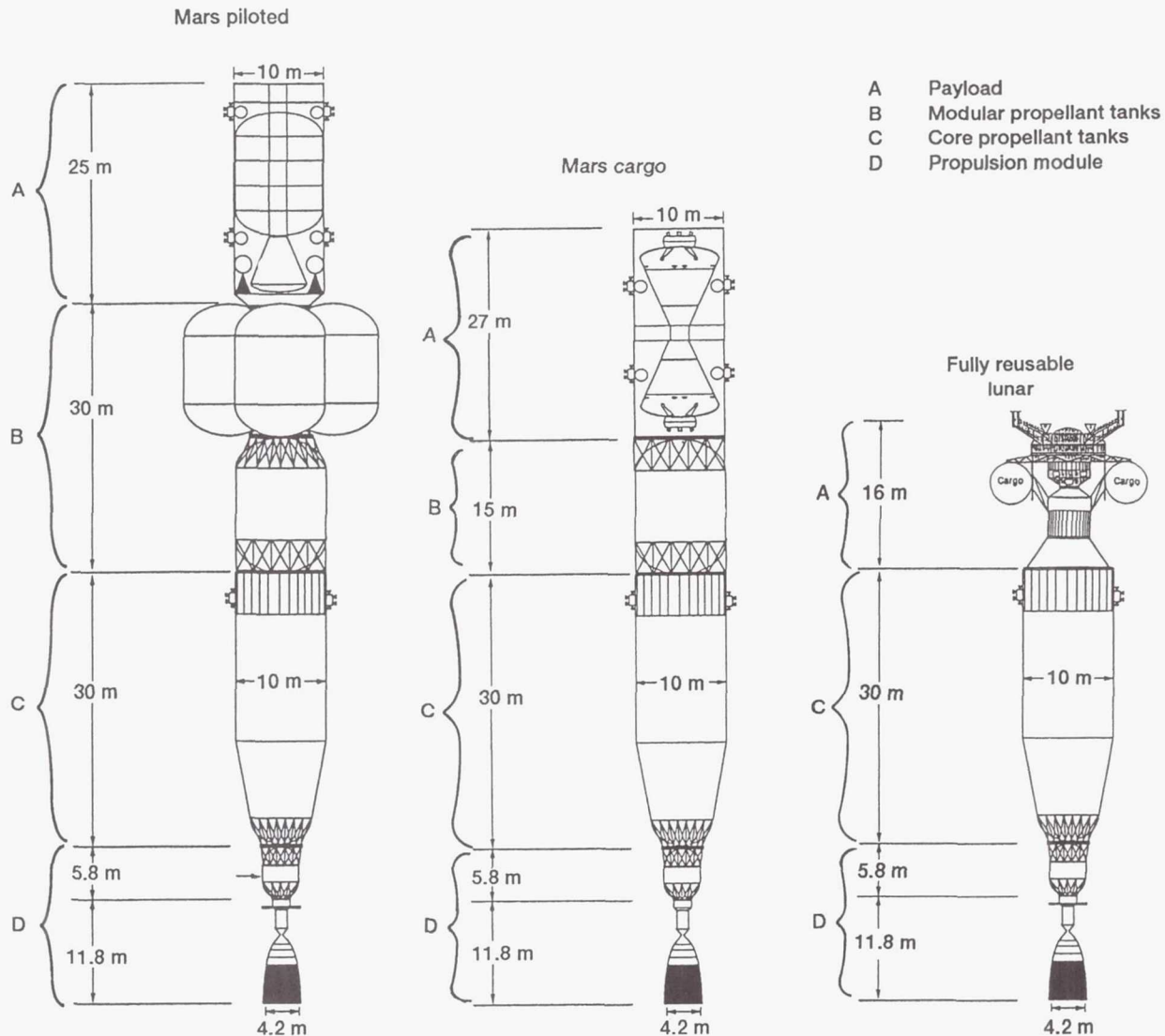
**Lewis contact:** Rafael Sanabria, (216) 433-2332  
**Headquarters program office:** OAST

## Nuclear Propulsion

### Common Lunar/Mars Space Transportation System Is Based on Nuclear Thermal Rocket Technology

The Stafford Report has identified the nuclear thermal rocket (NTR) as a key technology for implementing the Space Exploration Initiative. Thrust, power, and hydrogen exhaust temperature levels required for piloted missions to Mars were successfully demonstrated in the Rover/NERVA (Nuclear Engine for Rocket Vehicle Application) programs of the 1960's and 1970's. Integrated system and mission studies are being performed to better characterize engine and stage design features for lunar and Mars NTR-powered vehicles and to help focus technology development efforts.

Performance projections have been made for current NERVA-derived reactor systems utilizing higher temperature uranium carbide (UC)-zirconium carbide (ZrC)-graphite composite and UC-ZrC pure carbide fuel forms and state-of-the-art nozzle and turbopump technologies. The projections indicate substantial improvements in



Relative size of various NTR lunar/Mars vehicles: 75,000-lbf NERVA-derivative engines; composite fuel; 925-sec specific impulse.

both specific impulse and engine thrust-to-weight ratio over the 1972 NERVA reference design engine. In addition to NERVA-type systems a variety of other solid-core NTR concepts are also being studied. Examples include a uranium oxide ( $\text{UO}_2$ )-tungsten-fueled cermet reactor configuration with tungsten-rhenium fuel cladding and a particle-bed reactor (PBR) system. The PBR concept would directly flow hydrogen propellant over small (500- to 700- $\mu\text{m}$  diameter), coated fuel microspheres in an effort to improve heat transfer characteristics and to reduce engine mass. Modeling efforts are also under way in house and in cooperation with other NASA centers and Department of Energy national laboratories in the areas of nozzle and turbopump

performance, thermal hydraulic analysis, and reactor core neutronics.

With its potential for high specific impulse (~825 to 1000 sec) and high engine thrust-to-weight ratio (~4 to 20), the NTR can provide the basis for an efficient space transportation system capable of supporting both piloted and cargo lunar and Mars missions. For lunar missions the use of NTR technology enables a fully reusable, aerobraked chemical system having comparable outbound and return payloads. The lunar NTR stage consists of a propulsion module and a core propellant tank having liquid hydrogen propellant capacities of 3.9 and 127.5 tons, respectively. An aluminum-lithium alloy is used for tank



CHARACTERISTICS OF 75,000-lbf NERVA-TYPE ENGINE

Parameter	1972 NERVA engine <sup>a</sup>	State-of-the-art NERVA derivatives <sup>a</sup>				
		Graphite		Expander		
Engine flow cycle	Hot bleed/expander					
Fuel form						
Chamber temperature, K	2350-2500	2500	2350-2500	2700	2700	3100
Chamber pressure, psia	450	500	1000	500	1000	1000
Nozzle expansion ratio	100:1	200:1	500:1	200:1	500:1	500:1
Specific impulse, sec	825-850/ 845-870	875	850-885	915	925	1020
Engine weight, kg	11,250	7721	8000	8483	8816	9313
Engine thrust-to-weight ratio	3.0	4.4	4.3	4.0	3.9	3.7

<sup>a</sup>Engine weights contain dual turbopump capability for redundancy.

construction and a thermal protection system combining foam multilayer insulation with a vapor-cooled shield is used to minimize boiloff. By developing an additional modular propellant tank (having a liquid hydrogen capacity of ~70 tons), a variety of single and multiengine lunar and Mars vehicles can be configured. The Mars vehicles shown assume a split/sprint mission mode with separate piloted and cargo vehicles delivering the crews and Mars landing vehicles, respectively.

A common lunar/Mars space transportation system is expected to have a number of mission benefits. These include enhanced mission flexibility and safety, reduced development and procurement costs through standardization, simplification of design and in-space assembly, and a shortened development schedule.

**Lewis contact: Dr. Stanley K. Borowski, (216) 433-7091**  
**Headquarters program office: OAST**

### Nuclear Electric Propulsion Vehicle Studied for Piloted Mars Mission

An integrated system and mission study of a nuclear electric-propelled vehicle for a Mars piloted application has been performed. The study shows that critical figures of merit such as trip time and initial mass in low Earth orbit can be minimized with nuclear electric propulsion by leveraging existing space nuclear reactor and thruster technology programs.

Safety and cost considerations for a piloted Mars mission place requirements on transit time to and from Mars, as well as on the amount of initial mass that would need to be launched into low

Earth orbit at the beginning of a mission. Two-way transit times on the order of 400 days are desirable, with an initial mass in low Earth orbit of 500 metric tons or less.

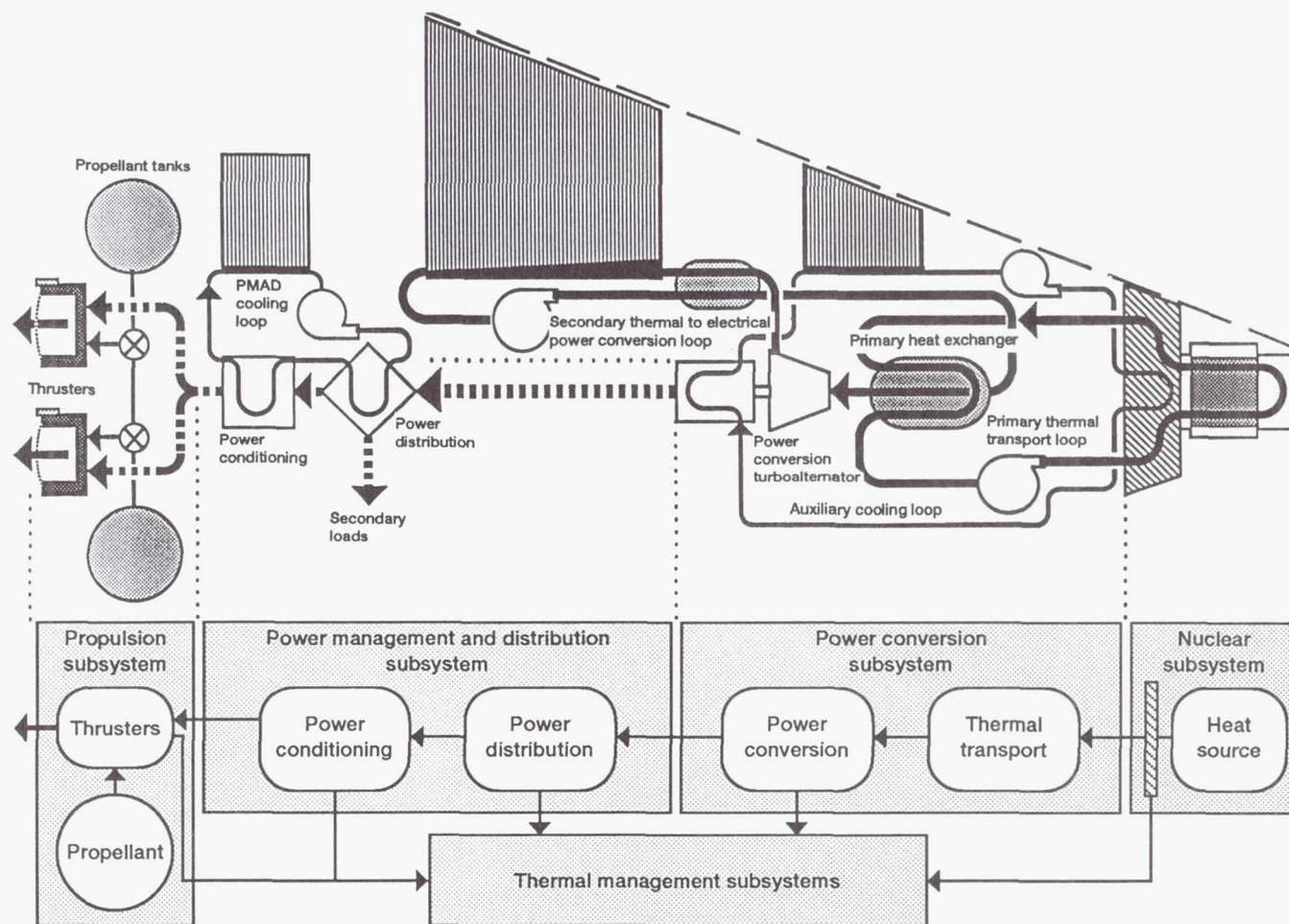
A nuclear electric propulsion system has been proposed that uses an SP-100 derivative reactor, potassium-Rankine power conversion, carbon-carbon heat pipe radiators, high-temperature-compatible power management and distribution, and ion electric thrusters. The reactor and the power conversion system produce 10 MWe of power to drive argon ion thrusters having 5000-sec specific impulse at an efficiency of 70 percent. A system mass breakdown (in kilograms) is as follows:

Reactors . . . . .	7,000
Shield . . . . .	12,200
Power conversion . . . . .	19,100
Radiators . . . . .	8,320
Power conditioning and distribution . . . .	20,000
Ion propulsion . . . . .	6,000
Total . . . . .	72,000

The resultant power/propulsion specific mass of 7.3 kg/kWe enables a safe piloted journey to and from Mars with a total transit time of 382 days and an initial mass in low Earth orbit of 360 metric tons, including a chemically propelled "crew taxi" for rapid transfer through Earth's radiation belts. A cargo mission is assumed to deliver a Mars ascent/descent vehicle prior to crew departures from Earth.

This study has the following implications for the development of nuclear electric propulsion technology:

No new space reactor program would need to be started, as the applicable nuclear fuel and reactor systems technologies have been or are



Schematic of nuclear electric propulsion system for piloted missions.

being developed under the existing SP-100 program.

- A new development program in potassium-Rankine technology would have to return to where the United States left off in the 1960's.
- Semiconductor technology for high-temperature power management and distribution would need to be developed.
- Carbon-carbon (or equivalent lightweight) radiator technology would be required.
- Existing technology programs in ion electric thrusters would be augmented for high-power performance.

**Lewis contacts:** Jeffrey A. George, (216) 433-7108; Kurt J. Hack, (216) 433-7060; Michael P. Doherty, (216) 433-7092; Leonard A. Dudzinski, (216) 433-7107  
**Headquarters program office:** OAST

## Space Experiments

### GaAs Crystal Growth Experiment Flown on Shuttle

Gallium arsenide (GaAs) substrates and devices are considered a leading contender for a new generation of electronics technology offering greater speed and durability than existing silicon-based systems. High-quality GaAs crystals are difficult to produce and the commercial crystal growth of this material is of significant interest. The effect of gravity-induced, buoyancy-driven convection on the types and distribution of defects in GaAs is the focus of a study being conducted by GTE Laboratories, Inc., of Waltham, Massachusetts. The work is cost shared by GTE, the Air Force Materials Laboratory, and NASA. NASA Lewis manages the project, has implemented numerical modeling of the furnace and fluid flow, and will characterize selected samples from the study.



The study, as proposed by GTE (the principal investigator is Dr. Brian Ditchek), consists of a systematic investigation of how buoyancy-driven fluid flow affects GaAs crystal growth. It includes GaAs crystal growth in the microgravity environment of the Space Shuttle. The program also involves a comparative study of crystal growth under a variety of Earth-based conditions with variable orientation (to change the direction of the gravity vector) and applied magnetic field (to partially damp flow). Earth-based growth will be performed under stabilizing as well as destabilizing temperature gradients. The boules grown in space and on Earth will be fully characterized to correlate the degree of convection with the distribution of impurities. Both macro- and micro-segregation of dopant will be determined.

In June 1991 the experiment was flown on the Space Shuttle *Columbia* as part of STS-40. The experiment was a qualified success. The hardware, software, electronics, and control routines all performed as designed; however, there was insufficient power in the primary battery supply to get the second furnace to operating tempera-

ture. At year's end the shortfall in total energy was under investigation. The thermal environment of the battery pack on orbit was a few degrees colder than predicted, and it appears that the batteries exhibited significantly reduced output during warmup of the second experiment. The crystal grown in the first experiment appears to be one of the finest grown in the program. Detailed analysis of the crystal was in progress at year's end.

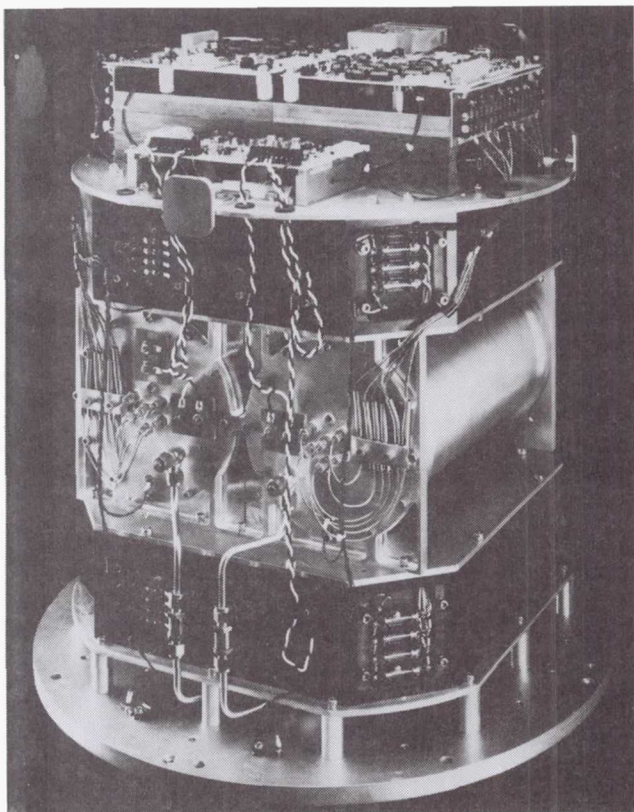
Conclusion of the ground-based science and consideration of a reflight of the payload are planned for 1992.

#### Bibliography

Bellows, A.; Matthiesen, D.; and Duchene, G.: Free Float Acceleration Measurements Aboard NASA's KC-135 Microgravity Aircraft. AIAA Paper 90-0742, Jan. 1990.

Matthiesen, D.; et al.: Interface Demarcation in GaAs Current Pulsing. AIAA Paper 90-0319, Jan. 1990.

**Lewis contact:** Richard W. Lauver, (216) 433-2860  
**Headquarters program office:** OSSA



*Self-contained dual furnace payload for GaAs Crystal Growth Experiment.*

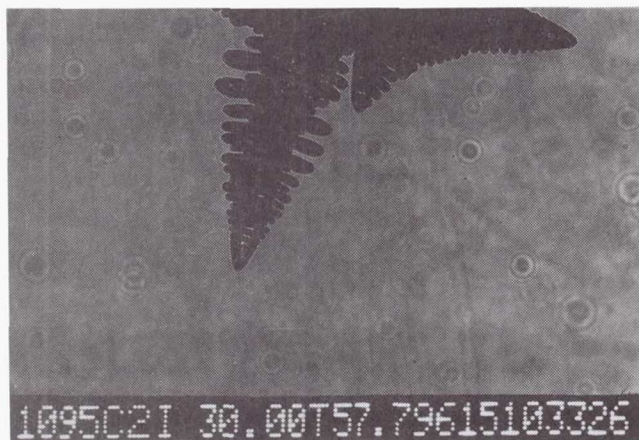
#### Apparatus Being Fabricated for Isothermal Dendritic Growth Experiment

The Isothermal Dendritic Growth Experiment (IDGE), to be conducted onboard the Space Shuttle beginning in 1993, will test fundamental theories that describe dendritic freezing of liquid metals on Earth. Rensselaer Polytechnic Institute scientists proposed the experiment to NASA. NASA Lewis then designed and is fabricating and testing the spaceflight apparatus.

The IDGE spaceflight apparatus will acquire data needed to correct current theories that predict metal dendrite growth kinetics during the freezing process. Experimentation on Earth has had limited success because gravity-driven convective effects cannot be separated from conductive and diffusive effects. Because steel, aluminum, and superalloys freeze dendritically, IDGE results should lead to improvement of their Earth-based production.

Three flights are planned for 1993 to 1997 on the NASA Marshall Space Flight Center-managed United States Microgravity Payload experiment





*Dendrite photographed in IDGE engineering unit during a mission simulation. (Scientifically relevant data are annotated on each photograph as it is taken with specially designed cameras.)*

carrier. Two will involve succinonitrile (a transparent material having a crystal structure similar to iron), and one will involve pivalic acid (a transparent material having a crystal structure similar to nickel).

The unique spaceflight apparatus will automatically carry out 25 dendritic growth experiments per flight. During each experiment it will maintain growth temperatures accurately to within 0.002 kelvin, automatically detect growing dendrites by analyzing slow-scan television images, and acquire 20 dendrite photographs. In addition, slow-scan television images of growing dendrites and over 100 other data items will be continuously communicated to Earth. Should a problem arise, the apparatus can be commanded from the payload operations control center on Earth.

Fabrication of the IDGE spaceflight apparatus began in 1990 and will be completed in 1992.

#### **Bibliography**

Glicksman, M. E., et al.: Isothermal Dendritic Growth—A Proposed Microgravity Experiment. *Metall. Trans. A*, vol. 19, no. 8, Aug. 1988, pp. 1945-1953.

Winsa, E. A., et al.: Flight Hardware and Tele-Operations Supporting the Isothermal Dendritic Growth Experiment Aboard the Space Shuttle. *AIAA Paper 89-0863*, Jan. 1989.

**Lewis contact:** Edward A. Winsa, (216) 433-2861  
**Headquarters program office:** OSSA

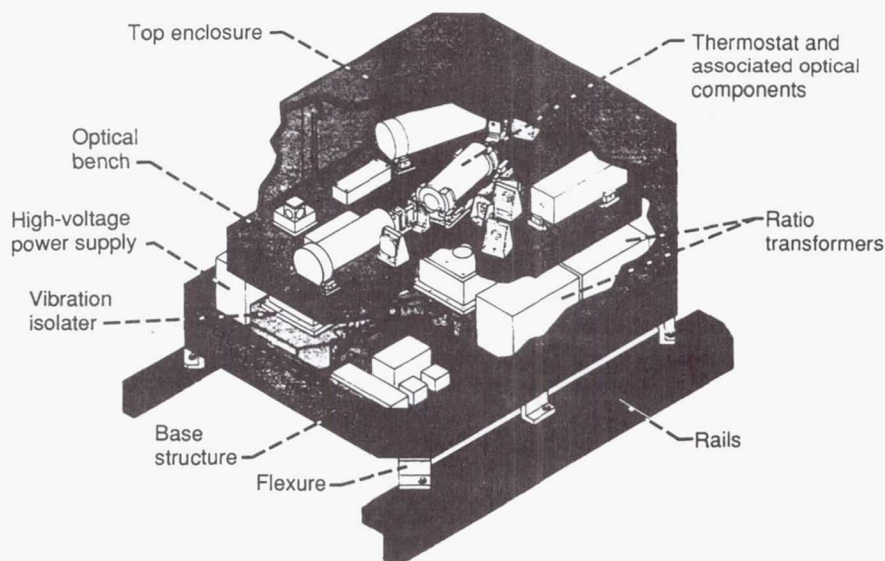
### **Design Completed for Critical Fluid Light-Scattering Experiment**

The Critical Fluid Light-Scattering Experiment (dubbed Zeno by the principal investigator in honor of the ancient Greek philosopher noted for descriptions of paradoxes of infinity) will use dynamic light-scattering spectroscopy and correlation analysis to study the density fluctuations of xenon at temperatures very near (within 100 microkelvin) the critical temperature for the vapor/liquid phase transition of this ideal fluid. These data will provide a test of theories describing such phase changes in realms that are theoretically interesting (very strong divergence of dynamic properties such as compressibility, thermal conductivity, heat capacity, and viscosity are predicted) but inadequately tested to date at the temperatures of most interest. Such measurements are severely limited on Earth owing to large density gradients created by normal gravity acting on the fluid as the compressibility of the sample increases (diverges) near the critical temperature. The ultimate effect of such theories will be far-reaching because the theories provide "universal" descriptions of many transitions, such as ferromagnetization, superconductivity, and binary fluid miscibility limits.

The principal investigator is Professor Robert W. Gammon of the Institute for Physical Science and Technology at the University of Maryland, College Park. Professor Gammon has assembled a team of 10 at the university including graduate research assistants, postdoctoral scientists, project engineers, and program/contract administrators. This team has responsibility, under NASA contract, both for defining the science requirements and developing the flight instrument. The flight hardware engineering, fabrication, integration, and testing is subcontracted to the Ball Aerospace Group of Boulder, Colorado. Although the implementation of the experiment is fully contracted, a significant team of NASA Lewis personnel support the effort in project management and scientific oversight, engineering oversight, product assurance support, and contract management and financial management.

During 1991 the detailed design was completed and the critical design review was held. The engineering model of the instrument was built and testing began; however, technical difficulties slowed progress and the test program was not





*Zeno optics module showing optics bench and selected support systems.*

completed as scheduled. Flight hardware fabrication was in progress at year's end, and integration and testing of the flight instrument is scheduled for early 1992. Flight acceptance testing should be complete by mid-1992.

The flight instrument is currently identified on the manifest for STS-67 in August 1993 as part of the second United States Microgravity Payload mission.

#### **Bibliography**

Boukari, H., et al.: Critical Speeding Up in Pure Fluids. *Phys. Rev. A*, vol. 41, no. 4, 1990, pp. 2260-2263.

Boukari, H., et al.: Critical Speeding Up Observed. *Phys. Rev. Lett.*, vol. 65, no. 21, 1990, pp. 2654-2657.

Law, B.M.; Gammon, R.W.; and Sengers, J.V.: Dynamic Light Scattering From Long-Range Density Correlations in a Nonequilibrium Liquid. *Photon Correlations Techniques and Applications*, J.B. Abbiss and A.E. Smart, eds. Optical Society of America, 1989, pp. 147-152.

Law, B.M., et al.: Light-Scattering Measurements of Entropy and Viscous Fluctuations in a Liquid Far From Thermal Equilibrium. *Phys. Rev. A*, vol. 41, no. 2, 1990, pp. 816-824.

Shaumeyer, J.N.; and Gammon, R.W.: Optimizing Fitting Statistics in Photon Correlation Spectroscopy, *Photon Correlations Techniques and Applications*, J.B. Abbiss and A.E. Smart, eds., Optical Society of America, 1989, pp. 14-17.

Shaumeyer, J.N.; Gammon, R.W.; and Sengers, J.V.: Measurement of Diffusivities With Photon Correlation Spectroscopy, *IUPAC Volume on Measurement of Transport Properties*, in press.

**Lewis contact: Richard W. Lauver, (216) 433-2860**  
**Headquarters program office: OSSA**

#### **Surface-Tension-Driven Convection Experiment Nears Flight-Readiness**

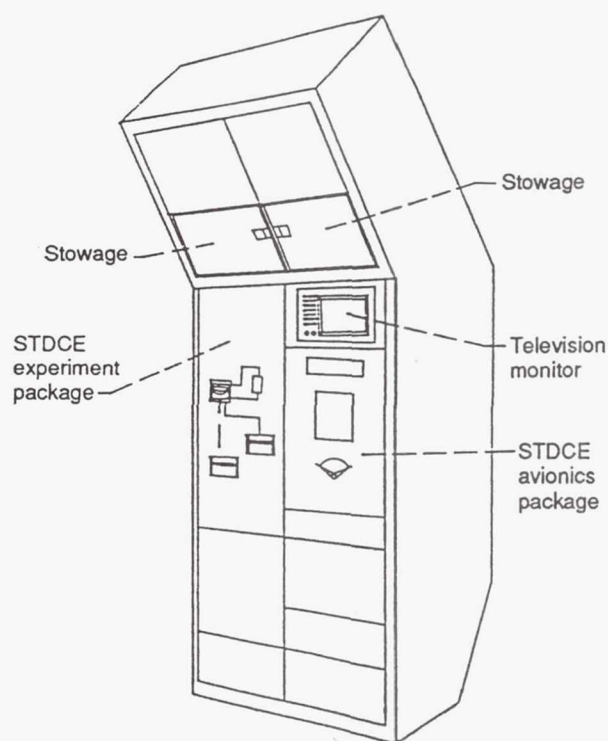
Materials processing that involves solidification and crystal growth is generally expected to be dramatically improved in the microgravity environment of space because natural convection and buoyancy effects are eliminated. However, convection currents due to surface tension forces are still present. These thermocapillary flows result from the fluid motions generated by the surface-tractive force that is caused by surface tension variations due to the temperature gradient along the free surface.

Changes in the nature and extent of these thermocapillary flows can cause deleterious fluid oscillations. Numerical modeling is not adequate to predict the parameters for which these

oscillations occur because of the complex three-way interaction between the imposed thermal signature, the surface flow, and the surface deformation. In order to complete an understanding of the physical process and develop an accurate numerical model, experimental data must be obtained in an extended low-gravity environment. Therefore, the Surface-Tension-Driven Convection Experiment (STDCE) was proposed for the Space Shuttle.

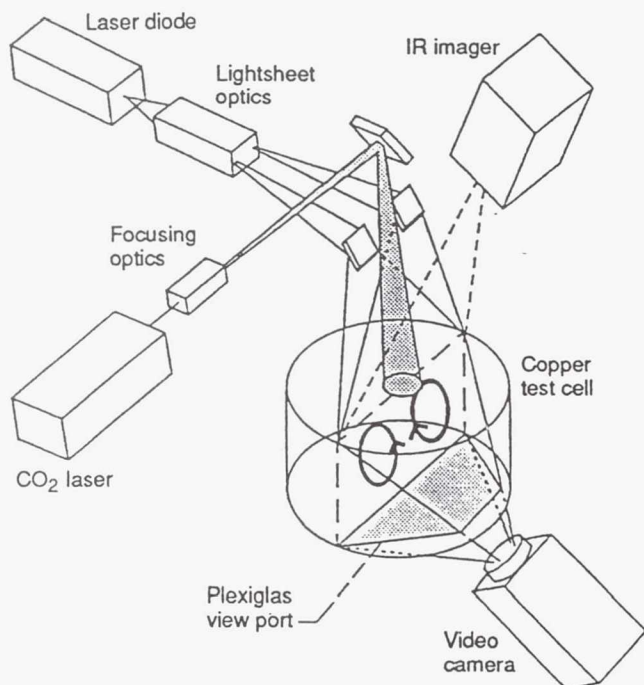
The STDCE consists of a copper test cell, 4 in. in diameter by 2 in. deep, filled on orbit with silicone oil to provide both a flat and a curved free surface that can be centrally heated either externally by a carbon dioxide laser or internally. The cross section is illuminated by a 1-mm-thick sheet of light, which scatters from small aluminum oxide particles mixed into the oil, allowing observation of the axisymmetric flow velocities.

The design and development of the STDCE for the United States Microgravity Laboratory (USML-1) mission in June 1992 was an in-house project at NASA Lewis. Major components were developed under contract: an infrared thermal imager for mapping the surface temperature gradients, a carbon dioxide laser for surface heating, and a laser diode system for illumination. These com-



STDCE experiment package in Spacelab rack.

ponents were integrated with the mechanical, optical, electrical, electronic, and structural systems that were designed, fabricated, and tested at NASA Lewis.



Optics module for STDCE.

Significant milestones were achieved during 1991. The STDCE team resolved many difficult problems during the final testing of the flight hardware. The flight hardware was shipped to NASA Kennedy Space Center in June 1991. Mechanical integration of the hardware into a double rack of the Spacelab module was completed in August 1991. In March 1991 the second crew training session was conducted at Lewis, and an engineering model of the STDCE was shipped to the Payload Crew Training Complex at NASA Marshall Space Flight Center. During August 1991 this engineering model was used for additional crew training proficiency and mission simulation. Training was also started for several STDCE team members at the Payload Operations Control Center at Marshall. During the USML-1 mission, which will be managed by Marshall, real-time data and videotapes will be obtained and analyzed to assist in determining results and in uplinking new experiment parameters for two additional test sequences.



## Bibliography

Kamotani, Y.; and Ostrach, S.: Design of a Thermocapillary Flow Experiment in Reduced Gravity. *J. Thermophys. Heat Trans.*, vol. 1, no. 1, Jan. 1987, pp. 83-89.

Ostrach, S.: Surface Tension Gradient Induced Flows at Reduced Gravity. NASA CR-159799, 1980.

Pline, A. D., et al.: Hardware Development for the Surface Tension Driven Convection Experiment. *J. Spacecraft Rockets*, vol. 27, no. 3, May-June 1989, pp. 312-317.

Pline, A. D.; and Butcher, R. L.: Spacelab Qualified Infrared Imager for Microgravity Science Applications. *Thermosense XII*, SPIE Proc. vol. 1313, S. A. Semanovich, ed., SPIE, 1990, pp. 250-258.

Wernet, M. P.; and Pline, A. D.: Particle Image Velocimetry for the Surface Tension Driven Convection Experiment Using a Particle Displacement Tracking Technique. *Proceedings of the Fourth International Conference on Laser Anemometry*, 1991, vol. I, pp. 315-326. (Also, NASA TM-104482.)

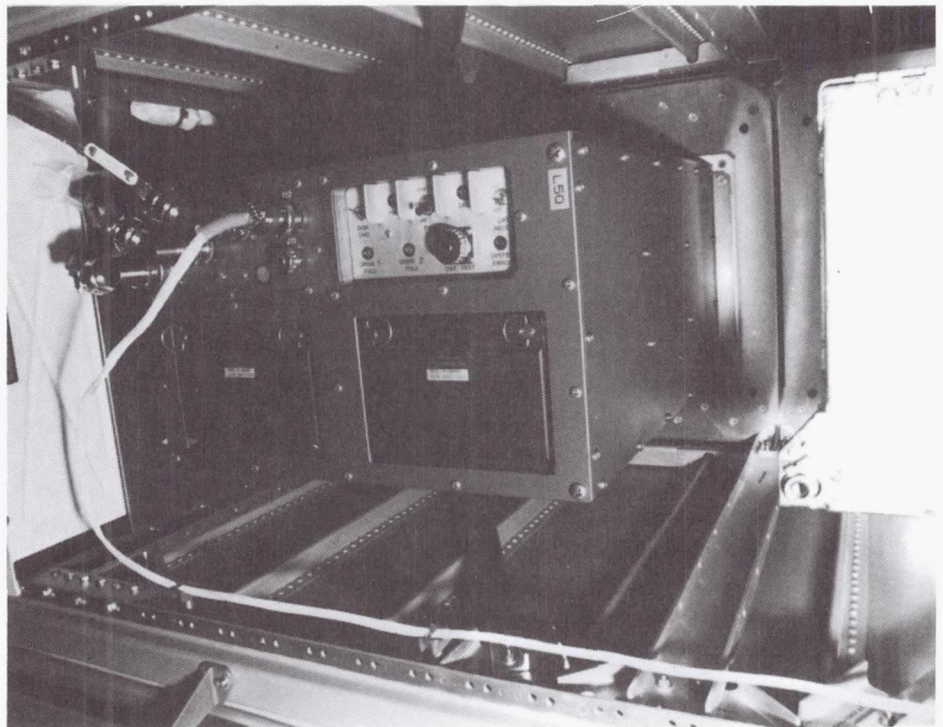
**Lewis contacts:** Thomas P. Jacobson, (216) 433-2872; Robert L. Thompson, (216) 433-3321; Alexander D. Pline, (216) 433-6614

**Headquarters program office:** OSSA

## Space Acceleration Measurement System Flown on Two Shuttle Missions

Many experiments are flown on the Space Shuttle to utilize the reduced levels of gravity during the orbital operations. The actual levels of acceleration and vibration experienced by the experiments quite often need to be measured to clarify the experimental results. The Space Acceleration Measurement System (SAMS) Project has designed and fabricated an instrument to measure acceleration at or near experiments on the Shuttle. The data are provided to the experimenter after the mission or, in some cases, in near-real time at a payload operation center. A data base of this acceleration environment will also be developed and maintained to facilitate future analyses and predictions of expected environments.

The SAMS project in 1991 delivered one flight unit to NASA Kennedy Space Center (KSC) for integration into a 1992 shuttle mission. The integration aspects of three other flight units delivered in 1990 were also worked with KSC in 1991. These efforts culminated in the first flight of a SAMS unit on STS-40 in June 1991 as part of the first Spacelab Life Sciences Mission. The second flight occurred in the middeck on STS-43



SAMS installed in SLS-1 module.

in August 1991. The engineering unit was completed in 1991 for a second configuration of SAMS units to be installed in the Shuttle cargo bay. Two additional flight units of this configuration were fabricated in 1991. These six flight units will be flown on numerous Shuttle missions in the coming years.

The SAMS project has developed a general-purpose instrument for measuring and recording the very low levels of acceleration (e.g., from gravity, vibrations, and thrusters) experienced onboard the Shuttle, both to document what the experiments experience and to help predict the expected acceleration environment prior to missions. The SAMS instrument is flexible in several ways to meet the needs of various types of experiments (e.g., fluid physics, crystal growth, and combustion) that will be located in the Shuttle middeck and cargo bay and the Spacelab module. Each SAMS main unit can have up to three remotely positioned three-axis sensor heads that are mounted in, on, or near the experiment apparatus and connected to the main unit by cables. Each of the three sensor heads may be independently set to one of six low-pass-filter frequencies depending on the requirements of the experiment. One style of main unit is configured for installation in the habitable areas of the Shuttle (the middeck and the Spacelab module). The other style of main unit is designed for installation in the Shuttle cargo bay.

Data are acquired and stored continuously during a typical mission of 7 to 13 days. Because gigabytes of data may be generated by a typical mission, a high-density storage medium is needed. The data recording is performed by optical disks that have a capacity of 400 megabytes. When filled with data, these disks can be changed by the crew, provided that the SAMS is installed in the middeck or the Spacelab module. Additional disk drives and data downlinking are utilized in the cargo bay configuration to increase the data capacity for the mission, since crew disk changeout is not possible.

The work is being performed at NASA Lewis by a team composed of NASA and Sverdrup Technology, Inc., engineers and NASA technicians. The component parts have been fabricated by commercial companies. Missions involving international participation with the European, Japanese, and Canadian space agencies are also supported.

SAMS is expected to support approximately three or four flights per year. This flight rate is expected to continue until Space Station *Freedom* is operational. A SAMS type of system will be among the first user experiments aboard *Freedom*.

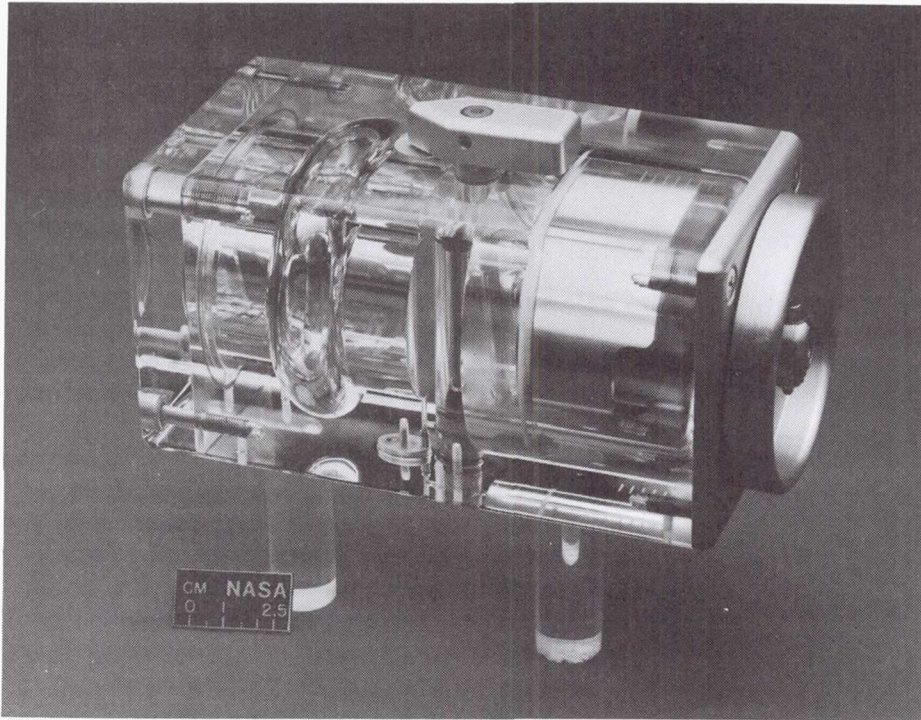
**Lewis contact:** Richard DeLombard, (216) 433-5285  
**Headquarters program office:** OSSA

### Glovebox Experiments Being Developed for USML-1

As part of the first United States Microgravity Laboratory (USML-1) mission scheduled for flight in 1992, five small-scale experiments in microgravity combustion and fluid physics are in final development at NASA Lewis.

- The Interface Configuration Experiment (ICE) is designed to determine the preferred orientation that fluids will take in a specially designed transparent chamber as the effect of gravity is reduced. The unique shape of the chamber was conceived and built by the investigators, Paul Concus of the University of California at Berkeley, Mark Weislogel of NASA Lewis, and Robert Finn of Stanford University. The experiment will be of critical importance to engineers and scientists designing equipment to store and transfer cryogenic fuels for use on Space Station *Freedom*.
- The Smoldering Combustion in Microgravity (SCM) experiment is designed to determine the potential effects of low gravity on the smoldering of common materials. Several samples of polyurethane foam will be used in this experiment. The investigators are Carlos Fernandez-Pello of the University of California at Berkeley and Dennis Stocker and Sandra Olson of NASA Lewis.
- The Wire Insulation Flammability Experiment (WIFE) is designed to determine the offgassing, flammability, and flame spread characteristics of overheated wire in a low-gravity environment. The investigators are Paul Greenberg and Kurt Sacksteder of NASA Lewis and Takashi Kashiwagi of the National Institute for Science and Technology.





*Transparent hardware for ICE.*

- The Candle Flames in Microgravity (CFM) experiment is designed to determine and demonstrate the unique burning characteristics of candles in low gravity. The investigators are Howard Ross of NASA Lewis, James T'ien of Case Western Reserve University, and Daniel Dietrich of Sverdrup Technology, Inc.
- The Oscillatory Thermocapillary Flow Experiment (OTFE) is designed to determine if fluid flows driven by surface tension variations can be made to oscillate in low gravity. The investigators are Simon Ostrach and Yasuhiro Kamotani of Case Western Reserve University and Alexander Pline of NASA Lewis.

These experiments will be conducted in the "glovebox," otherwise known as the glovebox experiment module (GEM), which is being designed and built by the European Space Agency in a cooperative agreement with NASA. Twelve other experiments in crystal growth and fluid physics under development at NASA Marshall Space Flight Center and the Jet Propulsion Laboratory will also be conducted in the glovebox during the USML-1 mission. The glovebox can be opened through a front port to install and remove each experiment. Before each experiment is

started, the front port is sealed and an internal ventilation system for the glovebox is switched on. After an experiment has been installed inside the glovebox, a crew member can still access the experiment by using rubber gloves attached to two airtight ports on two sides of the glovebox. Several video cameras viewing through the transparent top of the chamber will record each experiment. Experiments that generate temperature data through thermocouples will have that data indicated on liquid-crystal displays, light-emitting diodes, or both. The data can then be recorded on videotape.

The glovebox experiments differ from most other Space Shuttle experiments in that they are simpler and therefore less expensive and can be built and approved for flight in only 2 years instead of the usual 5- to 10-year cycle.

**Lewis contact: John B. Haggard, Jr., (216) 433-2832**  
**Headquarters program office: OSSA**

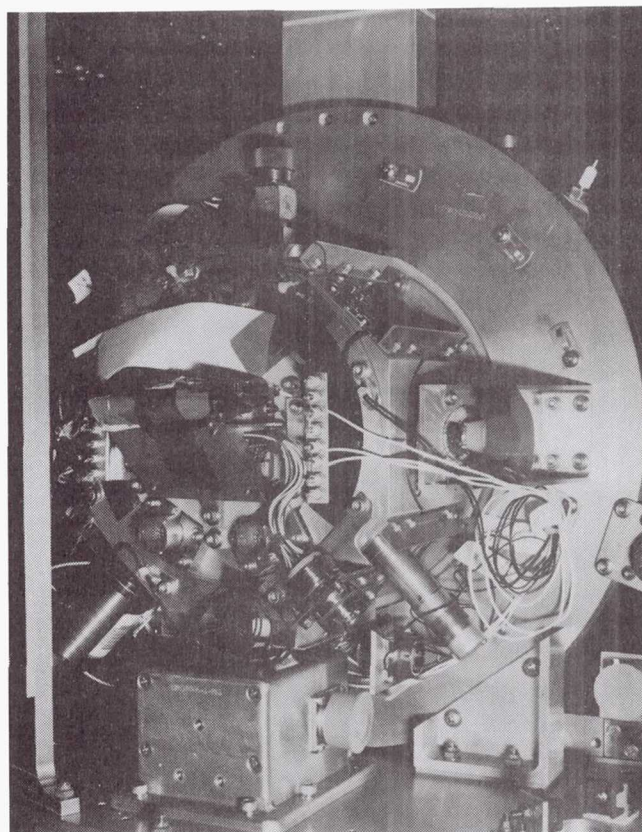


## Pool Boiling Experiment Prepared

The Pool Boiling Experiment (PBE) is scheduled to fly onboard the Space Shuttle in 1992 in a Get Away Special canister. This experiment for studying nucleate boiling under microgravity conditions was conceived by Dr. Herman Merte, Jr., of the University of Michigan and built by NASA Lewis. Its objective is to improve understanding of the fundamental mechanisms that constitute nucleate pool boiling. These mechanisms include nucleation, or the onset of boiling; dynamic growth of vapor bubbles near the heater surface; and subsequent motion and collapse of the vapor bubbles. A pool of liquid that is initially at a precisely defined pressure and temperature will be subjected to a step-imposed heat flux from a semitransparent thin-film heater that forms part of one wall of the container. This will allow boiling to be initiated and maintained for a defined period of time at a constant pressure level. Transient temperature measurements of the heater surface and the fluid near the heater surface will be made, noting especially the conditions at the onset of boiling. Motion photography will record the boiling process in two simultaneous views, one from beneath the heater surface, and one from the side. The control of the experiment and data acquisition will be completely automated.

This experiment will provide an understanding of how heat flux, initial subcooling, and time affect the growth and motion of vapor bubbles; will correlate the liquid-vapor behavior with observed heater surface temperature variation; will use initial liquid temperature distribution at nucleation to compute vapor bubble growth rate for comparison with observations; and will measure delay time to nucleation for correlation with nucleation theory by using heat flux, surface temperature, and liquid temperature distribution.

The PBE hardware includes a test chamber with two sections, one filled with degassed Fluorocarbon R-113 (Freon), and the other with gaseous nitrogen. The two sections are separated by a metal bellows. Constant pressure can be maintained within the Freon-filled section by introducing additional nitrogen into the nitrogen-filled section of the test chamber from a pressurized nitrogen storage bottle. Solenoid valves automatically increase the nitrogen pressure or vent it as required by the experiment. Thermistors



*Pool Boiling Experiment test chamber showing instrumentation.*

monitor the fluid temperature, and pressure transducers monitor the Freon and nitrogen pressure. The Freon will be heated by applying power to two thin-film heaters built into the bottom wall of the test chamber. These heaters are produced by sputtering 400 Å of gold onto a quartz substrate. The test chamber is sized so that vapor bubbles with a maximum diameter of 2 in. can be viewed. Two windows permit photographing the bubbles from beneath the heaters and from one side wall. Two additional windows are used for chamber illumination. The PBE hardware also includes a pressurized nitrogen storage bottle, a film camera and optical mirrors, a data acquisition and control system, and a power control unit and batteries.

Design engineering, qualification testing, and scientific support for the PBE have been furnished by NASA Lewis with assistance from Sverdrup Technology, Inc.

The information obtained from this experiment will be invaluable in designing equipment for use in Space Station modules and on space platforms



for temperature control, power generation, energy dissipation, and the storage, transfer, control, and conditioning of fluids, including cryogenic fluids.

**Lewis contacts:** Angel M. Otero, (216) 433-3878;  
Francis P. Chiaramonte, (216) 433-8040  
**Headquarters program office:** OSSA

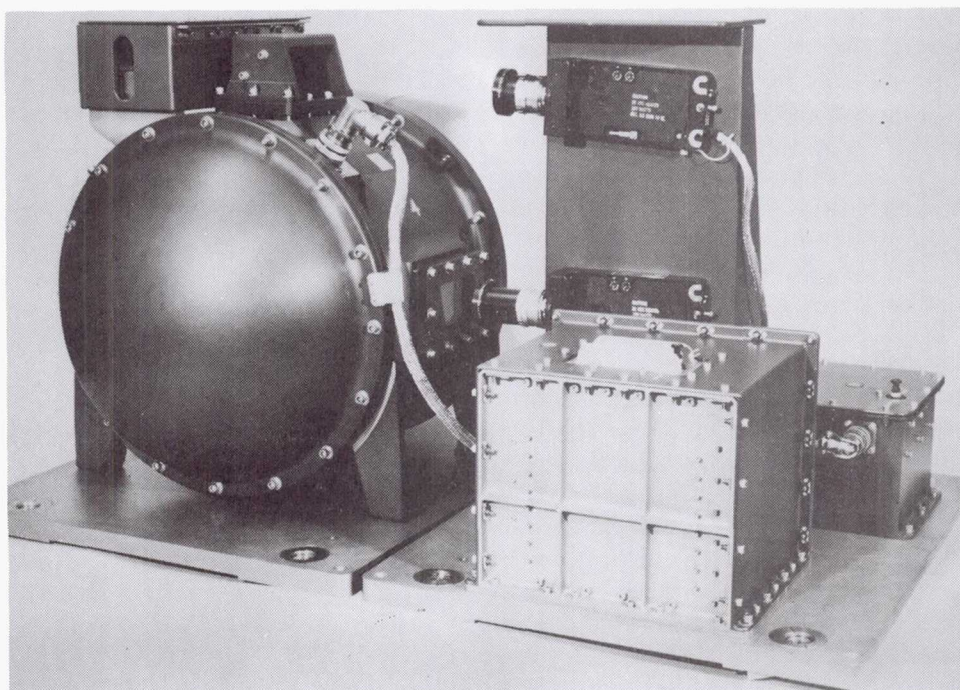
### **Solid Surface Combustion Experiment Analyzed**

The Solid Surface Combustion Experiment (SSCE) was flown for the second and third times during 1991 aboard the STS-40 (SLS-1) and the STS-43 Shuttle missions. The SSCE is the first combustion experiment to fly in the Shuttle, and the first such experiment in the NASA spaceflight program since Skylab. It was conceived by Professor Robert A. Altenkirch, Dean of Engineering at Mississippi State University, and built by NASA Lewis.

The purpose of the SSCE is to study the physical and chemical mechanisms of flame spread over solid fuels in the absence of gravity-driven buoy-

ant or externally imposed airflows. The controlling mechanisms of flame spread are different in low gravity and normal gravity; thus the results of the SSCE experiment have a practical application in the evaluation of spacecraft fire hazards. In these first three flights the fuel sample—ashless filter paper instrumented with three thermocouples—was mounted in a sealed chamber filled with a 1:1 mixture of oxygen and nitrogen at pressures of 1.5, 1.0, and 2.0 atm and ignited with an incandescent wire. Two 16-mm motion-picture cameras photographed the experiment from perpendicular perspectives, and thermocouple temperature and chamber pressure measurements were recorded with a digital data acquisition and control system. The SSCE is self-contained and battery operated and can be flown either on the Shuttle middeck or in the Spacelab module. For safety and simplicity, only one specimen is burnt in the test chamber during each mission. Reference 1 provides more information concerning the hardware configuration.

NASA Lewis designed and built the SSCE payload and also performed engineering, qualification testing, scientific support, and flight operations functions. The SSCE project was supported in some way by nearly every major element of the Lewis organizational structure.



*SSCE flight hardware in middeck configuration.*



The SSCE hardware was activated and performed without incident on the first two flights, igniting the test specimen and recording transducer and imaging data precisely as designed. Following the example of the first crew (STS-41), the STS-43 crew attached a video camera to the experiment for a welcome early downlinking of preliminary results. All three crews verbally reported evidence of a flame sustained for about 70 sec. The motion picture films showed that the initial spreading of the flame occurred during the first 20 to 27 sec and that fuel not consumed during the spreading burned sporadically thereafter. The flame spread rates were larger at the higher atmospheric pressures. Preliminary assessments of the thermocouple data indicate that pyrolysis models widely used in ground-based test analysis must be altered to account for microgravity behavior. An integrated analysis of the temperature, pressure, and imaging data has been performed and is being prepared for publication.

The principal investigator, Professor Altenkirch, has developed a numerical simulation of the flame spreading process from first principles (of fluid mechanics, heat transfer, and reaction kinetics). The spread rates, flame shape, and thermodynamic data from the SSCE flight are being compared directly with the results of the computational model. The flight temperature data indicate that the solid-phase kinetics parameters commonly used to model normal-gravity flame spread do not reproduce the flame structure observed. The results from these three tests will be used to formulate an improved solid-phase pyrolysis model.

The SSCE project is currently scheduled for a total of eight flights. Ashless filter paper will be tested on the next two flights in different mixtures of oxygen and nitrogen and pressure; the final three tests will use polymethylmethacrylate. The SSCE is currently manifested aboard the USML-1 Spacelab mission (June 1992).

#### Reference

1. Vento, D.M., et al.: The Solid Surface Combustion Space Shuttle Experiment Hardware Description and Ground-Based Test Results. AIAA Paper 89-0503, Jan. 1989.

**Lewis contacts:** John Koudelka, (216) 433-2852;  
Kurt Sacksteder, (216) 433-2857  
**Headquarters program office:** OSSA

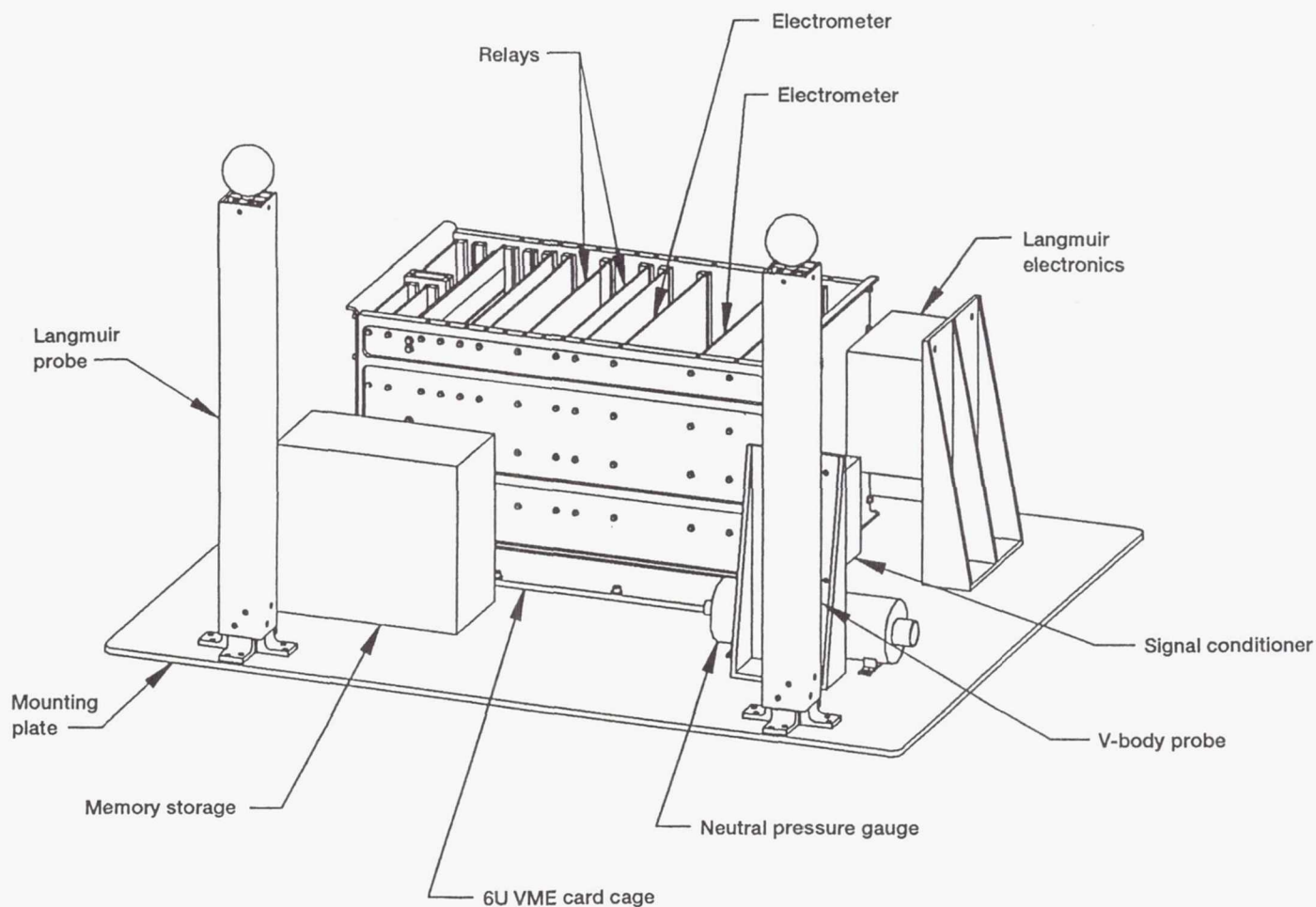
#### Solar Array Module Plasma Interactions Experiment Being Developed

Until now space power systems in low Earth orbit (LEO) have operated at low voltages and have not suffered from the effects of plasma interactions. High-power photovoltaic-based systems now under development for space applications will operate at higher voltages in order to increase system efficiency. Unfortunately, high-voltage systems suffer from adverse interactions with the LEO space plasma. The interactions, which are incidental results of power system operation, include arcing, which occurs when exposed metal surfaces attain a negative potential, and parasitic current collection, which occurs at a positive potential level. These interactions can cause damage to power system components and lower power system efficiency.

The Solar Array Module Plasma Interactions Experiment (SAMPIE) is a Space Shuttle-based flight experiment with a scheduled launch date of October 1993. SAMPIE will determine the effects of the LEO space plasma environment on state-of-the-art solar modules that are biased to high potentials relative to the plasma. In addition, specially modified solar cell modules will be tested to demonstrate the possibility of arc suppression during operation at highly negative potential levels. Finally, several metal test specimens will be included to study the basic nature of these interactions and for computer model validation. The experiment is being developed at NASA Lewis.

SAMPIE will consist of an enclosed metal container with an experiment plate fixed to the top surface. The entire package will mount directly to one of the top plates of a Hitchhiker-M carrier. A programmable, high-voltage power supply will bias the test specimens to direct-current voltages ranging from 300 V to -600 V with respect to the Space Shuttle ground. The transient current detector will detect the occurrence of arcing and measure the arc rate as a function of negative bias voltage. An electrometer will measure parasitic current collection versus voltage for both positive and negative bias potentials. A set of plasma diagnostic instruments will collect data on the plasma environment during experiment operation. A Sun sensor will measure the degree of insolation. An onboard data acquisition system will record and store the information to a solid-state, nonvolatile memory device.





*SAMPIE package.*

The experiment plate will measure 41 by 61 cm (16 by 24 in.). Solar cell samples will include standard silicon cells to provide a baseline, Space Station *Freedom* cells with copper interconnects, very thin ( $\sim 60 \mu\text{m}$ ), advanced photovoltaic solar array cells, and cells modified for arc suppression tests.

Various metal samples will be tested to investigate the effects of both current collection and arcing in the LEO plasma. The information from these tests will be used to help validate computer modeling codes that have been developed at NASA Lewis.

The SAMPIE flight experiment will be the most ambitious space power system plasma interaction experiment to date. SAMPIE has recently completed a preliminary design review and is proceeding with the buildup of the engineering model. It will be designed and built in a highly modular way that will facilitate refurbishment and reflight capability.

**Lewis contacts:** Lawrence W. Wald, (216) 433-5219;  
Dr. Dale C. Ferguson, (216) 433-2998  
**Headquarters program office:** OAST

# Space Station Freedom

## Systems Engineering and Integration

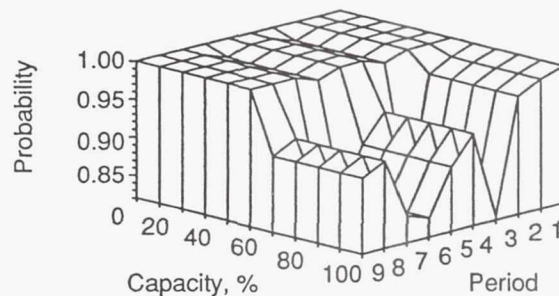
### Reliability Computer Program Developed

NASA has extensive experience in the development of highly reliable spacecraft. Very few of these spacecraft, however, have been maintained by scheduled resupply flights from Earth. Because of the unique challenges of maintenance support for Space Station *Freedom*, NASA Lewis has developed a computer program called ACARA. ACARA can assess performance (in terms of availability), reliability, maintenance, and life-cycle costs for a space-based power system subject to constrained resources.

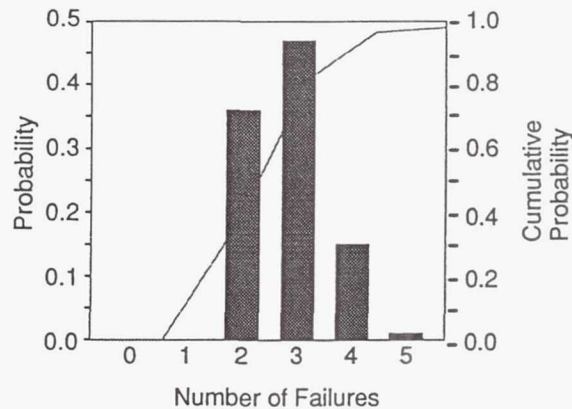
ACARA uses a statistical Monte Carlo method to simulate component failures and repairs, as well as capacity states of the subsystems throughout the life of a system. Component failures are modeled with multiple exponential and Weibull probability distributions. Resources are scheduled with the objective of maximizing system performance while complying with production, transportation, storage, crew, and equipment constraints. The scheduling method used was an approximate optimization approach that was verified by using an integer linear programming theory. The constraints are specified on a user-defined periodic basis over the life of the system and can thus be nonuniform over time. The life-cycle cost analysis is performed at the end of the simulation and presents the costs by time period in terms of hardware, transportation, crew, and equipment costs.

Because of the integrated approach of the ACARA analysis, many types of analyses and tradeoff studies can be performed. ACARA characterizes system performance in terms of both state and equivalent availability. The state availability is the probability that the system is in a particular capacity state (e.g., power level). The equivalent availability is a capacity-weighted average of the state availabilities. ACARA's ability to simulate partial capacity states is significant and not widely available in industry-standard reliability

MODULE 1, 200 runs, 18 years, period = 2 yrs  
Probability of Exceedence Results  
(Normalized to Installed Capacity)



MODULE 1, 200 runs, 18 years, period = 2 yrs  
Frequency of Occurrence Results  
Batteries, Period:18



ACARA's graphical analytical results.

modeling tools. ACARA can also determine the probability of exceeding a capacity state. This is useful in assessing reliability and loss-of-load probability requirements. Other types of analyses include evaluation of critical spares and the effect of resource constraints on system availability and life-cycle costs.

Although written to assess space-based power system designs, ACARA is quite general and can be used to model any system that can be represented by a block diagram of components in series or parallel combinations. ACARA's system assessment capabilities can be applied throughout the life of the system to influence the design and the logistics of a staged assembly, as well as aiding during the mission planning and operations phase.

ACARA incorporates a user-friendly, menu-driven interface with full-screen-input data entry and



editing. It is written in the programming language APL and runs on 386- and 486-based microcomputers.

Lewis contact: Dr. Larry A. Viterna, (216) 433-5398  
Headquarters program office: OSF

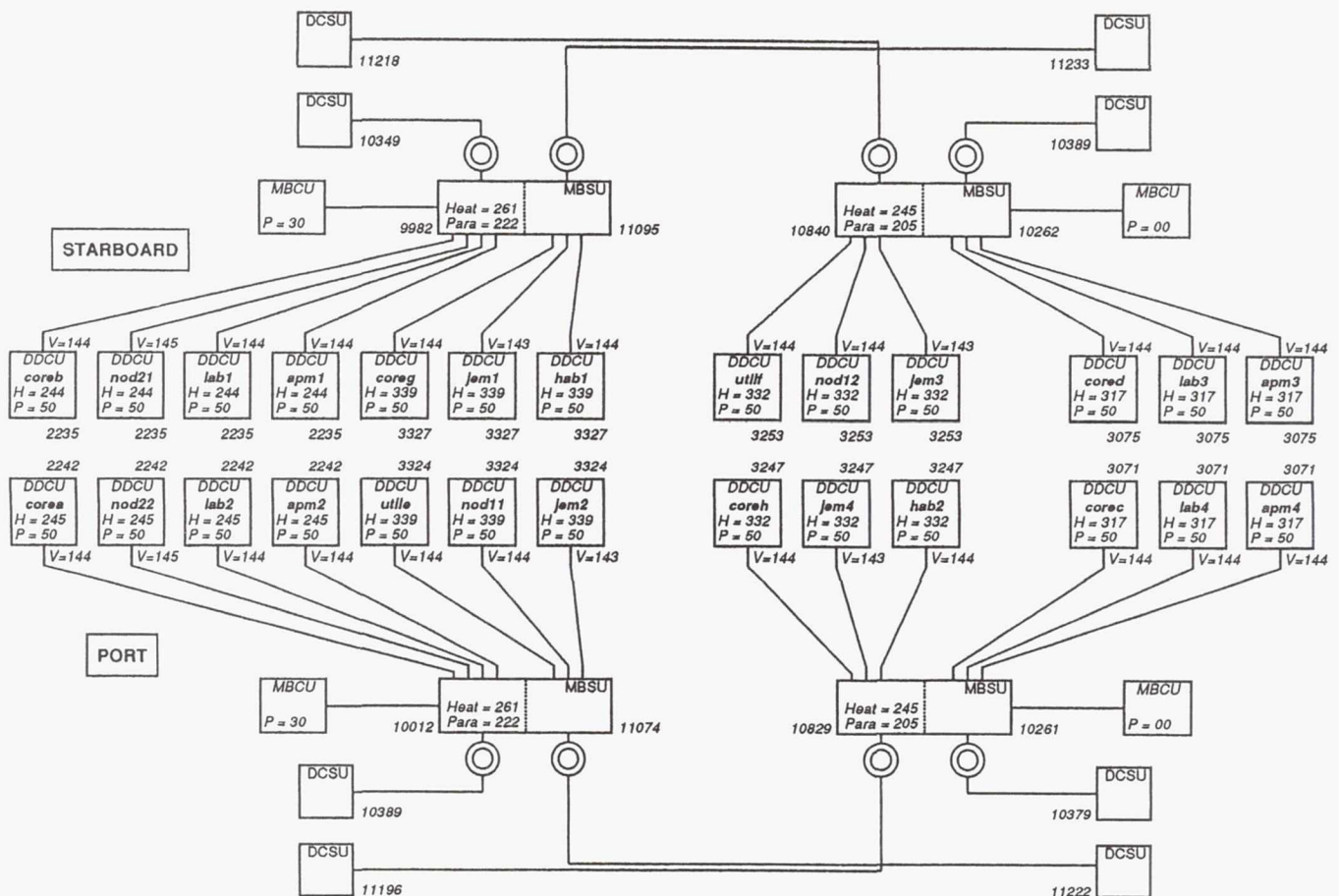
## Computer Code Analyzes Electric Power System Performance

SPACE is a computer code developed at NASA Lewis to model the performance of the Space Station *Freedom* electric power system (EPS). SPACE is used to predict the amount of power that the EPS can produce on orbit throughout its life. It was originally developed to assist in verifying the contractor's predictions of EPS performance but has evolved into a multipurpose tool for assessing EPS performance under a wide variety of orbital conditions and on-orbit configurations.

The model includes an orbital mechanics section, which calculates the parameters of the orbit, including the sunlight and eclipse times. Models of the solar arrays and the nickel/hydrogen batteries predict the amount of power that can be produced during the sunlight and eclipse portions of the orbit. These are coupled with a detailed load-flow model of the power management and distribution system (PMAD) to determine the amount of power that can be delivered to the housekeeping and user loads. SPACE uses a numerical iteration procedure to predict the highest power level that can be sustained throughout the specified orbit, taking into consideration any hardware constraints.

SPACE also contains a model of the photovoltaic thermal control system. This model predicts the temperatures of the batteries and other components under active thermal control and can assess the thermal environment.

In the past year SPACE has been used to assess the EPS performance under some severe off-



PMAD diagram at orbit midnight showing analysis of 5-year-old system.

normal operating modes. These include docking with the Space Shuttle orbiter and reboost of the Space Station. During each of these conditions the photovoltaic arrays must be turned so that they are not fully pointing at the Sun. SPACE has also been used to assess the performance of the EPS with some of the batteries removed to reduce the Shuttle launch weight, in order to ensure that the batteries achieve their required life.

Efforts are under way to expand the capabilities of SPACE by adding the ability to assess the performance of the EPS given a defined set of user and housekeeping loads. Also, SPACE is continually being updated with the latest information on the performance of various EPS components as the design progresses and higher fidelity information becomes available.

**Lewis contact:** Jeffrey S. Hojnicky, (216) 433-5393  
**Headquarters program office:** OSF

### Hypervelocity Impact Testing Performed on Solar Dynamic Radiator

One of the hazards Space Station *Freedom* will encounter in low Earth orbit is impact from micrometeoroids and orbital debris. Micrometeoroids are naturally occurring particles in orbit about the Earth; orbital debris arises from man-made material left in orbit. Both types of particles travel at hypervelocities, averaging between 10 and 20 km/sec. Even very small particles traveling at these speeds can cause a great deal of damage to space hardware.

Over the past 3 years NASA Lewis engineers teamed with scientists at NASA Johnson Space Center and engineers at LTV Missiles and Electronics Corp. have studied the effects of hypervelocity impact on the performance of *Freedom's* solar dynamic radiator. The radiator is designed to reject excess heat from the solar dynamic power module by pumping a liquid heat transfer fluid through a series of tubes embedded in radiator panels. The liquid fluid loop must be protected with a bumpering or armoring system because it could be damaged or ruptured if struck by a micrometeoroid or orbital debris particle.

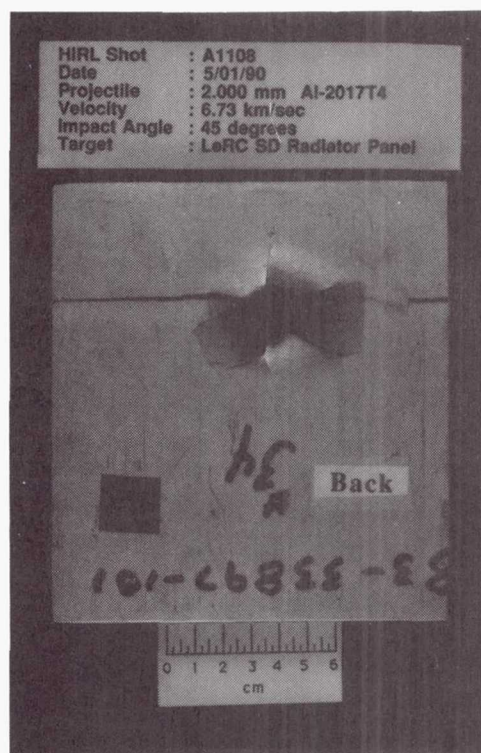
The protective bumpering designed for the solar dynamic radiator was tested by firing simulated debris particles at representative radiator panels from a light gas gun at NASA Johnson's Hypervelocity Impact Research Laboratory. Tests were conducted over a range of particle size, particle density, impact angle, and impact velocity. Damage to the samples was extensively analyzed. Testing showed that analytical penetration predictions overestimated the actual damage incurred by the radiator panel samples.

### Bibliography

Rhatigan, J.L.; Christiansen, E.L.; and Fleming, M.L.: On Protection of *Freedom's* Solar Dynamic Radiator From the Orbital Debris Environment, Part 1: Preliminary Analyses and Testing, *Proceedings of the 12th Annual International Solar Energy Conference*, ASME, 1990, pp. 349-356. (Also NASA TM-102458.)

Rhatigan, J.L.; Christiansen, E.L.; and Fleming, M.L.: On Protection of *Freedom's* Solar Dynamic Radiator From the Orbital Debris Environment, Part 2: Further Testing and Analyses. NASA TM-104514.

**Lewis contact:** Jennifer L. Rhatigan, (216) 433-8330  
**Headquarters program office:** OSF



Results of hypervelocity impact test.



# Photovoltaic Power Module

## Plasma Testing Performed on Solar Array and Structure

Plasma theory for low Earth orbit suggests that high-voltage arrays on Space Station *Freedom* will interact with space plasma and may "float" the entire structure to large negative potentials ( $-140$  VDC relative to space plasma ground is predicted). This large potential could result in structural arcing and possible damage to thermal control surfaces.

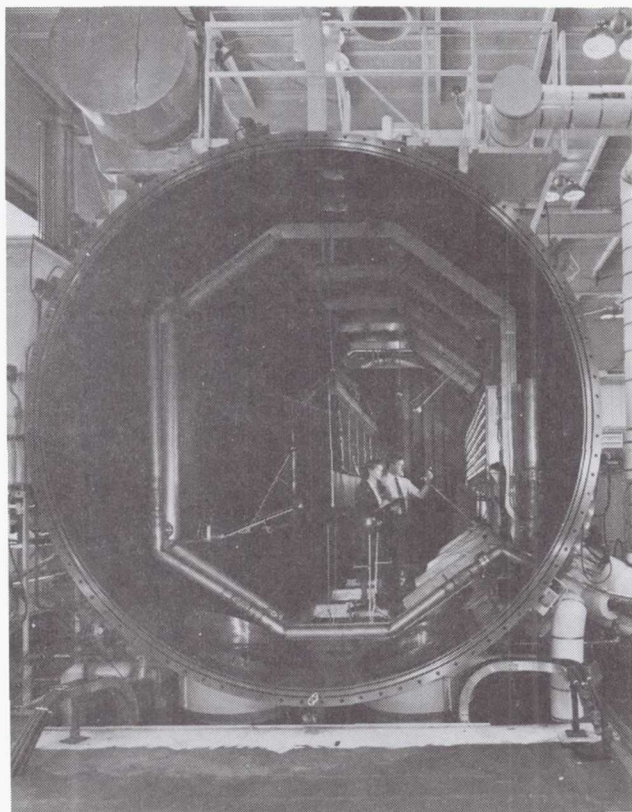
NASA Lewis has begun a system-level test program to investigate the vulnerability of *Freedom* and to measure the effectiveness of a plasma contactor in mitigating these effects. The test program used instrumented photovoltaic array environmental protection (PAEP) development hardware. This hardware consists of two panels that make up one complete solar array circuit (there will be 492 such circuits in the final *Free-*

*dom* configuration). Each circuit consists of 400 solar cells arranged on a Kapton blanket in a manner similar to the present *Freedom* solar array design. The panels were connected to a variety of simulated structural components and subjected to an environment similar to that found in space (i.e., high vacuum, solar illumination to  $1/3$  sun, a plasma density of  $1.66 \times 10^6$  ions/cm<sup>3</sup>, and an electron temperature of 0.18 eV).

Tests performed to date have demonstrated that floating potentials, although not as large as predicted, are still sufficient to allow structural arcing. Chromic-acid-process-anodized aluminum arced readily on the face of the samples. Sulfuric-acid-process-anodized aluminum was more resistant to arcing. Arcs that did occur on those samples were confined to the edge areas (edge arcing is not expected to affect bulk thermal control properties). Further tests are planned.

Tests using a plasma contactor showed it to be highly effective in eliminating large station potentials. Floating potentials were reduced from  $-120$  VDC (measured relative to plasma ground) to near ground potential. Structural arcing was eliminated. Parasitic currents resulting from use of the device were less than 1.5 mA.

**Lewis contacts:** Marian Felder, (216) 433-8310;  
Bernard L. Sater, (216) 433-5291; Phillip E. Paulsen,  
(216) 433-6507  
**Headquarters program office:** OSF



Operations engineers make final checks on solar array panels suspended in vacuum tank.

## Nickel/Hydrogen Cells Tested

NASA Lewis and its contractors are responsible for designing and fabricating the electric power system for Space Station *Freedom*. *Freedom* will circle the Earth every 90 min in a low Earth orbit (LEO), spending approximately 55 min in sunlight and 35 min in the Earth's shadow (eclipse). In order to supply continuous power over the orbit, the electric power system must not only provide power during the sunlight portion by means of solar arrays, but must also store energy for use during eclipse. Nickel/hydrogen (Ni/H<sub>2</sub>) cells were chosen as the energy storage system for *Freedom*. Because of the limited Ni/H<sub>2</sub> data base on life and performance characteristics in a LEO regime, NASA Lewis began two test programs:



one in house and one at the Naval Weapons Support Center (NWSC) in Crane, Indiana.

For the in-house test program NASA Lewis has built a computer-controlled Ni/H<sub>2</sub> cell laboratory with a data acquisition system to screen a large number of cell designs. Cells were purchased from Yardney Technical Products, Eagle-Picher Industries, and Hughes Aircraft Company. The resulting 39-cell test matrix comprises 13 different cell designs, including both 50- and 65-Ahr-capacity cells. All cells have successfully completed acceptance, vibration, and characterization testing and are currently undergoing LEO life testing at a 35-percent depth of discharge (DOD) and at either -5 or 10 °C. As of October 1991, 22 cells have successfully completed over 2 years of life testing (11,680 cycles); the rest have completed over 1 year. The number of completed life cycles ranges from 10,450 to 14,900 cycles.

The NWSC was contracted by Lewis to characterize and life test a statistically significant number of Ni/H<sub>2</sub> cells in order to verify *Freedom's* requirement of 5-year life at 35-percent DOD. The test matrix comprises 130 Ni/H<sub>2</sub> cells from each of three vendors: Yardney Technical Products, Eagle-Picher Industries, and Gates Aerospace Batteries. Each vendor will supply 50 "standard" 65-Ahr cells that represent a low-risk, state-of-the-art LEO design. They will also supply 20 "advanced" 65-Ahr cells and 60 "advanced" 81-Ahr cells. For the advanced design the vendors were directed to include at least two recent technology developments that improve cycle life and electrical performance. All life testing is performed in either 10- or 5-cell series-connected test packs, at 35- or 60-percent DOD, and at 10 or -5 °C.

As of October 1991, all Eagle-Picher and all Yardney cells have been delivered to NWSC and have successfully completed acceptance, vibration, and characterization testing, except for the Yardney 81-Ahr cells, which will begin characterization testing in November 1991 and life testing in January 1992. Sixty Yardney 65-Ahr cells (40 standard and 20 advanced) have started life testing and have accumulated between 4050 and 7090 cycles. Four test packs at 60-percent DOD have failed, with the longest one lasting 4700 cycles. Sixty Eagle-Picher 65-Ahr cells (40 standard and 20 advanced) have started life testing and have accumulated between 1170 and 2460

cycles. Forty Eagle-Picher 81-Ahr cells are just beginning life testing. All 60 Gates 81-Ahr cells have recently been delivered to the NWSC and will undergo acceptance testing shortly. Thirty additional 65-Ahr standard cells have been ordered from Gates for charge management testing. These and the other 60 cells from Gates are scheduled for delivery by December 1991. The NWSC will also perform storage tests on cells from each vendor.

In April 1991, NASA Lewis directed the NWSC to carry out a special 6-month test on 48 of the Eagle-Picher standard 65-Ahr cells to study the effects of charging at a constant current and then terminating charge at 94-percent state of charge (SOC). (The *Freedom* baseline charge profile is constant current to 94-percent SOC, taper to 100-percent SOC, trickle charge.) A constant current charge is more desirable for *Freedom's* electric power system because it allows for greater available continuous power over the sunlight period. However, the effects of terminating charge at less than 100-percent SOC are not well known and are therefore being studied.

**Lewis contact:** David T. Frate, (216) 433-8329  
**Headquarters program office:** OSF

## Electrical Systems

### Power System Monitor Design and Implementation Completed

The Advanced Development Program of Space Station *Freedom* has completed the design and implementation of a power system monitor for the NASA Lewis direct-current power-management-and-distribution (DC PMAD) testbed. The DC PMAD testbed is a reduced-scale representation of the electric power system (EPS) in *Freedom*. This testbed serves as the platform for evaluating power system control techniques that are candidates for implementation onboard *Freedom* or in the ground-based control center. The power system monitor, developed by NASA Lewis engineers, includes all the functions deemed essential to the safe operation of the testbed EPS. The Ada programming language was selected for implementation of the power system monitor algorithms. The power system monitor was tested



and verified in the Power System Facility. Ada software development and testing was performed by NASA Lewis.

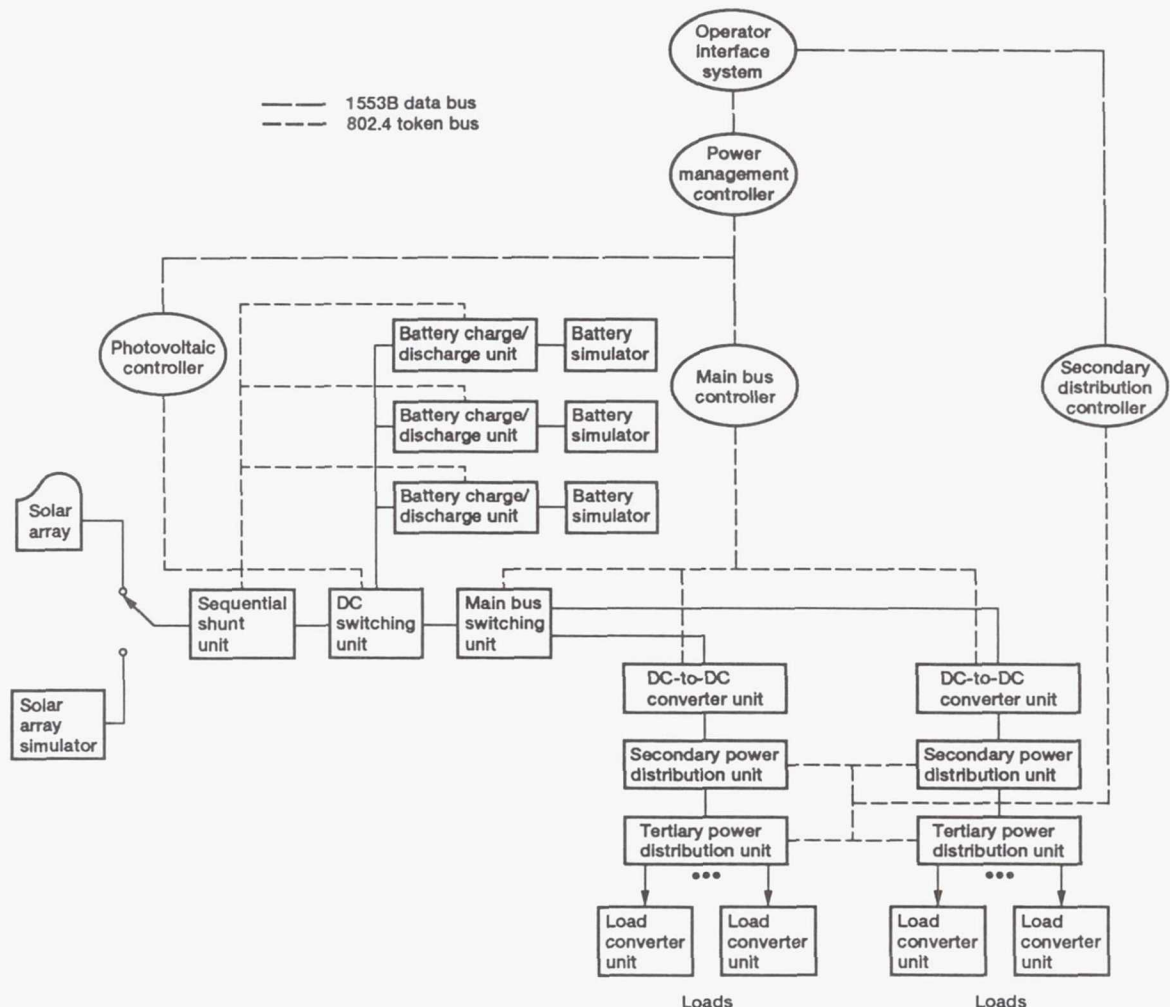
The EPS control system will play a major roll in the operation of *Freedom's* electric power system. In its initial configuration the control system functionality will be kept to a minimum to comply with program constraints. As the EPS evolves and becomes operational, the control system functionality is expected to approach that of an autonomous electric power system.

The DC PMAD testbed control system consists of five standard controllers arranged in a distributed, hierarchical architecture. The standard controllers are 20-MHz, Compaq 386/20e personal computers. Each standard controller is configured with operating Ada software and appropriate peripheral hardware to perform its

given function in the hierarchy. This hierarchical system monitors and controls the testbed power system.

The testbed control system has been developed by using a top-down approach based on classical control and conventional terrestrial power utilities design techniques. The design methodology used included development of a testbed operating concept, a functional design phase, and a detailed design and implementation phase.

The power system algorithms provide the necessary functions for performing periodic data acquisition, data smoothing, fault detection and validation, and status reporting. The Ada programming language was selected to provide a flexible and maintainable environment for the development of the control algorithms.



Block diagram of DC PMAD testbed control system.

## Bibliography

Baez, A.N.; and Kinnach, G.L.: Description of the Control System Design for the SSF PMAD DC Testbed. *26th IECEC Proceedings*, American Nuclear Society, 1991, vol. 2, pp. 334-339.

Beach, R.F., et al.: Description of the PMAD DC Testbed Architecture and Integration Sequence. *26th IECEC Proceedings*, American Nuclear Society, 1991, vol. 2, pp. 340-345.

Ludwig, K.; Wright, T.; and Mackin, M.: Description of Real-Time Ada Software Implementation of a Power System Monitor for the Space Station Freedom PMAD DC Testbed. *26th IECEC Proceedings*, American Nuclear Society, 1991, vol. 1, pp. 51-55.

Soeder, J.F.; Frye, R.J.; and Phillips, R.: The Development of Testbeds to Support the Definition and Evolution of the Space Station Freedom Power System. *26th IECEC Proceedings*, American Nuclear Society, 1991, vol. 2, pp. 346-351.

**Lewis contact: Anastacio N. Baez, (216) 433-5318**  
**Headquarters program office: OSF**

## Development of High-Voltage, Direct-Current Spacecraft Fuse Completed

Fuses are expected to be used on Space Station Freedom in the primary and secondary distribution systems to protect the electrical distribution hardware from faults. Past spacecraft have utilized low-voltage fuses, but no high-voltage, space-rated fuses were available for use on Freedom. The fundamental problem with higher voltage fuses is the prevention of an electrical restrike in the form of a current arc. This effort resulted in a fuse rated at 160 VDC with current ratings up to 150 A.

The high-voltage fuse was developed under NASA contract by the Mepcopal Company. The fuse is manufactured with thick film materials in a process similar to that used in fabricating semiconductors. The fuse element consists primarily of gold material deposited on an alumina substrate. A low-temperature sealing glass (arc suppressant) is laid down over the fuse element. When the fuse is subjected to an overload, the gold element melts and migrates rapidly into the arc-suppressant glass coating. This effectively prevents subsequent vaporization and ionization of the blown metal. Arc, plasma, and vapor are contained within the fuse package. The gold material has a high positive temperature coefficient of resistance, which tends to provide

inherent current limiting as the overload current increases. The fuse development effort resulted in breadboard fuses that were tested over a range of overload conditions. Further packaging and qualification of the fuses has subsequently been done by the Mepcopal Company.

**Lewis contact: Raymond F. Beach, (216) 433-5320**  
**Headquarters program office: OSF**

## Electric Power System Diagnostic Program Tested

A major Space Station objective is to maximize its productivity by developing products to enhance its efficient operation. To minimize restoration time, NASA Lewis is developing a diagnostic program that will improve a power system controller's ability to respond to anomalies.

A diagnostic program must understand all possible failures and their consequences before it can diagnose a problem. Lewis' program incorporates its failure knowledge into data tables, a technique known as set covering. Using set covering rather than a series of if-then rules to encode the failure knowledge makes the diagnostic program extremely flexible. The program uses a standard reliability analysis tool—the failure modes and effects analysis—to produce the symptom and failure data base. Symptoms are detected by using rule-based classifiers. Symptoms are then linked, by using antecedent-driven rules, to all related system failures. This linkage generates failure-cause hypotheses. Hypotheses are ranked primarily by the number of observed symptoms; the more symptoms, the more likely the failure cause. Explanations are provided for the failure causes and their symptoms, making the reasoning process readily understood by a power system controller.

This diagnostic program has been built and tested on a model of the Space Station power-management-and-distribution system's direct-current testbed. This model is being updated to accurately depict the current testbed configuration. Integrated failure detection testing will be performed during the fall of 1991.

**Lewis contact: James L. Dolce, (216) 433-8052**  
**Headquarters program office: OSF**



# Engineering and Computational Support

## Electronic and Control Systems

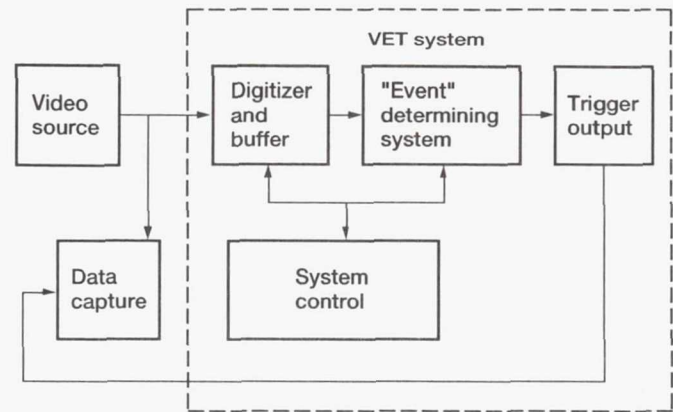
### Video Signal Analyzer Provides Trigger Pulse Based on Sensing Motion in Image

Ongoing and future microgravity experiments aboard the Space Shuttle or Space Station *Freedom* require high-resolution, high-frame-rate video technology (HHVT) to replace high-speed photographic motion picture film, which is heavy and bulky and cannot be processed in space.

In the 1990's advances in semiconductor charge-coupled device (CCD) and charge-injection device (CID) array camera sensor technologies will permit fabrication of very high-resolution video cameras with frame rates much higher than the commercial broadcast television standard of 30 frames per second. Digitized output from such a high-rate video stream will present a difficult data storage problem when data are produced at rates 300 Mbps or higher. As these data accumulate in onboard storage, total mission video data storage requirements will easily exceed 1 terabyte (1 trillion bytes). Without careful attention to cost of storage and transmission, such vast volumes of data will become very expensive to support.

An approach to minimizing data storage requirements and cost involves storing only the "important" digitized images. These are the images containing information about the experiment that are captured in the localized motion around some significant physical event. In microgravity experiments video events often happen after minutes or hours of prior inactivity.

To facilitate coping with the mounting HHVT data storage requirements, NASA Lewis has developed an implementation of a video event trigger (VET) that uses digital fuzzy logic technology and is packaged on printed-circuit hardware inside a personal computer testbed.



Video event trigger system.

The VET system can detect the onset of motion within less than 5 msec after a new video frame is acquired by a digitizer. It will support acquisition of many seconds of high-density frame storage when coupled with high-density memory capable of continuously recycling uninteresting video frames. With pre- and post-trigger capabilities, such memory could store an entire sequence of images, including all the subtle details and changes visible just before the main event.

The trigger event is extracted by a special processor capable of parallel processing 96 million pixels per second, searching for picture changes caused by one or more of the following events:

- Motion of an object in the area of interest
- Color change in the area of interest, with no motion
- Sudden and complete disappearance (or appearance) of an object in the area of interest

Built into the VET system is the capability to qualify and trigger on sudden image changes while ignoring slow changes or to trigger after detecting slow long-term image changes based on differences from a static reference image.

**Lewis contact:** Glenn L. Williams, (216) 433-2389  
**Headquarters program office:** OSSA



# Structural Systems

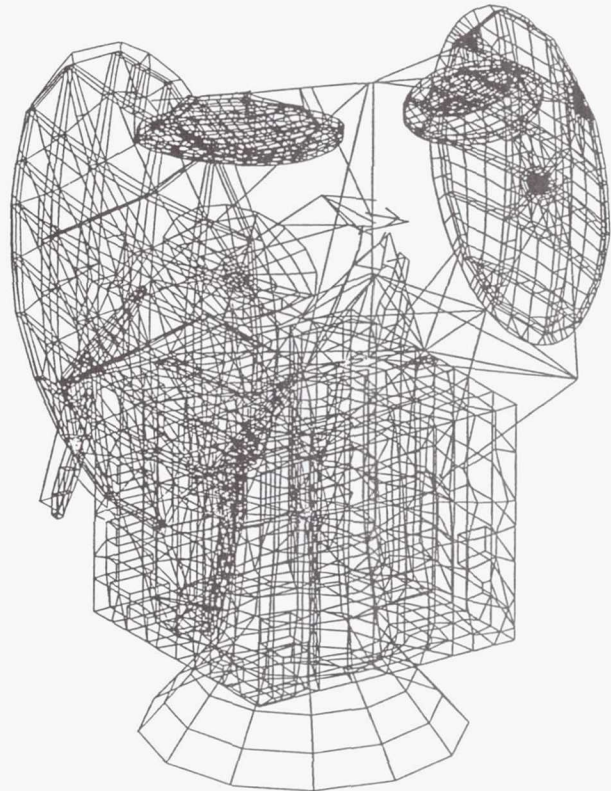
## Test Verification of Spacecraft Dynamic Models Applied to ACTS

Space Shuttle safety requires that the dynamic models used to calculate flight loads be test verified. Model verification is a part of the structural certification process that precedes all Space Shuttle flights. Advanced test and analysis techniques are being applied at NASA Lewis in the verification of dynamic models. These dynamic models are created by using finite element programs such as NASTRAN. These advanced techniques have been recently applied to the Advanced Communications Technology Satellite (ACTS).

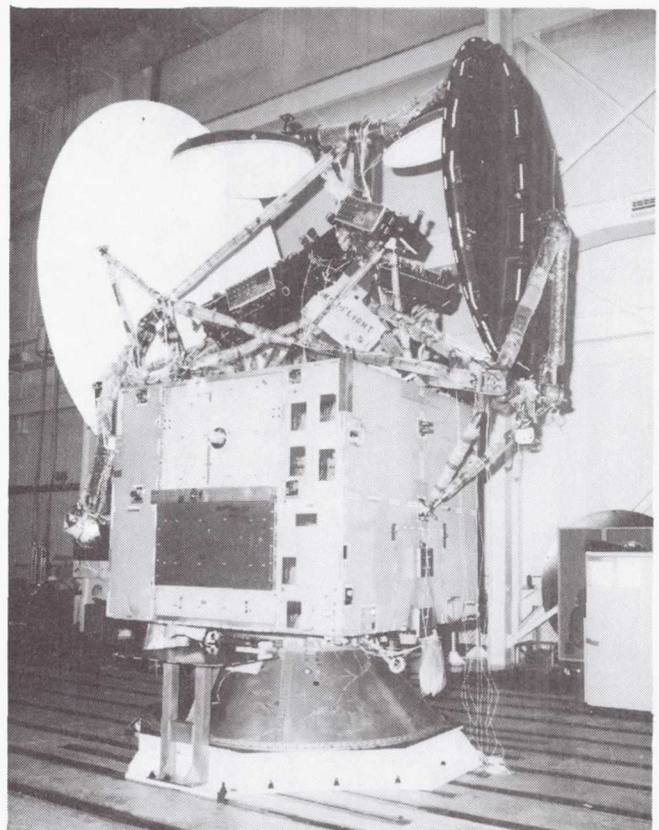
There are three phases in the verification of a model. The first phase is pretest analysis. In this phase the "target" or important loads that produce modes of vibration are identified. Modifications to NASTRAN called DMAP's have been written to calculate the mass associated with each mode. Modes with high mass produce high loads. Another important part of the pretest analysis is the development of a test analysis model (TAM). A TAM is the finite element model reduced from many thousand degrees of freedom to a few hundred that will be instrumented with accelerometers during the second phase, the modal survey. The TAM must predict the target modes as accurately as the full finite element model. For the ACTS TAM a new method called effective independence (ref. 1) was applied in addition to more standard techniques. These standard techniques include calculating the kinetic energy of each degree of freedom and instrumenting those with large kinetic energy.

During the modal survey phase different means of exciting the modes are used. For example, one method may work better in identifying closely spaced modes than another. In the ACTS modal survey continuous random, burst random, and multipoint stepped sine excitation were all used. Objective criteria have been developed that allow the best mode to be selected from all the data collected.

Correlation of the model with test data is the final phase of this activity. Changes are made to the model to improve agreement between it and test data. Both the frequency of a mode as well as its



*Finite element model of ACTS spacecraft.*



*ACTS spacecraft.*



shape must be adequately correlated. Design sensitivity analysis is helpful in identifying where changes will be most effective in improving correlation. Engineering judgment is also important in the correlation effort.

These techniques successfully verified the ACTS dynamic model. This technology is applicable to all Space Shuttle cargo bay payloads. It will be applied to the first Space Station *Freedom* launch that will place the first electric power module for *Freedom* into orbit. It is also applicable to spacecraft placed into orbit by expendable launch vehicles.

#### Reference

1. Kammer, D.C.: Sensor Placement for On-Orbit Modal Identification and Correlation of Large Space Structures. J. Guidance, Control Dynamics, vol. 14, no. 2, Mar.-Apr. 1991, pp. 251-259.

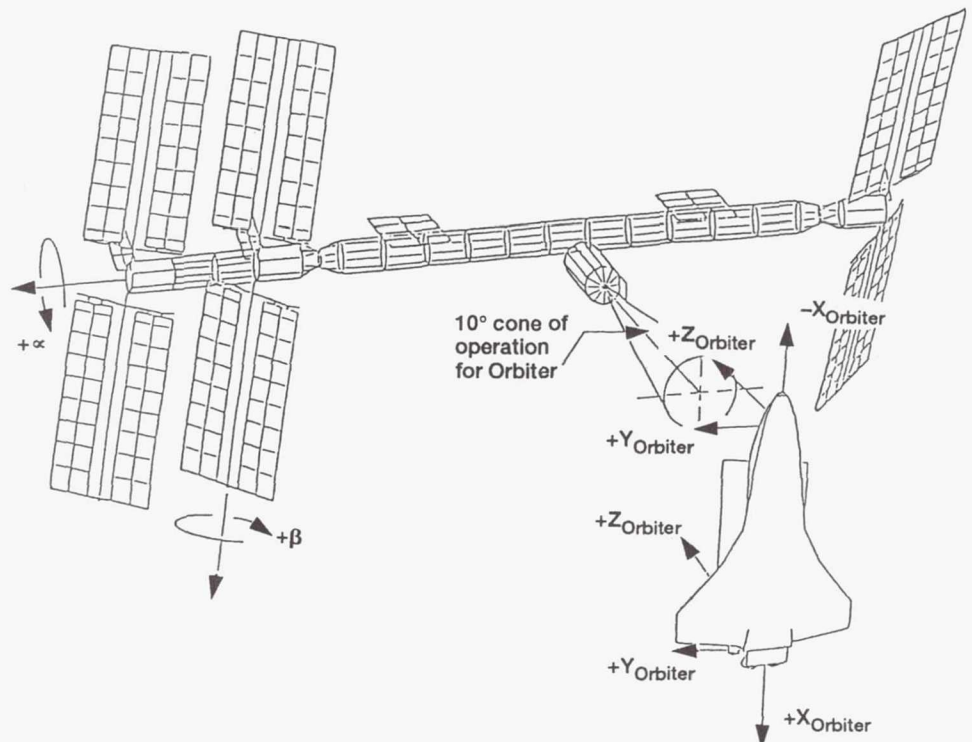
Lewis contact: Timothy L. Sullivan, (216) 433-2589  
Headquarters program office: OAST

### Space Station *Freedom* Photovoltaic Array Feathering Reduces Loads

The current evolution in spacecraft design is toward larger, lighter, and more flexible structures. Space Station *Freedom* is an example of such a structure. Even though it operates in the microgravity environment of low Earth orbit, it still must be designed to withstand several unique external disturbances.

Structural dynamic loads analyses conducted at NASA Lewis have indicated that Space Shuttle Orbiter plume impingement is one of the most severe load-inducing disturbances. Plume impingement is the result of the Orbiter firing its reaction control jets to maneuver toward a rendezvous with *Freedom*. In these loads analyses the computer program RCSFORCE was used to compute the reaction control jet forces. MSC/NASTRAN was then used to compute the resultant internal loads.

Initial rendezvous scenarios indicated that the photovoltaic array structure would not survive most Orbiter approaches. In these initial analyses the photovoltaic arrays were allowed to maintain their Sun tracking mode, and thus a large percentage of their structural area was exposed to



Optimum feather position for Space Station *Freedom* stage configuration 17.

the oncoming plume impingement jet forces. It was then decided that an operational fix of *Freedom*, the Orbiter, or both would be required. In searching for a possible operational fix, the RCSFORCE program was used to find the  $\alpha$  and  $\beta$  joint angles of *Freedom* for the lowest maximum plume loading. These angle combinations are called the feathered positions.

The plume impingement forces for these feathered positions were then run through MSC/NASTRAN to compute the actual dynamic loads. Results indicate that feathering lowers the resultant load by an order of magnitude.

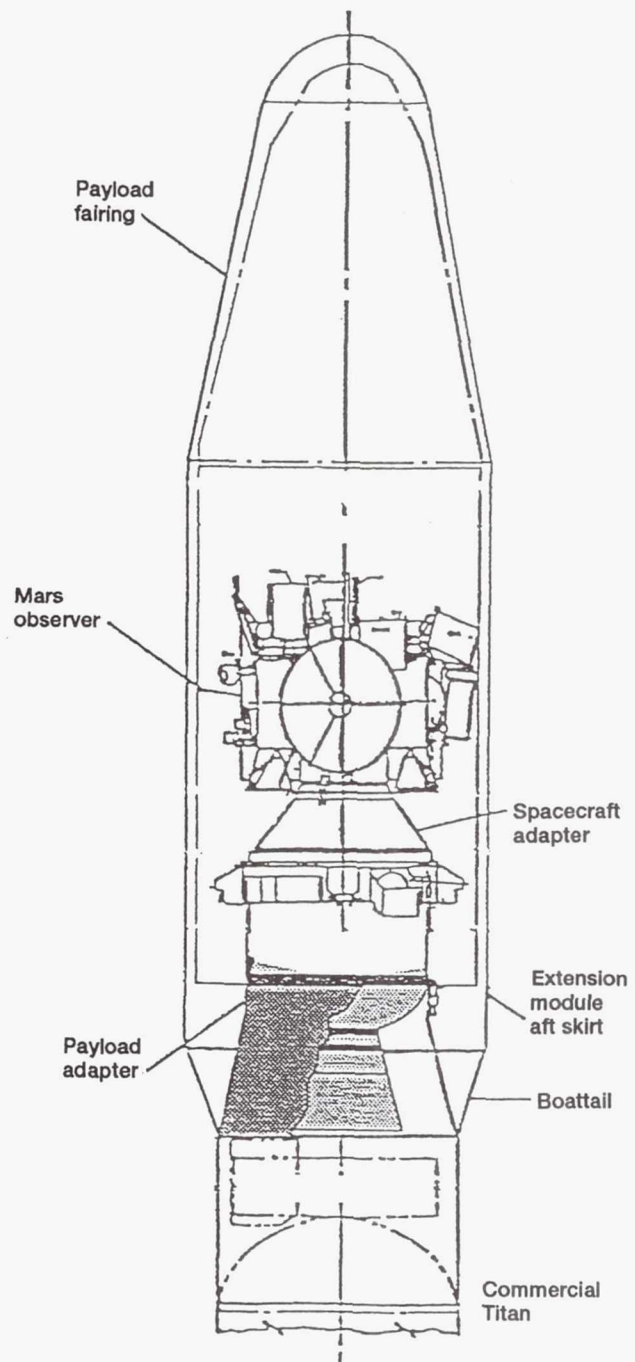
Additional analyses continue to be conducted to ensure that the most efficient feathered positions are used for the variety of Orbiter approach scenarios and *Freedom* stage configurations. Future work will be done to couple RCSFORCE with CO-ST-IN. CO-ST-IN is a computer program used to predict the very complex structure-control interactions occurring in modern spacecraft designs.

The results from these simulations, done at NASA Lewis, will be used to help design flight rules for both Space Station *Freedom* and the Orbiter fleet.

**Lewis contacts:** Damian R. Ludwiczak, (216) 433-2383; Isam Yunis, (216) 433-8393; Marsha Nall, (216) 433-5374  
**Headquarters program office:** OAST

### VAPEPS Predicts Acoustic Environment for ELV Payloads

Acoustic environment predictions for payloads launched by Atlas and Titan expendable launch vehicles (ELV) are critical for spacecraft design and testing. The prediction of the acoustic environment inside payload fairings is complicated by the recent advances in launch vehicle design, where greater lift capacity is combined with lighter and larger payload fairings. NASA Lewis has successfully developed and utilized two independent analysis methodologies for determining the maximum expected spacecraft acoustic environments. These methodologies were most recently applied to the Mars Observer mission. The Mars Observer spacecraft will be launched on Martin Marietta Corporation's newest launch vehicle, the Commercial Titan. The transfer orbit



Configuration of Commercial Titan, Mars Observer, and transfer orbit stage.

stage will make its initial flight for the Mars Observer mission.

Early in the Mars Observer Program, before flight data were available, the acoustic environment was predicted analytically by using the VAPEPS computer program. VAPEPS uses statistical energy analysis to predict the vibroacoustic response of a structure. VAPEPS is managed by



the Jet Propulsion Laboratory and is currently sponsored by NASA Lewis. VAPEPS predicted a noise reduction for the Commercial Titan's new honeycomb payload fairing. The payload fairing interior acoustics at the Mars Observer spacecraft and the transfer orbit stage was then predicted by combining the VAPEPS noise reduction prediction with a scaled estimate of the external acoustic environment derived from other Titan flight vehicles. This early prediction allowed the spacecraft and upper stage to be designed on schedule.

When the first flight data for the new Commercial Titan vehicle became available two years later, a second acoustic environment prediction was made for the Mars Observer mission. The Commercial Titan flight data were corrected for spatial variability, flight-to-flight variability, and payload configuration differences to arrive at a second acoustic prediction for the Mars Observer spacecraft and the transfer orbit stage.

The predictions obtained from these two independent methodologies agreed very well. NASA Lewis determined the final acoustic specification by enveloping the two predictions. This acoustic specification is incorporated into the interface control document for the mission.

The two acoustic prediction methodologies developed and utilized for the Mars Observer mission can be applied to any ELV mission to predict the required acoustic specifications. The fact that the VAPEPS analytical prediction agreed well with the flight data prediction increases confidence that VAPEPS can be used to make a good acoustic prediction early in an ELV mission program, even for a new launch vehicle.

#### **Bibliography**

Hughes, W.O.; and McNelis, M.E.: Dual Path Analysis for ELV Acoustic Environment Prediction. Spacecraft Dynamic Environment Technical Interchange Meeting, June 18, 1991.

**Lewis contact: William O. Hughes, (216) 433-2597**  
**Headquarters program office: OAST**

#### **Advanced Propfan Technology Works for Cruise Missiles**

A series of wind tunnel tests successfully demonstrated the performance of a U.S. Navy cruise missile with a counterrotating propfan propulsion system. A 55-percent scale model of the cruise missile with Lewis-supplied propfan blades completed extensive performance tests in the NASA Ames 14-Foot Transonic Wind Tunnel during the summer of 1991. The model is about 12 in. in diameter and 130 in. long and has a wingspan of 55 in. There are two blade rows with six blades in each row. Each blade was made from approximately 90 layers of graphite epoxy material; each layer was 0.0032 in. thick. Lewis designed and fabricated two different sets of propfan blades for this project. Each set simulates an operating design point representative of a particular propulsion system.

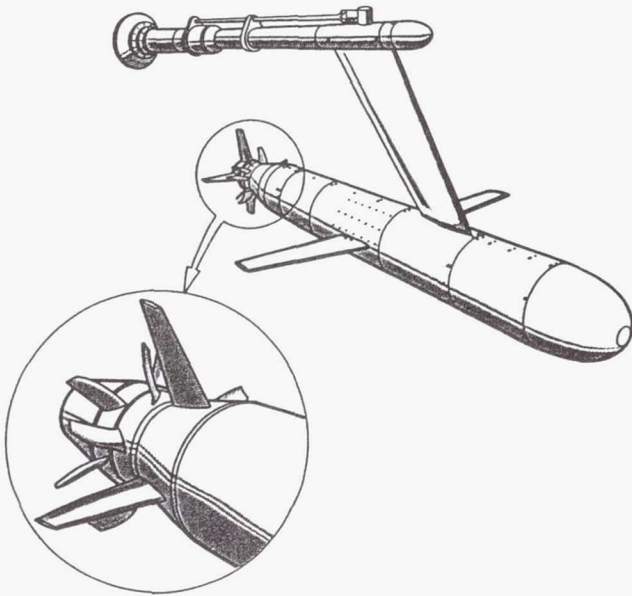
The U.S. Navy, at the request of the Department of Defense, is investigating unique missile propulsion systems that could increase fuel efficiency. Lewis has recently completed several aircraft flight projects that have demonstrated substantial increases in propulsive fuel efficiency through the use of propfan blades. Propfan blades are thin, highly swept propellers that are designed by using highly advanced computational aerodynamics and structural mechanics techniques. These advancements in design allow the blades to withstand high operating loads while maintaining high efficiency at high cruise speeds. A propfan offers a 50-percent fuel saving over equivalent-technology turbofan engines at comparable aircraft speeds and altitudes. As a result, the U.S. Navy selected the Lewis-developed propfan blade technology as a unique system for evaluating improvements in missile performance. The Naval Weapons Center at China Lake, California, had overall responsibility for the propfan-missile interaction project. This project required support from NASA Ames, NASA Lewis, the Naval Aviation Depot, the National Science Foundation, and industry. A primary goal of the project was to validate computational fluid dynamics analytical models of a complete missile configuration having counterrotating blades with experimental results from the wind tunnel test.

A Lewis and support service contractor team was formed to carry out this project. The two different Lewis-designed propfan blade sets were (1) a

## Bibliography

Krzycki, L.J.; and Strutz, L.W.: Analytical and Experimental Investigation of Propfan Propulsion for Cruise Missiles. Vol. 1. Program Overview and Summary, NWC-TM-6948, Naval Weapons Center, China Lake, CA.

**Lewis contact:** E. Brian Fite, (216) 433-3892  
**Headquarters program office:** OAST



*Propfan cruise missile.*

short-span, high-tip-speed design and (2) a longer-span, lower-tip-speed design. A totally integrated computer process was used to accomplish the design, analysis, and fabrication. The aerodynamic shape of the blades had to be correctly defined to achieve the necessary performance. The graphite epoxy laminate blades had to be designed to accommodate the proper three-dimensional aerodynamic shape and to withstand the high rotational speeds and fluctuating aerodynamic loads.

Once fabricated, the blades were instrumented, mounted to a test hub, and spin tested to verify that they could withstand the rotational speeds required during the actual wind tunnel tests. The wind tunnel model hubs were also spin tested over the test matrix.

A preliminary analysis of the wind tunnel test results indicated that counterrotating propfans make an excellent cruise missile propulsion system and can significantly improve vehicle aerodynamic characteristics. The test results matched the performance predictions made by the aeroelastic codes for almost all cases. Deviations were noted for high angles of attack.

The details of this work are being prepared for proposed NASA Technical Memorandums 105264 to 105272.

## Penetrable Linear-Gap Pressure Seal Designed

Flexible rubber tubes form a seal around a probe or other penetrating object, yet still allow movement. Through the use of inflatable rubber seals an instrumentation probe can penetrate and move along a wind tunnel wall without causing an air leak at the wall. A pair of opposed inflatable rubber tubes (or seals) create an airtight seal across a slot in a wind tunnel wall. The probe is equipped with a special teardrop-shaped section that causes the inflatable seal to deform and mold itself around the probe.

The design of the seal was completed in 1991, but hardware fabrication was postponed owing to lack of program funds. A prototype seal test

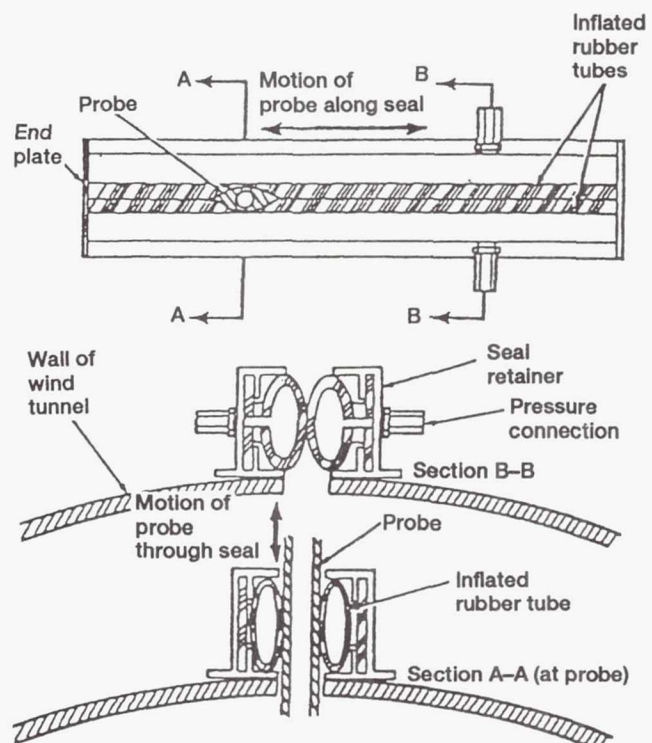


*Diagram of linear-gap pressure seal.*



apparatus was constructed and tested, however, and proved that the concept will create an airtight seal while still allowing probe movement. The prototype was tested at a "wind tunnel" pressure of 30 psi and a seal inflation pressure of 50 psi, with no net leakage. Frequent lubrication of the seal interface is critical in minimizing the force needed to move the probe. A U.S. patent is pending on the linear-gap pressure seal.

Current technology for traversing seals utilizes sliding plates with face seals. However, in this bulky method the seal assembly must be at least twice as long as the desired probe travel. The new linear-gap pressure seal assembly is only slightly longer than the desired probe travel. This size advantage of approximately 50 percent can make a tremendous difference when space is cramped and allows a researcher to probe close to an obstruction or flange.

The new seal concept is adaptable to other situations in which objects must penetrate pressure walls and move along them. It should work as well for vacuum chambers as for pressure vessels.

**Lewis contact:** Paul A. Trimarchi, (216) 433-3824  
**Headquarters program office:** OAST

## Computational Support

### Distributed Resource Computing Speeds Information Delivery

Recent advances in microprocessor and networking technology have shifted computer resources from centralized facilities to the desktops of computer users. Resources available to an application are no longer limited to a single computer but may now be distributed across a network between many different computer systems. This shift in computer resources presents system designers with new opportunities in computer resource utilization.

An information delivery system currently is being prototyped by Sverdrup Technology personnel of the Technology Demonstration Center (TDC) at NASA Lewis. Computer users at NASA Lewis use

the services of the TDC to obtain information on new computer hardware and software products. Information regarding TDC services is currently provided to the user community through a paper distribution system. The TDC is replacing the existing paper method with an automated information delivery system that provides centralized storage of information for quick and easy access by the user community.

The TDC information delivery system is an application program based upon the client/server model. A point-and-click graphical interface allows the user to obtain information on TDC events and services or to register for a specific event. A data base server residing on a remote host system processes requests for information and transfers them to the client through a network connection by using the standard Transmission Control and Internet protocols (TCP/IP). Although the client and server are two separate programs, the network connection glues them together to operate transparently as a single application program executing on a local computer system.

The server side of the TDC information delivery system has been implemented as a remote data base server program with Remote Procedure Call (RPC) library routines. Using RPC library routines simplifies the development of distributed applications by hiding the details of network programming from the programmer. The RPC library routines transparently handle all of the message passing from one process to the other, freeing the application programmer from the task of low-level interprocess communication programming.

The interoperability of heterogeneous computer environments can increase the capabilities and functionality of distributed applications by utilizing the unused processing power of today's high-performance desktop systems. The TDC information delivery system is an example of such an application. Its use will help alleviate the TDC's dependence on the paper distribution of information and will deliver schedule and announcement information faster. It may also serve as a model for future applications seeking to utilize distributed resource computing.

**Lewis contact:** Jeffrey A. Miller, (216) 433-8268  
**Headquarters program office:** OAST

## Multigrid Biharmonic Solver on a Parallel Computer

Parallel computers are a new style of computer. Instead of programming one computer and letting it execute, one programs several computers and lets them work together. The advantage is much faster execution than with even a Cray supercomputer, and at a fraction of the cost. But programming these computers is more challenging. One of NASA Lewis' first significant parallel computer applications was the multigrid biharmonic solver. The work was done in the Advanced Computational Concepts Laboratory (ACCL) on the Intel Hypercube parallel computer. This project has led the way for future work in parallel computing. The multigrid technique has been proven to improve the convergence rate of many numerical problems. But this project has shown that it can be used to even greater advantage in conjunction with a parallel computer. More importantly, the techniques learned are being applied to other problems at Lewis.

The multigrid biharmonic solver has attained 65 percent efficiency. This means that as the number of computing elements doubles, the speed with which the problem is solved increases by 65 percent. The number of computing elements can continue to be increased until the desired speed is achieved. A standard computer cannot increase its speed like this.

Besides solving some of the problems of parallel computing, this project has opened up new research possibilities. For example, a common Euler solver for jet engine configurations is now being modified to work on a parallel computer. This project also affects the Numerical Propulsion Simulation System (NPSS) community. They have problem spaces so large that they cannot be solved on traditional supercomputers. This project demonstrates that the promise of faster computing lies in parallel computing.

Especially important is the issue of scalability, or how to solve various size problems on a computer. Many programs that are written for parallel computing are limited to a certain number of computing elements. For example, although solving for 40,000 unknowns across a domain is much more time consuming than solving for 100 unknowns, many programs would use the same number of computing elements for both cases. Using many computing elements to solve a small

problem can be wasteful, and using only a few computing elements to solve a very large problem can be time consuming. Clearly, there is a need to be able to specify the number of computing elements for solving a given problem.

What makes the multigrid technique an interesting candidate for the parallel computing environment is its built-in scalability. The multigrid technique uses a user-specified number of grid levels to find a solution to the topmost grid level, but each lower level has half as many points as the level just before it.

Soon an entire jet engine configuration Euler solver will be implemented on the Intel Hypercube. This will be useful for the NPSS and other engine design applications.

### Bibliography

Briggs, W.L.: *A Multigrid Tutorial*. Society for Industrial and Applied Mathematics, 1987.

Anton, H.: *Elementary Linear Algebra*. Wiley, 1987.

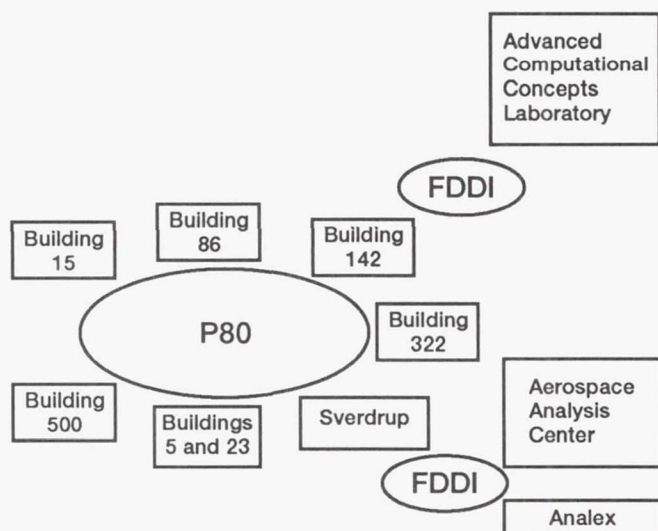
**Lewis contact:** Rodger W. Dyson, Jr., (216) 433-9083  
**Headquarters program office:** OAST

## High-Speed Fiber Networks Arrive at NASA Lewis

As NASA Lewis evolves from a facility with centralized computing to a facility with distributed computing resources, the need for higher speed networks becomes increasingly important. Lewis' networks have been continually upgraded. Networks using point-to-point copper connections at speeds less than 9600 bps have been replaced by Ethernets at 10 Mbps interconnected with fiber running at 100 Mbps.

Lewis' computing environment presently consists of Ethernets in each building interconnected across a laboratory-wide backbone. This topology allows users in any building on the backbone to interconnect to any resource on the laboratory and gives them access to the world via the Internet. The laboratory-wide backbone started as a portion of the bandwidth on Lewis' broadband cabling (CATV) network. Bridging devices caused Lewis to appear as one large network. Although this allowed any type of connection to





*Configuration of Lewis high-speed fiber networks.*

any resource available, it also created an environment where errors on one network would be propagated to every segment on the laboratory.

The bridged network is being converted to a routed one. This topology creates individual subnetworks on either side of the router. Although certain protocols are allowed through the router, errors do not get propagated. A routed network also allows for an additional level of security.

Higher performance routers are being explored to overcome some of the pitfalls of a purely routed environment. They have the segmentation and security advantages of routers but can drop back to a bridge configuration for protocols that are not routable.

A parallel effort as bridges are converted to routers is the conversion from the cable backbone to one of fiber. When this effort was begun in 1988, industry fiber standards were being created. One forerunner to the standard was an 80-Mbps network (P80) offered by Proteon, Inc. Buildings were brought onto the fiber ring by using Proteon's proprietary scheme until a standard was finalized by the industry. The industry standard, FDDI (fiber distributed data interface), is a 100-Mbps dual-redundant counterrotating fiber optic ring. This topology allows for fault tolerance and fiber redundancy.

As a new fiber optic backbone is installed around the laboratory, each building's Ethernets are being migrated to the FDDI standard. As of

September 16, 1991, 12 routers are installed on the fiber and plans are to add all of the buildings at Lewis with major computing and communications needs. This effort will ensure that Lewis' growing computer resources—mass storage, video, computer visualization, and other aspects of distributed computing—will be used in the most efficient way.

**Lewis contact:** Richard S. Kurak, (216) 433-8256  
**Headquarters program office:** OAST

### ISDN at NASA Lewis Explored

Integrated Services Digital Networking (ISDN) is a worldwide network concept that uses digital transmission and switching technology to provide an integrated set of voice and data (as well as non-voice and eventually video) services. A set of international standards is being formulated for a modular, layered framework that can deliver a variety of service features, management functions, and bandwidths. An initial survey of current and proposed ISDN technology was conducted at NASA Lewis to determine its applicability to the Lewis environment. The examination was performed with the assistance of faculty from Kent State and Cleveland State universities. Application testing involving ISDN functionality on Lewis' private branch exchange (PBX) continues to be performed.

The ISDN standards define a reference configuration of functional components and interface structures for connecting to an ISDN. Functional components include terminal adapters (TA), PBX's (NT2), and ISDN-compatible telephones (TE1). Interface structures include specifications for a basic rate interface that combines one 16-kbps D channel and two 64-kbps B channels and a primary rate interface that permits any combination of 64-kbps B, 64-kbps D, 384-kbps H0, and 1536-kbps H11 channels with an aggregate data rate limit of 1536 kbps.

A number of switching options are available with ISDN, including circuit switching, packet switching, and permanent virtual circuit. Call and network management information is conveyed on a separate channel from primary voice and data circuits by using a technique called common channel signaling. ISDN narrowband services

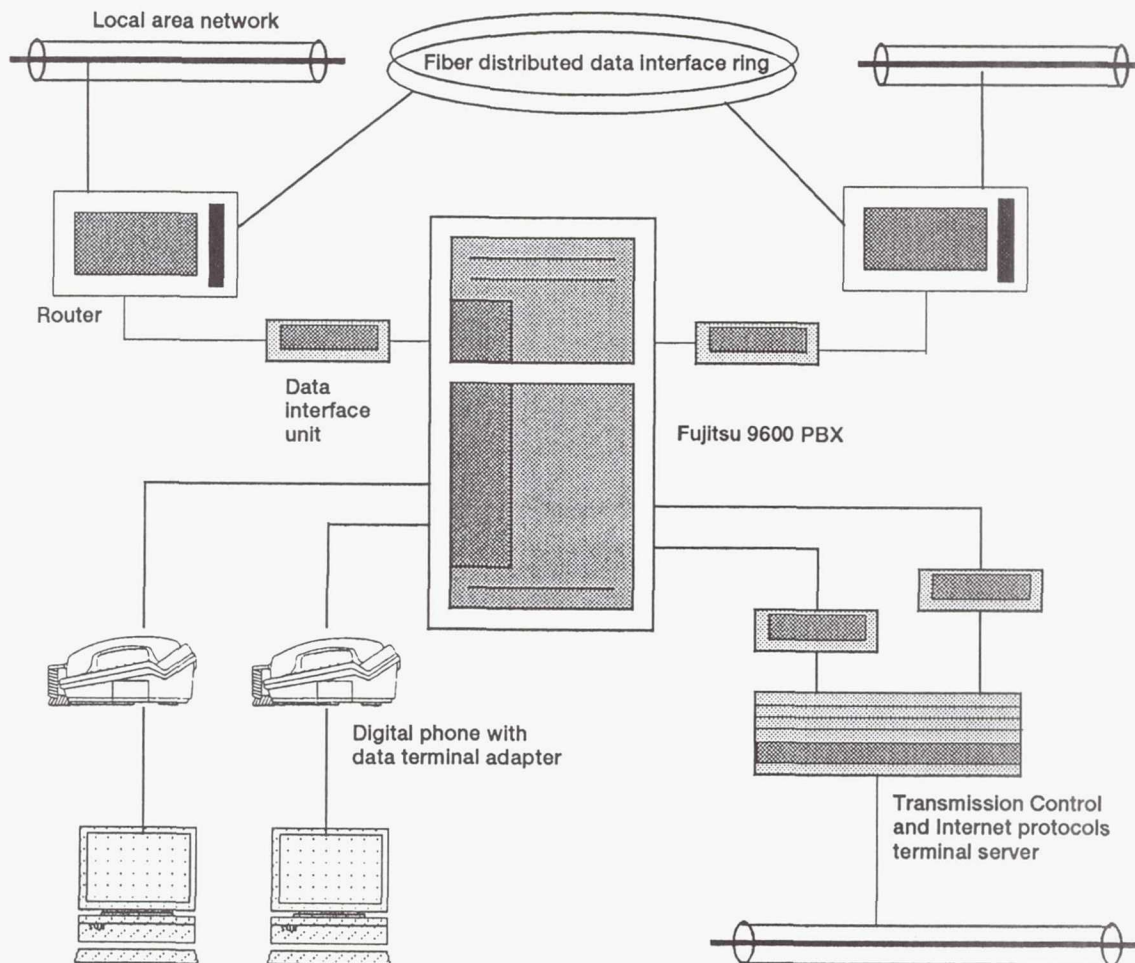
include such mandatory basic services as telephony and such supplementary options as callforwarding. Basic services are further divided into bearer services defining the "grade" of data service and teleservices describing applications-level services such as group 4 fax and telex.

New technologies are being developed to allow for higher bandwidth services. Asynchronous transfer mode (ATM) allows fast packet switching and satisfies diverse bandwidth and delay requirements, and synchronous optical network (SONET) transports ATM cells at data rates from 51.84 Mbps to 2.488 Gbps.

Lewis currently has limited ISDN capability through a Fujitsu F9600 PBX. Plans to upgrade the F9600 will add a basic rate interface to the existing primary rate interface capabilities as well as add compatibility with current AT&T and

Northern Telecom central office switches. Compatibility and interoperability are major concerns at Lewis. At present, long-distance carriers frequently use ISDN, common channel signaling, or both internally, but local exchange carriers find necessary equipment upgrades too costly, thus forming a barrier to widespread ISDN availability. NASA and Lewis are looking toward future inter-center testing and deployment through the new Federal telephone system, FTS2000, bypassing local barriers.

Preliminary experiments in providing point-to-point data circuits as well as connectivity to Lewis' central computing facilities have been successful. Computer users in buildings without normal local area network service can be supported through a data connection between their workstations and a digital telephone. In the long term broadband ISDN will also allow circuit-



Lewis ISDN testbed.



switched access to high-bandwidth services, such as video conferencing and digital video, as well as tighter integration between voice, data, and video services.

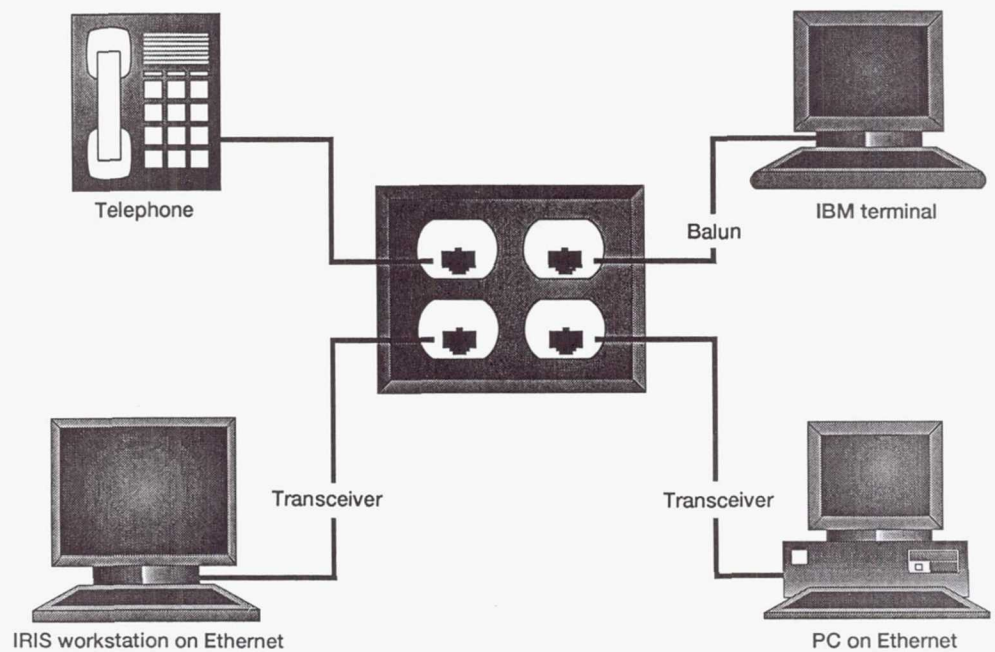
**Lewis contacts:** Steven W. Eubanks, (216) 433-9479;  
Fredric N. Goldberg, (216) 433-5074  
**Headquarters program office:** OAST

### Aerospace Analysis Center Opens

During late 1989 and most of 1990, NASA Lewis personnel designed a state-of-the-art communications network for the Aerospace Analysis Center, a building in the Aerospace Technology Park that houses the Advanced Space Analysis Office and the Aeropropulsion Analysis Office. The Aerospace Technology Park is an industrial park located adjacent to NASA Lewis where most of the larger Lewis support service contractors have offices and Lewis has located select NASA divisions.

The Aerospace Analysis Center was the first building occupied by Lewis personnel that has one type of cabling supporting all data and voice communications within the building. This network cabling was designed to simultaneously support voice and multiple types of data communications, including Ethernet, synchronous, asynchronous, and Apple Localtalk. The building is also cabled for broadband television distribution with standard CATV coaxial cable; two strands of multimode fiber optic cabling were pulled but not terminated at every faceplate. In most Lewis buildings the Ethernets utilize coaxial cable; synchronous data traffic utilizes a different coaxial cable; asynchronous traffic uses either broadband CATV coaxial cable or twisted pair; and Apple Localtalk networks use twisted pair.

The type of cabling used in the Aerospace Analysis Center's data and voice communications design was 24 American wire gauge unshielded twisted pair. Each of the two floors in the building has a centrally located wiring closet from which each of the offices is radially wired. Each two-person office has two faceplates. Each faceplate



*Typical faceplate at Aerospace Analysis Center.*

has four 4-pair unshielded twisted-pair cables terminated on RJ-45 connectors. Each faceplate has one connector designated for telephone and one connector for Ethernet, leaving the other two connectors available for another telephone, another Ethernet drop, or synchronous or asynchronous drops.

Because Lewis has given Aerospace Technology Park buildings the option of connectivity to the Lewis 80- to 100-Mbps fiber optic token ring backbone network, access to Lewis through multiplexed point-to-point T1 service, and connectivity to the Lewis broadband CATV distribution, the Aerospace Analysis Center was the first group to move off the Lewis laboratory who retained the same communications functionality as they had on the laboratory. Telephone service is provided by Ohio Bell Centrex, with tie lines installed between a remote Centrex telephone switch located in the Sverdrup Technology building and the Lewis telephone switches.

Ameritech, under contract to the Aerospace Technology Park developer, did the intrabuilding network installation for the Aerospace Analysis Center and installed the necessary interbuilding cabling to Sverdrup Technology, the building in the Aerospace Technology Park that houses the equipment which bridges the Park networks to the Lewis networks.

**Lewis contacts: Jennifer L. Lazbin, (216) 433-8252;  
Fredric N. Goldberg, (216) 433-5074  
Headquarters program office: OAST**



# Lewis Research Academy

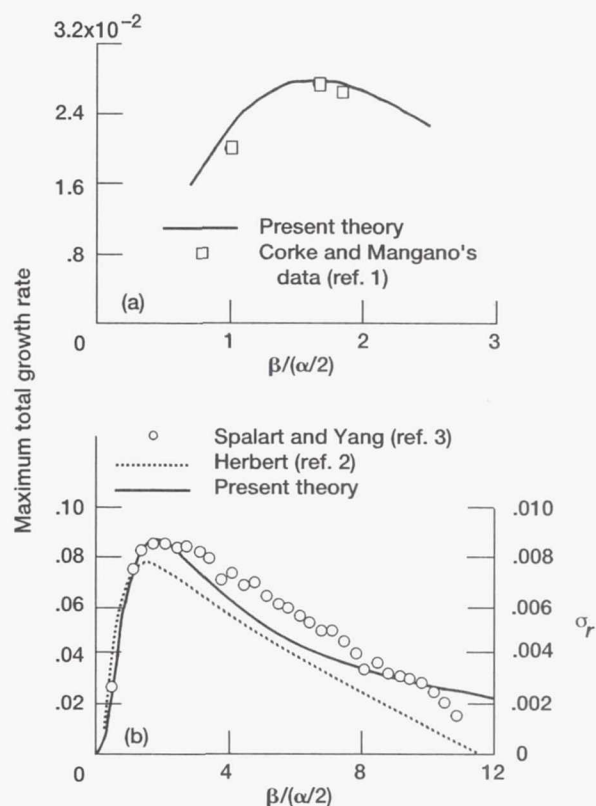
## Internal Fluid Mechanics

### Boundary Layer Transition Explained Further

The prediction of boundary layer transition is one of the major unresolved issues in aircraft design. Experimentalists usually study this phenomenon by artificially exciting their flows with two-dimensional, relatively small-amplitude, single-frequency excitation devices, such as a vibrating ribbon or an acoustic speaker. The resulting initial disturbances are well described by linear stability theory and, at the low Mach numbers at which most of the experiments have been carried out, are nearly two dimensional. This two-dimensional linear behavior can persist over very long streamwise distances when the excitation levels are sufficiently small, but the disturbance usually becomes three dimensional and nonlinear at sufficiently large downstream distances. Most experiments are carried out on a thin, flat plate that is carefully aligned with the upstream flow.

The linear regime and the initial three-dimensional regime are reasonably well understood. The latter is associated with the appearance of more or less periodic spanwise structures in the flow (peak-valley splitting, etc.). These spanwise structures are probably due to a resonant-triad interaction between a pair of oblique subharmonic modes and a basic fundamental two-dimensional mode.

The growth rate of the oblique modes in the initial three-dimensional regime is effectively linear because the oblique modes do not affect the plane wave. However, a new, fully nonlinear regime eventually develops, and a completely rational asymptotic analysis of this regime has been worked out. It shows that the oblique modes undergo a nonlinear self-interaction at this regime that completely controls their downstream development. This interaction produces nonlinear saturation of the instability waves in the absence of adverse-pressure gradients and an explosive growth of these waves when adverse-pressure gradients are present.



Effect of spanwise wavenumber on subharmonic growth rate: (a) comparison with experiment (ref. 1); (b) comparison with Floquet analysis (ref. 2) and with numerical simulation (ref. 3).

Analytical predictions are in excellent agreement with the zero-pressure-gradient, flat-plate boundary layer experiments and numerical investigations, not only at the exact resonance condition but also over a broad range of spanwise wavenumbers. Unlike previous analyses, they are able to explain the experimentally observed saturation phenomena that appear in these experiments.

### References

1. Corke, T.C.; and Mangano, R.A.: Resonant Growth of Three-Dimensional Modes in Transitioning Blasius Boundary Layers. *J. Fluid Mech.*, vol. 209, Dec. 1989, pp. 93-150.
2. Herbert, T.: Secondary Instability of Boundary Layers. *Ann. Rev. Fluid Mech.*, vol. 20, 1988, pp. 487-526.
3. Spalart, P.R.; and Yang, K.-S.: Numerical Study of Ribbon-Induced Transition in Blasius Flow. *J. Fluid Mech.*, vol. 178, 1987, pp. 345-365.

**Lewis contacts: Dr. Marvin E. Goldstein, (216) 433-5825; Dr. Reda R. Mankbadi, (216) 433-8569**  
**Headquarters program office: OAST**

## Insight Gained on Three-Dimensional Boundary Layer Separation

The mechanisms that cause a thin, viscous boundary layer to separate from the surface of a solid body are still not understood, even though considerable progress has been made in recent years—mostly for two-dimensional flows. Three-dimensional flows behave quite differently from the ideal two-dimensional situation, and very little is known about their separation behavior.

To gain some insight into this phenomenon, we consider the flow over a relatively thin, flat plate with a small-amplitude, three-dimensional distortion imposed on an otherwise uniform upstream flow. Two limiting cases have been considered.

In the first case the upstream vorticity field is entirely in the streamwise direction, so that there is little or no vortex stretching outside the viscous boundary layer on the plate surface. The streamwise velocity profiles first become inflectional within this boundary layer, and the boundary layer then undergoes a gradual separation along a continuous curve along which the normal component of the wall shear stress vanishes.

The second case is much more interesting. Here the upstream vorticity field is perpendicular to the plane of the plate, and considerable vortex stretching occurs. The boundary layer separation now occurs farther upstream, involves the collision of two different regions of the flow, and ends in the ejection of a strong vertical jet. The detailed morphology of this separation has been worked out by using a combination of analytical and numerical techniques.

This local structure can be quite unstable to small disturbances and could break down into turbulence. This local bursting phenomenon may contribute a kind of bypass mechanism that leads directly to boundary layer transition without involving the linear regime.

**Lewis contact:** Dr. Marvin E. Goldstein, (216) 433-5825  
**Headquarters program office:** OAST

## Turbomachinery Flow Modeling Continues

A mathematical analysis has yielded a set of equations governing the conceptual flow model currently used to design turbomachinery blading. These equations govern the time-averaged flow state within a typical passage of a blade row embedded in a multistage configuration. This mathematical exercise has been transformed into a number of computer simulation models and has aided in the formulation of two turbomachinery research programs.

The first research program is focused on advancing our understanding of the flow phenomena that affect the performance and life of multistage compressor blading. This research effort integrates computational fluid dynamics, flow modeling, and experimental fluid mechanics to develop flow models that designers can apply to advanced blading. Both university and industrial researchers have been and will continue to be active participants in this program.

The second research program will examine the control of secondary flow structures within turbomachinery. A viscous multistage code developed at NASA Lewis will be used in this study. This code has been used recently to examine the development of secondary flows within a mixed-flow turbine. The simulations revealed the existence of a strong vortical flow, at the exit of the rotor, whose origin was traced back to the rotor hub boundary layer.

In addition, this code has been used to examine the tip clearance flow of a transonic rotor. It was found that a strong interaction takes place between the leakage vortex and the in-passage shock, resulting in a rapid growth of the tip end-wall blockage as the rotor is throttled toward stall. It was hypothesized that this rapid growth triggers the onset of stall.

**Lewis contact:** Dr. John J. Adamczyk, (216) 433-5829  
**Headquarters program office:** OAST



## Characterization of Turbulence Shows That Nonlinearity Can Be Negligible

Because of the pervasiveness of turbulence, both in man-made fluid systems and in nature, the work at NASA Lewis on the characterization of turbulence is continuing. Turbulence is still not well understood, and much of our inability to predict turbulent flows stems from that lack of understanding. A main complicating characteristic of turbulence is its nonlinearity; we do not know how to handle the nonlinear terms in the equations of motion. There has been some disagreement as to whether that nonlinearity is ever small. A study at NASA Lewis has shown that when the turbulence is weak enough, the nonlinearity can be neglected.

The nonlinear terms in the equations of motion of a fluid are ordinarily large compared with the other terms when those equations are used to describe turbulent flow. However, one might expect intuitively that at very low turbulence Reynolds numbers (for weak turbulence) the nonlinear terms would become negligible. There has been, nevertheless, some uncertainty on that point. Some plausible analyses have indicated that the skewness factor, which is a measure of the nonlinearity of the turbulence, may not approach zero at vanishingly small Reynolds numbers. In particular reference 1, where the shape of the energy spectrum was assumed to remain approximately the same as the turbulence decayed, concluded that the skewness approaches a nonzero value in the final period of decay. That value did not differ greatly from those at earlier times. On the other hand, analyses where the assumption of similarity was not invoked (refs. 2 and 3) and an experiment (ref. 3) indicated that the skewness approaches zero as the turbulence decays.

In an attempt to resolve this discrepancy a numerical solution of the unaveraged equations of fluid motion for a decaying turbulent flow was used to determine how the skewness (nonlinearity) changes with time. The results show that as the Reynolds number approaches zero, so also does the skewness or the nonlinearity, in agreement with references 2 and 3 rather than with reference 1. This suggests that the change in shape with time of the turbulence energy spectrum can have an important effect on the ultimate character (linear or nonlinear) of the decaying turbulence. The results also show

that the flow, as the final period of decay is approached, is not truly turbulent, because the temporal fluctuations decayed earlier, leaving only the spatial fluctuations. Further details on the study are given in reference 4.

## References

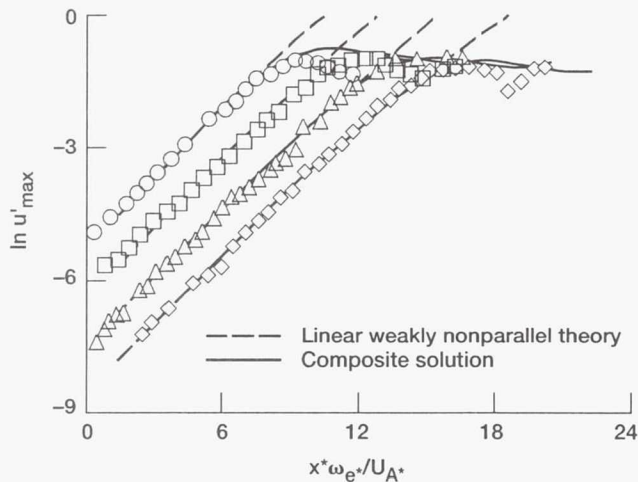
1. Reid, W.H.; and Harris, D.L.: Similarity Spectra in Isotropic Turbulence. *Phys. Fluids*, vol. 2, no. 2, 1959, pp. 139-146.
2. Deissler, R.G.: On the Decay of Homogeneous Turbulence Before the Final Period. *Phys. Fluids*, vol. 1, no. 2, 1958, pp. 111-121.
3. Tavoularis, S.; Bennett, J. C.; and Corrsin, S.: Velocity-Derivative Skewness in Small Reynolds Number, Nearly Isotropic Turbulence. *J. Fluid Mech.*, vol. 88, no. 63, 1978.
4. Deissler, R. G.: Numerical Solution for the Velocity-Derivative Skewness of a Low-Reynolds-Number Turbulent-Like Decaying Navier-Stokes Flow. *Computers Fluids*, vol. 20, no. 89, 1991.

**Lewis contact: Dr. Robert G. Deissler, (216) 433-5823**  
**Headquarters program office: OAST**

## Nonlinear Dynamics Studied for Mixing and Transition Control

Considerable progress has been made at NASA Lewis toward understanding nonlinear phenomena in both unbounded and wall-bounded shear flow transition by using a combination of high-Reynolds-number asymptotic and numerical methods. The objective of this work is to fully understand the nonlinear dynamics so that ultimately effective means of mixing and transition control can be developed.

The analyses has two important novel aspects. First, the disturbances evolve from strictly linear, finite-growth-rate instability waves on weakly nonparallel mean flows so that the proper upstream conditions can be applied in the linear region. Second, the question of proper outflow boundary conditions, which is still a research issue for direct numerical simulations (DNS) of convectively unstable shear flows, does not arise because the asymptotic formulations lead to parabolic problems. Composite expansion techniques are used to obtain solutions that account



Comparison of composite solution accounting for both nonlinear critical-layer effects and viscous mean-flow spreading with instability-wave amplitude data from Freymuth's (ref. 2) circular-jet shear layer experiment.

for both mean-flow-divergence and nonlinear effects.

For an incompressible mixing layer the amplitude evolution of a two-dimensional instability wave is completely controlled by a nonlinear critical-layer vorticity equation. Although the solution of this parabolic partial differential equation requires supercomputer resources, it is sufficiently simpler than a direct numerical simulation using the Navier-Stokes equations so that grid-resolution questions can be resolved.

Very good agreement with available experimental data for the first nonlinear saturation stage of a plane-jet shear layer, a circular-jet shear layer, and a mixing layer behind a splitter plate has been demonstrated (ref. 1). The composite solution was compared with Freymuth's (ref. 2; fig. 10) amplitude-evolution data for four different excitation levels in his circular-jet shear layer experiment. The comparison confirmed that there is an initial streamwise region where the disturbance is well described by weakly non-parallel linear stability theory and that the nonlinear saturation is well described by the composite solution. For subsonic and supersonic instability waves on compressible shear layers (ref. 3), the nonlinearity comes into play at smaller amplitudes than in the incompressible case; and their evolution is consequently determined by a nonlinear integro-differential equation. The nonlinear effects can give rise to either an explosive growth or an equilibrium solution.

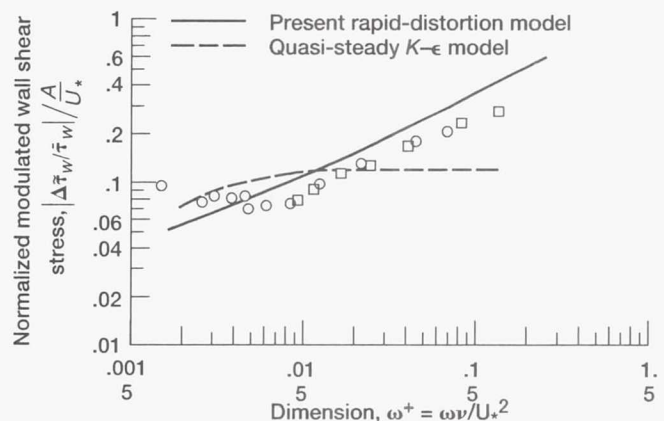
## References

1. Hultgren, L.S.: Nonlinear Spatial Equilibration of an Externally Excited Instability Wave in a Free Shear Layer. Submitted to J. Fluid Mech., 1991.
2. Freymuth, P.: On Transition in a Separated Laminar Boundary Layer. J. Fluid Mech., vol. 25, 1966, pp. 683-704.
3. Leib, S. J.: Nonlinear Evolution of Subsonic and Supersonic Disturbances on a Compressible Free Shear Layer. J. Fluid Mech., vol. 224, 1991, pp. 551-578.

Lewis contact: Dr. Lennart S. Hultgren, (216) 433-6070  
Headquarters program office: OAST

## Modeling of Unsteady Turbulent Flows Aided by Rapid-Distortion Theory

The study of unsteady turbulent flows is quite relevant to many technical applications, such as Stirling engine flow, rotor-stator interactions in turbomachinery, and internal combustion engines. In predicting these flows, off-the-shelf models, such as the  $K-\epsilon$  model, were used to describe the turbulent motion. These models were originally developed for steady flows, and using them in the unsteady case implies that the turbulence would respond in a "quasi-steady" manner to unsteady effects. But now there is increasing experimental evidence that this is not the case. In fact, experimental observations show that the structure of wall turbulence is distorted when



Modulated wall shear stress versus frequency in a turbulent wall layer subject to oscillatory pressure field. Predictions of the  $K-\epsilon$  model and the rapid-distortion model are compared with experimental data.



exposed to highly unsteady effects (the behavior near the wall lags behind that away from the wall) and that flow-history effects are important. The use of steady-state-based turbulence models in unsteady cases can thus result in considerable errors, because such models cannot account for the observed unsteady effects.

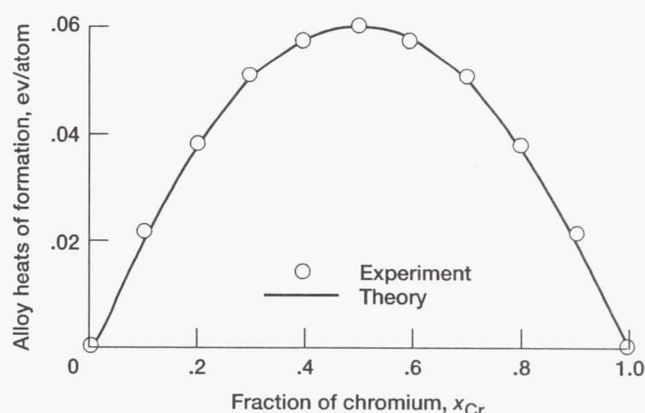
This difficulty was overcome by adapting rapid-distortion theory to introduce a truly unsteady closure into a simple phenomenological turbulence model in order to describe the unsteady response of a turbulent wall layer exposed to a temporarily oscillating pressure gradient. The closure model was built by taking the ratio of turbulent shear stress to turbulent kinetic energy to be a function of the effective strain. The latter accounts for the history of the flow. The computed unsteady velocity fluctuations and modulated turbulent stresses compared favorably in the "non-quasi-steady" frequency range, where quasi-steady assumptions fail. This suggests that the concept of rapid distortion is especially appropriate for unsteady flows.

**Lewis contact: Dr. Reda R. Mankbadi, (216) 433-8569**  
**Headquarters program office: OAST**

## Materials

### New Method Calculates Material Properties

Although solving the Schroedinger equation for a solid, which is based on first principles, is the most desirable approach to use in computational materials studies, it can prove to be cumbersome for complex problems of practical interest. Therefore, current theoretical research is directed toward the development of semiempirical techniques that have their grounding in first-principles approaches yet use some fitting parameters from experiment. These methods are then tested by how well they quantitatively predict both experiment and first-principles calculations for less complex situations. The objective of the research is the prediction of the energetics of defects in solids and at interfaces. Materials of practical interest span a wide range, including metals, ceramics, semiconductors, and polymers; consequently, it is necessary to develop approaches that treat each class of solids.



*Heats of formation versus composition for body-centered cubic alloys of chromium and iron.*

Progress has been made in predicting the energetics of single-component systems for metals and semiconductors. Extensive effort has been recently directed toward predicting the properties of face-centered, cubic metallic alloys (ref. 1). We now have developed techniques to predict the properties of body-centered, cubic metallic alloys, which have complex behavior in their heats of formation, and are in the initial stages of predicting the properties of semiconducting compounds such as silicon germanium (SiGe) or gallium arsenide (GaAs).

In order to develop techniques to predict the properties of ceramics, it is necessary to extend the previously developed methods to include the possibility of charge transfer between the interacting components. Progress has been made in extending the universal binding energy relation to these situations and on the approaches needed to develop semiempirical techniques for predicting the properties of ceramics (ref. 2).

In addition to developing methods for predicting interaction energies, it is also necessary to determine the minimum energy configuration of a defect and to treat dynamic problems. Monte-Carlo and molecular-dynamics approaches are being developed in conjunction with semiempirical methods in order to examine problems of practical interest in material science.

## References

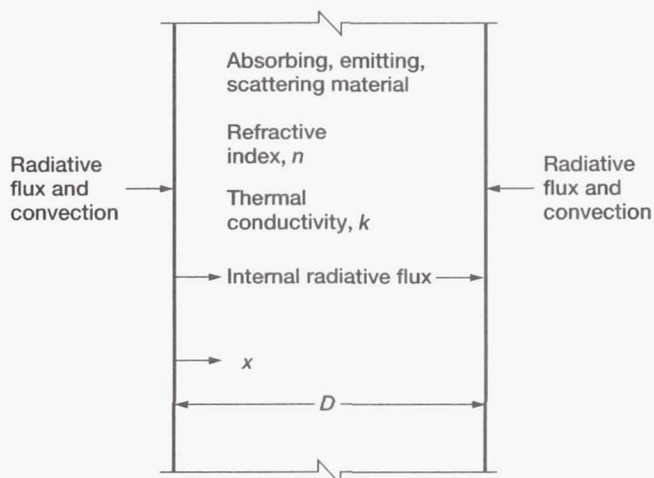
1. Bozzolo, G.; and Ferrante, J.: Equivalent Crystal Theory of Alloys. NASA TP-3155, 1991.
2. Schlosser, H.; Ferrante, J.; and Smith, J. R.: Global Expression for Representing Cohesive-Energy Curves. Phys. Rev. B, vol. 44, no. 17, Nov. 1, 1991, pp. 9696-9699.

Lewis contact: Dr. John Ferrante, (216) 433-6069  
Headquarters program office: OAST

### Radiation Heat Transfer Characteristics Obtained in Semitransparent Materials

Heat transfer can occur in some solid materials by the internal transmission, absorption, scattering, and emission of infrared and visible radiant energy. This energy transfer, which is in addition to heat conduction, can be appreciable when temperatures are elevated and materials are partially transparent to radiant energy. Radiant transfer can have a significant effect on the internal temperatures of some ceramic coatings and ceramic engine parts. Some heat storage materials, such as lithium fluoride, are partially transparent to radiative transfer. This is also true of some crystals to be grown in microgravity experiments, so that radiation influences the growth processes. The temperature distributions in windows used for viewing into experimental furnaces and combustion chambers are influenced by absorption of radiant energy. Analytical and numerical research is being done to develop improved methods for predicting heat transfer effects in these semitransparent materials. Local temperatures and heat flows within the material have been obtained. This work is being done in house and is a continuing effort.

Combined radiation and conduction heat transfer have been analyzed in plane layers with refractive indexes typical of ceramic materials. The materials partially absorb, emit, and scatter internal radiant energy. Each side of the layer is heated by differing amounts of radiation and convection, and the effect of interface reflections is included. When the refractive index is larger than 1, total internal reflections occur at the surfaces for some of the energy within the layer. These reflections



*Radiation heat transfer in heated semitransparent layer.*

substantially redistribute energy across the layer and considerably alter the temperature distribution from that when the refractive index is 1 and total internal reflections do not occur. Results were obtained for a gray layer and for a two-band spectral variation of the absorption coefficient. The solutions yield detailed temperature distributions that can be used to evaluate thermal performance and to perform thermal stress calculations. The radiant energy leaving the surface was examined to determine when it can be used to accurately measure the surface temperature. Most of the calculations were for a layer with absorption only, but the computer program has been extended to include scattering. Investigations are continuing to examine its effect.

An analytical solution has been found for the limiting situation of pure radiation in a plane layer. This applies when there are small heat conduction effects. The solution includes internal radiative absorption, emission, and scattering. By using the simple analytical expressions that were obtained, the temperature distributions for a material with a refractive index of 1 were extended to include internal interface reflections and a refractive index greater than 1. A higher refractive index tends to make the internal temperature distribution more uniform.

An analytical solution has been obtained for a two-dimensional radiating medium in a rectangular geometry. The medium is well mixed so that it is at uniform temperature. The absorption coefficient is spectrally dependent. The solution



predicts the local heat flux received along the rectangular boundary as a function of position. Because the solution is in analytical form, very accurate heat flux results can be evaluated from it. These can be used as a reference to check solutions from general numerical computer programs.

#### **Bibliography**

Spuckler, C.M.; and Siegel, R.: Refractive Index Effects on Radiative Behavior of a Heated Absorbing-Emitting Layer. J. Thermophys. Heat Trans., vol. 6, 1992.

Siegel, R.; and Spuckler, C.M.: Effect of Index of Refraction on Radiation Characteristics in a Heated Absorbing, Emitting and Scattering Layer. Submitted to J. Heat Trans., 1991.

Siegel, R: Boundary Heat Fluxes for Spectral Radiation From a Uniform Temperature Rectangular Medium. J. Thermophys. Heat Trans., vol. 6, 1992.

**Lewis contact: Dr. Robert Siegel, (216) 433-5831**  
**Headquarters program office: OAST**

# Author Index

- Adamczyk, Dr. John J., 149  
 Alger, Donald L., 87, 88  
 Alterovitz, Dr. Samuel, 99  
 Anderson, Robert C., 7  
 Ansari, Dr. Rafat R., 38  
 Appelbaum, Dr. Joseph, 81  
 Baez, Anastacio N., 135  
 Banks, Bruce A., 90  
 Baker, Karl W., 93  
 Barankiewicz, Wendy S., 27  
 Barth, Richard L., 35  
 Beach, Raymond F., 135  
 Benson, Thomas J., 19  
 Bents, David J., 86  
 Bhasin, Dr. Kul B., 99, 100  
 Blech, Richard A., 13  
 Bobinsky, Eric A., 104  
 Borowski, Dr. Stanley K., 116  
 Bowles, Kenneth J., 51  
 Bresnahan, Donald L., 112  
 Budinger, James M., 101, 103  
 Bulzan, Dr. Daniel L., 15  
 Burkhardt, Leo A., 3  
 Burley, Richard R., 34  
 Capaldi, Russell J., 72  
 Carlile, Julie A., 70, 74  
 Chamis, Dr. Christos C., 53, 54, 55, 60  
 Chiaramonte, Francis P., 126  
 Chima, Dr. Roderick V., 30  
 Chomos, Gerald J., 106  
 Curlett, Brian P., 2  
 Curren, Arthur N., 96  
 Davidian, Kenneth J., 78  
 Decker, Dr. Arthur J., 8  
 de Groh, Kim K., 90  
 Deissler, Dr. Robert G., 150  
 DellaCorte, Dr. Christopher, 49, 50  
 DeLombard, Richard, 123  
 DiCarlo, Dr. James A., 44  
 Doherty, Michael P., 117  
 Dolce, James L., 135  
 Dreshfield, Dr. Robert, 41  
 Dudzinski, Leonard A., 117  
 Duffy, Dr. Steve, 66  
 Dyson, Rodger W., 143  
 Eckel, Andrew J., 43  
 Ellis, Dr. David, 42  
 Esker, Barbara S., 28  
 Eubanks, Steven W., 146  
 Felder, Marian, 132  
 Ferguson, Dr. Dale C., 128  
 Ferrante, Dr. John, 153  
 Fite, E. Brian, 141  
 Frate, David T., 133  
 Fralick, Gustave C., 6  
 Fricker, David M., 16  
 Fujikawa, Gene, 104  
 Gaby, Joseph D., 110  
 Garg, Dr. Sanjay, 9, 11  
 Gayda, Dr. John, 41  
 George, Jeffrey A., 117  
 Glover, Daniel R., 108  
 Gokoglu, Dr. Suleyman A., 48  
 Goldberg, Fredic N., 146, 147  
 Goldstein, Dr. Marvin E., 148, 149  
 Gray, Dr. Hugh R., 36  
 Grady, Dr. Joseph E., 58  
 Guo, Dr. Ten-Huei, 10  
 Hack, Kurt J., 117  
 Haggard, John B., Jr., 124  
 Harding, Dr. David R., 45  
 Hardy, Terry L., 72  
 Hathaway, Dr. Michael, 14  
 Heidelberg, Laurence J., 32  
 Herbell, Dr. Thomas P., 43  
 Herr, Joel L., 89  
 Hojnicki, Jeffrey S., 131  
 Holanda, Raymond, 5  
 Holdeman, Dr. James D., 17  
 Hughes, William O., 140  
 Hultgren, Dr. Lennart S., 151  
 Iek, Chanthay, 34  
 Jacobson, Thomas P., 122  
 Jankovsky, Robert S., 71  
 Jones, Robert E., 101  
 Kazaroff, John M., 71  
 Kerczewski, Robert J., 105  
 Kerwin, Paul T., 21  
 Kim, Dr. Suk C., 20  
 Knoll, Richard H., 109  
 Kohout, Lisa, 84  
 Koudelka, John, 127  
 Krantz, Timothy L., 24  
 Kunath, Richard R., 95  
 Kurak, Richard S., 144  
 Lauver, Richard W., 118, 120  
 Lawrence, Dr. Charles, 61  
 Lazbin, Jennifer L., 147  
 Lee, Ho-Jun, 58  
 Lee, Dr. Richard Q., 94  
 Lei, Dr. Jih-Fen, 4  
 Lerch, Dr. Bradley A., 59  
 Linne, Diane L., 76  
 Liou, Larry C., 68



Liou, May-Fun, 12  
 Ludwiczak, Damian R., 139  
 MacKay, Dr. Rebecca A., 40  
 McGaw, Michael A., 73  
 Madzsar, George C., 69  
 Mankbadi, Dr. Reda R., 148, 152  
 Melis, Matthew E., 56  
 Merrill, Dr. Walter C., 9  
 Meyer, Claudia M., 77  
 Meyer, William V., 38  
 Miller, Dr. Christopher J., 31  
 Miller, Jeffrey A., 142  
 Mirtich, Michael J., 90  
 Misra, Dr. Ajay K., 46  
 Morscher, Gregory N., 44  
 Mularz, Dr. Edward, 16  
 Murthy, Durbha V., 61  
 Murthy, Pappu L.N., 57  
 Nall, Marsha, 139  
 Nathal, Dr. Michael V., 40  
 Nemeth, Noel N., 65  
 Niedzwiecki, Richard W., 22  
 Oswald, Fred B., 25  
 Otero, Angel M., 126  
 Palaszewski, Bryan, 75, 76  
 Palko, Joseph L., 66  
 Patterson, Richard L., 83  
 Paulsen, Phillip E., 132  
 Pavli, Albert J., 71  
 Piszczor, Michael F., Jr., 80  
 Pline, Alexander D., 122  
 Powers, Lynn M., 65  
 Proctor, Margaret P., 74  
 Quentmeyer, Richard J., 70  
 Ramins, Peter, 97  
 Reinmann, John J., 23  
 Rhatigan, Jennifer L., 131  
 Richter, Scott W., 92  
 Roelke, Richard J., 29  
 Romanofsky, Robert R., 99  
 Roth, Dr. Don J., 67, 68

Roth, Mary Ellen, 82  
 Sacksteder, Kurt, 127  
 Saiyed, Naseem H., 113  
 Sanabria, Rafael, 114  
 Sanders, William A., 44  
 Sater, Bernard L., 132  
 Shalkhauser, Kurt A., 95  
 Shuen, Dr. Jian-Shun, 16  
 Siegel, Dr. Robert, 154  
 Sliney, Harold E., 49  
 Smialek, Dr. James L., 47  
 Smith, C. Frederic, 34  
 Snyder, David B., 89  
 Spalvins, Talivaldis, 50  
 Stankiewicz, Norbert, 98  
 Starlinger, Dr. Alois, 66  
 Stefko, George L., 61, 63  
 Steinetz, Dr. Bruce M., 62  
 Stephens, Joseph R., 37  
 Stochl, Robert J., 111  
 Stubbs, Dr. Robert M., 20  
 Sullivan, Timothy L., 138  
 Taylor, William J., 112  
 Thompson, Robert L., 122  
 Trefny, Charles J., 26  
 Trimarchi, Paul A., 142  
 Troudet, Dr. Terry, 9  
 Vanderaar, Mark J., 103  
 Viterna, Dr. Larry A., 130  
 Wald, Lawrence W., 128  
 Whalen, Margaret V., 72  
 Whittenberger, Dr. J. Daniel, 39  
 Whyte, Wayne A., 107  
 Williams, Glenn L., 136  
 Winsa, Edward A., 119  
 Woodward, Richard P., 32  
 Wright, William D., 23  
 Yunis, Isam, 139  
 Zaman, Dr. Khairul, 18  
 Zaretsky, Erwin V., 52

REPORT DOCUMENTATION PAGE			Form Approved OMB No. 0704-0188	
Public reporting burden for this collection of information is estimated to average 1 hour per response, including the time for reviewing instructions, searching existing data sources, gathering and maintaining the data needed, and completing and reviewing the collection of information. Send comments regarding this burden estimate or any other aspect of this collection of information, including suggestions for reducing this burden, to Washington Headquarters Services, Directorate for Information Operations and Reports, 1215 Jefferson Davis Highway, Suite 1204, Arlington, VA 22202-4302, and to the Office of Management and Budget, Paperwork Reduction Project (0704-0188), Washington, DC 20503.				
1. AGENCY USE ONLY (Leave blank)	2. REPORT DATE	3. REPORT TYPE AND DATES COVERED Technical Memorandum		
4. TITLE AND SUBTITLE Research & Technology 1991		5. FUNDING NUMBERS  None		
6. AUTHOR(S)				
7. PERFORMING ORGANIZATION NAME(S) AND ADDRESS(ES) National Aeronautics and Space Administration Lewis Research Center Cleveland, Ohio 44135-3191		8. PERFORMING ORGANIZATION REPORT NUMBER  E-6677		
9. SPONSORING/MONITORING AGENCY NAMES(S) AND ADDRESS(ES) National Aeronautics and Space Administration Washington, D.C. 20546-0001		10. SPONSORING/MONITORING AGENCY REPORT NUMBER  NASA TM-105320		
11. SUPPLEMENTARY NOTES Responsible person, Walter S. Kim, (216) 433-3742.				
12a. DISTRIBUTION/AVAILABILITY STATEMENT  Unclassified - Unlimited Subject Categories 01 and 31			12b. DISTRIBUTION CODE	
13. ABSTRACT (Maximum 200 words)  This report selectively summarizes the NASA Lewis Research Center's research and technology accomplishments for the fiscal year 1991. It comprises approximately 150 short articles submitted by the staff members of the technical directorates. The report is organized into six major sections: Aeronautics, Aerospace Technology, Space Flight Systems, Space Station <i>Freedom</i> , Engineering and Computational Support, and Lewis Research Academy. A table of contents by subject has been developed to assist the reader in finding articles of special interest. This report is not intended to be a comprehensive summary of all the research and technology work done over the past fiscal year. Most of the work is reported in Lewis-published technical reports, journal articles, and presentations prepared by Lewis staff or by contractors. In addition, university grants have enabled faculty members and graduate students to engage in sponsored research that is reported at technical meetings or in journal articles. For each article in this report a Lewis contact person has been identified, and where possible, a reference document is listed so that additional information can be easily obtained. The diversity of topics attests to the breadth of research and technology being pursued and to the skill mix of the staff that makes it possible.				
14. SUBJECT TERMS  Aeronautics; Aerospace engineering; Space flight; Space station power supplies; Materials; Structural analysis; Computational fluid dynamics; Computer programming			15. NUMBER OF PAGES 170	
			16. PRICE CODE A08	
17. SECURITY CLASSIFICATION OF REPORT Unclassified	18. SECURITY CLASSIFICATION OF THIS PAGE Unclassified	19. SECURITY CLASSIFICATION OF ABSTRACT Unclassified	20. LIMITATION OF ABSTRACT	



